INFORMATION TO USERS

UMI®

University of Alberta

**Petroleum Hydrogeology of the Nisku Aquifer in the
Western Canadian Sedimentary Basin**

by

©

Arif Alkalali

A thesis submitted to the Faculty of Graduate Studies and Research in partial
fulfillment of the requirements for the degree of Master of Science

Department of Earth and Atmospheric Sciences

Edmonton, Alberta

Fall 2002

0-612-81354-1

Canada

University of Alberta

Library Release Form

Name of Author: Arif Alkalali
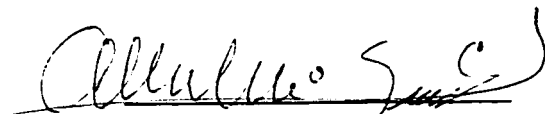
Title of Thesis: Petroleum Hydrogeology of the Nisku Aquifer in the Western
Canadian Sedimentary Basin

Degree: Master of Science

Year Degree Granted: 2002

Permission is hereby granted to the University of Alberta Library to reproduce single
copies of this thesis and to lend or sell such copies for private, scholarly, or scientific
research purposes only.

The author reserves all other publication and other rights in association with the
copyright in the thesis, and except as herein before provided, neither the thesis nor
any substantial portion thereof may be printed or otherwise reproduced in any
material form whatever without the author's prior written permission.

P. O. Box 5741
Dhahran, 31311
Saudi Arabia

Date: October 3, 2002
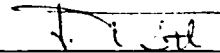
University of Alberta

Faculty of Graduate Studies and Research
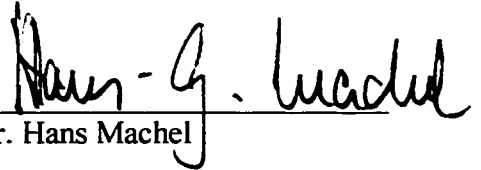
The undersigned certify that they have read, and recommended to the Faculty of
Graduate Studies and Research for acceptance, a thesis entitled *Petroleum
Hydrogeology of the Nisku Aquifer in the Western Canadian Sedimentary Basin*
submitted by *Arif Alkalali* in partial fulfillment of the requirements for the degree of
Master of Science.

Dr. Benjamin Rostron

Dr. József Tóth

Dr. Hans Machel

Dr. Mauricio Sacchi

Date: *OcTOBER 2, 2002*

Abstract

A petroleum hydrogeological study was conducted in order to evaluate the effects of moving groundwater on the distribution of hydrocarbons in the Nisku Aquifer over the Western Canadian Sedimentary Basin. The study involved the utilization of pressure, temperature, water density, structure, and the development of a program code to model the oil driving forces in the Nisku Aquifer. The study revealed several correlating patterns of sites that are highly likely to be hydrocarbon accumulation sites and actual hydrocarbon distributions. Those hydrogeologically favorable hydrocarbon accumulation sites developed as a result of varying basinal-scale factors relating to the source of energy that drive groundwater flow, the permeability distribution in the sedimentary section, and the basin tectonics and erosional history.

In northern Alberta and British Columbia, as well as the Karr basin in central Alberta, underpressuring drives flow inward, and also steering the oil driving forces into those potentiometric minima. In west central and south central Alberta, significant cross-formational flow from the underlying Leduc Aquifer introduces energy into the Nisku Aquifer and drives the groundwater flow outward from these potentiometric highs. In southern Alberta and northwestern Montana, topography driven flow creates downdip flow steering the oil driving force vectors in a northerly, northeasterly, and a northwesterly direction, creating several areas of converging vectors. At West Pembina, overpressuring creates a local potentiometric high leading to an outward directed flow and oil driving force vectors. In the Williston basin, the low hydraulic gradients and high structural gradient create oil driving forces that are dominated by buoyancy forces. In the east central part of the Alberta basin, the area acts as a regional discharge due to the low

land surface topography and the trapping could potentially be affected by recharge in local flow system due to small-scale land surface topography variations.

Acknowledgements

TO MY WIFE

HANAN ALMUBARK

Table of Contents

List of Tables

List of Figures

1.0 Introduction and Theoretical Background

1.1 Purpose

The Nisku Formation, and its lateral equivalents (Figure 1.1) in the Western Canadian Sedimentary Basin (WCSB) span almost the entire basin from its southern to northern boundaries (Switzer et al., 1994), and host large accumulation of hydrocarbons distributed at accumulation-preferred sites (Table 1.1). Furthermore, several petroleum geochemical studies have suggested that major oil pools in the Nisku Formation are sourced from within the formation (Chevron Exploration Staff, 1979; Allen and Creany, 1991; Obermejer et al., 1999; Fowler et al., 2001).

The distribution of hydrocarbons at preferred sites in the Nisku Formation could potentially be highly influenced by moving groundwater. The effects of moving groundwater on hydrocarbon migration and entrapment have been proposed and studied by several workers including Munn (1909), Hubbert (1953), and Tóth (1980), and a number of studies have expanded on the theories already established by those workers like, among others, Schowalter (1979), Davis (1987), England et al. (1987), Bethke et al. (1991), and Dahlberg (1994). While significant hydrocarbon accumulations were discovered and produced from the Nisku Formation in the WCSB, no published study is known to exist investigating the effects of moving groundwater on the hydrocarbons' lateral migration and entrapment in this formation on a basinal scale. Thus, this is a regional study assuming the Nisku Formation to be a carrier bed for migration of hydrocarbons conducted to evaluate such effects in view of the theoretical foundation of

1

Central Alberta	Southern Alberta	N. Alberta/N. B.C..	Saskatchewan	N. Dakota/Mont.
Calmar	Calmar/Stettler	Red Knife	Three Forks	Three Forks
Nisku	Arcs	Jean Marie	Birdbear	Birdbear/Nisku
Ireton	Duperow/Ireton	Fort Simpson	Duperow	Duperow

Upper Devonian

Frasnian — Famennian

Woodbend — Winterburn — Wabamun
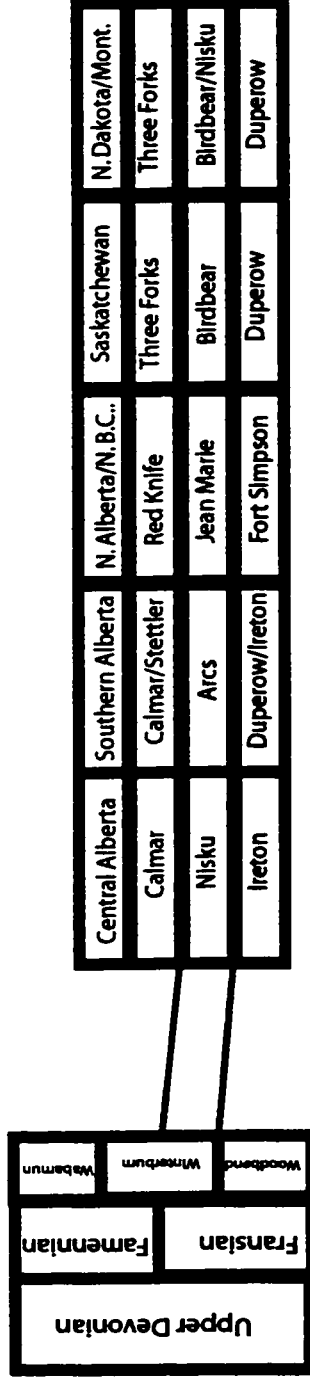
Figure 1.1 The Nisku Formation and its lateral basinal equivalents (compiled from Switzer et al. (1994) and a stratigraphic correlation chart by Western Atlas International, undated).

Field	Number of Pools	Marketable Reserves (10^6 m^3)	Discovery Year
Fenn-Big Valley	3 oil; 4 gas	49.1 oil; 2,060 gas	1952
Pembina	27 oil (with Blue Ridge pools), 25 gas	28.4 oil; 3,337 gas	1976
Leduc-Woodbend	6 oil; 4 gas	18.0 oil; 2,676 gas	1947
Joffre	1 oil	10.1 oil	1956
Brazeau River	10 oil; 27 gas	9.4 oil; 11,644 gas	1977
Bigory	10 oil	8.0 oil	1977
West Pembina	3oil; 5 gas	7.2 oil; 1,719 gas	1977
Meekwap	6 oil	5.3 oil	1966
Drumheller	3 oil	4.7 oil	1951
West Drumheller	2 oil	4.7 oil	1952
Hamlet North	1 gas	5,434 gas	1976
Calling Lake	2 gas	2,705 gas	1964
Obed	2 gas	2,593 gas	1956
Figure Lake	22 gas	2,522 gas	1951
Kaybob South	5 gas	1,944 gas	1958

Table 1.1 Largest oil and gas fields of the Nisku Formation in the WCSB (after Switzer et al., 1994).

hydrocarbon migration, and is based on detailed regional hydrogeological utilization of subsurface pressure, temperature, geology, and water density derived from the total dissolved solids in groundwater at the formation pressure and temperature. Such a study is carried out to understand the variety of hydrogeological factors that can influence the distribution of hydrocarbons in the Nisku Formation and determine sites preferred for hydrocarbon accumulations as influenced by those factors.

The objectives of this work consists of two primary parts; the first is to characterize present-day regional-scale lateral hydrocarbon movement in the Nisku Formation based on Hubbert's (1953) theory and as applied by other workers for practical applications such as Schowalter (1979), Davis (1987), and Bethke (1991). The second part is to study potential tilt in the oil-water contact in the Nisku Formation reservoirs based on regional scale groundwater flow. Such characterization is feasible only by proper characterization of lateral and vertical movements of groundwater, augmented with other relevant published studies of hydrogeology, lithology, basin history, and hydrocarbon geochemical studies relevant to the Nisku Formation.

1.2 Fundamental Considerations

1.2.1 Scope and Limitations

The nature and scale of this study intends to identify basinal scale effects of moving groundwater on hydrocarbon distribution in the Nisku Formation. Observed patterns should serve as a lead to further smaller scale investigations, based on this large-scale petroleum hydrogeological evaluation, represented by the resulting set of maps (Chapters 4 & 5). Furthermore, the conclusions to be drawn from this study will only suggest the hydrogeological component of petroleum prospecting, which is by no means conclusive, but rather an integral part of a suite of other tools traditionally used in the oil industry for hydrocarbon exploration, which includes structural, basinal, and geochemical analyses. It should be stated here that petroleum hydrogeology cannot serve as the only basis for identifying regions of high probability of hydrocarbon occurrences, but it must be integrated with other tools for risk minimization in the petroleum exploration process.

4

1.2.2 The Nisku Formation as a Hydrogeological Unit

An aquifer has been traditionally defined in the context of groundwater use such as "...
a saturated permeable geologic unit that can transmit significant quantities of water under
ordinary hydraulic gradients ..." (Freeze and Cherry, 1979, p. 47). On the other hand, an
aquitard is a stratum that can transmit appreciable amounts of water significant at
geological time scale, but its permeability is not sufficient to allow the completion of a
well (Freeze and Cherry, 1979). On a human time scale, The Nisku Formation and its
lateral equivalents can take several forms as a hydrogeological unit due to the large scale
of this study. That is, it can be an aquifer, part of an aquifer, partly an aquifer, an
aquitard, or a host of more than one aquifer. The precise identification of those forms
with respect to human time scale is beyond the scope of this study, and the regional top
of the Nisku Formation will be considered as the upper aquitard in considering the lateral
migration of hydrocarbons, although upward flow of hydrocarbons through the upper
aquitard cannot be ruled out.

Choosing only the Nisku Formation to perform a petroleum hydrogeological analysis on
for this study, the first one of its type at this scale, does not necessarily imply that the
formation is hydraulically isolated from its encompassing sedimentary section. Given
sufficient time, groundwater flow will occur even in rocks with very low permeability,
and groundwater will ultimately reach a state of equilibrium (Tóth, 1995). According to
Tóth (1995, p. 4), "the recognition of regional hydraulic continuity is, therefore,
indispensable for the correct interpretation of numerous natural processes and
phenomena." The choice of a single formation for analysis here is just a simplification
analogous in objective to the traditional practice of selecting a rectangular area of a basin
and performing a hydrogeological evaluation of the entire sedimentary section in that
rectangle, and not including data from out of that area. Furthermore, the Nisku
Formation has been mapped and considered as an Aquifer by several authors including
Hannon (1984), Hugo (1985), Toop (1992), Paul (1994), Wilkinson (1995), Rostron et
al. (1997), Simpson (1999), Kirste (2000), Anfort (2001), Putnam (2001), and Michael
(2002). Also, studying a single formation's hydrogeology on a basinal scale may reveal
more varied hydrogeological factors that may influence a single formation according to
location within a basin and the flow-driving mechanism operating within that particular

location. Varied flow-driving mechanisms can result from different factors such as gravity, compression, compaction, dilation, thermal, and chemical (Tóth, 1995). Boundaries between the effects of those mechanisms is formed as a result of areal extent of propagation of energy originated by any of those mechanisms, which is a function of time and rock properties (Tóth and Miller, 1983). Thus, based on supporting local and regional studies highlighting the Nisku Formation and its lateral equivalents as an aquifer, those formations are combined here to represent an aquifer of basinal extent, called the Nisku Aquifer.

1.3 Theoretical Background

1.3.1 Groundwater Movement in the Subsurface

The main driving force affecting moving groundwater, either vertically or horizontally, is the fluid potential gradient, which can be represented by the hydraulic head gradient. Water will flow from high fluid potential to low fluid potential, assuming that no groundwater density variations exist in the aquifer. According to Hubbert (1940, 1953)

$$\Phi = gz + \frac{p}{\rho} = gh \qquad (1.1)$$

thus

$$h = z + \frac{p}{\rho g} \qquad (1.2)$$

where Φ is the fluid potential, h is the hydraulic head, z is the elevation of the point where the pressure measurement was made, p is the fluid pressure, ρ is the fluid density, and g is the acceleration due to gravity. In equation 1.2, z represents elevation head and $\frac{p}{\rho g}$ represents pressure head.

6

1.3.2 Detection of Lateral Movement of Groundwater

Traditionally, maps of potentiometric surface are used to detect flow direction in deep saline aquifers, and flow is assumed to be normal to equipotential lines. A potentiometric surface is defined as an imaginary surface, commonly expressed as a contour map of freshwater hydraulic head, representing lateral distribution of energy contained by a unit mass of fluid in a confined aquifer. Freshwater hydraulic head represents a column of fresh water in equilibrium with pore pressure at the point of measurement (Tóth, 1978). Inferring groundwater flow directions to be normal to equipotential lines can be problematic in saline, dipping aquifers, as will be discussed in Section 1.3.4.

1.3.3 Detection of Vertical Movement of Groundwater

In the case of vertical groundwater flow, pressure-versus-depth (p(d)) plots can be used to detect vertical variations in fluid potential (Tóth 1978, 1980). Those vertical variations in fluid potential can cause upward or downward movement of groundwater, often crossing through aquitards, given that flow is observed over a sufficient time period (Tóth, 1995). Large-scale features in potentiometric surface maps that indicate diverging or converging flow can be attributed to sources or sinks, respectively. Sources in this case represents a source of energy, which can be attributed to either an introduction of energy into the aquifer from a source within or introduced into from a source outside the aquifer from above or below, the latter indicating cross-formational flow (The method of applying pressure-versus-depth plots to this study is discussed in Chapter 3). Sinks, on the other hand, represent locations where energy dissipates.

1.3.4 Effect of Groundwater Density Variations on Groundwater Flow

Traditionally, it has been the practice to assume groundwater flow direction to be normal to equipotential lines for the lateral movement of groundwater in deep saline aquifers, which can be problematic. Effects of variable density groundwater on regional scale flow systems have been addressed previously by Lusczynski (1961), DeWiest (1965), Davies (1987), Barson (1993), Bachu (1995b), and Bachu and Michael (2002). The main interest of these studies is how to adjust for errors introduced by using freshwater head to calculate hydraulic head gradients, where there exist significant density variations in

7

groundwater, especially in regional scale studies, that introduce a flow-driving mechanism termed here "negative buoyancy", acting downdip in the case of heavy brines.

In order to correct for the effect of negative buoyancy, Davies (1987) wrote Darcy's Law in the form:

$$q = -K[\nabla h_f + \frac{\Delta \rho}{\rho_f} \nabla E]$$ (1.3)

where q is groundwater flux, h_f is freshwater head calculated at a reference density ρ_f, E is elevation of the top (or bottom) of aquifer, $\Delta \rho$ is difference in density between the reference and the formation water densities, and K is hydraulic conductivity. The water driving force vector (WDFV) component of this equation is the quantity between brackets, and consists of a pressure-related driving force vector represented by the hydraulic head gradient, and a density-related driving force vector, represented by a product of elevation gradient vector and the ratio of the difference in density to the freshwater density (Figure 1.2). This assumes, according to Davies (1987), a confined, isotropic, gently sloping aquifer where the flow is parallel to the aquifer plane.

Davies (1987) introduced the driving force ratio (DFR), which is used as a measure of amount of error introduced by using freshwater heads to assess the direction of flow in groundwater of variable density. According to Davies:

$$DFR = \frac{\Delta \rho}{\rho_f} \frac{\nabla E}{\nabla h_f}$$ (1.4)

Areas where DFR exceeds 0.5 are considered areas of possible introduction of significant error, which needs to be corrected while analyzing groundwater flow magnitude and direction.
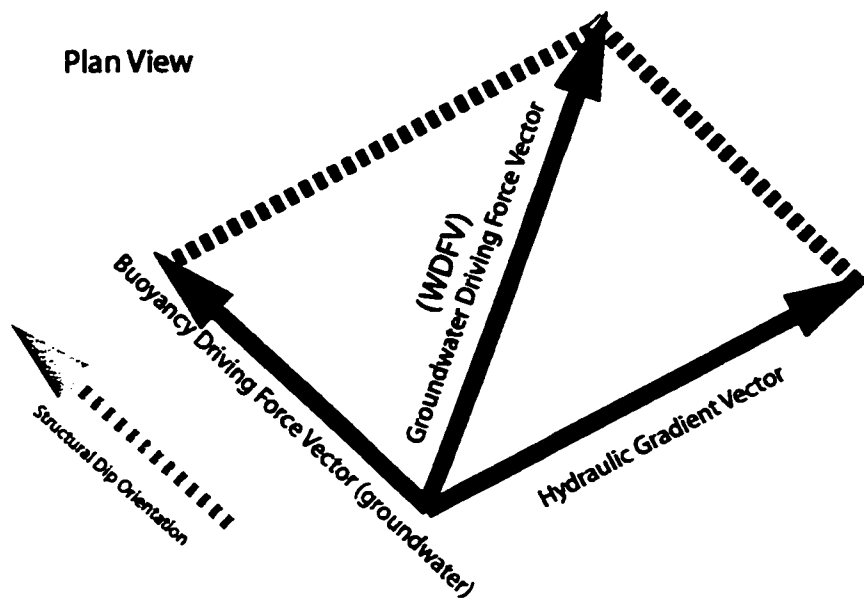
Plan View

Figure 1.2 Illustration of the components of the water driving force vector (Plan view).

Plan View
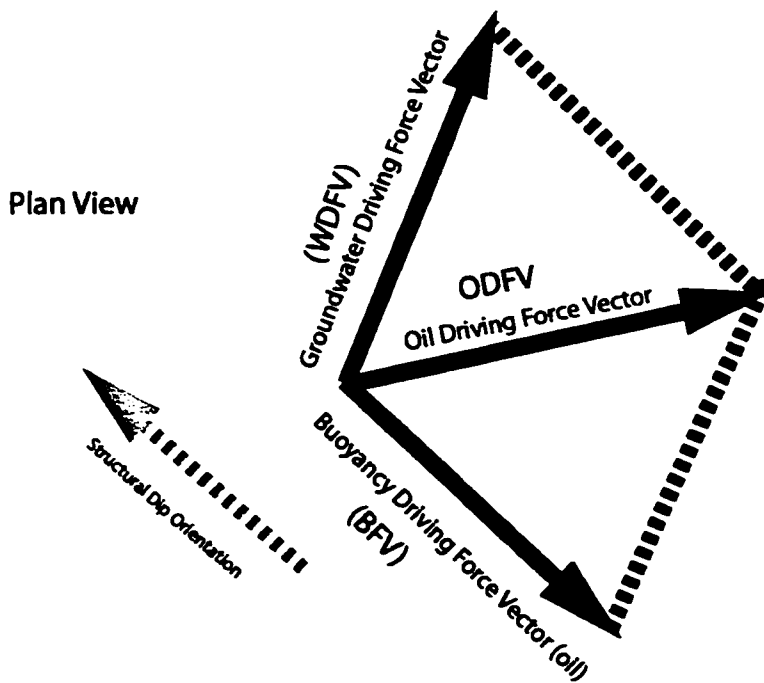
Figure 1.4 Illustration of the components of the oil driving force vector (ODFV).

9

1.4 Effects of Moving Groundwater on Hydrocarbons

Tóth (1980, p. 164) concluded that ". . . groundwater mobilizes, transports, and deposits hydrocarbons as it moves along its flow paths from regions of high energy to regions of low energy." According to the theory of regional groundwater flow system (Tóth, 1980), water descends at relative higher elevations of land surface, moves laterally, and ascends at areas of relative lows of land surface topography.

The movement of groundwater and its effect on hydrocarbon has been quantitatively investigated by Hubbert (1953). The "impelling force" for oil (Hubbert, 1953) can be mathematically expressed as (Figure 1.3):

$$F_o = g + \frac{\rho_w}{\rho_o}(F_w - g) \qquad\qquad (1.5)$$

where F_o is the force acting on a unit mass of oil, g is acceleration due to gravity, ρ_w is density of the water, ρ_o is density oil , and F_w is the impelling force for water, which represent the fluid potential gradient for water. Units of force as defined in equation 1.5 are in Pascal/m, and are given a different designation from those defined in Section 1.5. These forces as stated here reflect the original designations stated by Hubbert (1953) and should not be confused with forces defined in sections 1.3.4 and 1.5. Forces defined in sections 1.3.4 and 1.5 are used for modeling groundwater and hydrocarbon driving forces in an aquifer throughout this work, based on the work of Hubbert but modified for the condition of oil flow in a carrier bed and transformed into a dimensionless quantity (expressed in m/km in this work). For the practical modeling of hydrocarbon driving forces in an aquifer, equation 1.5 is combined with Darcy's law in order to arrive at the definition of the dimensionless forces used throughout this study. The detailed mathematical combination is not included here, and the reader is referred to Verweij (1993, Chapter 4) and references therein for a detailed treatment of the combination. In the case of hydrocarbons moving laterally in an aquifer, the capillary forces are also into account in order to determine the flow direction and entrapment as suggested by several
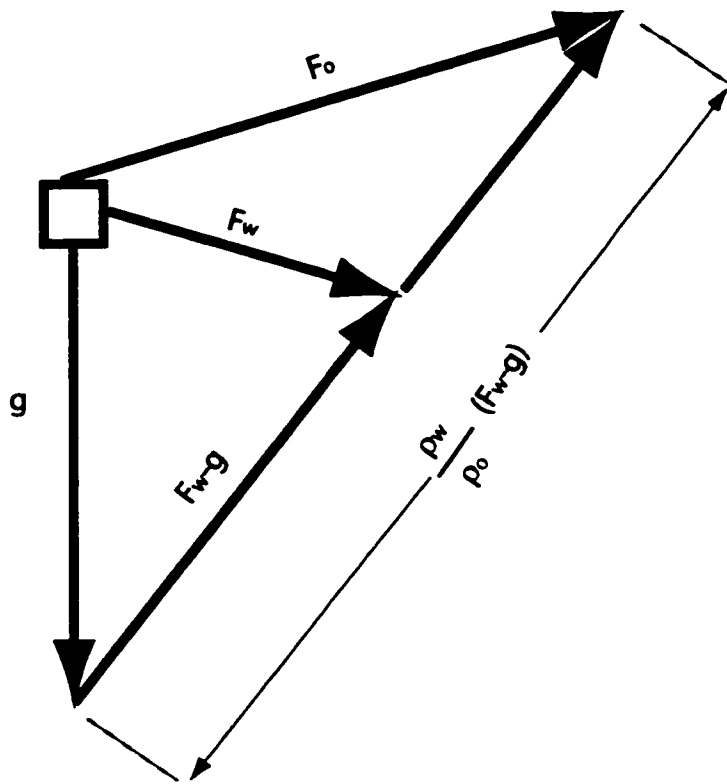
Figure 1.3 Forces acting on an element of oil in hydrodynamic environment (Modified after Hubbert, 1953).

workers (Hubbert, 1953; Schowalter, 1979; Davis, 1987; Bethke, 1991). Section 1.5 describes the formulation used in this study to quantify lateral driving forces for hydrocarbons.

1.5 Buoyancy Driving Force (BDFV) and Oil Driving Force (ODFV)

In order to perform a complete quantitative analysis of forces acting on oil in the subsurface, three force vectors have to be analyzed. Those are WDFV, buoyancy driving force vector (BDFV), and capillary forces. Trapping of hydrocarbon occurs when the net effect of these three forces is equal to zero (Davis, 1987). It is not feasible to quantify the lateral capillary forces on the scale used in this study. The only capillary barrier to oil flow assumed here is at the top of the Nisku Aquifer. Thus, with the available geological structure, pressure, temperature, and water density data, it is feasible to quantify both the WDFV and the BDFV. The WDFV has been discussed earlier; practical formulation of the BDFV is needed here. The mathematical formulation of the BDFV has been discussed by Davis (1987), England et al. (1987), Bethke et al. (1991), Barson (1993), Rostron (1993), and Verweij (1993).

For the BDFVs for hydrocarbons, one can arrive at a term that is of similar, dimensionless quantity of the WDFV expressed in m/km. If we have a fluid of density ρ_o that is lighter than freshwater (oil for example), the buoyancy force vector arrived at by Davies (1987) can be used to represent the ODFV. Following the derivation illustrated by Barson (1993), we can combine the WDFV with the BDFV to have:

$$q = -\frac{k}{\mu}\rho_f g[\nabla h_f + \frac{\Delta\rho}{\rho_f}\nabla E] + \frac{k}{\mu}[g(\rho - \rho_o)\nabla E] * \frac{\rho_f}{\rho_f} \qquad (1.6)$$

thus

$$q = -\frac{k\rho_f g}{\mu}[WDFV - \frac{(\rho - \rho_o)}{\rho_f}\nabla E] \qquad (1.7)$$

12

The second term between brackets is the BDFV for lighter hydrocarbon. It has to be noted here that in order to calculate the flow rate for hydrocarbon, one must use fluid properties of the hydrocarbon to calculate the term left of the brackets.

The quantity between the brackets in equation 1.7 is a vector quantity representing the oil driving force vector (ODFV). From above we have:

$$BDFV = -\nabla E \frac{(\rho - \rho_o)}{\rho_f} \tag{1.8}$$

where ∇E is dip of the aquifer. The buoyancy force for hydrocarbons acts in the direction of maximum updip, at any point in the flow field.

1.6 Tilted Oil-Water Contact

According to Hubbert (1953), groundwater movement can cause a tilt in the oil-water interface as illustrated in Figure 1.5. The first published mathematical description that demonstrates effects of moving groundwater on the tilt of the oil-water interface is by Hubbert (1953). Cases of tilted oil-water contact have been observed in West Texas (Adams, 1936), Arkansas (Goebel, 1950), Wyoming (Hubbert, 1953; Stone and Hoeger, 1973), and Algeria (Chiarelli, 1978) in addition to several other published examples. The following is the theoretical and mathematical foundation for tilted hydrocarbon-water contact. To calculate tilt, the following equation is used (Hubbert, 1953) (Figure 1.5):

$$\frac{\Delta Z}{\Delta X} = \frac{\rho}{\rho - \rho_o} \times \frac{\Delta h}{\Delta X} \tag{1.9}$$

where ρ is groundwater density, ρ_o is hydrocarbon density. In the case of equation 1.9, tilt is calculated considering that driving force for water is caused only by the hydraulic gradient. However, in the case of a sloping aquifer with variable density, the water driving force is expanded to include the negative buoyancy in the force vector, and equation 1.9 becomes:

13
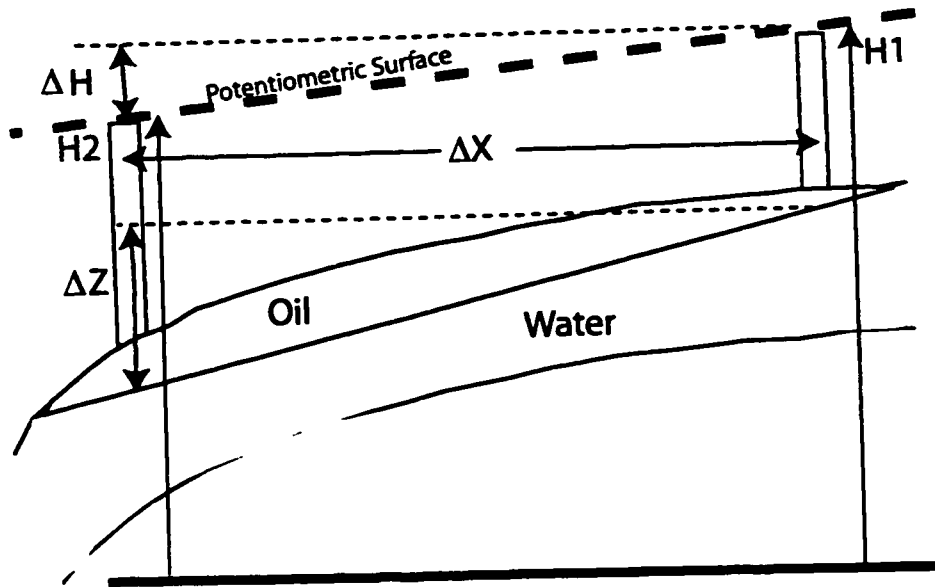
Figure 1.5 Schematic showing the configuration of a tilted oil water contact for freshwater. The quantities are used for equation (modified after Dahlberg, 1994).

$$\frac{\Delta Z}{\Delta X} = \frac{\rho}{\rho - \rho_o} \times WDFV \qquad (1.10)$$

1.7 Implication of Tilt Angle on Distance of Oil Migration

In cases where tilt in the oil-water interface exceeds the structural gradient of a potential structural trap, flushing can occur. It can be observed from equation 1.10 that the higher the density of the hydrocarbon (the lower the API gravity), the more the resulting tilt increases, and flushing of hydrocarbons from traps is more likely. This concept indicates that the relatively lower API will migrate farther downstream within an aquifer, if the water driving forces are sufficient to tilt the oil-water interface to an angle greater than the structural dips of the top of the aquifer.

1.8 Forms of Hydrocarbon Transport

Hydrocarbons can be transported as different phases depending on the thermodynamic state of the water environment at the time and space of migration. These forms can be as a molecular solution, as a micellar solution, or as a separate hydrocarbon phase (Verweij, 1993). In the case of molecular solution, Price (1976) found that the solubility of hydrocarbons in water increases significantly at a temperature of around 100 °C and .that the increase of solubility is very significant at a temperature of 150 °C.

The transport of hydrocarbons as a separate phase is controlled by buoyancy and hydrodynamic forces (Schowalter, 1979). Buoyancy forces are affected by the density of both oil and groundwater as can be inferred from equation 1.8. Both of these densities depend on pressure, temperature, and gas content. On the other hand, hydrodynamic forces depend on hydraulic gradients, groundwater density, and structural gradients as can be seen from the WDFV described in equation 1.3. The interplay between all of these factors dictates the movement of oil in the subsurface, as can be inferred from equation 1.7.

15

2.0 Study Area, Geology, and Hydrogeology

2.1 Study Area

The study area encompasses the extent of the Nisku Formation across the WCSB and portions of the Williston basin in the United States (data permitting). This includes Alberta, British Columbia, Saskatchewan, and Manitoba, and extends by two degrees in latitude into Montana and North Dakota of the United States as shown (Figure 2.1).

Geologically, the study area covers the Alberta and the Williston basins, and each of the two basins is characterized by its own evolution history, geology and hydrogeology. Understanding the regional geological and hydrogeological controls in the Nisku Aquifer requires a summarized description of geology and hydrogeology of both basins. Also, the general character of a basin and its genesis can give an insight on possible flow-driving mechanisms, their evolution, and their dissipation during the geological history. Basin evolution history is a key factor in analyzing the movement of fluids, which may dictate the flow regimes in the sedimentary succession of which the Nisku Formation is only a part a hydraulic continuum.

2.2 Geology

2.2.1 Generalized Geology of the Alberta Basin

The geology of Alberta basin has been widely studied, and the most comprehensive description of the basin is presented in the Geological Atlas of the Western Canada Sedimentary Basin (Mossop and Shetsen, 1994). The following description has been extracted from Bachu (1999). The Alberta basin is situated on a Precambrian platform and is bounded by the Rocky Mountain Trench in the west and southwest, the Bow Island Arch in the southeast, and the Canadian Shield to the northeast (Figure 2.2). During the geological period of Middle Cambrian to Middle Jurassic, the basin was in a passive margin stage leading to the formation of shallow water carbonates and evaporites with intervening shales. Starting with the Late Jurassic, an eastward movement of the sedimentary strata was caused by the Columbian and Laramide orogenies. As a result of
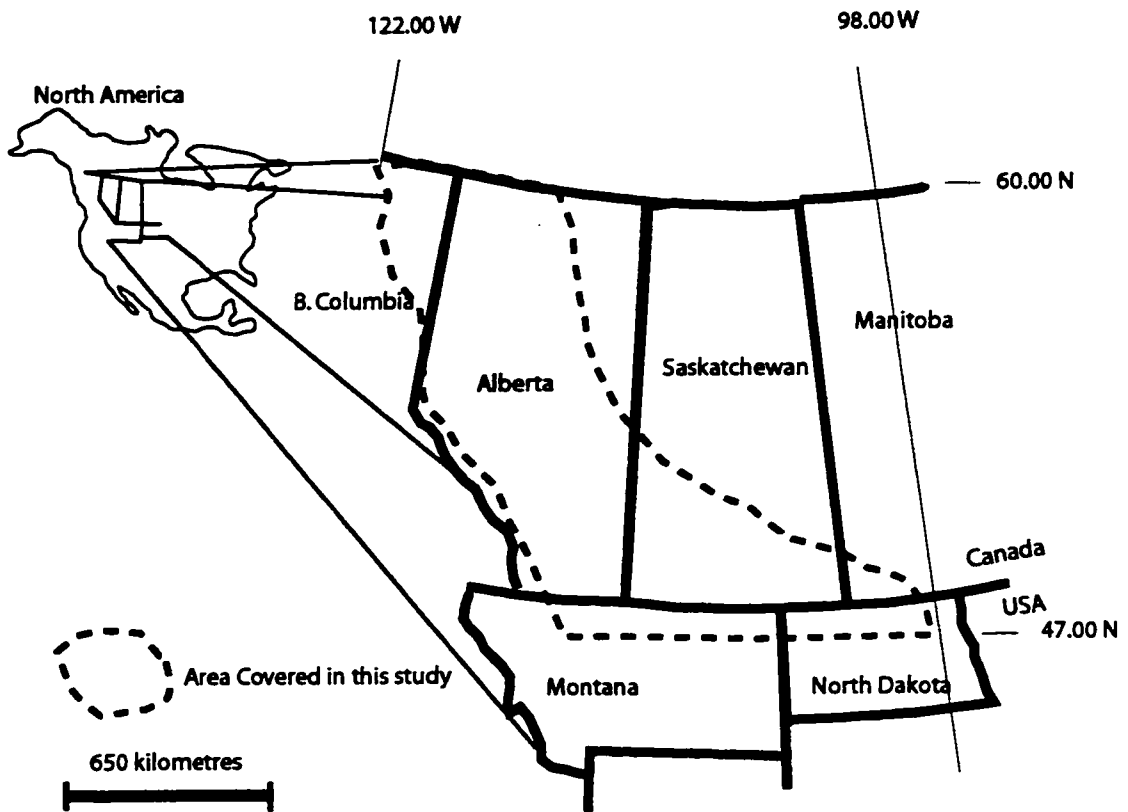
Figure 2.1 Location of the study Area
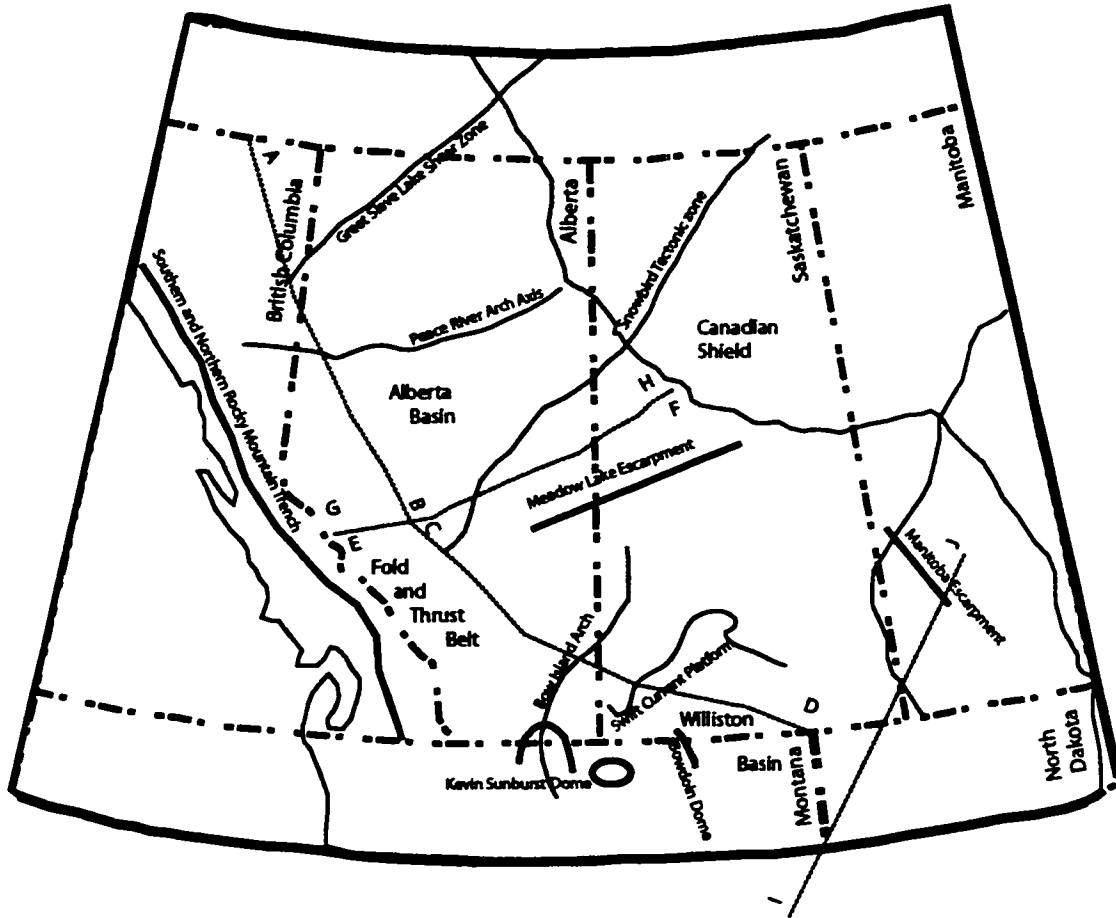
Figure 2.2 Map showing major structural features of the WCSB and Transects of
Cross-sections A-B, C-D, E-F, G-H, I-J (inferred) (basemap modified from
Mossop and Shetsen, 1994)

sediment loading and isostatic flexure, the basement tilted westward, whereby the slope of the strata is gentler in the east and steeper at the fold and thrust belt, the typical setting for a foreland basin, which lasts until present. The foreland sequence in the Alberta basin is primarily composed of siliciclastics beds with regionally extending aquitards. The basin was at its maximum thickness in the Paleocene. On the other hand, erosion, extending from Tertiary to Recent, is estimated at 2000 to 3800 m in the southwest (Nukowski, 1984; Bustin, 1991), and about 1000 m in the north (Kalkreuth and McMechan, 1988). The resulting configuration of the basin as a result of this sequence of deposition and erosion is a wedge-shaped sedimentary package (in a cross section view) that increases in thickness from 0 m at the Canadian Shield to 6000 m at the fold and thrust belt (Figures 2.2 and 2.3).

2.2.2 Generalized Geology of the Williston Basin

The Geology of the Williston basin has been widely studied including Gerhard et al., (1982), Crowley et al. (1985), and Peterson and MacCary, (1987). The following geological description of the Williston Basin has been extracted from Bachu and Hitchon (1996). The Williston Basin is an intracratonic sedimentary basin with relatively simple structure, which straddles the northwestern United States and western Canada. It spans over the northern Great Plains of the United States, and of the Prairie region in Canada. This includes parts of Montana, North Dakota, and the northern part of South Dakota, southwestern Manitoba, and the southern part of Saskatchewan. According to Ahern and Mrkvicka (1984), the Williston basin subsided as a result of a thickening process of the lithosphere that resulted from cooling, which initiated the depocenter in North Dakota. The basin is bordered in the southwest and west by a number of arches, to the north with the Canadian Shield, and to the east by Siouxia uplift and the Transcontinental arch. The Williston basin contains an almost continuous geological record from middle Cambrian to Tertiary age. The geological formations are, in simple description, composed of carbonates from the early Paleozoic to middle Paleozoic, and primarily siliciclastics in the late Paleozoic, Mesozoic, and Tertiary. The upper Devonian formations consist of a sequence of interbedded shallow-water carbonates, shaley carbonates, shales, or evaporites (Gerhard et al., 1982; Peterson and MacCary, 1987).

19
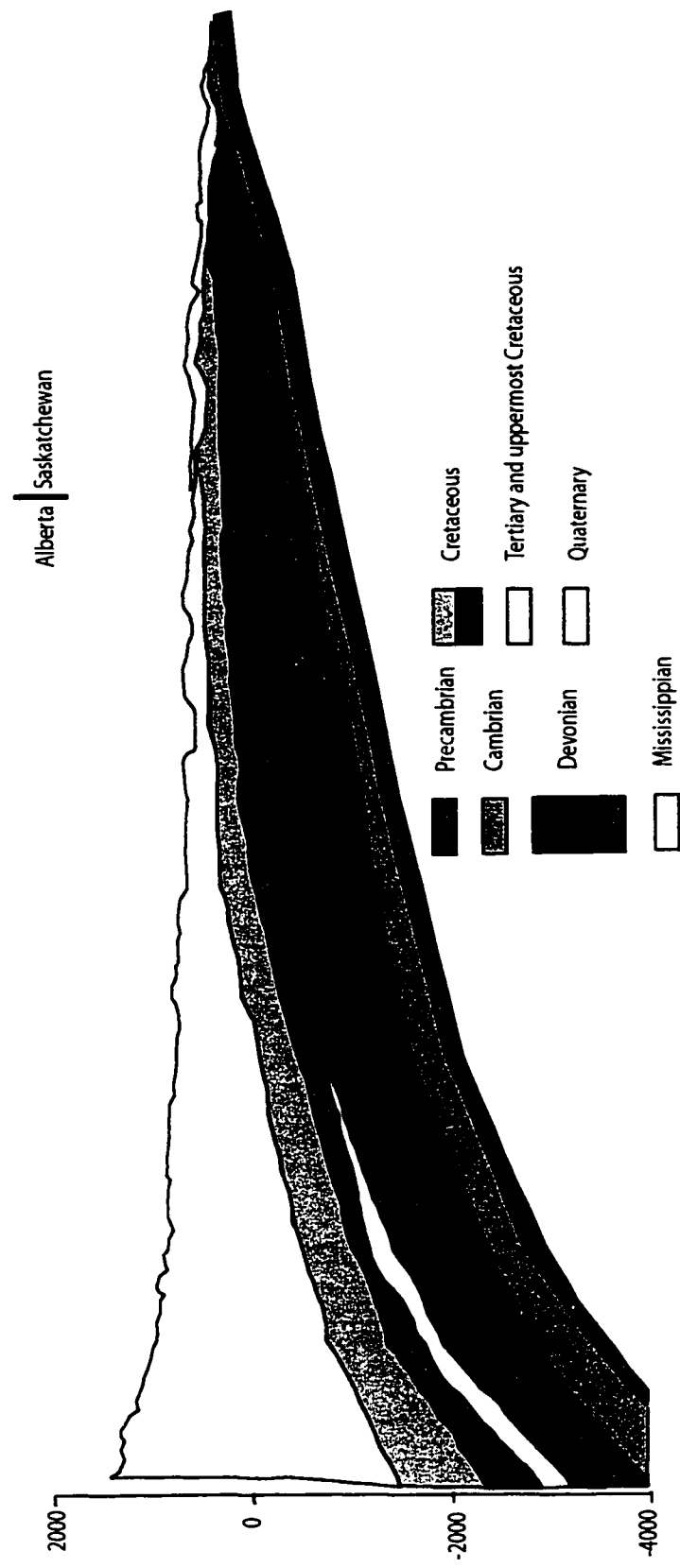
Figure 2.3 Generalized cross section of the Alberta basin (modified after Mossop and Shetsen, 1994; colors indicate reference's stratigraphic subdivisions; location is shown in Figure 2.2)

G

H

Alberta | Saskatchewan

2000

0

-2000

-4000

	Precambrian		Cretaceous
	Cambrian		Tertiary and uppermost Cretaceous
	Devonian		Quaternary
	Mississippian		

2.2.3 Geology of the Nisku Formation

The Nisku Formation and its lateral equivalents (Figure 1.1) belong to the Winterburn Group of the Upper Devonian (Switzer et al., 1994). The major features that distinguish the Winterburn group from the underlying depositional sequence are the deposition of extensive carbonate shelves and the development of isolated pinnacle reefs and reef trends. Those reef trends play an important role in the transport of hydrocarbons and in providing the reservoir rock for hydrocarbon accumulations.

In the Alberta basin, the Nisku Formation, depositionally, represents the oldest member of the Winterburn Group (Figure 1.1) and is underlain by the Ireton Formation (Figures 2.4, 2.5, and 2.6). Above the Nisku Formation is the Calmar Formation, which represents a general sea level rise coupled with increase of siliciclastic sediment influx. Much of the geological features observed in the Nisku Formation can be related to the isopach of the underlying Woodbend Group, which represents the paleotopography just prior to the time of the deposition of the Nisku Formation (Switzer et al., 1994). For example, the water depth dictated by the paleotopography preceding the deposition of the Nisku Formation and the sea level controls the formation of reefs in the Nisku Formation.

A structure contour map of the Nisku Formation is presented in Figure 2.7. The data for this figure has been collected from Switzer et al. (1994) and augmented with data from Montana and North Dakota (see Chapter 3 for details). Following the generalized wedge-shaped configuration of the Alberta basin, the Nisku Formation drops in elevation tens of m above present sea level near the eastern edge of the formation and dips to an elevation of 3500 m below sea level. The strike of the Nisku Formation is in a northwesterly trend over the entire basin. Contrary to its structure in the Alberta basin, the Nisku Formation in the Williston basin takes a semi-circular configuration, with its highest elevations near the Canadian Shield and at the divide between the Alberta and the Williston basins in the range of 250 to 0 m below sea level. Minimum elevation is attained at the center of the basin at 2750 m below sea level. The strike of the Nisku Formation structure takes a radial shape, increasing in elevation in a circular trend.

The regional isopach and lithofacies of the Nisku Formation has been presented by Switzer et al., (1994), from which the description given here is extracted. In southern

21

A

British Columbia | Alberta

Datum Base of Graminia Silt

b-97-A-94-0-3
a-58-E-94-I-5
a-97-G-94-H-14
a-3-K-94-H-8
10-13-94-13W6
15-2-90-9W6
7-8-87-6W6

Blue Ridge Member

Figure 2.4 Strtigraphic cross section thrcugh A-B showing the N
(modified after Switzer et al., 1994; location is shown i

sh Columbia | Alberta

Basement

Granite Wash

metres

0

kilometres

0   50

150

Shale   Mixec

Siliciclastics   Lime:

Dolomite   Siltst

Mixe
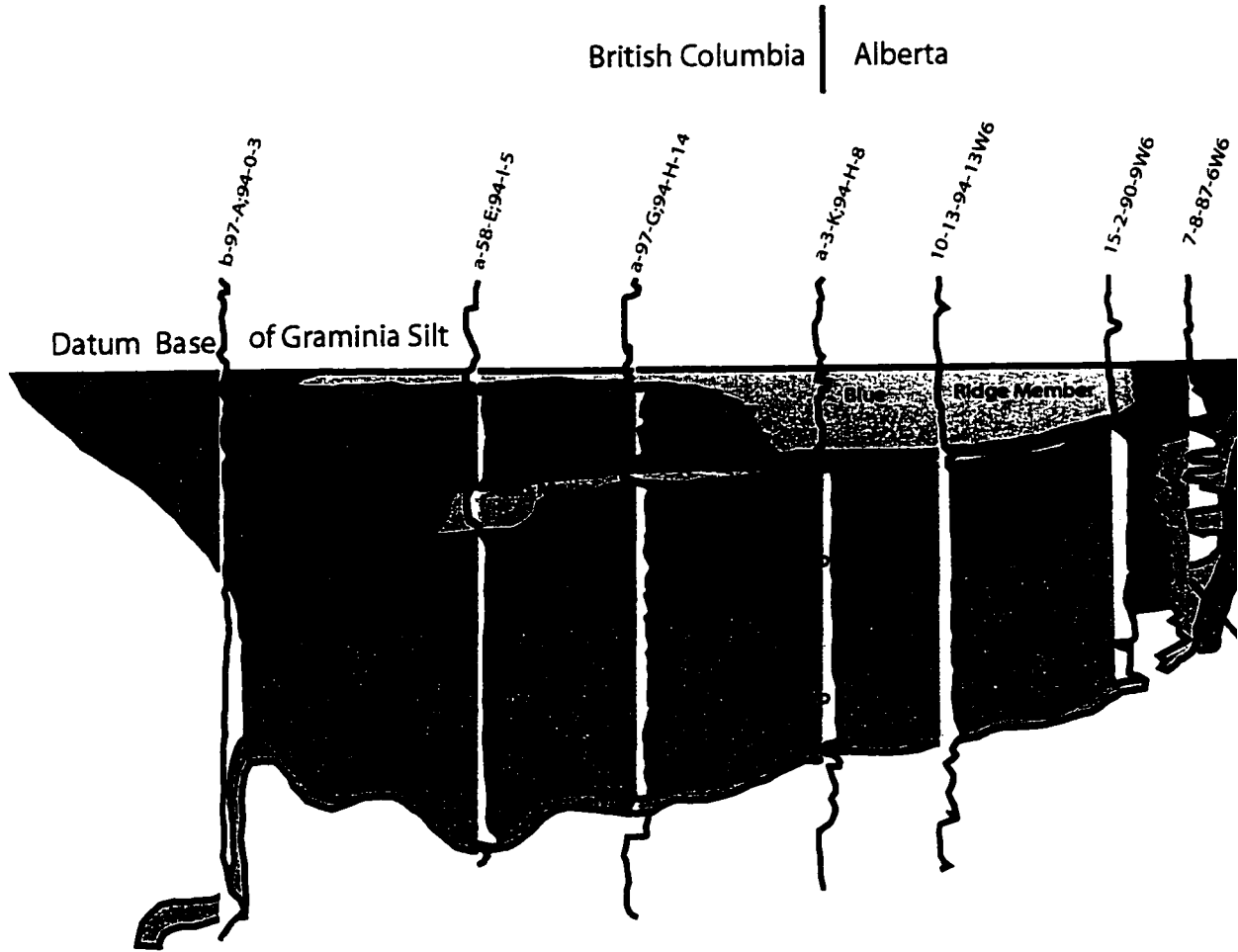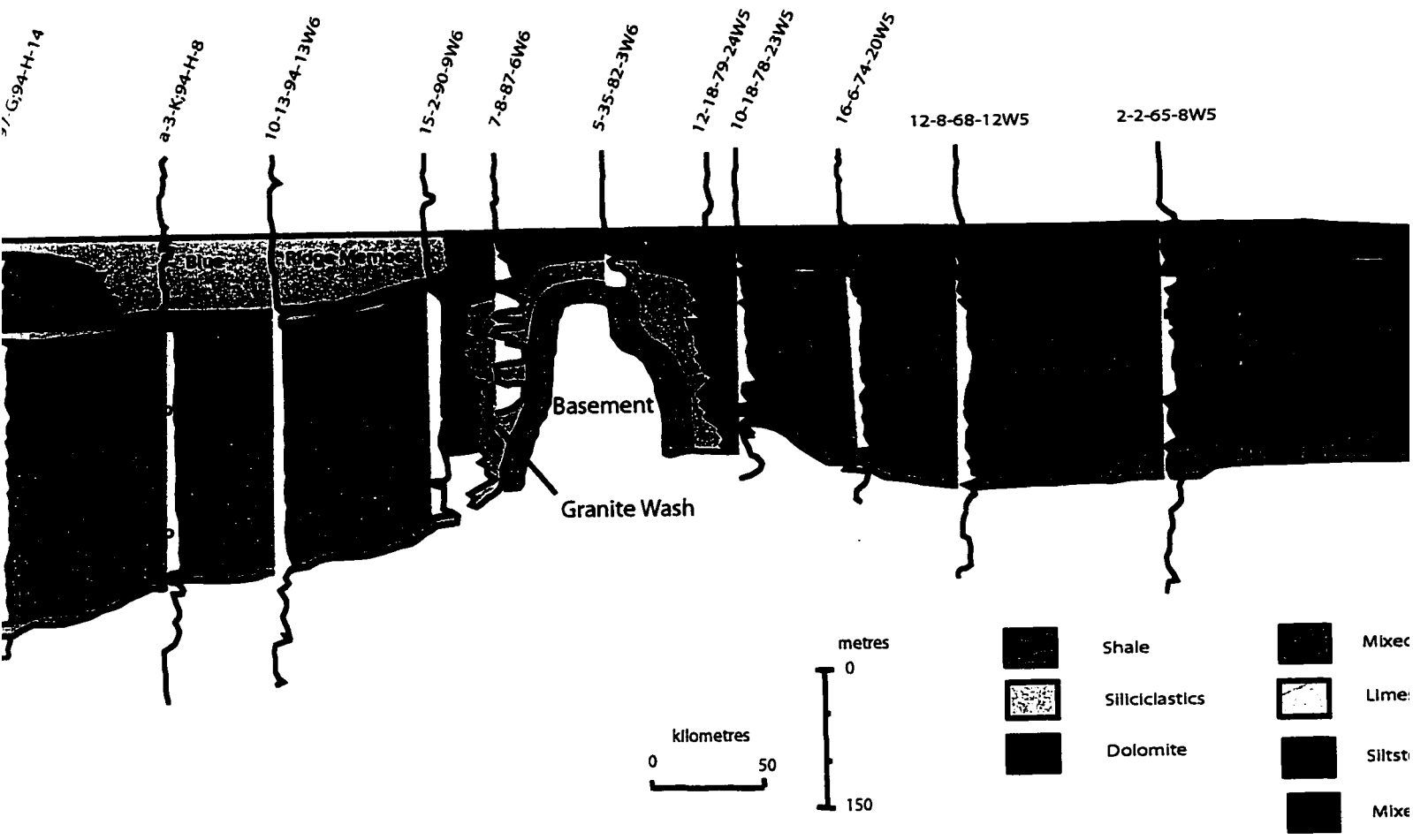
ss section through A-B showing the Nisku Formation and the related geological units
Switzer et al., 1994; location is shown in Figure 2.2).

22

B

Legend:
- Shale
- Siliciclastics
- Dolomite
- Mixed carbonates and clastics
- Limestone
- Siltstone/silty shale
- Mixed carbonates and evaporites

Wells: 7-8-87-6W6, 5-35-82-3W6, 12-18-79-24W5, 10-18-78-23W5, 16-6-74-20W5, 12-8-68-12W5, 2-2-65-8W5

Basement

Granite Wash

metres
0
150

kilometres
0   50

ie Nisku Formation and the related geological units
wn in Figure 2.2).

22

C

8-17-53-21W4
4-19-50-19W4
16-17-48-20-W4
8-28-43-12-W4
13-38-35-2W4
15-8-35-27-W3
16-36-36-26W3
16-10-34-22-W3

Alberta | Saskatchewan

10-15-42-11W-4

Torquay

Nisku (Birdbear)

Lower Cooking Lake

Figure 2.5 Stratigraphic cross section through B-C showing the Nisku Formation and the
(modified after Switzer et al., 1994; location is shown in Figure 2.2).

13-38-35-2W4 15-8-35-27-W3 16-36-36-26W3 16-10-34-22-W3 8-14-29-14W3 4-11-23-10W3 10-3-19-9W3 16-27-15-6W3 14-12-9-28W2 16-11-

Alberta | Saskatchewan

Torquay

Nisku (Birdbear)

metres

0

150

kilometres

0   50

	Shale		Mixed carbonate
	Siliciclastics		Limestone
	Dolomite		Siltstone/silty sl
	Mixed clastics and carbonates		Mixed carbona

ıugh B-C showing the Nisku Formation and the related geological units
994; location is shown in Figure 2.2).

23

D

8-14-29-14W3 4-11-23-10W3 10-3-19-9W3 16-27-15-6W3 14-12-9-28W2 16-11-6-25-W2 12-20-4-21-W2 16-36-1-18W2

metres
0

kilometres
0   50

150
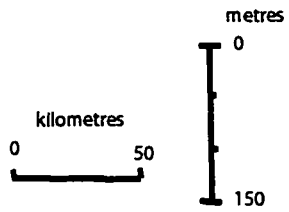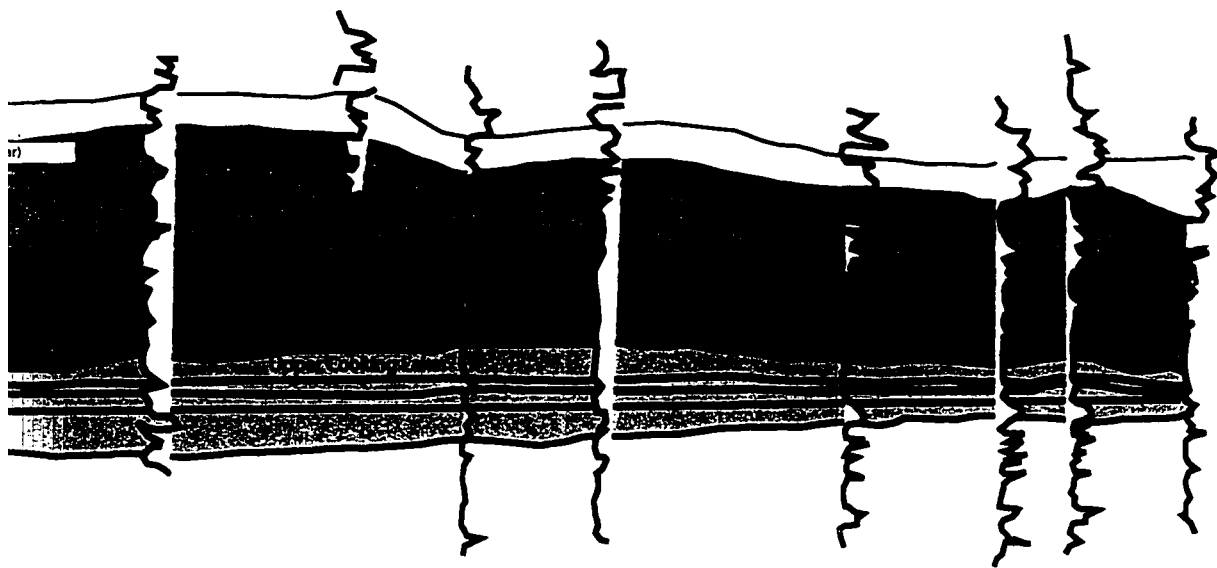
	Shale		Mixed carbonates and clastics
	Siliciclastics		Limestone
	Dolomite		Siltstone/silty shale
	Mixed clastics and carbonates		Mixed carbonates and evaporites

e related geological units

23
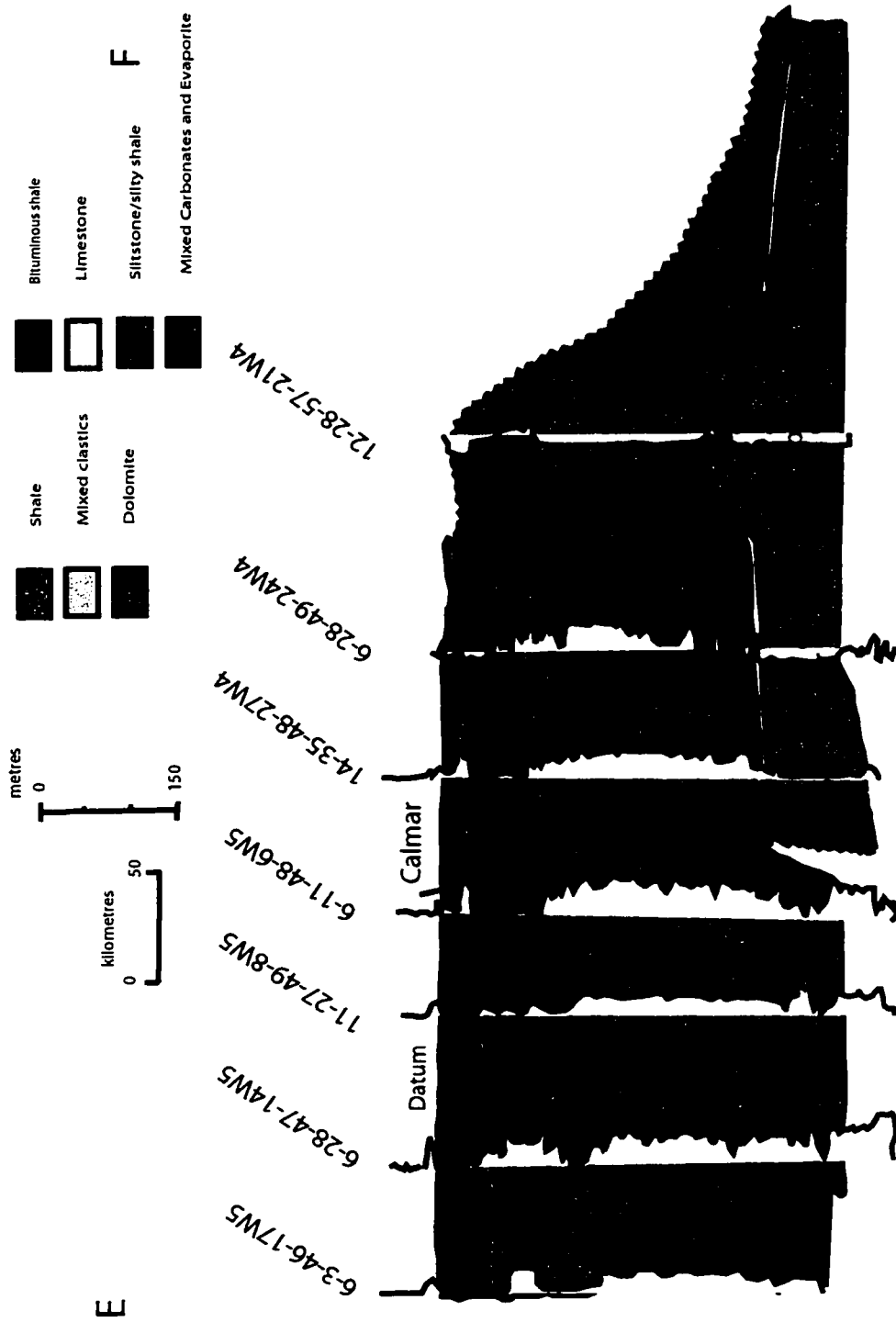
Figure 2.6 Stratigraphic cross section through E-F showing the Nisku Formation and the related geological units (modified after Switzer et al., 1994; location is shown in Figure 2.2)
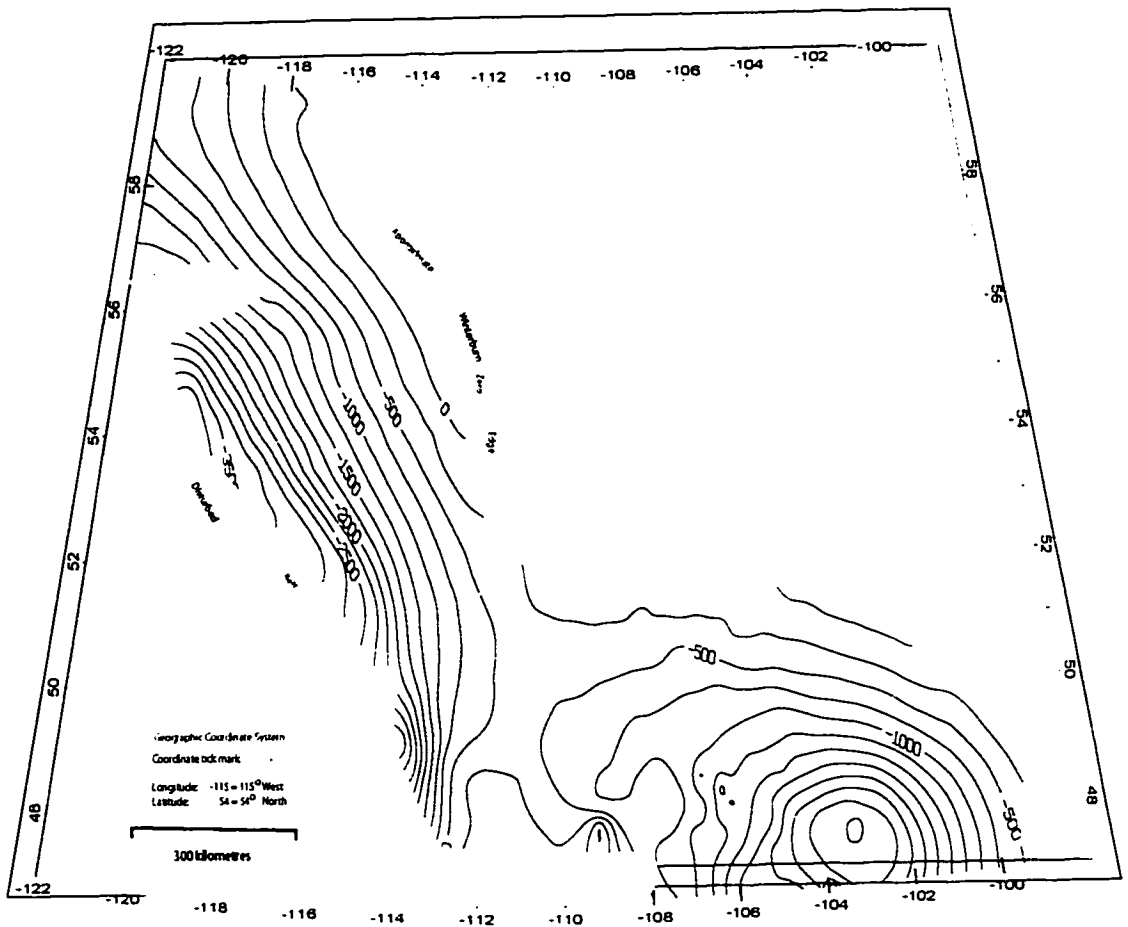
Figure 2.7 Structure contour map of the top of the Nisku Formation, WCSB (C. I. =250 metres).

Alberta, the Nisku Formation generally ranges in thickness from 10-30 m to about 50 m to the northwest of southern Alberta (Figure 2.8). It consists predominantly of dolostone and evaporites. In west-central Alberta, the Nisku Formation ranges in thickness between 60 to 100 m. The thickening coincides with the development of the reef buildups known as the Zeta Lake Member (Figure 2.6). In east-central Alberta, the Nisku Formation is characterized by an irregular surface. The Nisku Formation's interval thickness increases from about 20 m in the east to 60 m to the west and northwest. Areas of moderate thickening occur along some margins of the underlying Leduc Formation reefs. In northern Alberta, and along the Peace River axis, the Nisku Formation contains several large isolated carbonate banks that are often encased by sandstone and siltstone and supported by an extensive basal carbonate platform. North of the Peace River Arch, no lower Nisku Formation carbonates have developed. Even during the progradational stage, additional filling by shale was required before an upper Nisku Formation shelf could develop. This forming shelf complex is typically 15 to 20 m in thickness but can reach up to 100 m at the transition from shelf to basin.

A generalized, basin scale permeability distribution map can be associated with the lithofacies of the Nisku Formation (Figure 2.9). Those variations can usually be attributed to the paleogeography during the deposition of the formation or subsequent diagenetic processes. The Nisku Formation represents a shallow carbonate platform containing patch reefs and isolated reefs preferentially distributed throughout the WCSB (Switzer et al., 1994). Areas where the Nisku Formation reflects lithofacies of restricted depositional environment, where evaporites are dominant, are usually expected to have low reservoir quality. However, dissolution or fracturing of those rocks can create good reservoirs as a result of rock collapse features development. Areas of low energy depositional environment within the platform are also expected to have low permeability. On the other hand, reefs act as high permeability areas and hence, if continuous, act as conduits for flow.

The development and preservation of porosity and permeability can be associated with the effects of diagenesis, primarily, by dolomitization. The diagenesis of the Nisku Formation has been the focus of studies by several workers, among them are Machel (1986), Machel and Anderson (1989), and Whittaker and Mountjoy (1996) (Figure 2.10).
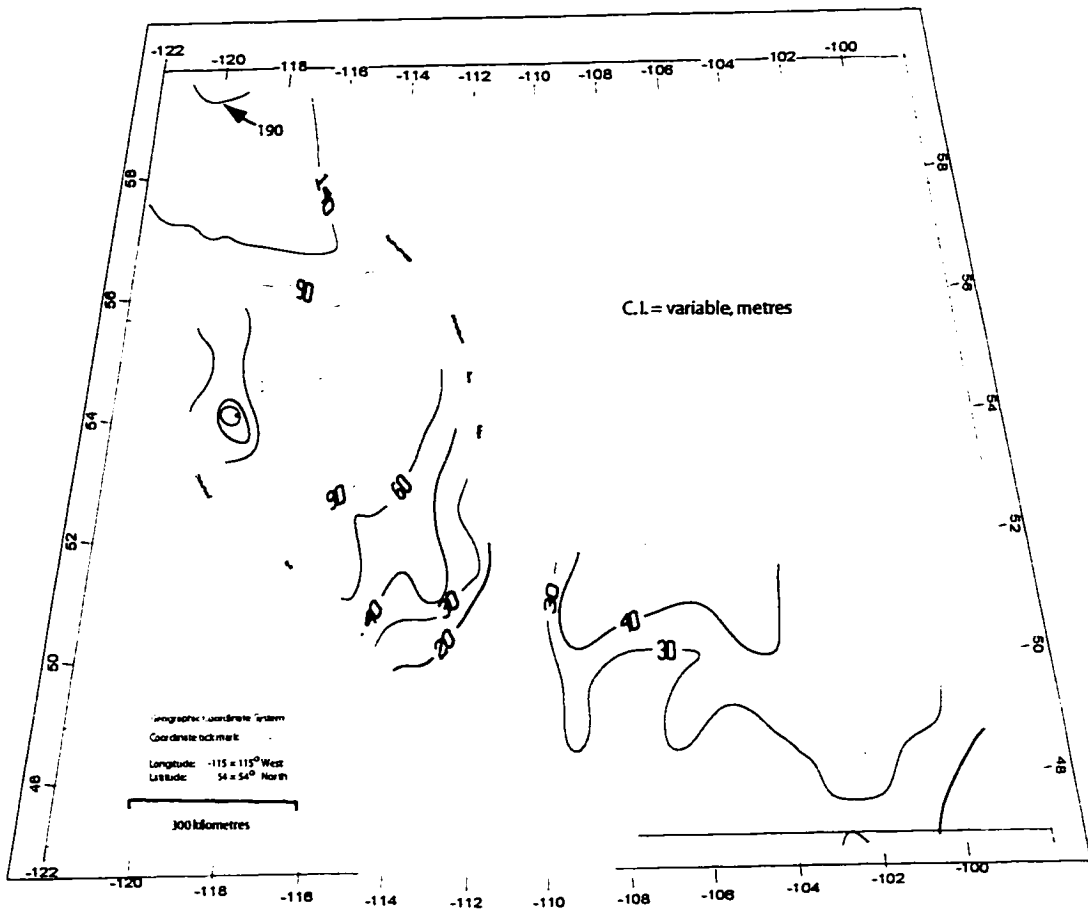
Figure 2.8 Regional isopach of the Nisku Formation, WCSB. (Compiled from Switzer et al. (1994), Halabura (1983), and NDIC digital data).
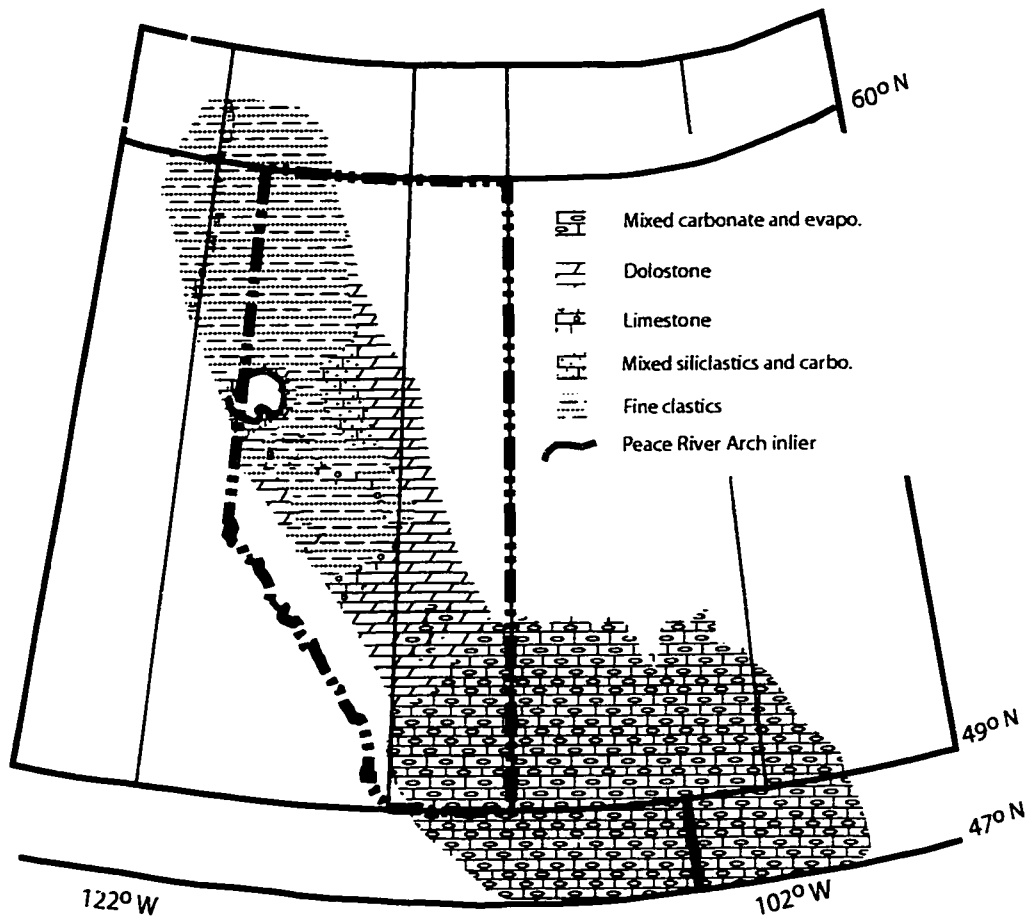
Figure 2.9 Generalized lithofacies map of the Nisku Formation
(modified after Switzer et al., 1994).
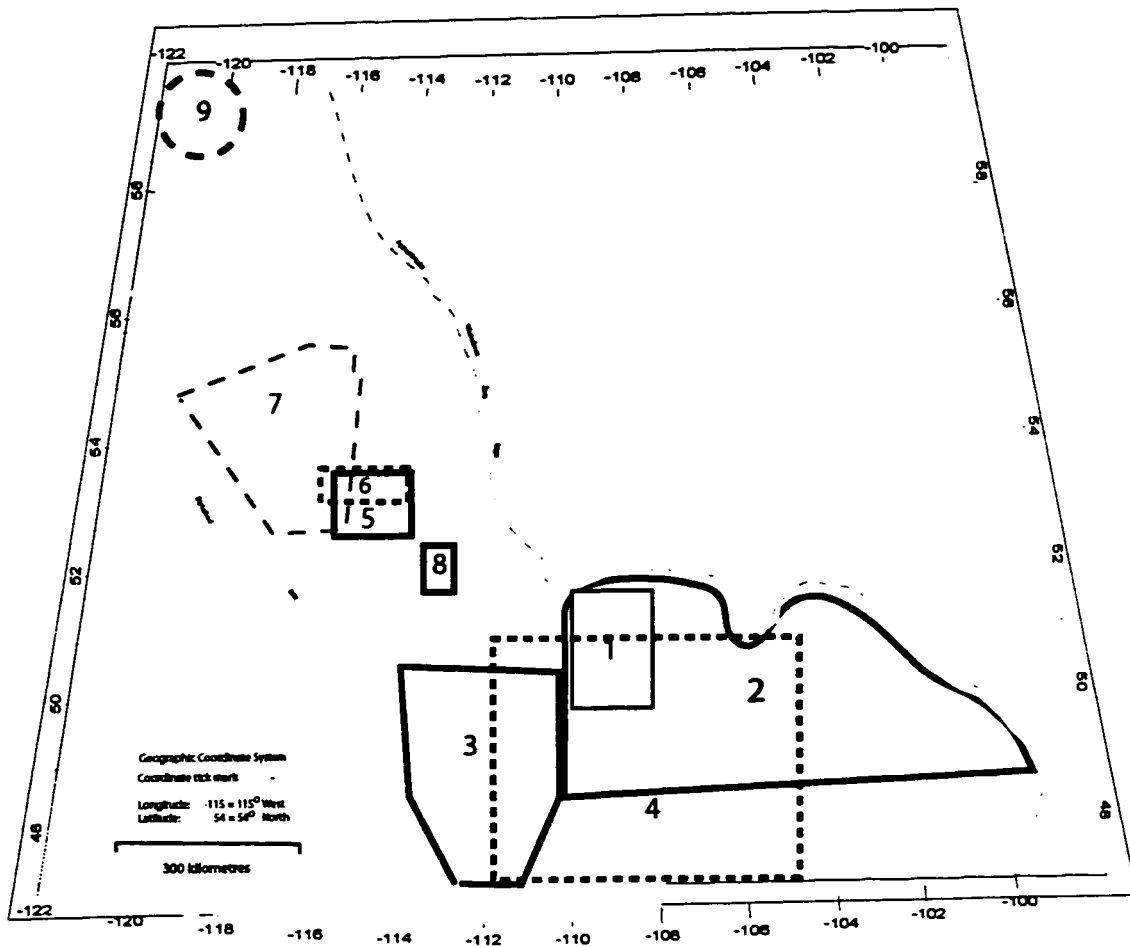
1- Cisyk (1991)
2- Halabura (1983)
3- Kissling (1997)
4- Whittaker and Mountjoy (1996)
5- Exploration Staff: Chevron Standard Limited (1979)
6- Machel (1986); Machel and Anderson (1989)
7- Skilliter (2000)
8- Hearn (1996)
9- Hudema (1991)

Figure 2.10 Location of selected geological studies in the Nisku Formation.

Machel and Anderson (1989) presented detailed studies of the diagenesis (dolomitization) of the Nisku Formation in central Alberta. Dolomitization is an essential process that can significantly enhance the porosity and permeability of the rock framework and aid in its preservation (Machel 1986, 1989). Machel and Anderson (1989) suggested two flow mechanisms that could have caused the dolomitization and gypsification/anhydritization. The first is that due to compaction driving chemically-altered seawater upward from deeper parts of the basin, and the second is that it is due to thermal convection of formation water from underlying or overlying formations.

Whittaker and Mountjoy (1996) studied the diagenesis of the Nisku Formation in southeastern Alberta and southwestern Saskatchewan utilizing isotopes. They concluded that the Nisku Formation consists of carbonates and evaporites that evolved in hypersaline conditions. karstification is a dominating feature marking the top of the Nisku Formation, which is overlain by thick, anhydritic units of the Stettler and Torquay formations.

Kissling (1997) studied the Nisku Formation reservoirs in southern Alberta and Northwest Montana plains. He studied 914 logs that penetrated the Nisku Formation, and extend from Great Falls of Montana to Calgary. Relating to this study are the descriptions of the structures of the reservoirs as well as the main structures controlling the geology of the region. In the area of Kevin-Sunburst Dome, thinning in both the Cambrian and the Devonian strata is evident, indicating that the area is a paleostructure. Two oil pools are located east of Kevin-Sunburst Dome, East Kevin and Nine Mile are developed in Nisku Formation tidal flats that are elevated, and leached shoals of peloid and packstone in a linear trend. Porosity is mainly inter-crystalline, and rarely fracture and vuggy. The reservoirs are both structural and stratigraphic. The API gravity of these pools is 37-39.

The Hays-Enchant pools were discovered in 1985, in reservoirs that vary from cross-bedded peloid-calcisilite grainstone to laminated mudstone (Kissling, 1997). The pools are trending along crests of ridges in a northwest, southeast-orientation. The trapping is associated with the dissolution of halite, which is at least 25 m in thickness, and the dissolution is associated with similarly trending basement faults. The API of these pools is reportedly between 27-30 (Kissling, 1997).

Chevron Exploration Staff (1978) reported a detailed study of the geology of the Western Pembina area, which is a host of some of the largest Nisku Formation hydrocarbon accumulations in the Alberta basin. In a trend of southwest-northeast, in a northwestern direction, the Nisku Formation shelf extends until it undergoes a drastic change in thickness, which forms the barrier reef (see Figure 2.10 for study area location). This is followed westward by the Nisku Formation outer shelf which extends until it terminates in a northeast-southwest trending shelf front. Basal carbonate dominates the lithofacies northwest of the edge of the outershelf, which later constitutes the platform on which the reefs of Western Pembina grow. The reefal member of the Nisku Formation is named the Zeta Lake Member, and is characterized by a uniform, low reading of gamma ray, which demonstrates an efficient leaching process. In the study area of Western Pembina (Chevron Exploration Staff, 1979), the Zeta Lake member is entirely dolomitized, with abundant vuggy porosity, although later studies contradicted those findings (Machel, 1986; Machel and Anderson, 1989).

2.3 Hydrogeology

2.3.1 Regional Hydrogeology of the WCSB

Hitchon (1969 a, b) presented a basin-scale hydrogeological study of the WCSB, in which he examined the fluid flow and the effect of topography and geology on the regional flow system. Hitchon considered that flow in the WCSB is under a steady state condition (Hitchon utilized the regional flow models suggested by Tóth (1962, 1963) and Freeze and Witherspoon (1967) to analyze the flow in the basin). Hitchon (1969a) used "stabilized" formation pressure, and horizontally sliced the sedimentary section into intervals of 152 m (500 feet). He observed a correspondence between high hydraulic heads and high topographic elevations especially at the disturbed belt and Cypress Hills. He thus concluded that flow in the WCSB is controlled by topography and is at a steady state. Hitchon further concluded that there is a thick, low fluid potential zone that coincides with the upper Devonian and Carboniferous carbonates. This forms a drain to the Alberta Basin, which discharges at the Athabasca oil sands. In his second paper

(Hitchon, 1969b), Hitchon constructed potentiometric surface maps based on stratigraphy for 27 units from Cambrian to Upper Cretaceous.

Hitchon (1984) examined the relationship between geothermal gradients, hydrodynamics, and hydrocarbon. His primary conclusion states that there is a correlation between topography, hydrodynamic regime, and geothermal gradient in the Alberta basin. The correlation is such that areas of high topographic elevations have a low geothermal gradient due to recharge. Areas of medium topographic elevations exhibit intermediate geothermal gradient, and areas of low topographic elevations exhibit high geothermal gradient. High geothermal gradients at low elevation were interpreted to be a result of warm water discharging from deeper aquifers. Hitchon (1984) also noted that there is a link in many cases between the Upper Devonian hydrocarbon accumulations and hydrodynamic regime.

Tóth (1978) examined the flow system in the Red Earth region (Figure 2.12) and proposed that the flow from the Upper Devonian to surface is driven by present-day topography. However, below the Ireton Aquitard, Tóth (1978) concluded that groundwater flow is in transient state of adjustment to a paleotopographic configuration. Tóth and Corbet (1986) examined the flow system in the Taber area, which included the post-Devonian sedimentary succession. They identified three flow systems: mainly the post-Colorado succession driven by present day topography, the Colorado succession driven by rebound due to erosion, and the Carboniferous-Manville succession which was interpreted as a relict flow system driven by a paleotopographic configuration.

A Current model of flow in the Alberta basin has been presented by Bachu (1995, 1999) (Figure 2.11a). According to Bachu (1995, 1999), the flow system in the northern part of the Alberta basin is driven by present-day topography and is in equilibrium, recharging at the fold belt and discharging at the Great Slave Lake, at elevations of 200 m. The succession from the Winnipegosis to the upper Devonian aquifers interpreted as "open flow systems" that receive recharge at the fold belt and Bovie Lake fault, and discharge at the Great Slave Lake and the edge of the Pre-Cambrian Shield. Another large-scale flow system is where the succession from the Devonian to the Cretaceous aquifers crop out at higher elevations of Montana and flows towards the north, discharging at the Peace River. The aquifers spanning the Upper Devonian to the Jurassic are in hydraulic

32

contact at their subcrop due to the absence of the intervening aquitards. High permeability of the aquifers induces low, sub-hydrostatic pressures (Belitz and Bredehoeft, 1988).

Intermediate, topography-driven flow is present in the area spanning the Athabasca to Great Slave Lake, where relatively higher elevations in the Caribou, Birch, and Pelican mountains receive recharge and discharge is at the Athabasca low elevations. Local flow systems driven by topography are also present in areas such as Swan Hills, Cypress Hills, Pelican Mountains and Caribou Mountains, and discharge at their respective relative topographic lows.

Several flow systems have also been reported to be driven by erosional rebound. It is estimated that up to 3800 m of sedimentary package have been removed by erosion (Nurkowski, 1984; Bustin, 1991). In southern Alberta, regions of rebound have created underpressured zones in small and large scales. Those have been reported in the clastic Cretaceous succession (Tóth and Corbet, 1986; Corbet and Bethke, 1992; Parks and Tóth, 1993; Bachu and Undershultz, 1995, Anfort et al, 2001).

Tectonic compression is generated by lateral movement of the sedimentary succession, which generates pressure pulses during the mountain-building tectonics. Those pulses diffuse over geologic time scale, depending on the permeability and storage properties of the aquifer-aquitard system (Ge and Garvin, 1989, 1994). Bachu (1995 a) hypothesized that high hydraulic heads in the Paleozoic aquifers associated with the high salinity could be driven by compression. According to Bachu (1999) this hypothesis is supported by the isotopic signature of the water from those deeper formations, as being expelled from deeper parts from underneath the orogenic belts (Machel et al., 1996). However, this is questionable since Ge and Garven (1994) used numerical simulation and concluded that transient flow induced by such a mechanism would last for a relatively short time. A numerical simulation by Ge and Garven (1994) applied to the McConnell Thrust suggests that an average displacement of 100 m would induce a transient flow in the order of 10^5 m^3. A total of 9 x 10^7 m^3 of expelled groundwater may have resulted from a 30-km movement over a period of 9 million years in Late Cretaceous.

Cross-formational flow has been reported by Tóth (1978) in the Red Earth region, by Bachu and Underschultz (1993) in the Athabasca area Clearwater and Watt Mountain

aquitards. Rostron and Tóth (1997) and Anfort (2001) report it in the Calmar in the Upper Devonian aquifer system, and in the Ireton Aquitard (Rostron et al., 1997).

Connolly et al. (1990 a, b) discussed the origin and evolution of formation waters in the Alberta basin. Based on chemical composition, they classified formation waters into three types. Those are: 1) Waters from dominantly carbonate reservoirs, 2) waters from clastics, and 3) a group different from 1 and 2 in that it is dilute meteoric water from clastic reservoirs. They also used isotopes to investigate the groundwater regimes. According to Connolly et al. (1990 b), results of the investigation "cross-formational upward water migration, superimposed on lateral fluid flow, is required to explain the geochemistry and isotopic systematic in the brines from Devonian-Lower Cretaceous reservoirs.

Generally, in the Alberta basin, the total dissolved solids (TDS) of groundwater increases with depth. The salinity of the Upper Devonian in southern Alberta is lower than that in central and northern parts of the basin, as recharge water in Montana forms an advancing front of fresh water. Zones of mixing between meteoric waters and connate waters are present at the subcrop of the Devonian aquifers at the sub-Cretaceous unconformity (Bachu, 1995 a; Rostron and Tóth, 1997; Anfort et al., 2001).

2.3.2 Generalized Hydrogeology of the Williston Basin

The Williston basin is composed of a sequence of aquifers and aquitards and the flow is reportedly driven by land surface topography (Downey, 1982, 1984; Bredehoeft et al., 1983; Downey et al. 1987; Downey and Dinwiddie, 1988; Bachu and Hitchon,1996;) (Figure 2.11b). The aquifers of the Williston basin are exposed at topographically high land surface elevations in the west and southwest of Montana and South Dakota, where they are recharged by meteoric water and streams, and flow at slow rates towards the east and northeast part of the basin. The Devonian aquifer system sub-crops in Manitoba on the Canadian side.

Hannon (1987) mapped the potentiometric surface in the Canadian portion of the Williston basin. Hannon considered the effects of topography on pressure systems in aquifers to be invalid, contrary to the wealth of literature supporting the effect of topography on groundwater flow. However, Hannon (1987) concluded that flow in the

SW   Interior Plains   NE

Local-scale topography driven flow
Basin-scale S to N topography driven flow
Mixing zone
Flow driven by erosional rebound
Flow driven by past tectonic compression
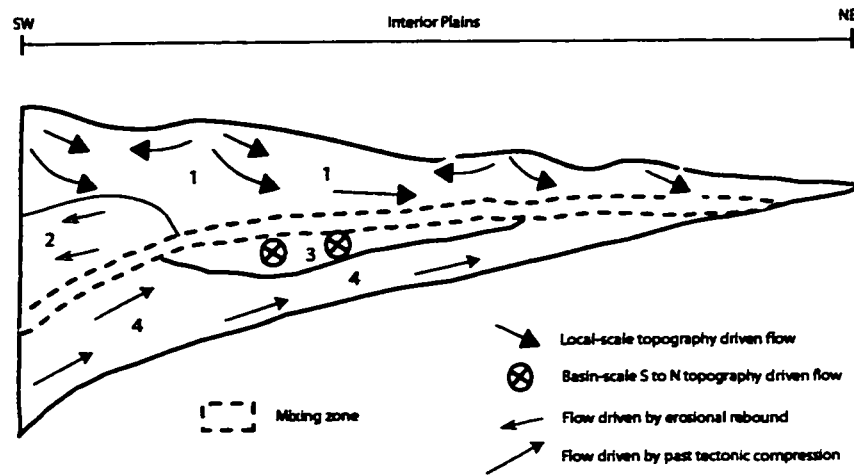
Figure 2.11a Generalized hydrogeological cross section of the Alberta basin showing major flow systems (modified after Bachu, 1999; and Michael, 2002)

Aquitard
Aquiclude
Aquifer
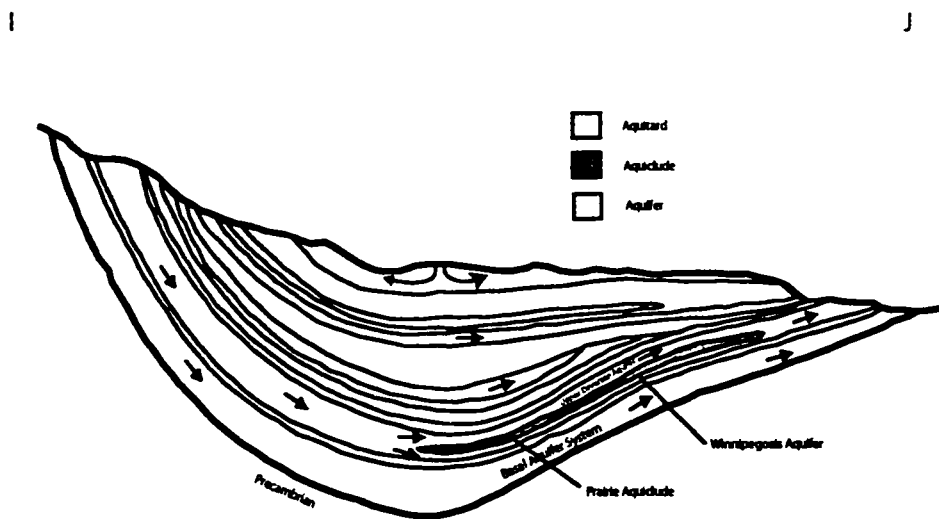
Figure 2.11b Generalized hydrogeological cross section of the Williston basin (modified after Bachu and Hitchon, 1996, based on Neuzil et al., 1982; Downey and Dinwiddie, 1988; and Bachu and Hitchon, 1996)

35

Canadian sector of the Williston basin is to the northeast, originating at higher elevations in South Dakota, central Montana, and discharge at low elevations outcrops on the Canadian Shield of Manitoba and Saskatchewan.

According to Bachu and Hitchon (1996), little cross-formational flow is known to exist and has been attributed to the existence of strong aquitards. However, this is in contradiction with previous models suggesting that most aquitards in the Williston basin are leaking due to fracturing (Downey and Dinwiddie, 1988). The presence of high TDS waters of the Paleozoic aquifers causes the freshwater to divert its flow direction around the high-density water (Bachu and Hitchon, 1996).

Benn and Rostron (1998) mapped the total dissolved solids, ions, and ionic ratios in the Williston basin for Cambrian to Devonian Strata. Based on the identified types of formation waters, they concluded that there are distinct hydraulic flow regimes and that water chemistry reflects a major role of hydrodynamics.

The primary causes for high salinity water in the Williston basin have been investigated by Iampen and Rostron (2000), who suggested the presence of high TDS water as a result of ancient evaporated sea water, in addition to halite dissolution.

2.3.3 Hydrogeological Studies of the Nisku Aquifer

Several hydrogeological studies have covered the Nisku Aquifer in portions of the WCSB (Figure 2.12). Hugo (1985) studied the hydrodynamics associated with the Leduc Reefs of the Rimbey-Meadowbrook trend area, in an attempt to identify the sources of energy that drive flow, in view of the observed flow system, and the existing geological patterns and possibly through the oil migration. Hugo concluded that the Ireton and Duvernay Formation shales underwent a compaction of 120 m during their burial. He also suggested that fluids expelled during the process of compaction flowed upward or downward, which then moved laterally and then moved vertically upward through the reefs into the overlying geological horizons or continued to flow in the underlying horizons towards the edge of the basin at the Canadian Shield. Hugo also concluded that the Rimbey-Meadowbrook reef trend acts as a high permeability lens, which collects flow in the upstream end and disperses it at the downstream end.

36
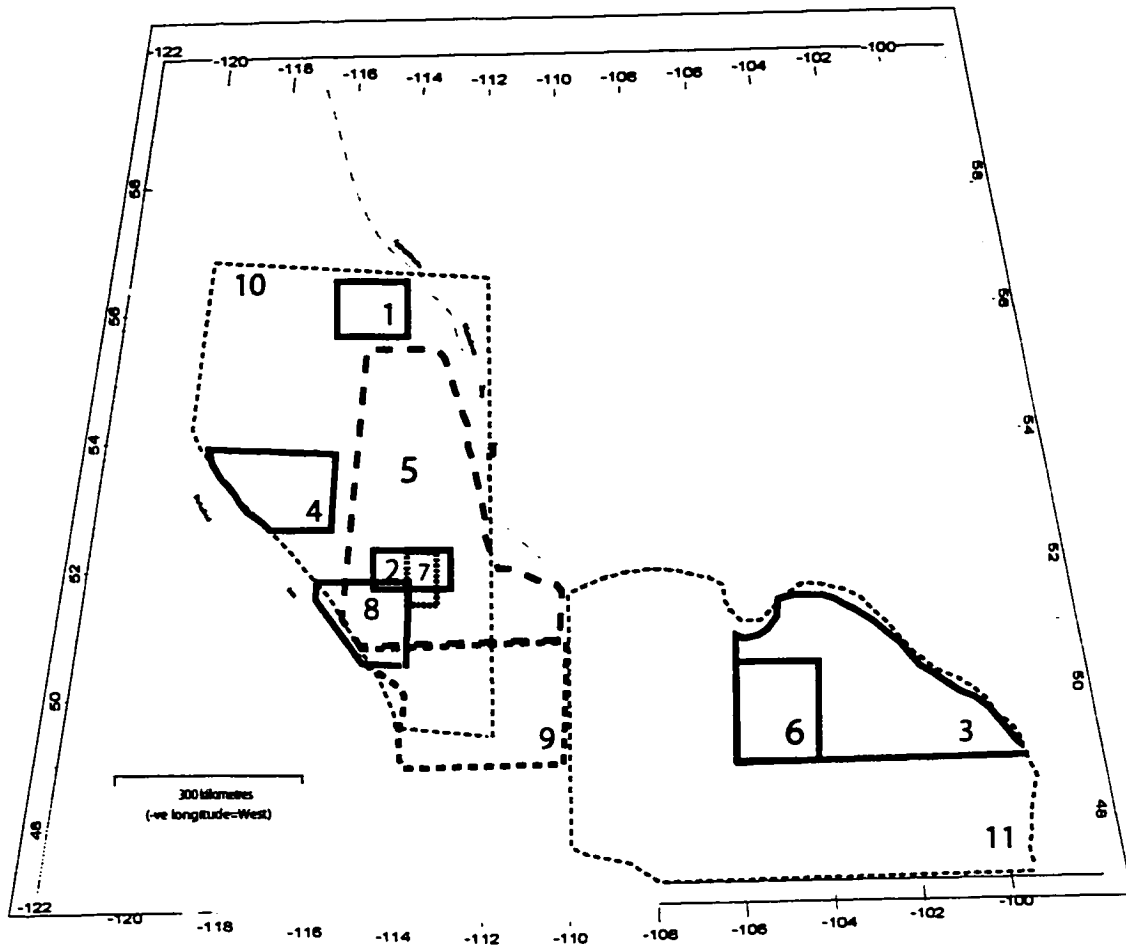
1- Tóth (1978)

2 - Rostron et al. (1997)

3- Hannon (1984)

4- Putnam and Ward (2001)

5- Anfort (2001)

6- Toop (1992)

7- Paul (1994)

8- Wilkinson (1995)

9- Kirste (2000)

10- Simpson (1999)

11- Benn and Rostron (1988)

Figure 2.12 Selected Hydrogeological studies related to the Nisku Aquifer.

37

Hannon (1987) studied groundwater flow in the Canadian section of the Williston Basin, and concluded that flow in all aquifers is mainly northward towards the discharge zones in areas where aquifers subcrop by the Canadian Shield. According to Hannon (1987), the Nisku Formation does not outcrop on the Canadian Shield, but is overlain by younger formations in the subcrop areas to the northeast of the Williston Basin. Values of equipotential lines decline from highs of 760 m to the south and southwest of the study area (Figure 2.7) to 305 m at the northern and northeastern edge of the Nisku Aquifer. In his interpretation of the potentiometric surface map with regard to hydrocarbon accumulations, Hannon (1987) ruled out the existence of large-scale barriers to flow in the Nisku Aquifer, which are thought to cause trapping of hydrocarbons.

Rostron (1995), Rostron et al. (1997) examined the possibility of cross-formational flow in west central Alberta. The study involved mapping of the potentiometric surface in an area covering from 52.05° to 52.93° north latitude and 115.45° to 112.9° west longitude for both the Cooking Lake-Leduc Aquifer and the Nisku Aquifer. Rostron et al. observed a decrease in the potentiometric surface of the Cooking Lake-Leduc Aquifer associated with an increase in the potentiometric surface of the Nisku Aquifer accompanied with flow that is radiating outward. A pressure depth plot in the Leduc Aquifer illustrated that the slope in the pressure depth line is greater than the nominal pressure gradient in the two aquifers indicating ascending flow. Those findings were further substantiated by the increased total dissolved solids in the area of suspected cross-formational flow, which indicated upward brine migration into the Nisku Aquifer. The study outlined the isopach of the Ireton Aquitard using some wells and showed that the breach of the aquitard is the main control in the intensity of cross-formational flow.

Hearn (1996) conducted an evaluation of the Ireton Aquitard in the Bashaw reef complex in order to determine locations of possible breaching and relate it to hydrocarbon migration and entrapment in the reef trend. Hearn concluded that the Ireton Aquitard ranges in thickness from 25 m to 1 m at the Bashaw reef complex, with the latter case likely to have been deposited on paleotopographic highs. Moreover, the Ireton Aquitard contained 30 percent more carbonate content over those paleotopographic highs. He further suggests that in areas where the draping of the Ireton Aquitard is less than 10 m, upward migration of hydrocarbons from the Leduc Aquifer to the Nisku Aquifer can be

expected. Hearn also concluded that the breaching could occur due to either thinning of the Ireton Aquitard or a lithofacies change in the aquitard, i.e., the more dolomitized the shale, the more likely the aquitard will be breached.

Physical evidence of upward hydrocarbon migration throughout the Bashaw reef complex was demonstrated by Hearn and Rostron (1997). The evidence was represented by the presence of oil/bitumen stain in the core of the Ireton Aquitard. Also, Rock-Eval analyses were used to rule out the Ireton Formation as the source of such hydrocarbons in the aquitard. Out of the 45 cores that were examined, eight wells showed evidence of oil leakage; this is in addition to the 28 wells identified by Rostron (1995) where the aquitard is absent. Breaching of the aquitard could have occurred where the thickness is up to 10 m. Migration through the aquitard occurred through inter-crystalline pores and often by the presence of fracture porosity. Hearn and Rostron (1997) also presented the controls on trapping, and those included dolomitization, which enhanced the permeability of the rock, and fractures in the aquitard, which can be attributed to reduced clay content.

Anfort et al., (2001) studied the regional hydrogeology of the Lower Cretaceous to middle Devonian aquifers in southeastern Alberta, in the area falling between 51.5° to 56° north latitude and 110° to 115° west longitude (Figure 2.11). In their study of the Nisku Aquifer, Anfort et al. concluded that the main flow system is northward, with the meteoric recharge originating from south of 51.5° north latitude. The study also suggested strong updip flow that directs flow towards the areas of low fluid potential existing in the northern end of the study area. They also observed that the TDS ranges between 200 g/l in the deeper parts of the aquifer to 20 g/l in the northeast and southeast. Other studies of relevance to the Nisku Aquifer shown in Figure 2.12 have contributed to its characterization and will be discussed as needed in the syntheses (Chapter 5).

2.4 Petroleum Geochemistry

Several studies addressed the question of potential source rock for the Nisku Formation, ranging from small pool-size studies, to large-scale studies that attempt to classify the Nisku Formation as having a single petroleum system.

Allen and Creany (1991) established the oil families and the hydrocarbon migration system in the WCSB. They described a number of petroleum systems in the basin, and among them is the Beaverhill Lake and Woodbend Group (Late Devonian). Based on the work of Stoakes and Creaney, they identified the Duvernay Formation as being the source rock that is equivalent to the Leduc reefs, and extends over a relatively large area, which includes areas of the Leduc reef trends. The mature part of this formation is in the west. In the area of the Bashaw reef complex, oil generated from the Duvernay Formation has migrated into the Leduc Pinnacles, and the leakage did occur to the Nisku Formation (based on geochemical evidence), which was trapped in Nisku Formation drape structures.

In the area of Western Pembina, it has been proposed by the Chevron Exploration Staff (1979) that the shales of the Cynthia Member of the Nisku Formation form the source rocks for oils in the pinnacle reef buildups. However, this proposal is not supported by laboratory analyses of the TOC of the Cynthia shale, which shows only 2 percent. Oils of Western Pembina show progressive increase in API gravity from northeast to southwest along the trend, which is believed to support the hypothesis that the oil is sourced from the Nisku Formation's basinal shale. Fowler et al. (2001) conducted a re-evaluation of the potential source rock in the West Pembina to resolve a controversy as to what the source is for the hydrocarbons within the Nisku Formation reservoirs in West Pembina. The study suggested that the Bigoray Member of the Nisku Formation could be a potential source rock for the oils in the area. However, it was suggested that the Duvernay Formation is the main source rock for the oils in West Pembina, but the sourcing from the Bigoray Member of the Nisku Formation oils cannot be ruled out. The study also suggested that the Cynthia Member is extremely unlikely to be a source rock in the area, due to its low content of TOC.

In the area of Stettler and Drumheller, Nisku Formation oils have pristane/phytane less than 1, indicating an evaporitic source, and may suggest that the Nisku Formation oils are sourced from the Nisku Formation evaporites (Fowler et al., 2001).

In the Area of southern Saskatchewan, it has been believed that the Nisku (Birdbear) Formation oils belong to oil Family D together with the Devonian Winnipegosis pinnacle reefs (Ostadetz et al., 1992). This was based on compositional analysis, mainly n-

alkane/acyclic isoprenoid and terpane, particularly C_{34} hopane prominence. A study by Obermajer et al., (1999) demonstrated that oil from the Nisku Formation could be differentiated from the Middle Devonian Winnipegosis oils using several biomarkers that have genetic indications of the oil analyzed. Those analyses included biomarkers such as, but not limited to, steranes, which showed to be different for the oils of the Nisku Formation. The study suggested a different petroleum system operating within the Nisku Formation in the Williston basin. Fowler et al. (2001) indicated the presence of excellent oil-generating potential in the Nisku (Birdbear) Formation. The lithology of the Middle to Upper Devonian in the Williston basin forms a succession of open marine carbonates and evaporitic sequences. Organic rich laminae are known to exist and are interpreted to reflect varying depositional environments, among which are organic rich laminae formed in mesosaline anoxic conditions resulting from lack of ocean circulation. Although those laminae are thin, they can constitute a significant amount of organic material and be an effective source rock.

Fowler et al. (2001) identified two new areas where source rocks within the Nisku Formation are present. The first area is in east central Alberta where, based on stratigraphic, sedimentological, and organic geochemical analyses, a significant source rock was identified within the Nisku Formation. The potential source rock is located in the area falling approximately between $51.2°$ to $52.7°$ north latitude and between $112.7°$ to $113.5°$ west longitude. Other potential source rocks were found in the evaporite succession of the Nisku Formation, which are not considered a significant source rock potential. The lower, more significant source rock is 1 to 7 m in thickness.

Fowler et al., (2001) reported Nisku Formation oil samples from Bashaw, Erskine, and Wood River fields that have very different geochemical character to that of the Duvernay Formation and similar to the significant potential source reported in this area within the Nisku Formation. Also, a sample from Milkman is reported to be likely a mixture of Duvernay and Nisku formations source rocks.

In Southern Alberta, Fowler et al. (2001) reported three significant potential source rock units within the Camrose Member/Nisku Formation. Potential source rock unit one is approximately 0.5 to 3.0 m in composite thickness and is present in the Camrose Member and directly overlays the Ireton Formation. This unit constitutes 10 to 50

percent of the source. Potential source rock unit two is at the top of the Camrose member and ranges in thickness from 1.0 to 2.3 m in composite thickness. Unit three is present in the middle of the Nisku Formation and restricted to southeast corner of Alberta. The composite thickness of this unit is from 3.0 to 4.0 m and constitute one third of the Nisku Formation in that area. Oils from the Enchant-Hays and the East Kevin oil fields appear to be sourced from the above source rocks in Southern Alberta.

3.0 Data Sources and Methods

3.1 Database

A comprehensive structured digital database was assimilated for this study, which included pressure, temperature, formation water chemistry, formation top, isopach, oil API gravity, and production data.

3.1.1 Pressure Data

A drill stem test (DST), which is a temporary completion of a well in order to measure reservoir parameters and find the types of fluid in a formation, is the only pressure data source used in this study. Geooffice database provided by the International Datashare Corporation and made available by the Department of Earth and Atmospheric Sciences of the University of Alberta, provided detailed pressure data for the Canadian side of the basin. The interface software for the database allows creating a customizable template, which formats the data to be acquired according to the user's design. A template was designed that provided as much data details about the test as needed for the data culling process. Geooffice database also provided a digitized form of DST charts.

Pressure data for Montana and North Dakota were obtained from data collected by previous students affiliated with the Hydrogeology Group at the University of Alberta, and are stored in digital format. Those raw data were originally obtained from industry and government agencies including the American Institute of Formation Evaluation and well files of the North Dakota Geological Survey.

3.1.2 Culling of Pressure Data

In order to eliminate the influence of production on the Nisku Aquifer pressure system, the method of Cumulative Interference Index (CII) proposed by Barson (1993), Rostron (1994), based on the Interference Index suggested by Tóth and Corbet (1986) was used.

This method is based on Theis equation to calculate the drawdown (s) in an aquifer in response to well pumping, where

$$s = \frac{Q}{4\pi T} W(u) \qquad (3.1)$$

and

$$u = \frac{r^2 S}{4Tt} \qquad (3.2)$$

Here, Q is the pumping rate, T is transmissivity, S is storage coefficient, t is time since pumping started, and r is the distance to the pumping well.

Drawdowns calculated from W(u) are

$$s \; \alpha \; \frac{4Tt}{r^2 S}$$

For a regional study, aquifer parameters such as S and T cannot be practically estimated. Also, and as seen from equation 3.2, the value of u can become dominated by values of t and r^2 as the time since start of pumping and distance to the pumping well increase. Thus the drawdown is essentially directly proportional to the time since the start of the pumping and inversely proportional to the square of distance to the pumping well. By the principle of superposition, the total drawdown at a point in the flow field is the sum of the drawdowns caused by the pumping at all the wells causing a drop in head at that point, at a certain time. From this concept, thus, the log of $\Sigma t/r^2$ is called the Cumulative Interference Index (Barson, 1993)[1] which gives an indication of the influence of any pumping at a certain point in the flow field. The resulting index is an indicator of how much a well has been influenced in terms of drawdown as a result of hydrocarbon

---

[1] The formula given in Barson (1993) is erroneous which is attributed to a typographical error.

production (or water injection) and serves as a criterion to describe how much the virgin pressure in the aquifer is disturbed at a well when the DST is carried out.

In order to apply the above method for culling pressure data in the Nisku Aquifer, a Visual Basic code[2] has been developed by the author that can be used in association with Microsoft Excel. The program takes geographic coordinates (which eliminates the necessity for coordinate conversions[3]) and facilitates the calculation of distances across UTM zones, a quality necessary for mapping at the scale of this study. In this program, the search radius, i.e. the radius in which points of production will be taken into account, can easily be specified by the user. The use of this program in association with Microsoft Excel eliminates the sometimes time consuming formatting effort associated with using other program codes and also expedites the process of exporting and importing, which is needed in intensive and repeated mapping associated with the culling procedure.

After calculating the CII for each DST, the study area was discretized into a set of smaller quadrangles that could be visually inspected by plotting. The size of these quadrangles depends on the areal density of the pressure data distribution; where the denser the data distribution, the smaller the quadrangle.

This process resulted in the discretization of the study area into 28 individual quadrangles. Freshwater head maps for those quadrangles were generated, and on each map, data point the CII and test quality code were posted. Several maps with a specified maximum CII are plotted, and improvement in response to this specified maximum CII in the generated map is observed. It was found that with a search radius of 20 km, tests having CII of −1.5 and less are not influenced by production in most cases. Once this is done, the maps are further refined by visual examination where data such as the tested interval, the quality of the test, formations tested, recovery, and type of recovery are posted, and certain restrictions are applied on these qualities. This is done in order to identify data of poor quality, which in turn are causing erroneous anomalies in the potentiometric surface. Due to the regional nature of this study, no specific rule was applied to these criteria when dealing with data culling, yet the completeness of the data

---

[2] For inquiries regarding this code, contact Dr. Benjamin Rostron, EAS Dept., University of Alberta (e-mail: ben.rostron@ualberta.ca)
[3] The raw data for this study are in geographic coordinates, or TRS converted to geographic coordinates.

was sought in areas of low-density data distributions, and more strict criteria were applied in areas of high-density data.

Further culling is performed using the method of nearest neighbor, where data that are obviously odd in an area of high-density data distribution are eliminated. Out of 4050 raw pressure data points (which were of quality D or better; see Table 3.1 for description of those quality codes), only 1750 (43 %) pressure data points survived this culling procedure. The resulting pressure data distribution is given in Figure 3.1.

3.1.3 Nisku Aquifer Test Verifications

In order to assign a DST to the Nisku Aquifer interval, the tested interval of the DST was verified to be within the aquifer or the aquifer and an adjacent aquitard. A grid of elevations of the Nisku Formation tops was generated, and then subtracted from a grid generated for the top of tested intervals in all the acquired Nisku Aquifer DST data. The difference between the two grids should give indication weather whether the tested interval falls within the Nisku Aquifer. Areas with an anomalously high difference between the test interval and the top of the formation show up as concentric circles on the map. These anomalies were further examined and resolved at smaller scale maps. For this step, the study area was discretized into 21 individual quadrangles, and tops of the Nisku Formation and the tops of the tested interval data points were numerically posted for each of those quadrangles at the locations of control points for a more detailed visual examination. Only a handful of tests were removed in this step. This is probably because the pick of the top of the Nisku Formation is obvious, both on the log, and probably the drilling rig's penetration rate, which is used to pick the formation top in the field (N. Hannon, 2001, personal communication).

3.1.4 Water Chemistry Data

Geofluids, a product of Rakhit Petroleum Consulting Ltd. provided the water analyses data for wells within the WCSB. Geofluids, which is available at the Department of Earth and Atmospheric Sciences of the University of Alberta, is a formation water
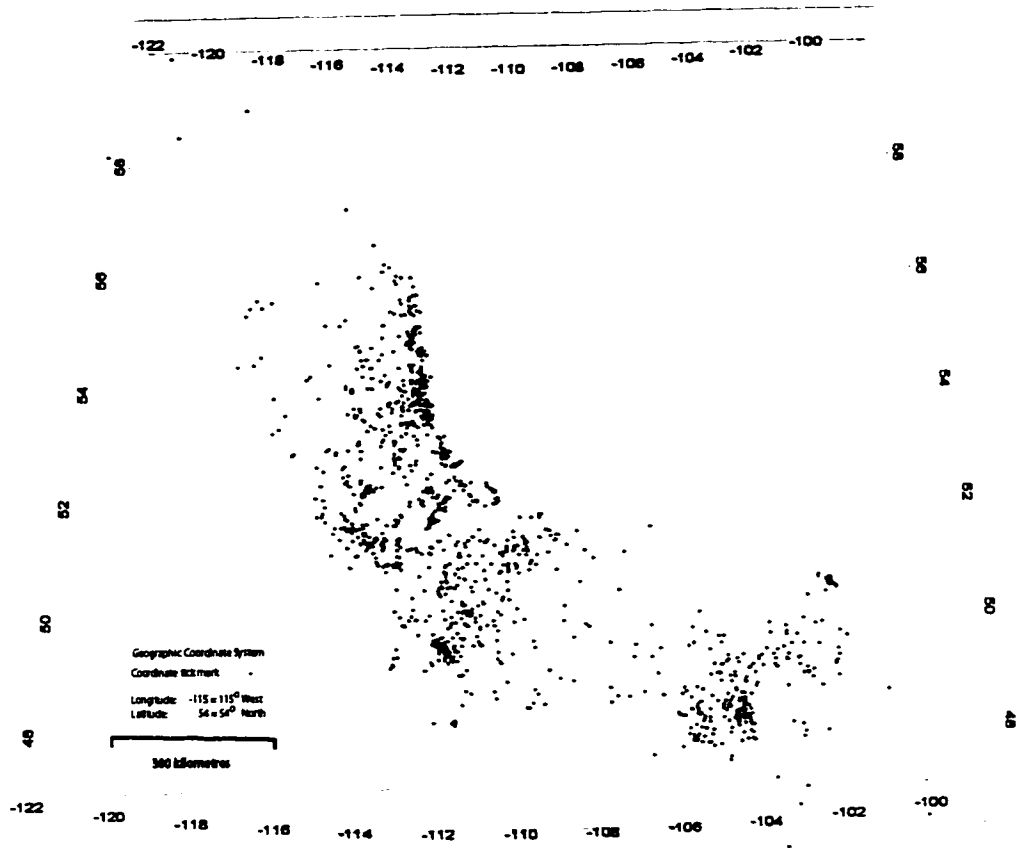
Figure 3.1 Distribution of culled pressure data. Total = 1750 data points.

Quality Code	Description
A	Best quality
B	Nearing stabilization
C	Caution (DST tool plugging)
D	Questionable
E	Low permeability, low pressure
F	Low permeability, high pressure
G	Misrun

Table 3.1 Description of DST quality codes

chemistry database created from hardcopy files of the Alberta Energy Utilities Board. These water analyses are for samples that were collected during drill stem tests, during production, or by several other possible means (Hitchon and Brulotte, 1994). The database provides individual ionic concentration as well as pH, sample source, depth of sample, and formation sampled. The database is in the format of Microsoft Access, and thus water chemistry data for the Nisku Aquifer were extracted according to the assigned formation names. Water chemistry data within Montana and North Dakota were obtained from data compiled by previous students of the Hydrogeology Group at the University of Alberta. The availability of the individual ionic concentration as well as the other parameters facilitates the culling of the water chemistry data.

3.1.5 Water Chemistry Data Culling

Water chemistry analyses reported by Geofluids include data that are not representative of the formation of interest. Geofluids database provides a flag for every sample indicating the possible source of the sample, based on certain criteria (Block, 2001). Those criteria identify samples as either formation waters or as any possible contaminant may have been introduced to the sample during the many processes carried out during the drilling or development of a well. Other sources of errors can result from sample handling or the lab analyses. According to previous works performed to cull formation water chemistry data, the process of culling can result in the elimination of up to about 70% of the total number of raw water samples based on the work by Hitchon and Brulotte (1994). The following is a summary of the method used in Geofluids (Block, 2001) for flagging the samples.

Incomplete Analysis:

Those are the analyses that are missing chloride, bicarbonate, sulfate, calcium, and magnesium. Should the sodium be missing, it can be calculated by the difference between the total dissolved solids and the sum of the above ions.

Analytical Error:

This error is determined by subtracting the sum of the milliequivalents cations from the sum of the milliequivalent anions. If the absolute value of the difference is more the 10 % then the sample is flagged as erroneous.

Completion Fluid or Acid Water:

The following are diagnostics that are used to indicate samples falling in this criteria:

PH < 4.5

Ca/Cl > 0.3 and pH < 5.7

Na/Ca < 1.2

Na/Ca < 5 and Na/mg < 10 and pH < 6

Corrosion Inhibitor:

SO4/Cl > 1.5 and TDS Ratio > 1.5

SO4/Cl > 1 and TDS Ratio > 1.5 and pH > 8.5 (TDS ratio = TDS @ 110 C/TDS @ ignition)

SO4/Cl > 10

KCL Mud Filtrate/Kill Fluid:

Na/K < 20

Alcohol:

Density of the sample < 0.95 and > 0

Gel Chem Mud Filtrate:

Na/Cl > 5

Na/Cl > 3.5 and SO4/Cl > 1.5

These criteria were applied to the samples using an automated spreadsheet, and each sample is assigned a flag for each of the criteria above; as 0 if the criterion is not matched, and 1 if the criterion is matched. The sum of these scores for each sample gives an indication of the quality of the sample, where the higher the score, the lower the quality of the sample. The study area was then discretized into 10 quadrangles for easier handling of data during posting. This was followed by a process where maps of TDS for those individual quadrangles were generated, and both of the scores from the automated spreadsheet and sample flags from Geofluids were posted. A series of maps with certain criteria restrictions were then generated and the quality of data were plotted. Just like the case with pressure data, in areas with high density of data, accuracy was sought; but, in areas with scarce data, completeness was sought, while not compromising the fact that only formation water are accepted. Out of the 5000 raw data samples collected for this
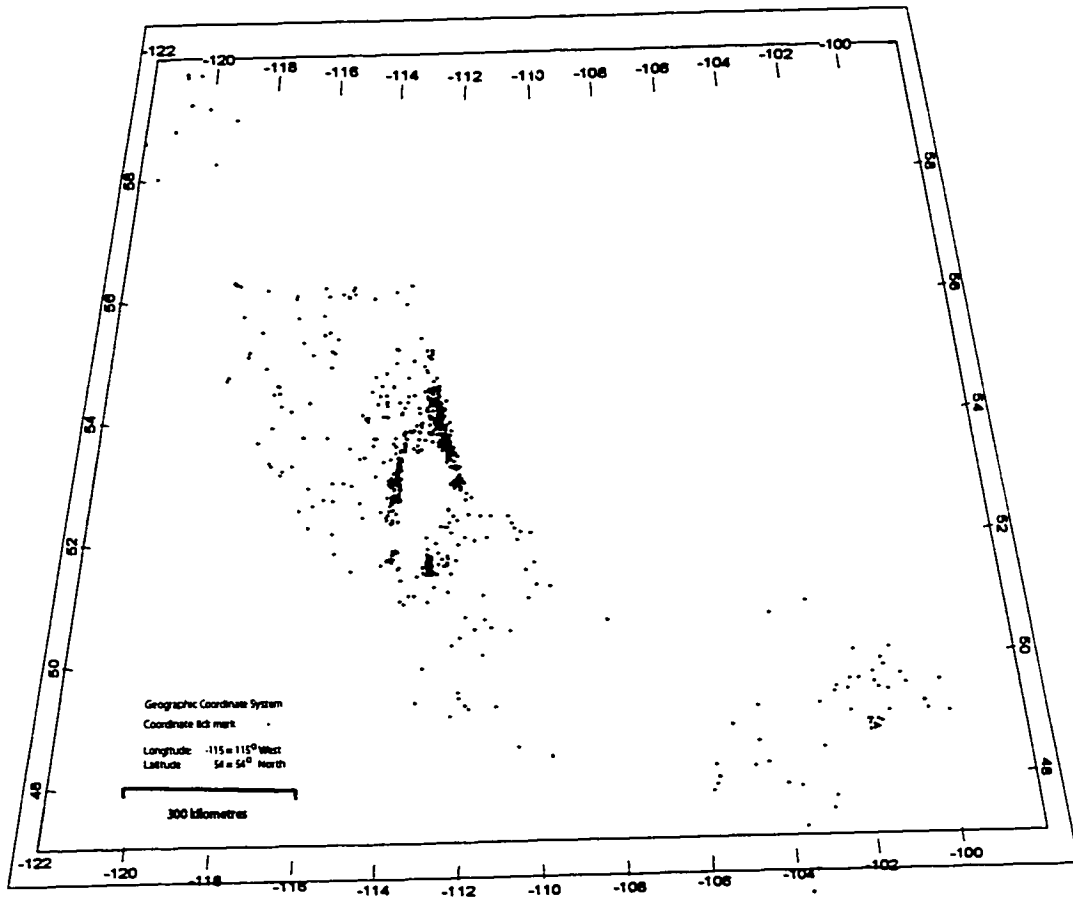
Figure 3.2 Distribution of culled water chemistry data. Total = 870 data points.

51

study, only 870 were accepted as representative values. The distribution of the culled chemistry data is shown in Figure 3.2.

3.1.6 Temperature Data

Temperature data were obtained from DST records in Geooffice. Temperature is usually measured from within the inside of the DST tool, and thus this measurement depends on the fluid temperature entering into the tool. In high permeability wells, it is expected that the measurement is more representative of the actual formation temperature than those wells with lower permeability. The well bore as well as the formation can be cooled by the circulation fluids used during drilling, and thus the degree of adjustment of the temperature at the temperature gauge will be directly proportional to the time allowed for the test and the amount of formation fluid entering the tool. The detailed treatment and classification of temperature data is beyond the scope of this study. However, those facts are mentioned here to clarify that error can be introduced using the DST temperature data. In much of the areas within the basin, the temperature data obtained from DST's are the most representative of the subsurface temperature (H. W. Reid, 2002, personal communication). A total of 2510 data points were used; distribution of temperature data is shown in Figure 3.3.

3.1.7 Production Data

The Geooffice database delivers production data, which just like the pressure data can be designed according to need. Primary fields of the production database are well location, producing reservoir, production start date, and production end date. Those are data columns were used in the pressure data culling procedure, discussed in Section 3.3. Production from Montana were manually assimilated from data accessed through the website of Montana Board of Oil and Gas Conservation (MBOGC) (MBOGC, 2001). The website offers production data classified by formation. For North Dakota, production data were extracted from the annual production report of the Oil and Gas Division of the North Dakota Industrial Commission (NDIC) (NDIC, 2000). The number of production data points collected is 3950 and their distribution is shown in Figure 3.4.
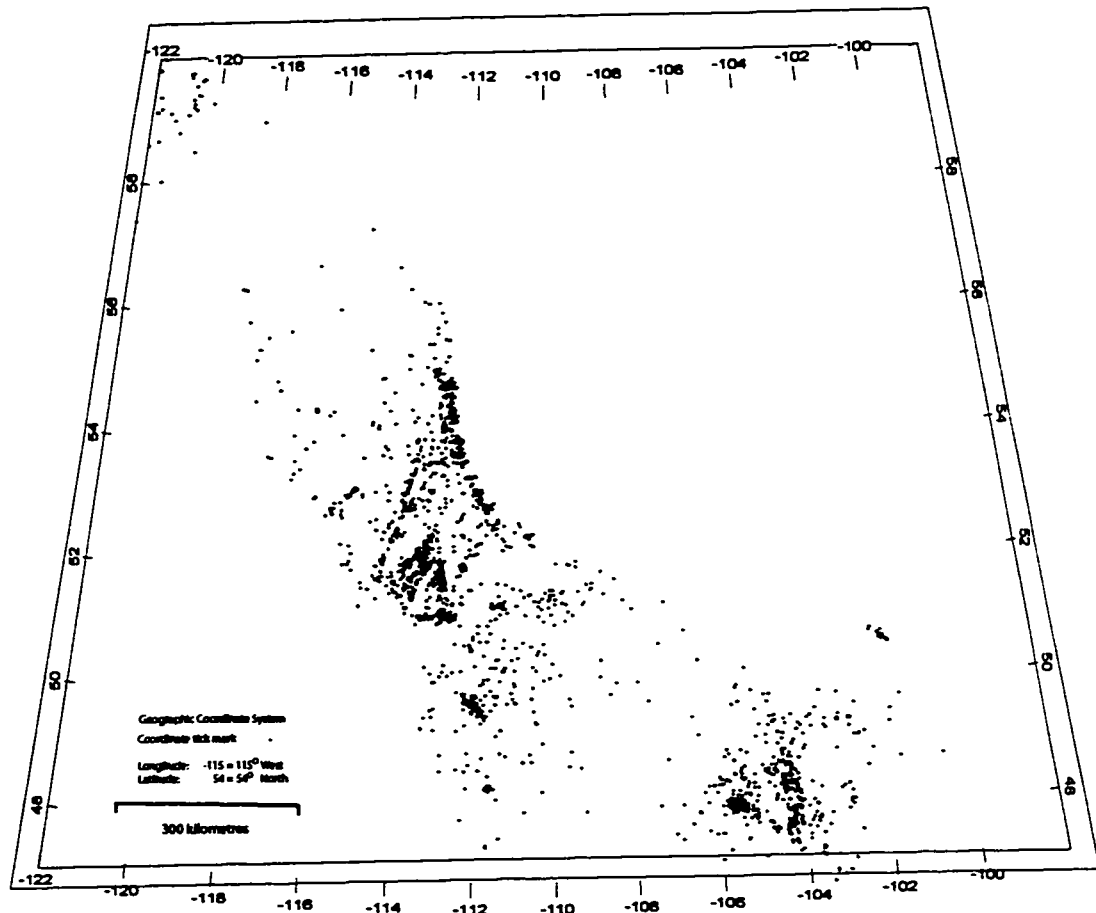
Figure 3.3 Distribution of temperature data. Total = 2510 data points.
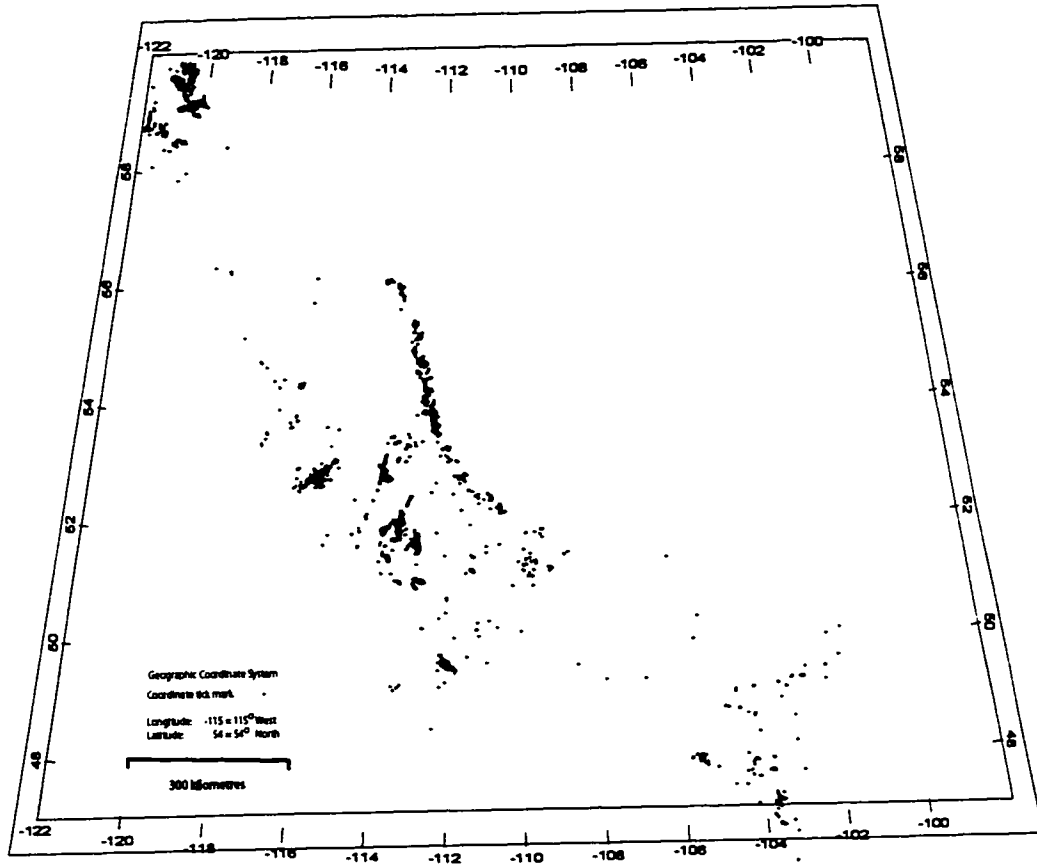
Figure 3.4 Distribution of the Nisku production data. Total = 3950 data points.

3.1.8 Geological Structure Data

Regional structure data were obtained from digital records of well control provided with the Atlas of WCSB (Mossop and Shetsen, 1994). Those data were originally assimilated by a team of geologists who obtained data from oil companies, and the data cover the whole WCSB for certain geological horizons. For Montana, structure data were obtained from online access to the website of the Montana Board of Oil and Gas Conservation (MBOGC) (MBOGC, 2001). Additional data were obtained from data provided on CD by MBOGC. Data for North Dakota were obtained from digital file compiled by North Dakota Industrial Commission, Oil and Gas Division. A total of 6800 structure data points were acquired and their distribution is shown in Figure 3.5.

3.1.9 Topography Data

The National Geophysical Data Center (NGDC) in Colorado, USA, offers online, 5-minute-spaced digital elevation grid model for the entire earth, based on a user-defined quadrangle. Topographic data were obtained from the NGDC site (NGDC, 2001) and triangulation interpolation was used to contour the data since they are provided as a grid. The website allows the retrieval of such data in geographic coordinates and elevation in a text format which can be taken to a spreadsheet or directly imported to the mapping software.

3.2 Vector Representation and Calculation

In order to give a visual representation of the water and oil driving forces, a procedure was developed to account for all the inputs in those vectors and to carry out necessary mathematical manipulations. To illustrate how this was accomplished, a background about the softwares used and their capabilities are given here.

Surfer:

Surfer is a mapping software that has the capability of kriging data in order to generate a grid distribution based on a given variogram. The data are input as X, Y, and Z values. The result is a grid that is in binary format, but is exportable as a text format. This
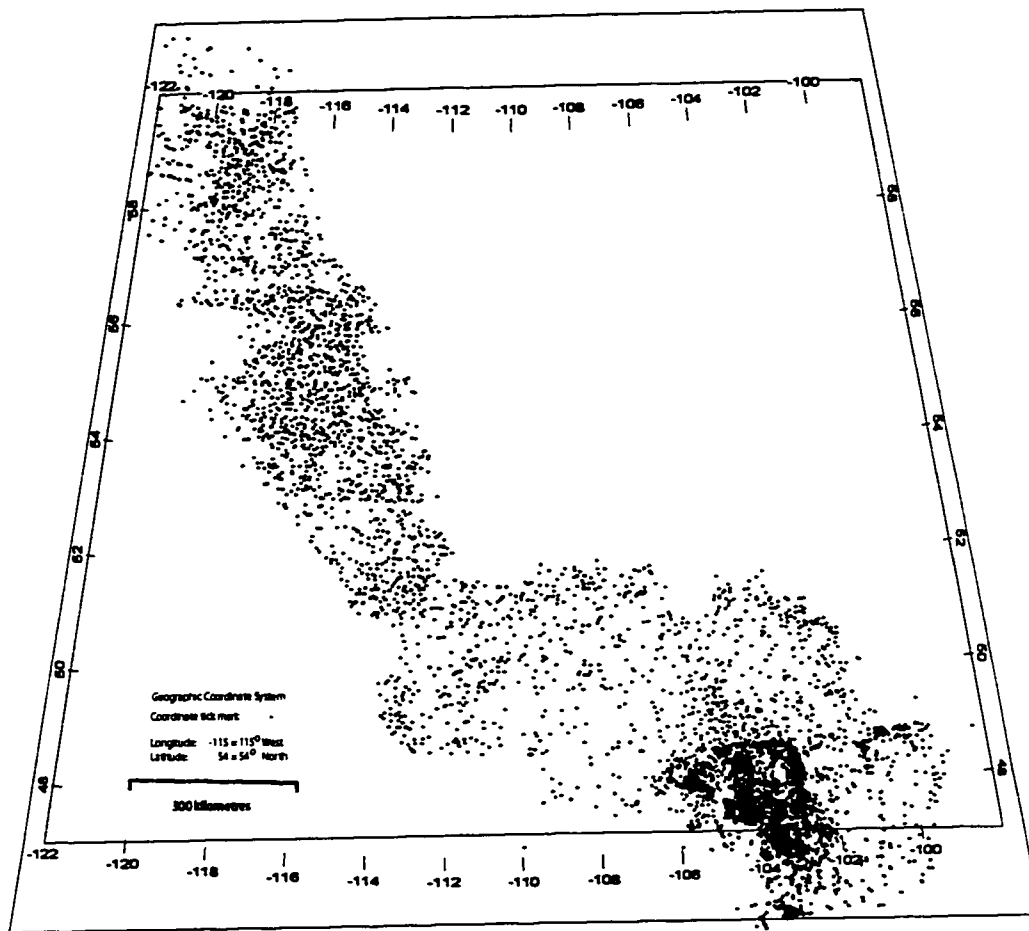
Figure 3.5 Distribution of Nisku Formation structure data. Total = 6800 data points.

56

represents a grid, which can be imported and manipulated in a spreadsheet according to need. Surfer's kriging engine was used to generate a grid for the potentiometric surface, TDS, structure, and temperature. Prior to any kriging, the coordinate system is converted to a UTM forced into zone 12.

Rockworks99:

Rockworks99 is a mapping software with multiple packages for geological, hydrogeological, and geophysical applications. Rockworks99 offers an engine called Directional Analyses, where the user can input a grid file, and Rockworks99 can calculate the maximum slope and the azimuth of the maximum slope at pre-specified grid node locations. This is an essential feature which was used to calculate gradient vectors given in equations 1.3 and 1.7. The directional analyses provide both a magnitude, expressed as slope angle dip from the horizontal, and an azimuth of the dip, expressed in a 0-360 degree angle.

3.3 Modeling Water and Oil Driving Forces

One of the primary goals of this study is to characterize the lateral movement of groundwater in the Nisku Aquifer, and to study the influence of this movement on that of hydrocarbons. In order to achieve that, and using the values of WDFVs and ODFVs, a Visual Basic code was developed by the author and used in conjunction with Microsoft Excel in order to carry out the vector addition needed to find the driving forces for water and for oil (Figures 1.2 & 1.4). The grids resulting from the vector addition process are used to define the coordinates of the tails and heads of arrows representing these vectors. The magnitude of the vector is directly proportional to the length of the arrow. However, due to the high variability of magnitudes of vectors generated for this study area, a classed scale was used for different magnitude ranges, in order to offer clarity in the presentation of results. The coordinates of heads and tails of vectors were then used to create an arrow map by Rockworks99. Due to the fact that this work involves extensive vector resolution in addition to the incorporation of the density calculations at subsurface conditions, numerous automated Excel files with linked Visual Basic codes were developed by the author and standard procedures for calculating each product were

57

```
        ┌─────────────┐
        │  Operation  │
        └──────┬──────┘
               │
               ▼
┌──────────────────────────────────────┐        ──→      -Exce
│  -Apply culling criteria to raw data  │        ←──      -Surfe
│  -Perform iterative mapping           │
│  -Extract good quality data           │
└──────────────────┬───────────────────┘
                   │
                   ▼
┌──────────────────────────────────────┐        ──→      -Rock
│  -Perform coordinate conversions to UTM│       ←──      -Surfe
│  -Generate grids for temperature,      │
│   pressure, EFWH, structural           │
│   elevation and TDS                    │
└──────────────────┬───────────────────┘
                   │
                   ▼
┌──────────────────────────────────────┐        ──→      -Rock
│  -Calculate structural and hydraulic  │        ←──
│   gradients                           │
│  -Obtain grids of slopes and azimuths │
└──────────────────┬───────────────────┘
                   │
                   ▼
┌──────────────────────────────────────┐        ──→      - Excel
│  -Export data to modeling spreadsheets│        ←──        codes
│  -Calculate WDFV, ODFV, DFR           │
│  - Calculate coordinates of heads and │
│   tails of arrows representing vectors │
└──────────────────┬───────────────────┘
                   │
                   ▼
┌──────────────────────────────────────┐        ──→      - Roc
│  -Plot WDFV, ODFV, DFR, and           │        ←──      - Roc
│   sensitivity analyses results        │
└──────────────────────────────────────┘
```

Figure 3.6 Flow chart describing the procedure used for generating maps of WDFV, ODFV, DFR, and sensitivity a
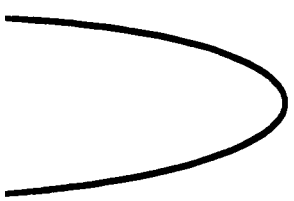
Tools
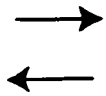
-Excel sheets with linked Visual Basic codes
-Surfer mapping software

TM
sure, EFWH, structural
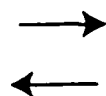
-Rockworks99 coordinate conversion engine
-Surfer

adients
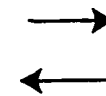
-Rockworks99 directional analysis engine

ts

:ails of arrows
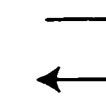
- Excel sheets linked to specially designed Visual Basic codes.

y analyses results
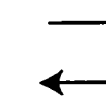
- Rockworks99 directional statistics engine
- Rockworks grid-based mapping engine

for generating maps of WDFV, ODFV, DFR, and sensitivity analyses.

established. The procedure for modeling ODFVs and WDFVs are summarized in the flow chart shown in Figure 3.6.

3.4 Calculating Water Density From TDS

The calculation of the water density, ρ_w, at aquifer conditions was adopted from Chierici (1959) where

$$\rho_w(p,T,C) = 730.6 + 2.025 - 3.8 \times 10^{-3} T^2 + [2.362 - 1.197 \times 10^{-2} T + 1.835 \times 10^{-5} T^2]p +$$
$$[2.374 - 1.024 \times 10^{-2} T + 1.49 \times 10^{-5} T^2 - 5.1 \times 10^{-4} p]C$$

$$(3.3)$$

where: p is pressure in mPa, T is temperature in degrees Kelvin (K), and C, the salinity, in kg m^{-3}. Equation 3.3 is valid for the following (Chierici, 1959):

Pressure: 0-50 MPa

TDS: 0-300 kg/m^3

Temperature: 293-373 K^0

Equation 3.3 was also programmed in Visual Basic in order to automate the process of calculating water density at grid nodes, when calculating the water and the driving forces.

3.5 Oil Density

Oil density for a certain API gravity, depends on temperature, pressure, and gas to oil ratio. In order to account for oil density variations according to subsurface temperature and pressure conditions, a Visual Basic code was developed by the author to automatically calculate the density of oil at the grid node, based on a combination of methods suggested by Lasater (1958) and by Glaso (1980), and reported in Chierici (1994). The reader is referred to petroleum engineering text books such as Chierici (1994) and references therein for detailed description of the parameters used in the mathematical formulation. According to this method:

$$\rho_o(p,T) = \frac{\rho_{o,sc} + 1.225\gamma_g R_{sf}(pT)}{B_{of}(p,T)}$$ (3.4)

where $\rho_o(p,T)$ is the oil density at the given pressure p and temperature T, $\rho_{o,sc}$ is the density of oil at standard conditions, γ_g is the gas gravity, R_{sf} is the solution gas/oil ratio by flush liberation, and B_{of} is oil formation volume factor resulting from the flush liberation of gas.

To calculate B_{of} the following equation is used, according to Glaso (1980):

$$B_{of} = anti\log[-6.58511 + 2.91329\log B* -0.27683(\log B*)^2]$$ (3.5)

where $B*$ is a correlation parameter, obtained from

$$B* = 212.5 \cdot [R_{sf}(\frac{\gamma_g}{\rho_{o,sc}})^{0.526} + 8.2 \cdot 10^{-3}T - 2.094]$$ (3.6)

where R_{sf} can be calculated, according to Lasater (1958):

$$R_{sf} = 23.645\frac{\rho_{o,sc}y_g}{M(1-y_g)}$$ (3.7)

where y_g is the gas mole fraction, which can be obtained from the graphic correlation given by Chierici (1994, Figure 2.9 p.31) correlating $p*$ to y_g which was digitized, and the following equation was generated describing the correlation as:

$$y_g = [.2411 \cdot \ln(p*)] + .3577$$ (3.8)

$$p^* = \frac{80.58p\gamma_g}{T}$$ (3.9)

The coding of these equations facilitated automated calculation of the density of hydrocarbon at a given temperature, pressure, and API, a technique needed where pressure and temperature vary drastically across the WCSB.

3.6 Pressure-versus-depth (p(d)) Plots

There are three objectives for constructing pressure-versus-depth (p(d)) in this study. The first objective is to characterize, if possible, the pressure system in the Nisku Aquifer within a certain area as normally or abnormally pressured. If a pressure data point is significantly less or more than hydrostatic pressure calculated using freshwater p(d) gradient, then this represents underpressuring or overpressuring, respectively. The second objective, at selected locations, is to detect the types of pressure systems in the sedimentary section and where the Nisku Aquifer pressure system belongs. The third objective is to detect the vertical sense of groundwater movement in a particular area and to what extent such movement affects the Nisku Aquifer.

Choice of the depth interval to be shown on the p(d) plot is subject to the type of analysis at the location being investigated, and may vary from one location to another. Only tests of qualities A and B were allowed for pressure data in the sedimentary succession. This is because in the p(d) plot, only clear patterns of the data are considered. Data that were obviously anomalous were removed, and trends of the maximum pressure data population were considered. The consideration of the maximum pressure data as the most representative in the trend on a p(d) plot has been reasoned by Orr and Kreitler (1985), and suggested by Jiao and Zheng (1998).

In order to construct p(d) plots with the above objectives at a certain area, pressure data population are classified according to the elevation ranges of the kelly bushings (KB) of the wells where pressures were measured. For each KB elevation range, a different color is assigned on the p(d) plot. Only tests with water recoveries were included in this study except for the Nisku Aquifer, where pressures measured in gas, oil, and water are

61

included and appropriately shown in different colors. Hydrocarbon phase data are included in order to 1) highlight the depth where hydrocarbons are found in the Nisku Aquifer and 2) to identify abnormal pressures, i.e. if the hydrocarbon phase is significantly overpressured or significantly underpressured (Appendix B).

This method of constructing a pressure p(d) plot should serve the objectives mentioned above. The flow direction can be read from the slope of the line trending through the maximum pressure data for a certain KB elevation range. A p(d) gradient greater than the p(d) gradient for freshwater indicates upward flow, while a p(d) gradient less than the p(d) gradient of freshwater indicates downward flow (in the case of saline formation water, this is true using the ambient water density of the formation instead of freshwater) (Tóth 1978, 1980; Barson, 1993). A change in slope that is inversely proportional to the KB elevation range is probably indicative of a flow system that is affected by local topography, while parallel lines for different KB elevation ranges may represent a system not responding to the local changes in land surface topographic elevations. Also, shown on the p(d) plots are the p(d) gradients of freshwater and ambient Nisku Aquifer groundwater densities.

3.7 Summary of Petroleum Hydrogeological Method

Lateral movement of hydrocarbons within the Nisku Aquifer, considered as a carried bed, is modeled by calculating the WDFVs ODFVs. First, pressure, temperature, TDS, and structure data were collected, and necessary culling procedures were applied. Those data are then kriged, mapped, and the resulting grids are imported to a data sheet in Rockworks99. The purpose of this importing is to convert the coordinate system from geographic longitude and latitude to UTM. The conversion to UTM coordinates involves the forcing of the all locations into Zone 12, which means that the distances are referred to a single origin. This prevents errors that can be introduced in vector calculations at the edges of standard UTM zones. These data are then entered in specially designed spreadsheets and the mathematical procedures needed to calculate the force vectors and the needed densities are coded using Visual Basic. After the relevant vectors are calculated, in terms of slope and aspect, they were exported for plotting. This was done

for groundwater and oils with different API's in order to assess the influence oil densities on oil migration patterns. To understand the vertical sense of groundwater movement and hydrocarbons into (and out of) the Nisku Aquifer, p(d) plots were constructed and interpreted. Published geological, hydrogeological, and petroleum geochemical studies were incorporated for the purpose of interpretation.

3.8 Possible Sources of Errors

Several sources of errors are associated with carrying out petroleum hydrogeological studies. Knowledge of the kinds of errors that can be introduced while conducting such a study can give an insight into the reliability of a certain conclusion drawn from the investigation. Following is a discussion of some sources of errors.

3.8.1 Top of Aquifer Versus Top of Formation

The stratigraphic top of the Nisku Formation is not necessarily the top of the aquifer, which is really the geological medium through which the hydrocarbons effectively flow (considering that the top of the aquifer will not transmit oil due to capillary forces) The structure data used in this study are obtained from the Atlas of the WCSB, and are utilized for the calculation of the WDFVs and ODFVs. However, for a regional study such as this, the gradient in structure is the controlling factor, which can be considered as parallel to the aquifer top. Thus, the maps generated in this study represent the regional trends, and may represent most of the local trends, but one should be aware of this point while determining a flow direction in a local scale area.

3.8.2 Temperature

As mentioned earlier, the temperature data can be erroneous due to the fact that during a DST, recovery may not be sufficient to allow fluids that have attained the formation temperature to enter the DST tool and be sensed by the temperature gauge. Errors in temperature measurements are introduced by the cooling effect of mud circulation during drilling (Gretener, 1981). Temperature gauges, on the other hand, are reliable and have accuracies that range between 0.1 to 0.01 °C (Gretener, 1981).

63

3.8.3 Pressure Data:

The pressure data are obtained using gauges that have a finite accuracy. Those accuracies are usually provided by the manufacturers of the gauges, and vary according to type and sometimes according to the scale of the specific gauge. The accuracy of some gauges is provided appendix A. Other errors are introduced during the extrapolation of the Horner plot, depending on the degree of stabilization of the shut in pressure (H. W. Reid, 2001, personal communication).

Other sources of error in the data can be introduced by digitizing non-digital DST charts. Those are usually generated by industry using computer digitizing devices. The accuracy of the process is subject to human errors and hardware abnormalities (N. Hannon, 2001, personal communication).

For a regional study, and in this case the contour interval is 50 meters of head, it is likely that such errors do not make a significant effect on the interpretations drawn from the maps. Errors introduced by gauge accuracies fall short of causing anomalies in the potentiometric surface with such a contour interval.

3.8.4 Permeability

Aquifer permeability data are not included in this study. The permeability distribution is not usually well defined for such a scale of study. The permeability data distribution is biased to areas with interest near areas of oil field development, and thus may introduce errors in the process of permeability mapping. However, for a basin scale study, the potentiometric surface is usually a distribution of hydraulic head that is affected by the aquifers' permeability variations (Tóth and Rakhit, 1988). Furthermore, the latter point can be substantiated by our knowledge of lithofacies which can in most cases provide a qualitative indication of the permeability distribution.

3.8.5 Permeability Anisotropy

Permeability anisotropy data are not included in this study. Anisotropy can be of great influence on diverting groundwater flow. In general, parallel to bedding, the aquifer can be considered isotropic in the X-Y (horizontal) plane. However, in the Z direction, which is usually normal to the bedding plane in a stratified sedimentary succession,

permeability can be significantly reduced. Possible diversion from this generalization is when the strata are deformed, in karstification and collapse features, or in some reef buildups where the stratification is absent.

4.0 Observations and Results

This chapter presents maps of physical quantities that were constructed using the raw data described in Chapter 3, which includes the distribution of hydraulic head, total dissolved solids, and temperature in the Nisku Aquifer over the WCSB. Quantities directly derived from those observations, which are relevant to the type of analyses conducted in this study, are also presented including horizontal hydraulic gradients, density differences between freshwater and actual groundwater, and the distribution of vertical temperature gradients. Oil API gravity values of wells producing from the Nisku Formation are mapped to help in the interpretation. A Topographic map of the study area is also presented (Figure 4.9) showing the Nisku Formation subcrop and the formation's outcrops in northwestern Montana.

4.1 Hydraulic Head Distribution in the Nisku Aquifer

The regional hydraulic head distribution in the Nisku Aquifer is shown (Figure 4.1). In the Alberta basin, there is a general decrease in hydraulic head from values of 1100-1400 m near the disturbed belt (excluding the localized high hydraulic head anomalies and decreasing to values of around 350 m at the formation subcrop in the east. (subcrop of the Nisku Formation is shown in Figure 4.9). Such a decrease in hydraulic head indicates a generally northeastward-directed flow in the Alberta basin.

For the Williston basin, the regional expression of the hydraulic head distribution shows a somewhat radially-outward decrease from the highest areas in the southern limit of the study area towards the north and northeast. Those highest hydraulic heads at the southern limit of the study areas reach 1100 m, and decrease to values of 400-550 m at the northern and northeastern subcrop of Nisku Formation in Saskatchewan and Manitoba. A relatively flatter potentiometric surface occurs at the northwestern part of the Williston basin. Flow directions inferred from the hydraulic head distribution indicate that regional flow is to the north and northeast.
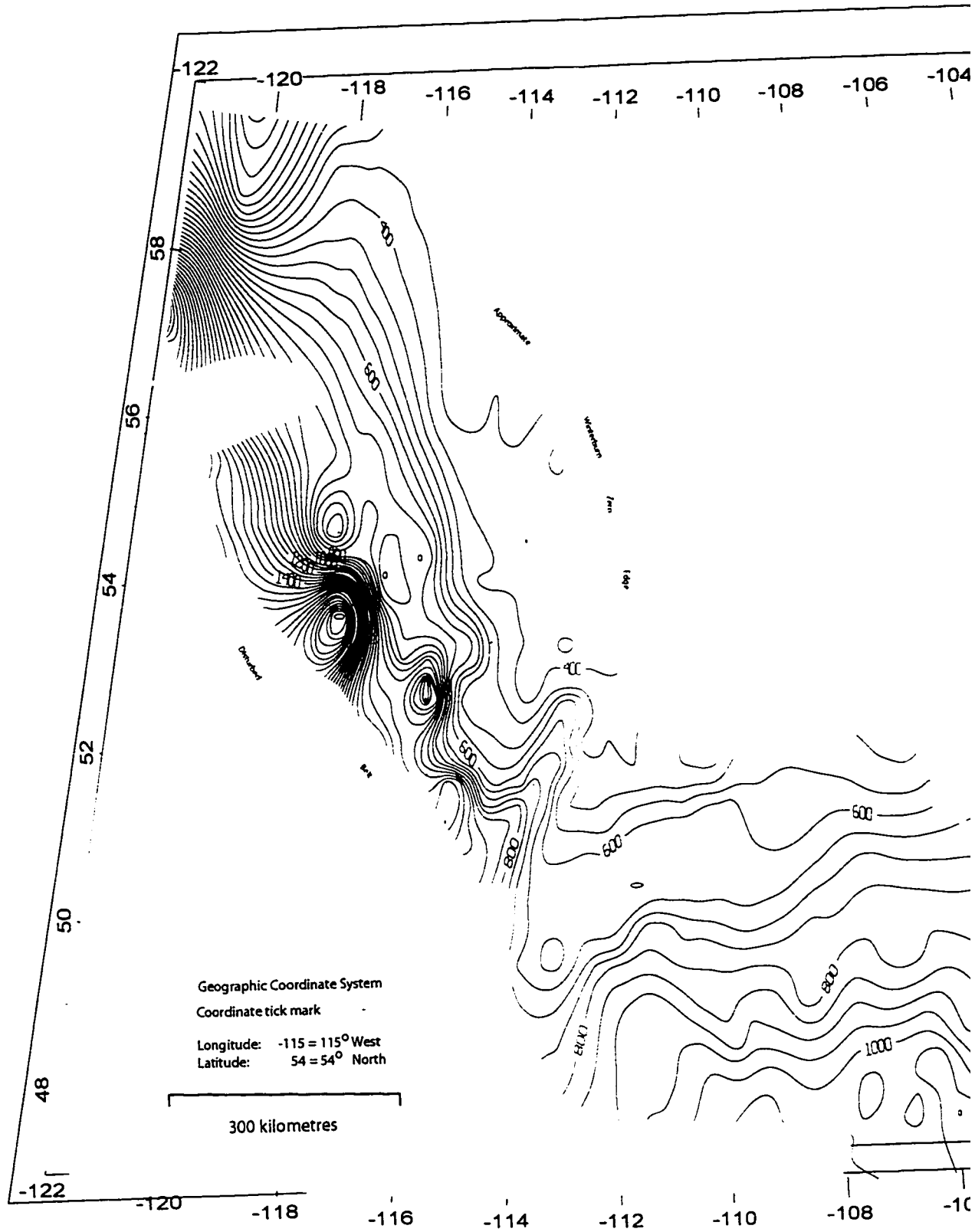
Figure 4.1 Hydraulic head distribution in the Nisku Aquifer, WCSB (C.I. = 50 m)
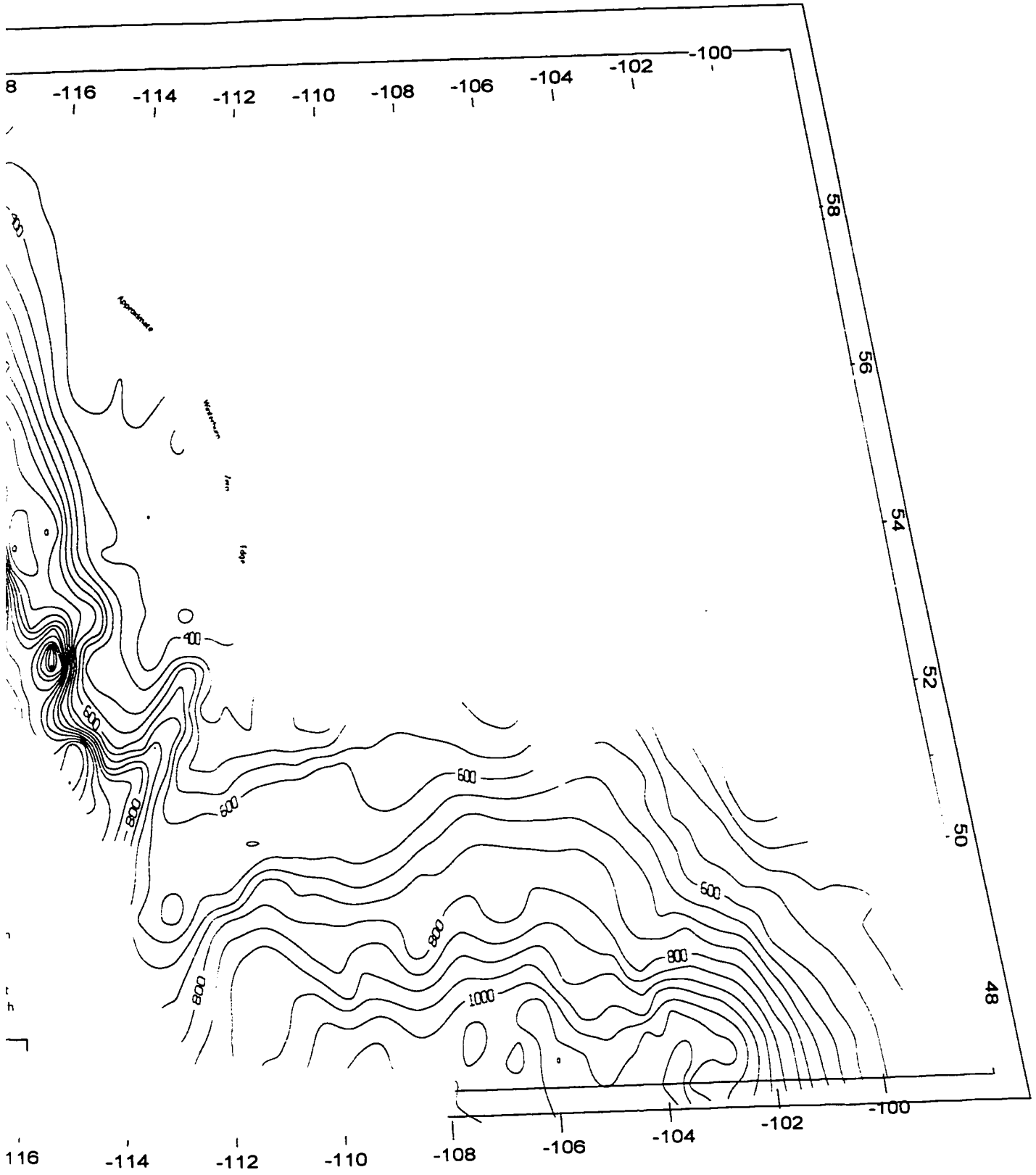
n in the Nisku Aquifer, WCSB (C.I. = 50 m)

Two primary regional features in the hydraulic head distribution are observed in the Alberta basin. A relatively high hydraulic head distribution is present in southern Alberta and originating in northwestern Montana reaching 1050 m and decreasing towards the north, northeast, and the north west (area F, Figure 4.2). A regional potentiometric low in the Nisku Aquifer is observed close to the eastern subcrop of the Nisku Formation in the Alberta basin, with hydraulic head values dropping to a low of 350 m, and a flattening of the potentiometric surface is observed (area C, Figure 4.2).

Three hydraulic head features are highlighted in the Williston basin. Generally high hydraulic head located at the southern portion of the study area in the Williston basin reaching 1100 m (area G, Figure 4.2) and decreasing with a moderate hydraulic gradient towards the north and the northeast. A northeasterly trending trough in the potentiometric surface is observed in southeastern Saskatchewan (area H, Figure 4.2). At the basin divide, there are relatively low hydraulic heads of 500 m, which represent relative lows to both the Alberta and Williston basins (area I, Figure 4.2).

Several regional-scale anomalies are observed in the hydraulic head map. Three regional mounds of hydraulic heads are observed that suggest radially outward flow from their respective maximum heads. They are located in south central Alberta, west central Alberta, and in the West Pembina area (areas E, D, and J, Figure 4.2). In south central Alberta, a northeast-southwest trending mound in hydraulic head distribution, reaching high values of 800 m and extending towards the disturbed belt in the west and to the Nisku Formation subcrop in the east. General flow directions inferred from such hydraulic head distribution are towards the northwest, southeast, and the northeast. In west central Alberta, hydraulic heads are at a high of 2200 m decreasing radially with an observable high hydraulic gradient expressed by the congestion of the contour lines. In West Pembina, hydraulic heads reach 1100 m and drop with a high hydraulic gradient in a radial manner.

In contrast, two anomalies showing regional sinks or low hydraulic heads are located at the Hamlet North area in northwestern Alberta and northeastern British Columbia and at the Karr Basin (areas A and B, Figure 4.2). In the North Hamlet area, hydraulic heads decrease to a minimum of −50 m with a clearly expressed high hydraulic gradient

68

A : Hamlet North
B : Karr Basin
C : East-Central Alber
D : West-Central Albe
E : South-Central Alb
F : Southern Alberta
G : Montana
H : SE Saskatchewan
I : Basin Divide
J : West Pembina

Location of a P(d) p

Geographic Coordinate System

Coordinate tick mark   -

Longitude: -115 = 115° West
Latitude: 54 = 54° North

300 kilometres
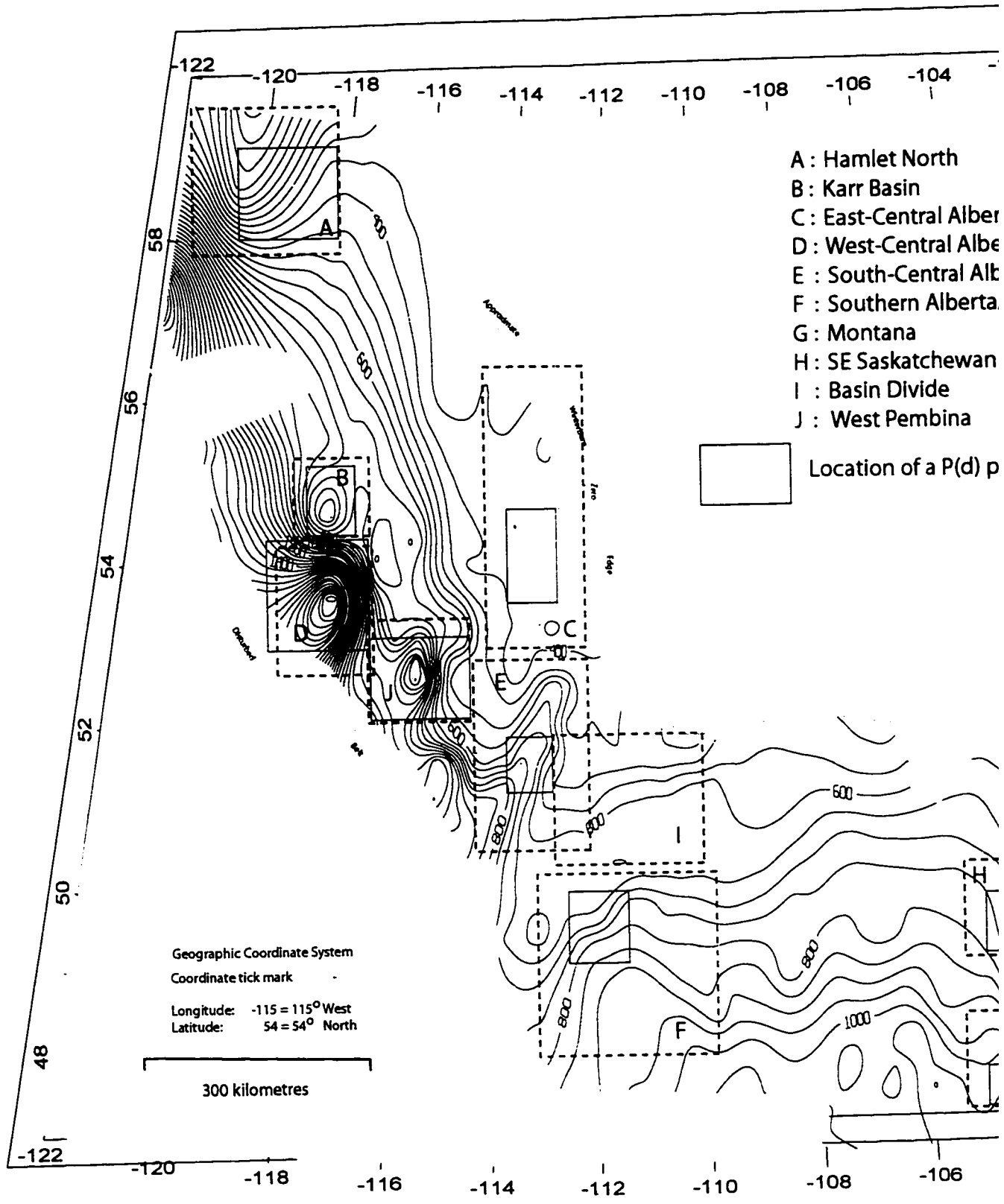
Figure 4.2 Index map for features in hydraulic head distribution and P(d) plots.

A : Hamlet North
B : Karr Basin
C : East-Central Alberta
D : West-Central Alberta
E : South-Central Alberta
F : Southern Alberta/ NW Montana
G : Montana
H : SE Saskatchewan
I : Basin Divide
J : West Pembina

Location of a P(d) plot
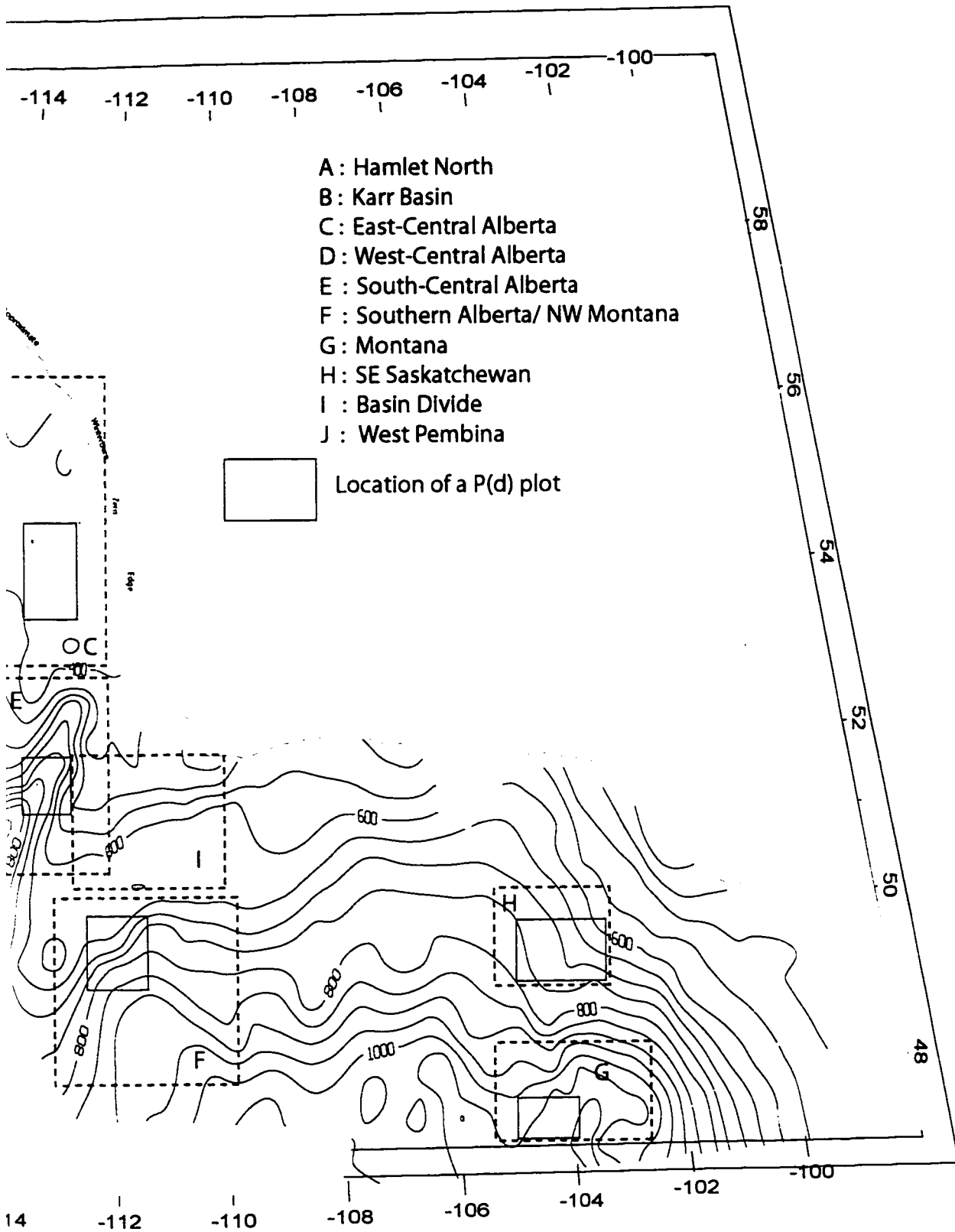
d distribution and P(d) plots.

directed away from this regional hydraulic head minimum. Hydraulic heads in the Karr basin area, on the other hand, drop to a relative minimum of 600 m in an area characterized with a general hydraulic head of greater than 800 m.

4.2 Horizontal Hydraulic Gradient Distribution, Nisku Aquifer

Hydraulic gradients in the Nisku Aquifer are in the range of 1 to 3 m/km for most of the basin (Figure 4.3). In the Alberta basin, horizontal hydraulic gradients generally decrease from the west to the east, while in the Williston basin, horizontal hydraulic gradients can be characterized as homogenous and their magnitudes is around 1 m/km for most of the basin.

In the Alberta basin, two areas showing elevated magnitudes of horizontal hydraulic gradient are located at the high hydraulic heads of west-central Alberta (Area D[1]), West Pembina (area J) with horizontal hydraulic gradients reaching a magnitude of 18 m/km. Relative high gradients are located around the Bashaw area (area E) reaching 3 m/km. In the Hamlet North area (area A), hydraulic gradient magnitudes reach 9 m/km.

Horizontal hydraulic gradients have direct relevance in the analyses of groundwater and hydrocarbon movements as discussed in Chapter 1.

4.3 Total Dissolved Solids in the Nisku Aquifer

Regional distribution of TDS in the Nisku Aquifer is shown in Figure 4.4. Over the entire WCSB, TDS values vary between 10 and 300 g/l, and generally the increase in TDS is associated with the increase of depth. Extending almost over the entire Alberta basin are TDS contour lines trending north-south to northwest-southeast and somewhat parallel to the disturbed belt, with some anomalies to the western half of the basin. In the Williston basin, TDS contour lines generally decrease in value from highs in the south to lows in the north, west, and east.

In the Alberta basin, the TDS map shows two major areas of high concentration flanking the Alberta disturbed belt and extending to approximately the middle of the study area part of the Alberta basin (Figure 4.4). The first area of anomalously high TDS extends

---

[1] Those areas have been defined in Figure 4.2.

70
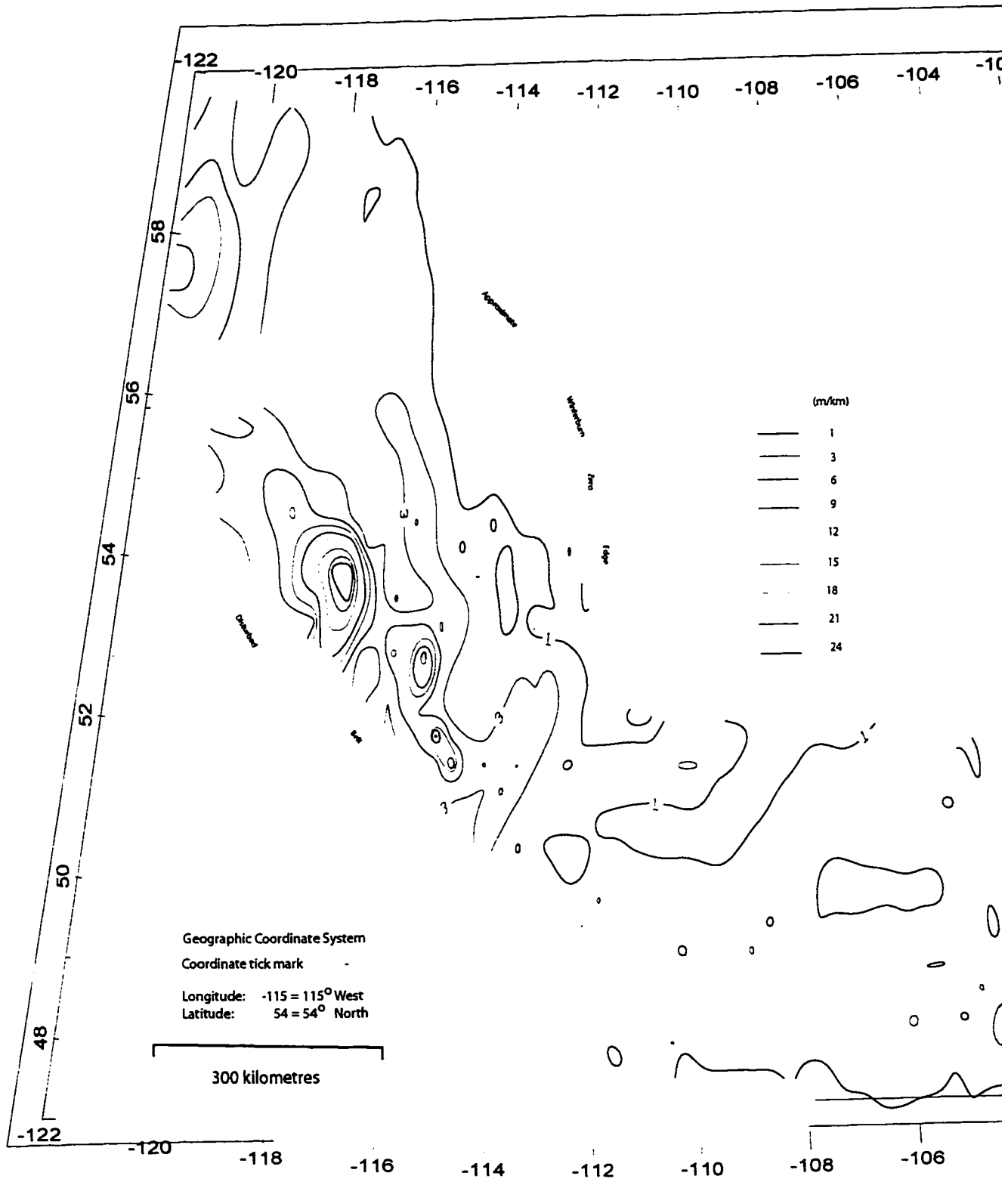
Figure 4.3 Magnitude of horizontal hydraulic gradients in the Nisku Aquifer, WCSB.
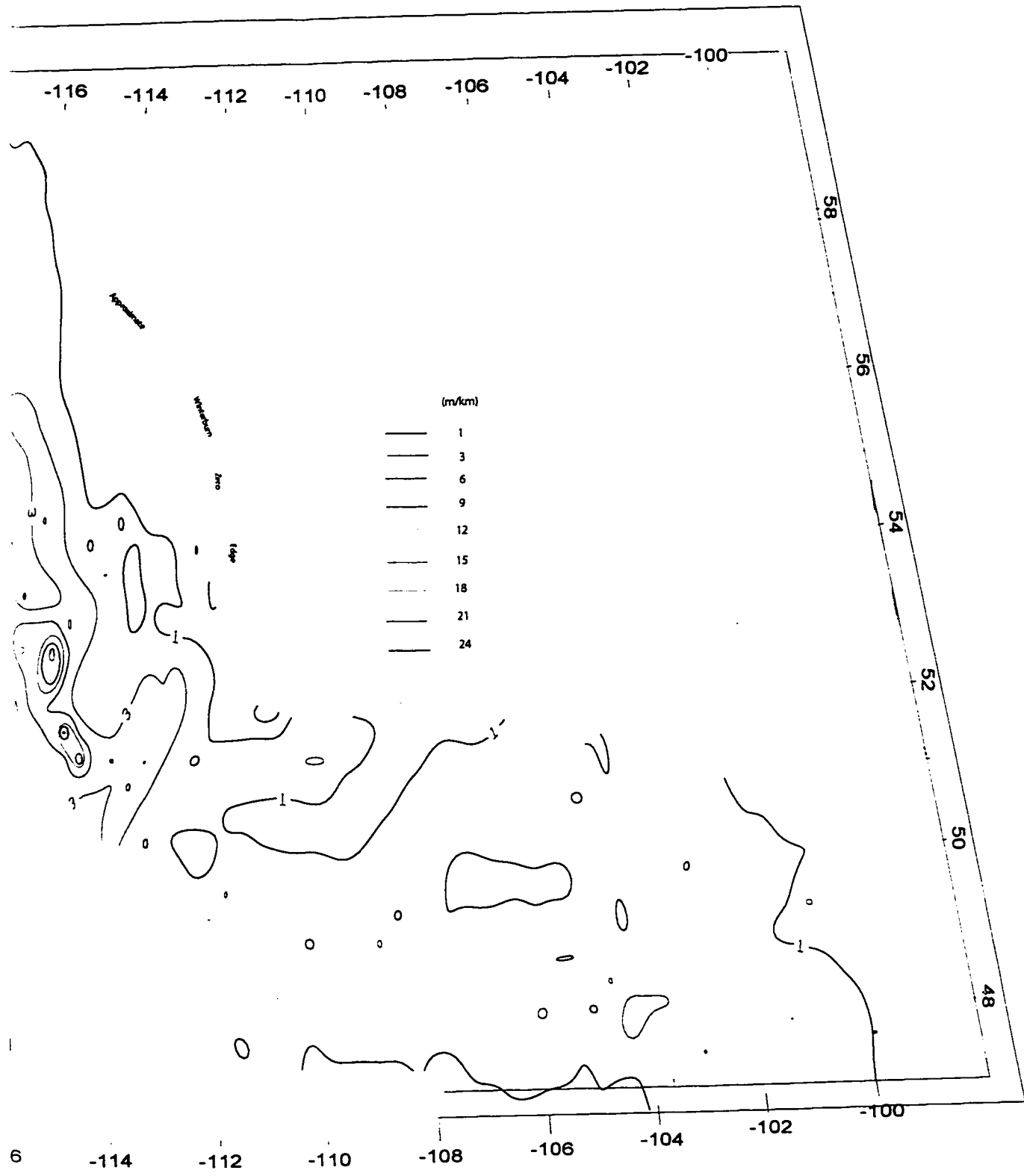
ydraulic gradients in the Nisku Aquifer, WCSB.
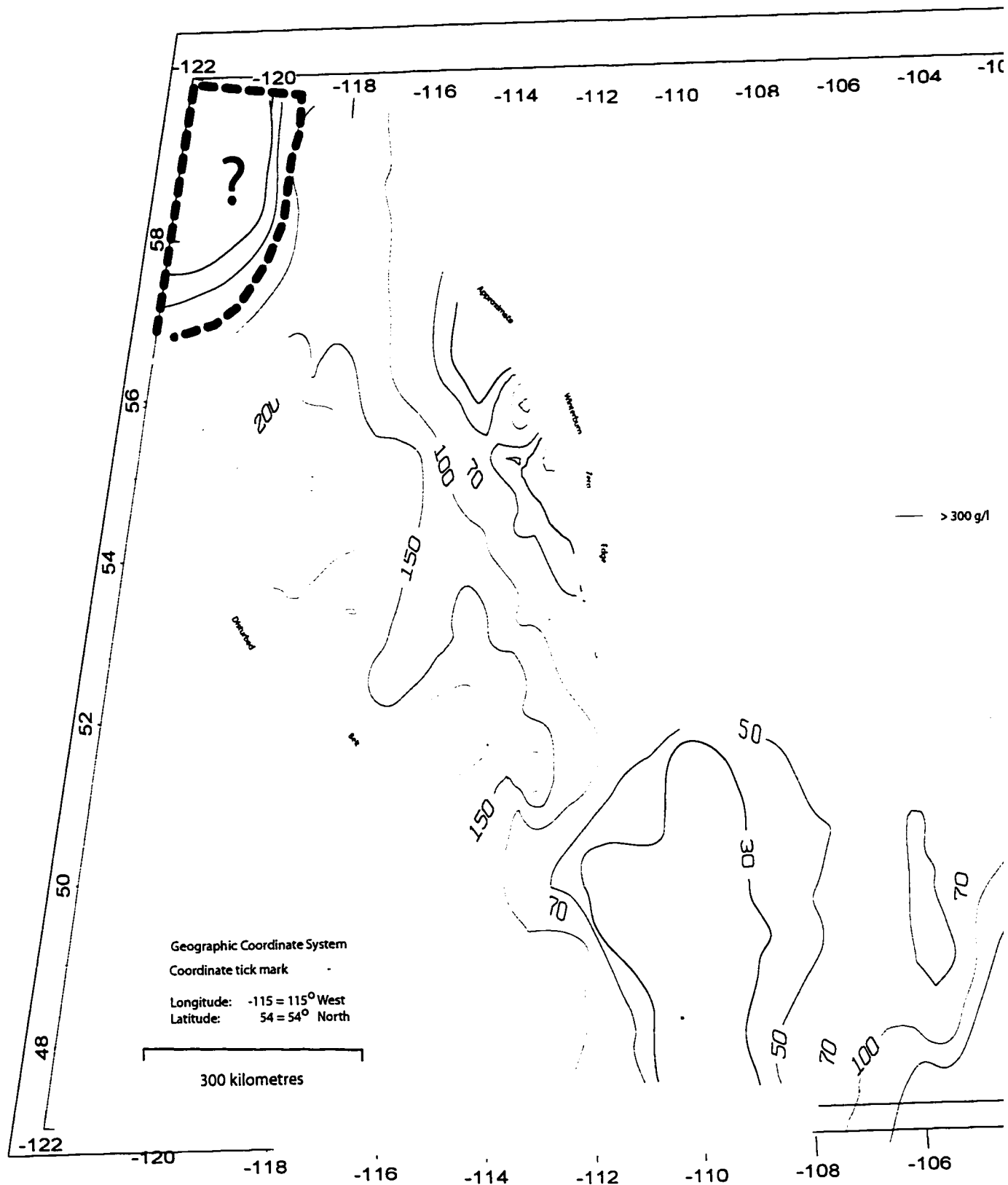
Figure 4.4 Distribution of Total Dissolved Solids (TDS) in the Nisku Aquifer (C. I. = Variable, in g/l).

-116   -114   -112   -110   -108   -106   -104   -102   -100

58

56

54

Approximate

Wenbun

Ian

Edge

100   70

150

> 300 g/l

52

150

50

50

30

50

70

100

70

150

70

200

50

48

50

70   100

250

-100

16   -114   -112   -110   -108   -106   -104   -102   -100

Ived Solids (TDS) in the Nisku Aquifer (C. I. = Variable, in g/l).

72
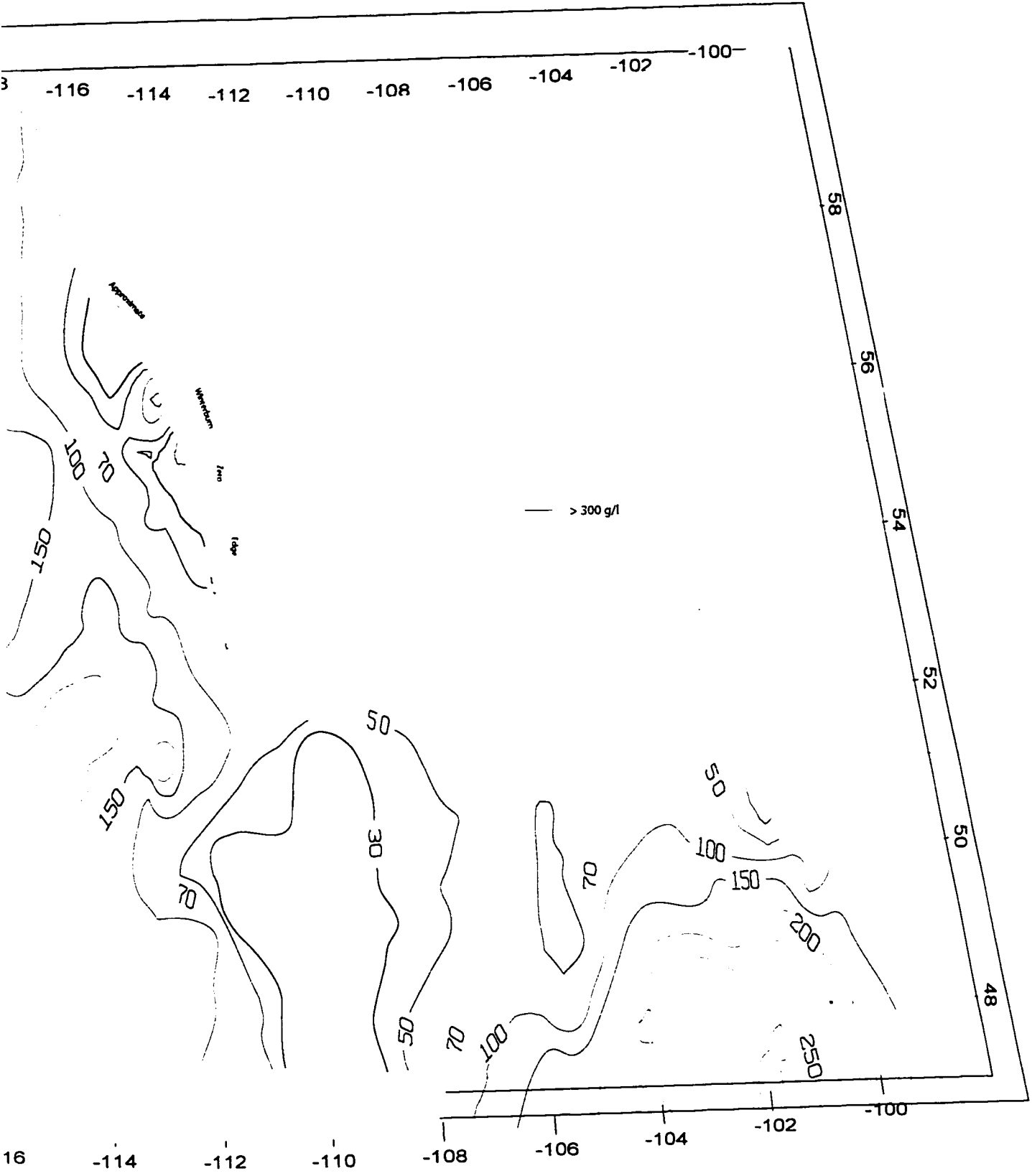
between 53° to 57° north latitude and 116° to 120° west longitude. The contour lines show a concentric shape with a high TDS of 250 g/l at the center and decreasing radially away from the center to a value of 200 g/l. Another somewhat elongated high TDS area is located between 51° to 53° north latitude and 113° to 116° west longitude, with TDS values reaching 200 g/l. In northern Alberta, the TDS decreases with a northwesterly trend, starting at a value of 100 g/l at approximately 56° north latitude and 120° west longitude decreasing to a value of 20 g/l. However, the samples in those areas are questionable as highlighted on the map.

In the Williston basin, two primary features divide the basin in two parts, an area of high TDS with values reaching the range of 300 g/l, located around 47° north latitude and 102° west longitude, and radially decreasing, with a high degree of irregularity towards the east, north, and west. An area of low TDS is observed at the western flank of the Williston basin, with an abrupt change in concentration towards the east. This abrupt change is located in the area around 48° north latitude and 105° west longitude where contour values increase from 50 to 250 g/l over a distance about 100 km. A freshwater tongue extends over the area bounded by 48° to 51° north latitude and 111° to 109° west longitude. The TDS in this area is 30 g/l or less.

4.4 Density Differences Between Freshwater and Nisku Aquifer Water

The density differences between actual aquifer water and freshwater mostly follows the pattern of the TDS map (Figure 4.5). The differences, reaching maximum values in the deeper parts of the Williston basin up to 140 kg/m^3, and at the Karr basin with values up to 120 kg/m^3 (Figure 4.5). Minimal density differences are observed at the divide between the Alberta and the Williston basins and in east central Alberta. A somewhat elongated trend of a difference in density of 80 kg/m^3 is observed in the general area of south-central Alberta and extending to the disturbed belt. The density difference between freshwater and actual aquifer water is considered in the analysis of groundwater movement, as described in Chapter 1.
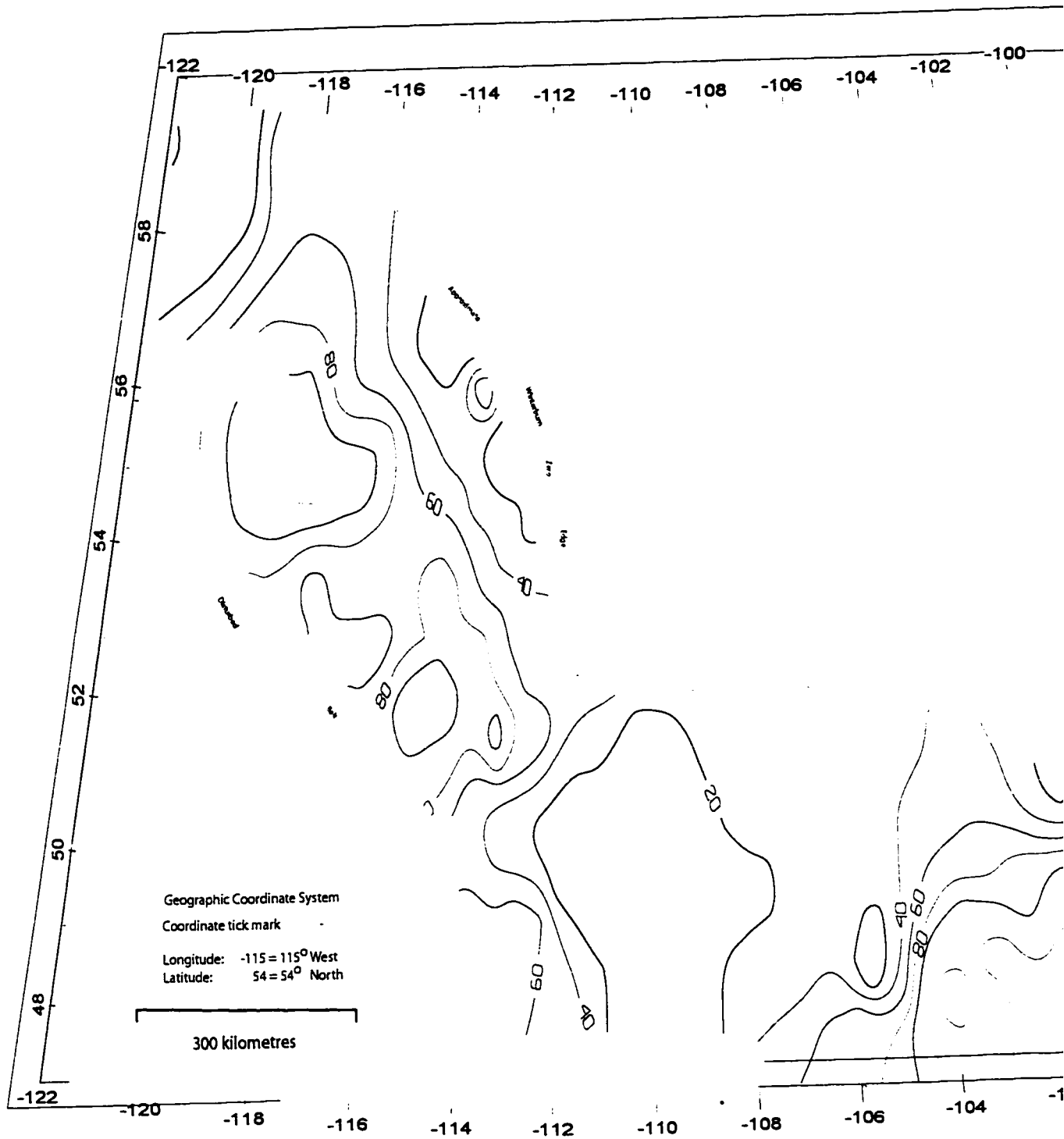
Figure 4.5 Differences between freshwater density and the ambient water density in the Nisku Aquifer ((
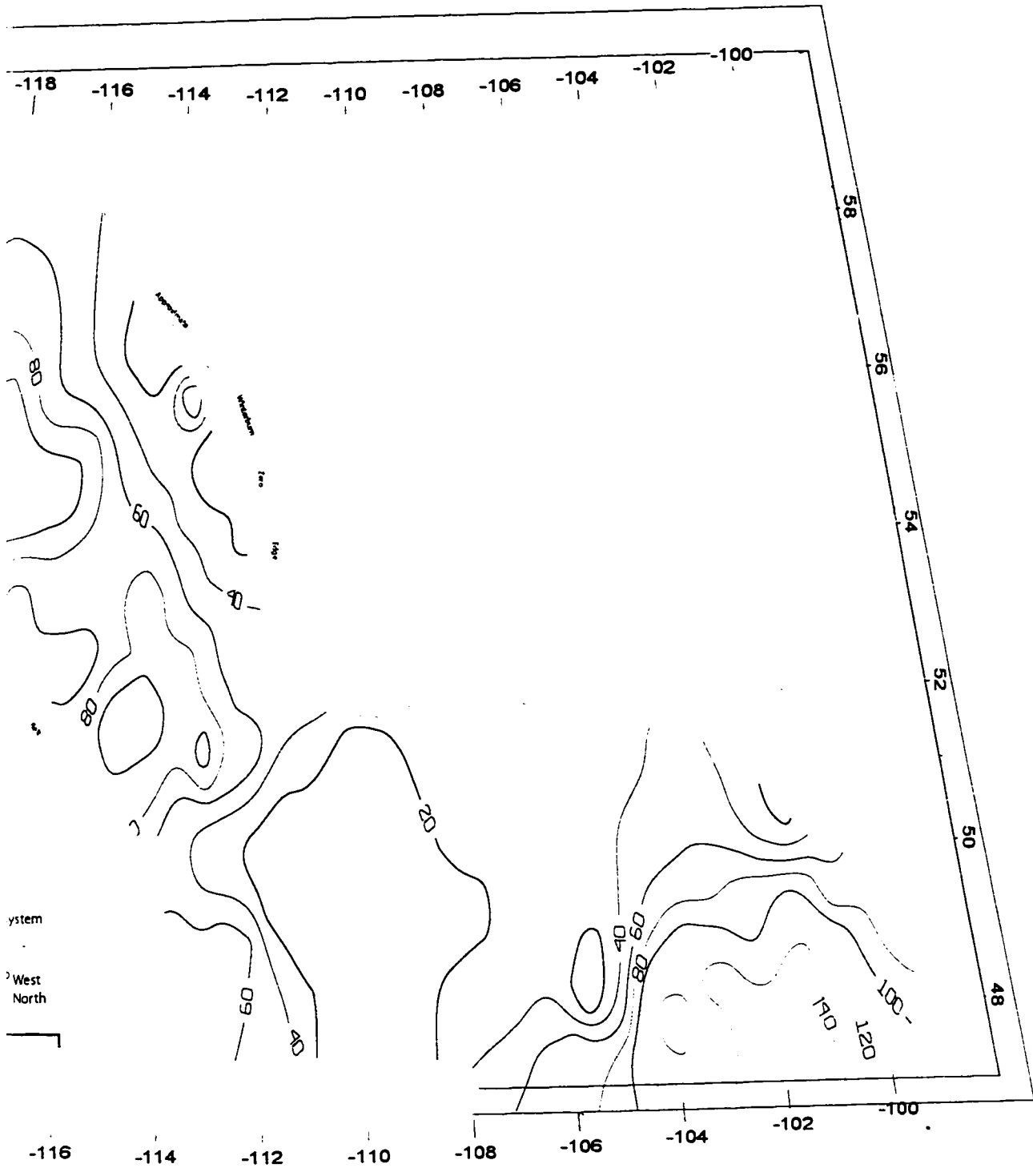
freshwater density and the ambient water density in the Nisku Aquifer (C.I. = Variable, kg/m³)

4.5 Temperature in the Nisku Aquifer

The temperature contour map of the Nisku Aquifer is presented in Figure 4.6. Temperatures in the aquifer range between 120 to 30 °C, and generally increase with depth. Highest values are observed in the area bounded by 47° to 48° north latitude and 104° to 102° west longitude in the Williston basin and the area bounded by 52° to 53° north latitude and 118° to 116° west longitude in the Alberta basin.

In the central and southern part of the Alberta basin, the temperature contour lines, in general, take semi-circular shapes, with the highest temperatures in the range of 110-120 °C located at 53° north latitude and 117° west longitude. From this area, the temperature decreases towards the east, north, and southeast, with the contour lines becoming more parallel to the disturbed belt towards the eastern part of the basin. Horizontal temperature gradients in the Alberta basin are variable, but can be generalized as high, moderate, and low, based on visual examination of the contour lines. The highest horizontal temperature gradients are observed in the area bounded by 53° to 54° north latitude and 116° to 114° west longitude. Moderate values of horizontal temperature gradients are observed in the eastern and southern parts of the Alberta basin, while low values are observed in the north.

In the Williston basin, temperature contour lines have semi-circular shapes with values decreasing towards the northern subcrop of the Nisku Formation in Saskatchewan and Manitoba, and towards the basin divide in the northwest. The horizontal temperature gradients increase towards the deeper, higher temperature parts of the basin, based on visual observations.

4.6 Vertical Temperature Gradients in the Nisku Aquifer

The distribution of vertical temperature gradients in the Nisku Aquifer is shown in Figure 4.7. Those gradients were calculated by dividing the temperature measured in the aquifer by its depth. Units of temperature gradients are in °C/km. Production data points are posted on this map in order to give visual reference to the geographic location of some of the features in the map.
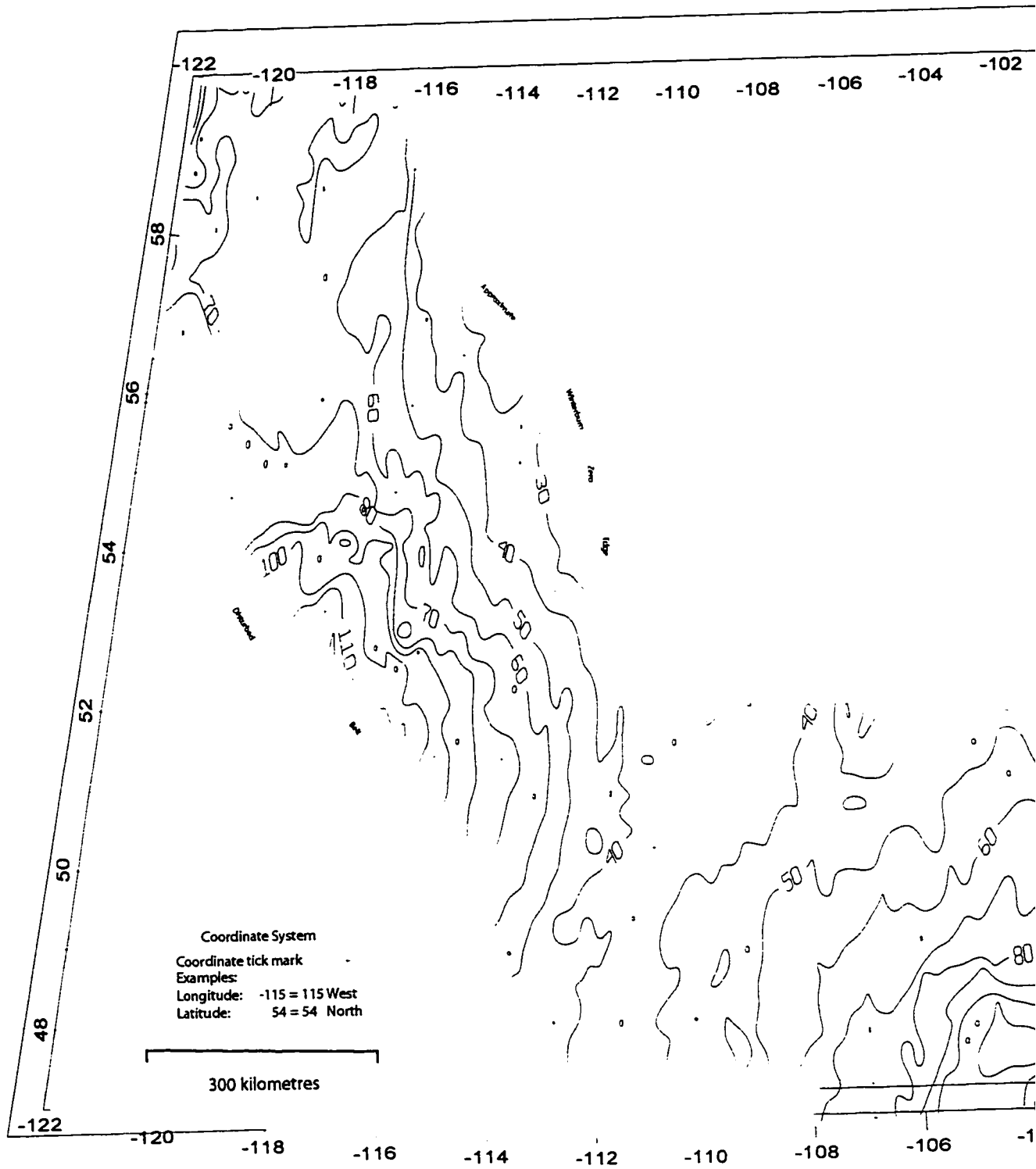
Figure 4.6 Temperature distribution in the Nisku Aquifer, WCSB (C. I. = 10 °C).
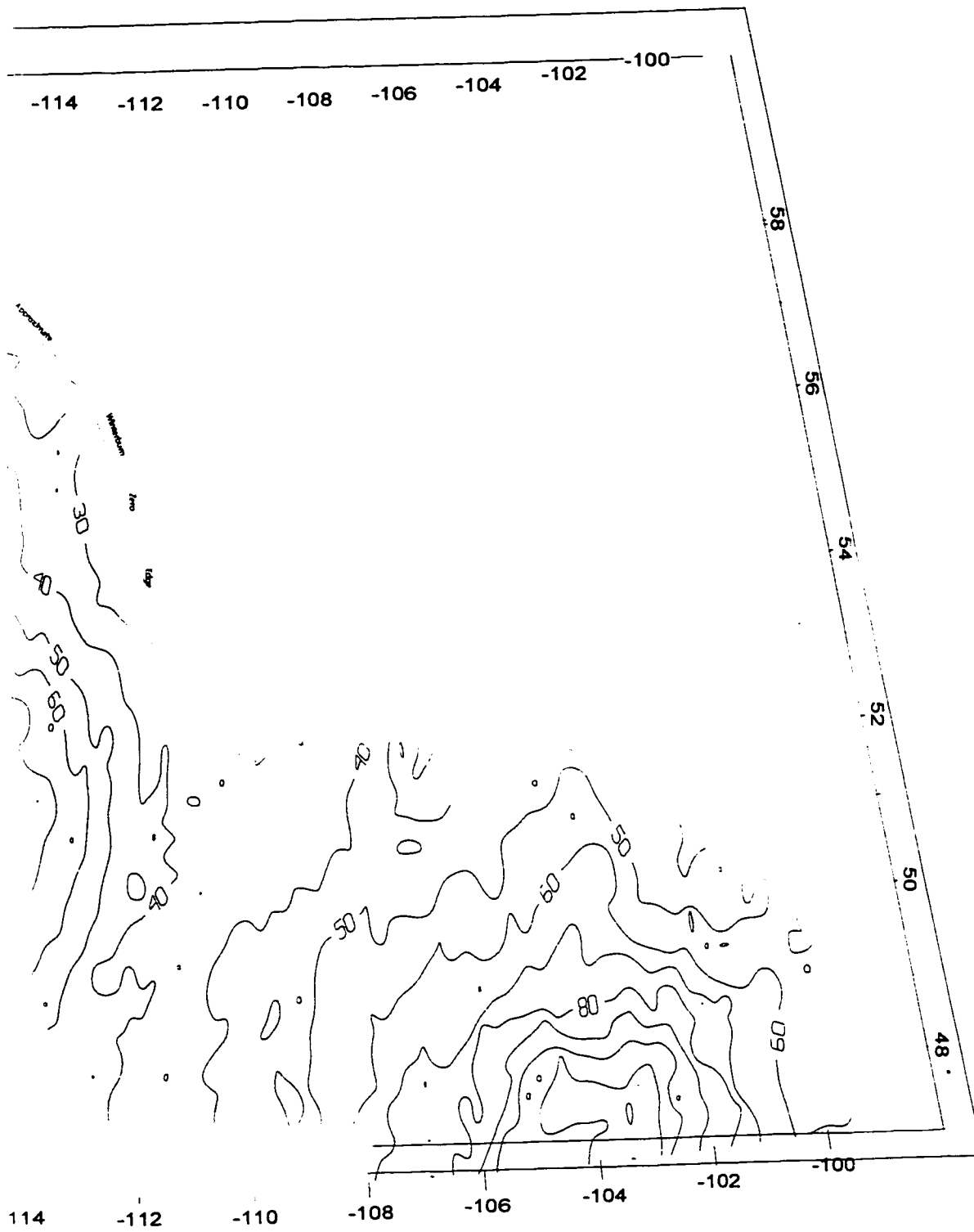
sku Aquifer, WCSB (C.I. = 10 °C).
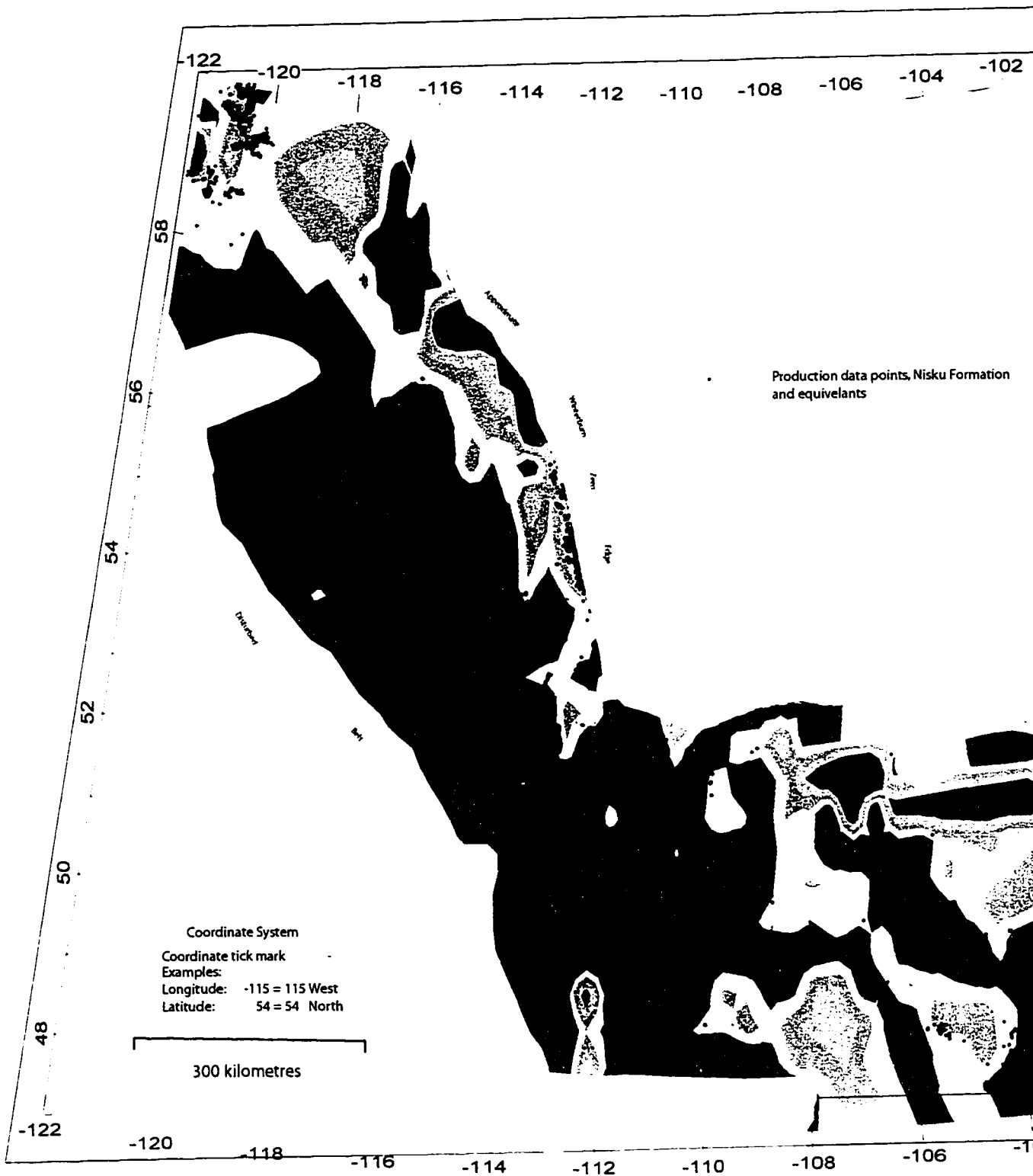
Figure 4.7 Vertical temperature gradients (temperature/depth) for the Nisku Aquifer, WCSB (°C/km).

-114   -112   -110   -108   -106   -104   -102   -100

52

58

56

Production data points, Nisku Formation
and equivelants

54

52

32

50

48

16

-100

114   -112   -110   -108   -106   -104   -102
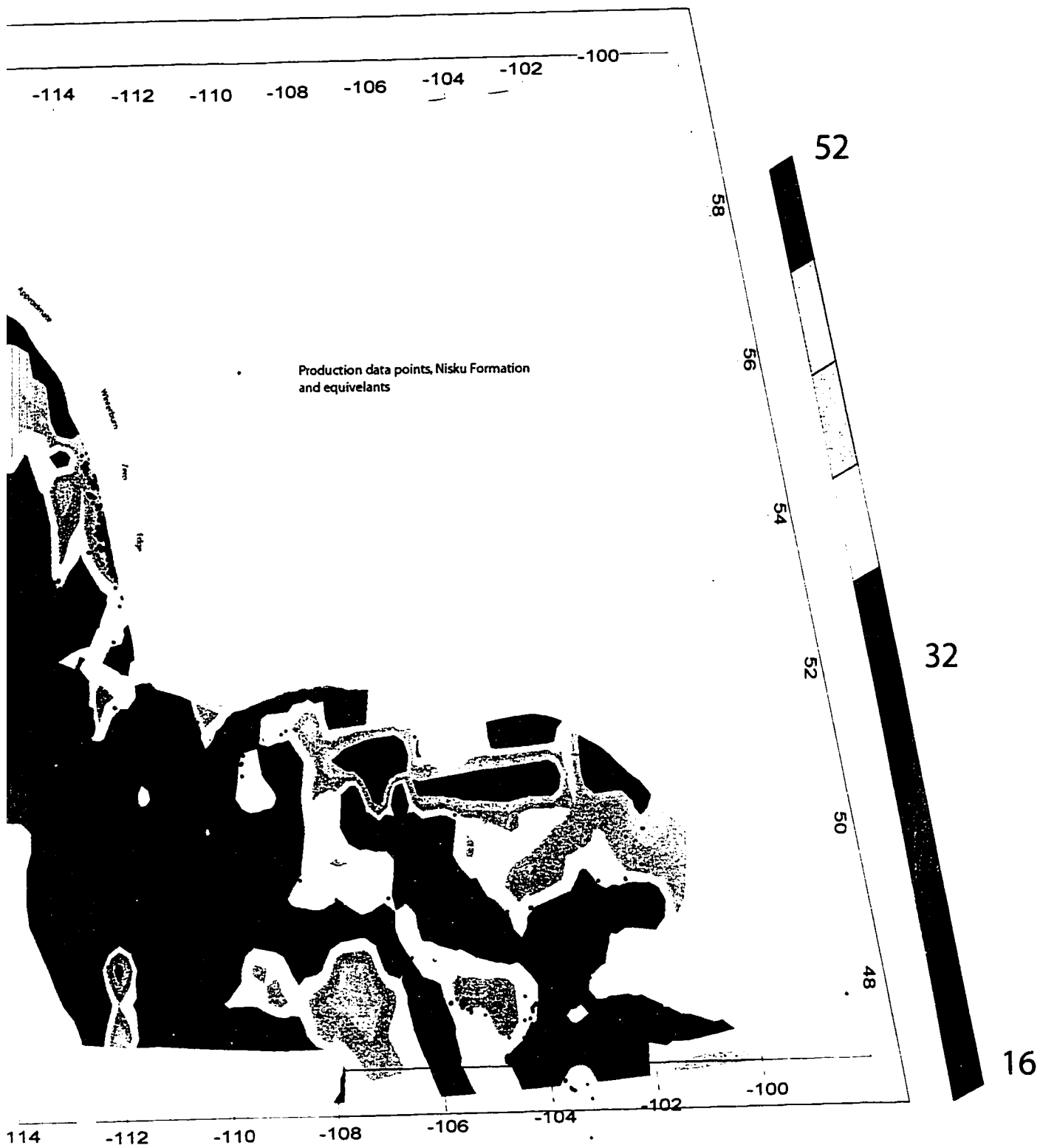
mperature/depth) for the Nisku Aquifer, WCSB (°C/km).

In general, vertical temperature gradients for the Nisku aquifer in the WCSB range between 16 to 52 °C/km, with the lowest vertical temperature gradients in the deeper parts of the basin and highest values in the shallower parts. In the Alberta basin, vertical temperature gradients increase from 28 °C/km in the western flank near the Disturbed Belt, and increase up to values of 52 °C/km near the Nisku Formation subcrop at the east of the Alberta basin. Several relative high or low vertical temperature gradient areas exist in the Alberta basin. An area of relative low temperature gradient is observed between 56° to 57° north latitude and 116° to 117° west longitude where temperature gradients drop to 20-24 °C/km. Low vertical temperature gradients are also observed in southern Alberta and northwestern Montana, where temperature gradients drop to relatively low values ranging between 20 to 28 °C/km. Those are located at 48° north latitude and 109° west longitude, 50° north latitude and 111° west longitude, and flanking the disturbed belt in a thin band extending in the southwestern part of the study area between 48° and 51.5° latitude north. High vertical temperature gradient values reaching 44 to 48 °C/km are located at 48.5° north latitude and 112° west longitude. The northern part of the Alberta basin is characterized by high temperature gradients which range between 32 and 48 °C/km, generally increasing from the west to the east. Relatively higher temperature gradients are observed in west central Alberta, and near the Bashaw area, where a tongue of high temperature gradient is observed, extending from the eastern subcrop of the Nisku Formation to approximately 150 km westward, trending to the south. In west central Alberta, vertical temperature gradients increase to 40 °C/km over a relatively small area, and decrease radially to reach the regional values of western Alberta.

In the Williston basin, high temperature gradients reaching up to 52 °C/km form a band near the subcrop of the Nisku Formation in Southern Saskatchewan and Manitoba. Two major areas of high temperature gradients are located in the area bounded by 47.5° to 49° north latitude and 104° to 109° west longitude.

4.7 Oil API Gravity Distribution of the Nisku Formation

The purpose of mapping the API gravity is to correlate density-related migration patterns that are strongly related to either hydrodynamics or buoyancy. The API gravity map
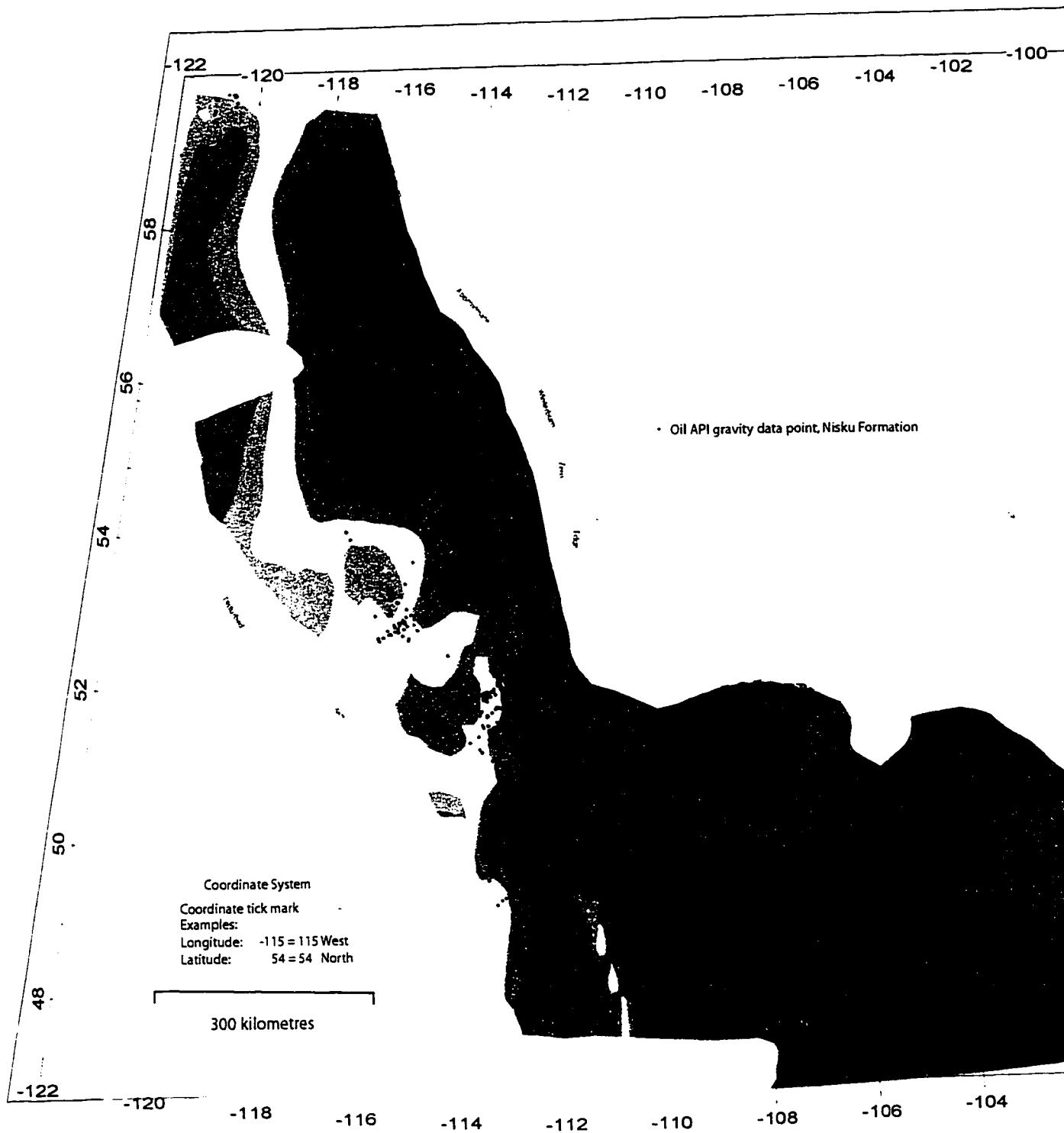
Figure 4.8 API gravity distribution of oils produced from the Nisku Formation, WCSB.

-116 -114 -112 -110 -108 -106 -104 -102 -100

60

58

56

• Oil API gravity data point, Nisku Formation

40

54

52

20

50

48

5

-100

-116 -114 -112 -110 -108 -106 -104 -102
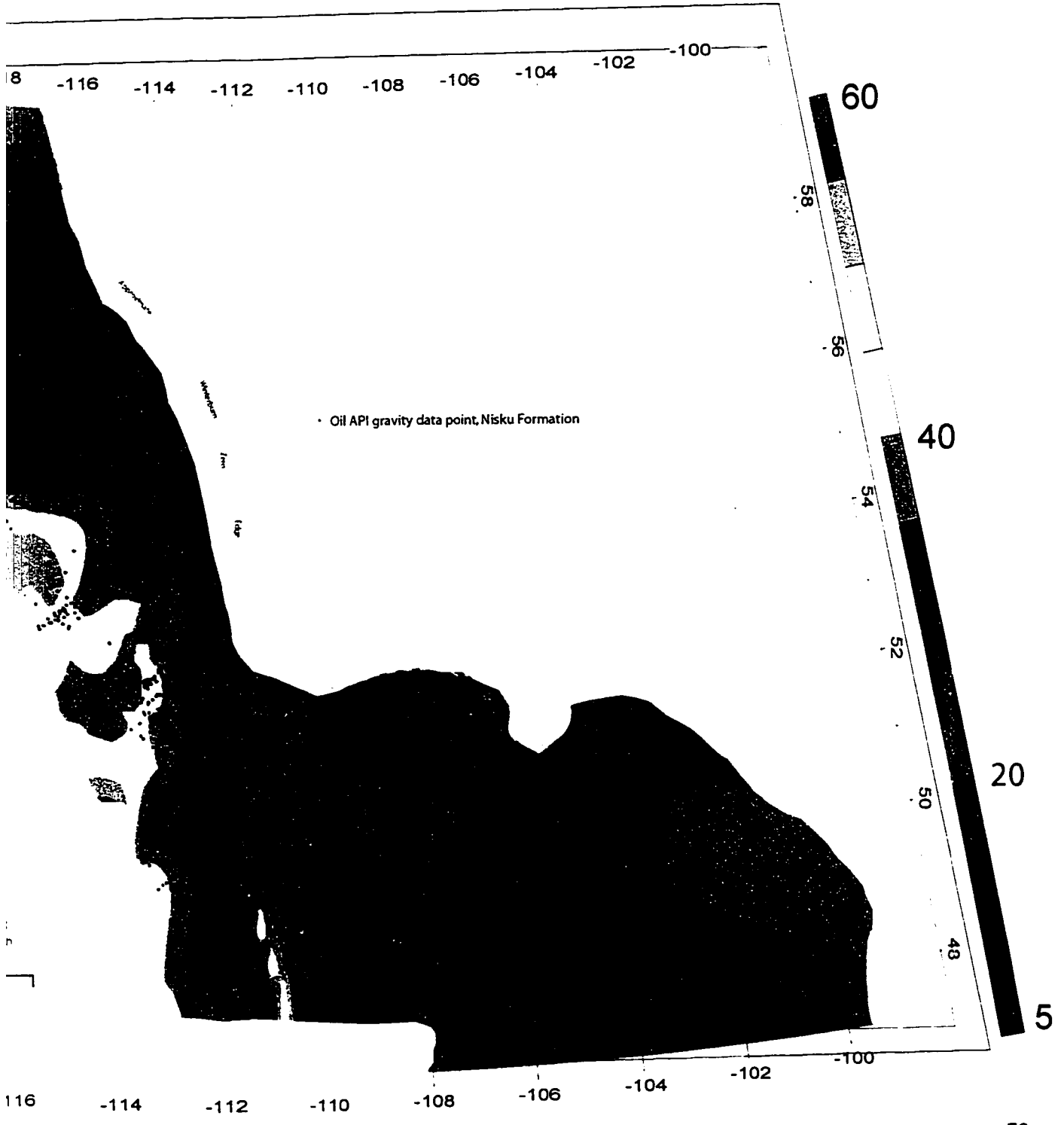
)ution of oils produced from the Nisku Formation, WCSB.

presented in Figure 4.8 shows several basinal-scale features. Due to the fact that a multitude of factors can influence the geographic distribution of the API gravity, the observations are going to be limited to those used for interpretation in Chapter 5, and which are supported by adequate data distribution posted on the map. It can be observed that there is a decrease in the oil API on the flanks of the Bashaw reef complex, and in general, away from the potentiometric high of south-central Alberta. On both flanks, the oil accumulations show a clear pattern of lower API than those in the Bashaw reef trend. The area of the Rimbey-Meadowbrook reef trend shows distribution of API gravity that is less than those observed at the Bashaw reef trend.

Corresponding to the potentiometric high of west-central Alberta is a high API gravity semi-circular shaped feature. The API decreases to the east, to the north, and to the southeast. To the southwest of West Pembina area is a tongue of high API gravity oil extending for tens of kilometers in distance.

4.8 Topography of the Study Area

A Topographic map of the study areas with the Nisku Formation subcrop and the outcrops in northwestern Montana is shown (Figure 4.9). Salient features in the Alberta basin include the decrease of land surface elevations from the range of 1100-1400 m near the disturbed belt to 500-300 m near the eastern subcrop of the Nisku Formation. In the Williston basin, land surface elevations decrease from a high of 900 m in the southwest to 500 m near the northeastern subcrop of the Nisku Formation.

At the highlighted outcrops of the Nisku Aquifer, elevations reach 1100-1400 m. Those are observed in northwestern Montana.
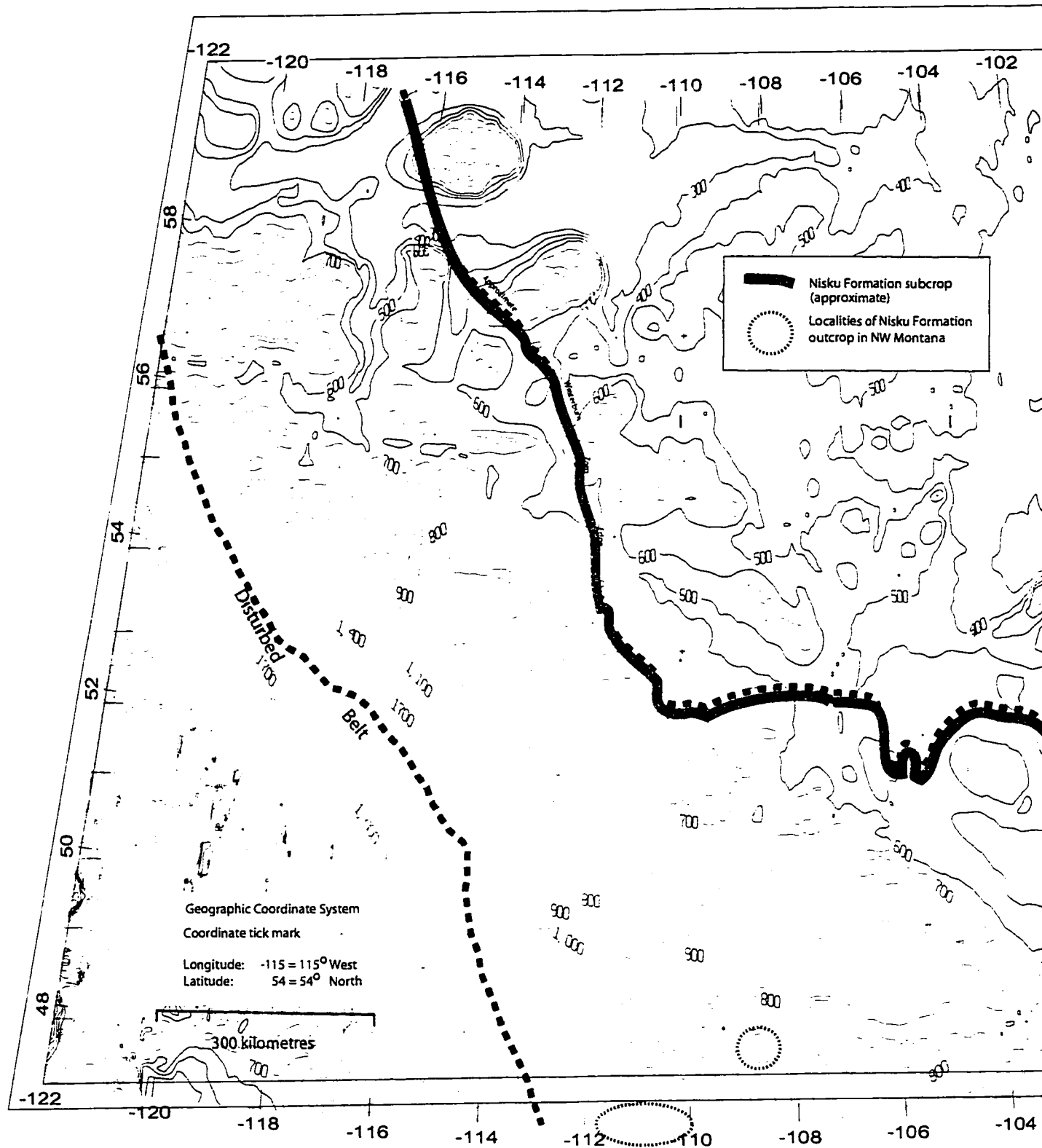
Figure 4.9 Topographic map of the WCSB. Elevations are in metres a.m.s.l. (C. I. = Variable).

Nisku Formation subcrop
(approximate)

Localities of Nisku Formation
outcrop in NW Montana
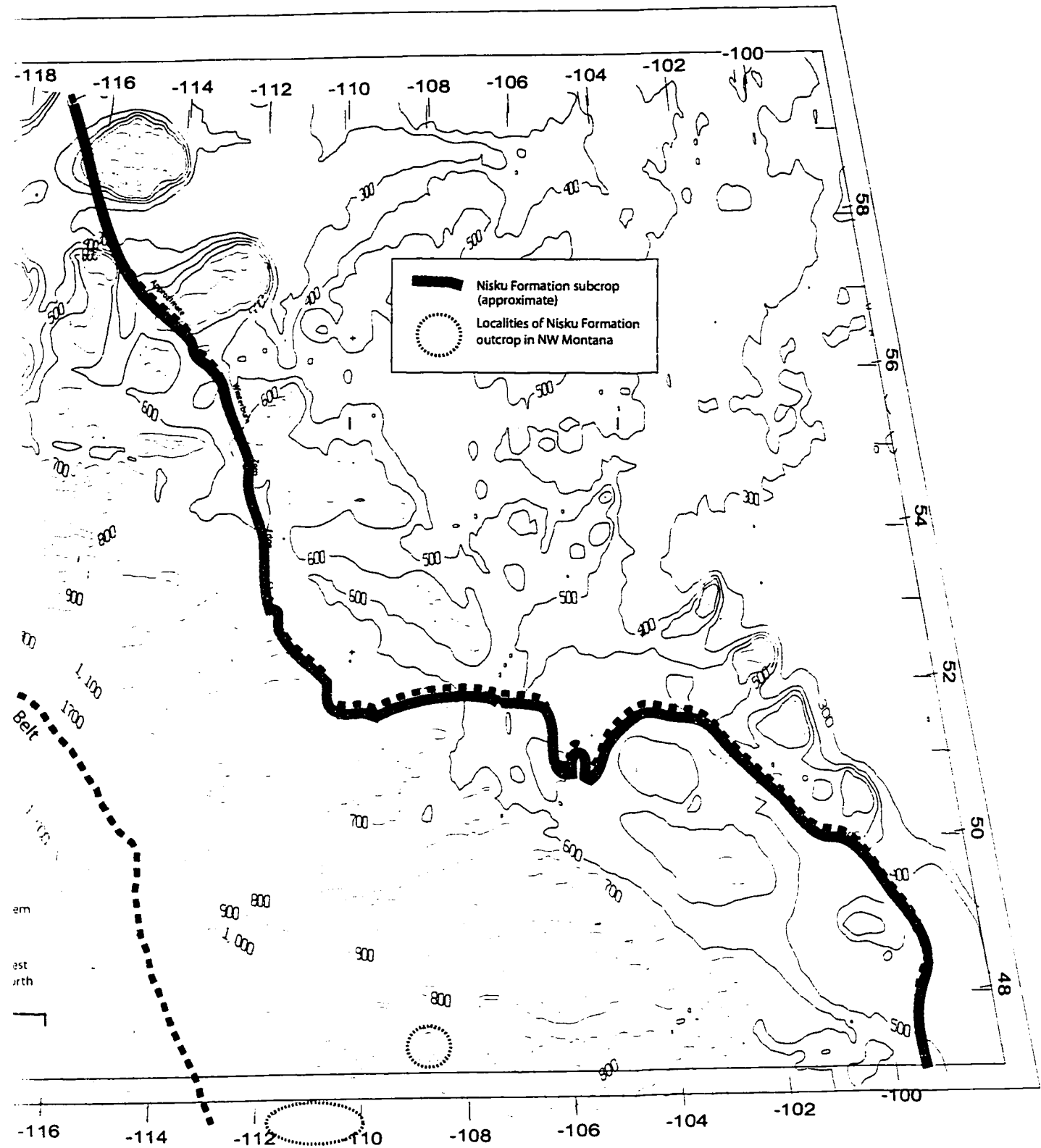
WCSB. Elevations are in metres a.m.s.l. (C. I. = Variable).

5.0 Hydrogeological and Petroleum Hydrogeological Syntheses

This chapter presents syntheses of the regional hydrogeology of the Nisku Aquifer, and its potential effects on hydrocarbon migration and entrapment. First, groundwater flow in the aquifer is discussed with an emphasis on groundwater density effects. Regional features and anomalies observed in the hydraulic head distribution (Figure 4.2) are also examined, aided by the p(d) plots constructed in areas of these features. Second, syntheses of hydrocarbon migration patterns dictated by groundwater flow systems in the Nisku Aquifer are given, in terms of WDFVs and the ODFVs (Section1.2.4 and & 1.5) analyses, and in terms of potential tilt in the oil-water contact.

5.1 Effects of Density on Groundwater Flow in the Nisku Aquifer

Groundwater density has a major effect on flow in the Nisku Aquifer in some areas of the WCSB. Different geological and hydrogeological factors may play different roles in enhancing or reducing such effects. Those factors are translated into the three quantities used in evaluating the DFR for groundwater: structural gradients, horizontal hydraulic gradients, and differences in density between freshwater and groundwater. Understanding those effects on the Nisku Aquifer was possible with the aid of a number of maps to be presented here.

Map of vectors representing the directions of fluid-driving forces in the Nisku Aquifer based on negative horizontal hydraulic gradients is presented in Figure 5.1. Those vectors are normal to contour lines of hydraulic heads calculated using freshwater density. As stated in Chapter 1, flow directions derived in such a manner can be erroneous in cases where the DFR increases above 0.5, according to Davies (1987).

The DFR map for the Nisku Aquifer in the WCSB is shown (Figure 5.2). In most of the basin, the groundwater DFR for is less than 0.5. However, DFR values exceed 0.5 in four major parts of the WCSB. In the Williston basin, DFR values exceed the 0.5 in the eastern part and in the southern part of the study area. In the Alberta basin, the DFR exceeds 0.5 in east-central Alberta, on both flanks and some distance away of the Bashaw reef trend, and around the area of the Karr basin.
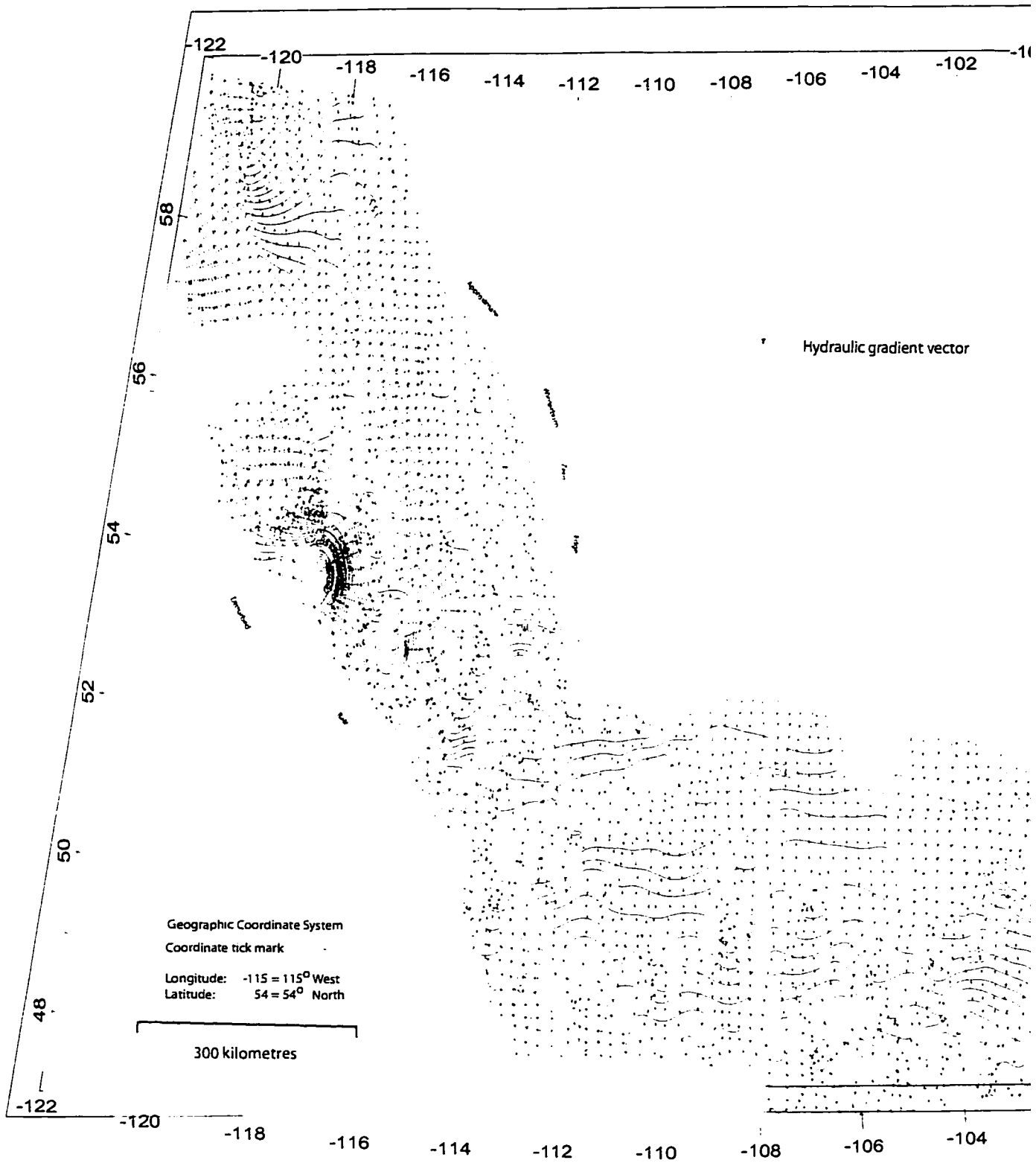
Figure 5.1 Hydraulic gradient vectors superimposed on a contour map of hydraulic head distribution in t
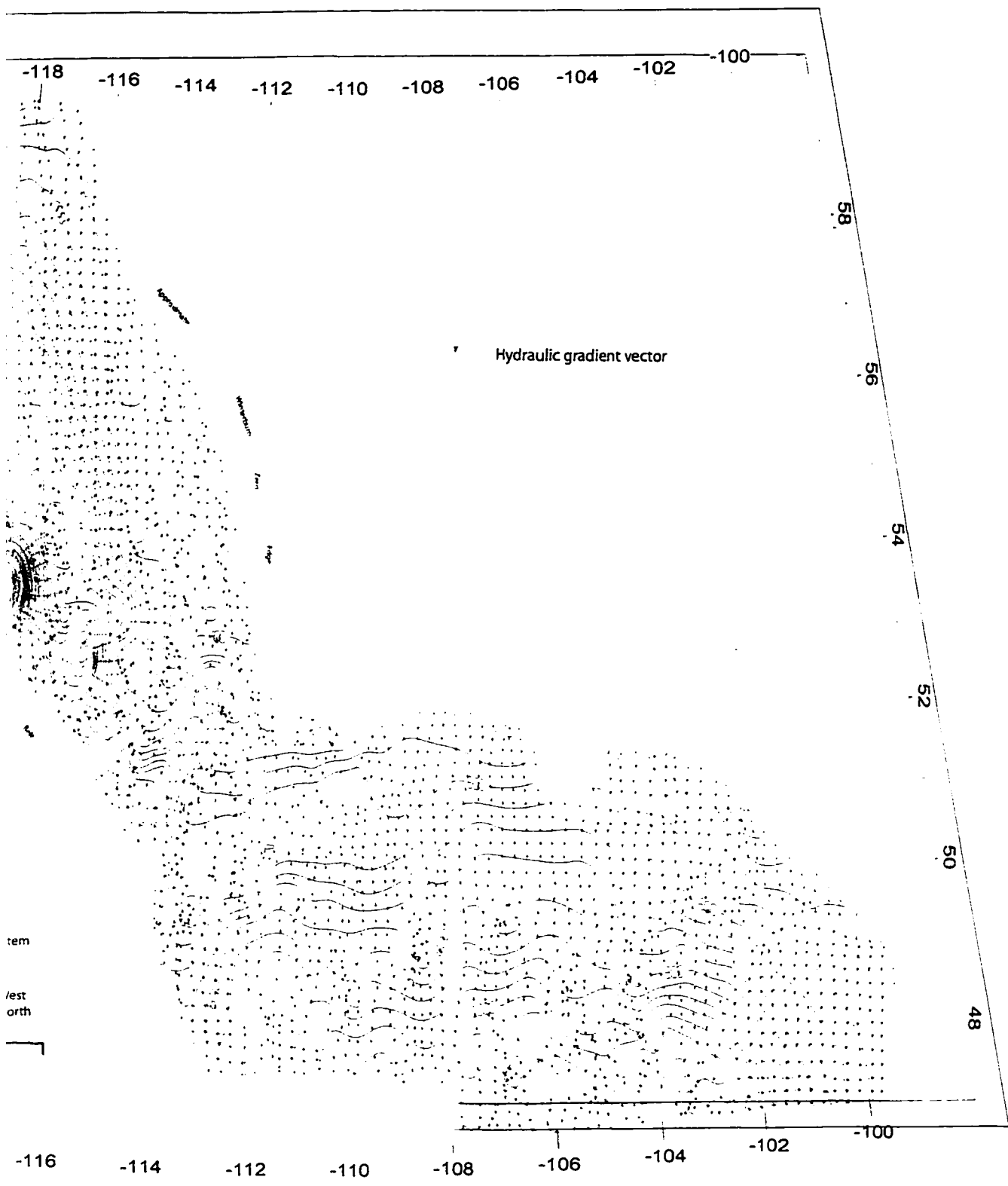
ctors superimposed on a contour map of hydraulic head distribution in the Nisku Aquifer, WCSB (C.I. = 50 m).
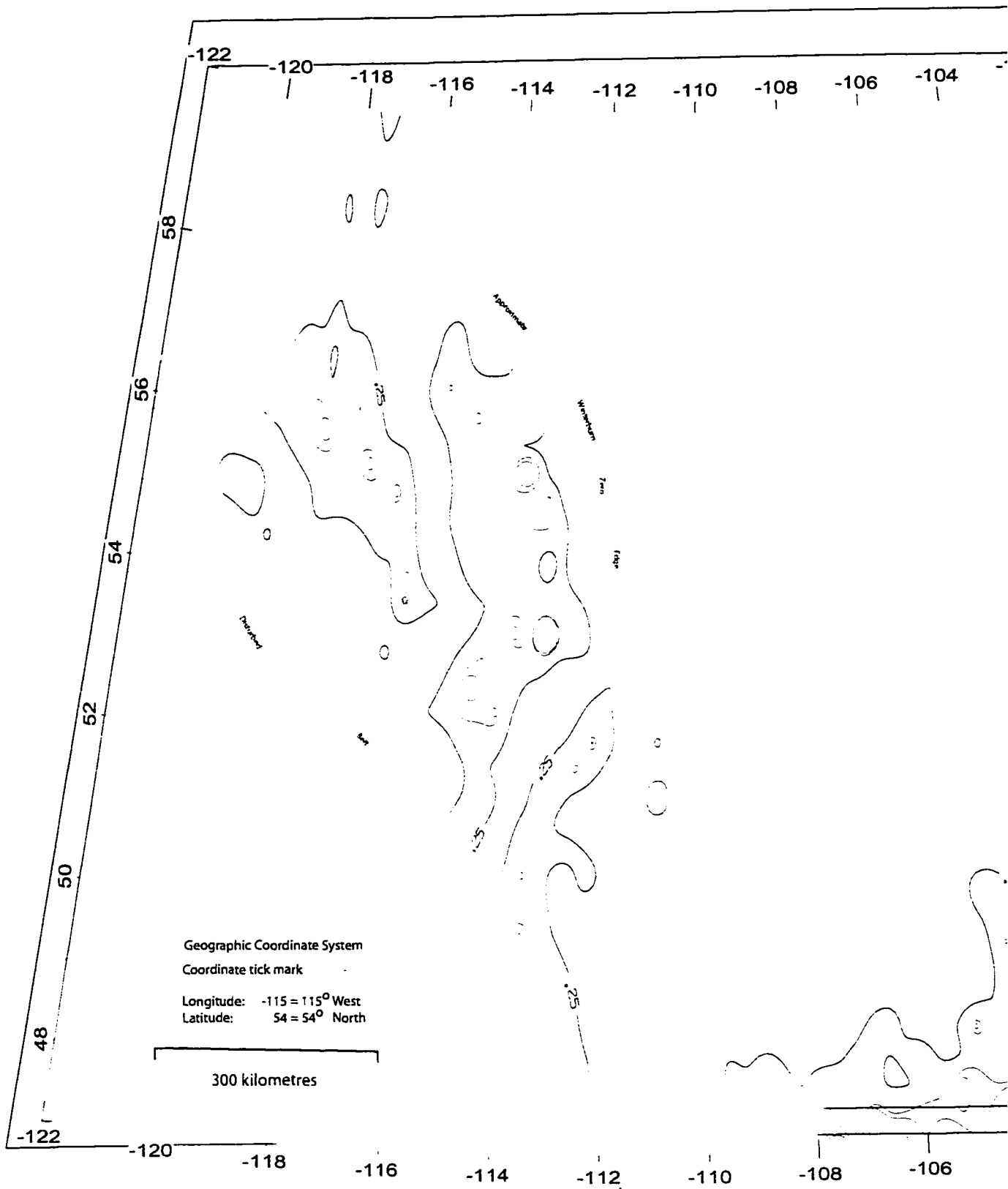
Figure 5.2 Distribution of the Groundwater DFR values for the Nisku Aquifer, WCSB (C.I. = .25).

-116 -114 -112 -110 -108 -106 -104 -102 -100

58

56

54

52

50

48

-100

-114 -112 -110 -108 -106 -104 -102 -100

FR values for the Nisku Aquifer, WCSB (C.I. = .25).

84
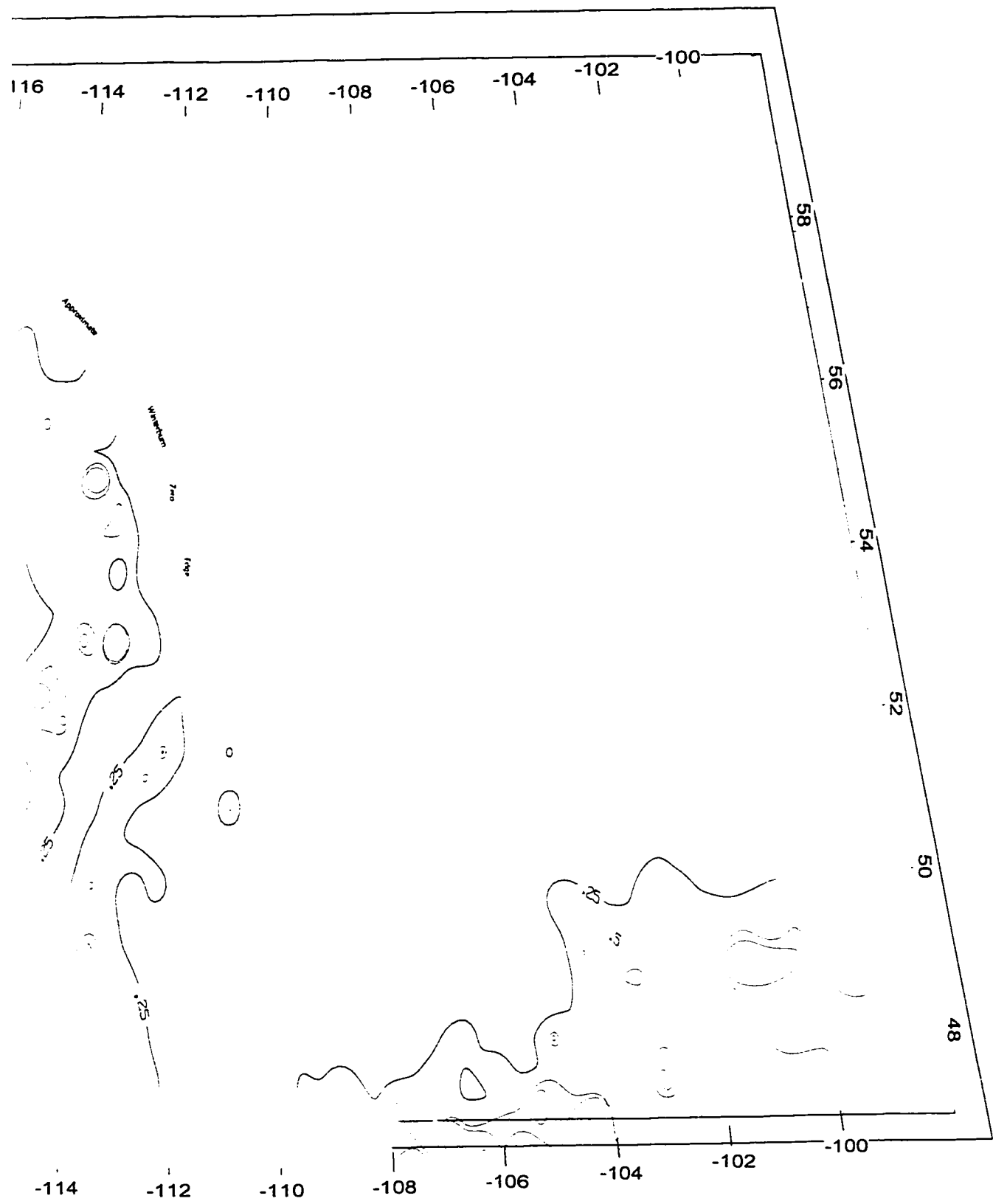
Visual examination of the DFR map (Figure 5.2), and maps of the quantities used in the calculation of the DFR in the Nisku Aquifer can give an indication as to which of those quantities has the direct influence of the DFR values in a particular area. Horizontal hydraulic gradients and density differences have already been described in Chapter 4. Structural gradients of the Nisku Aquifer show that they fall in the range of 3 to 24 m/km (Figure 5.3). In the Alberta basin, the structural gradient is highest in the western, deeper parts and in the area straddling the border between southwestern Alberta and northwestern Montana, where the gradients reach values of 24 m/km. In the Williston basin, the structural gradients range between 1 m/km in the northern tip of the Williston basin to 12 m/km in the deeper parts of the basin. A more detailed reasoning for changes in the DFR values are given in Section 5.2.

Corrected flow directions are shown in Figure 5.4 (blue arrows). Arrows in this map represent the WDFVs, whose magnitude is directly proportional to the arrows' lengths (shown in a classed scale for presentation purposes), and direction is read from their orientations. Manifestation of error introduced by using freshwater heads can be in flow direction, or in the magnitude. Such errors can be observed by examining maps shown in Figures 5.4, and 5.5. Figure 5.4 shows a visual comparison between horizontal hydraulic gradient vectors and WDFVs, where both are shown on the same map, the angles of differences between those two forces are contoured and shown in Figure 5.5.

From the differences in angle between the orientations of horizontal hydraulic gradient vectors and WDFVs, it is observed that largest errors overlap the general areas where the DFR values have exceeded 0.5. Due to the variety of hydrogeological conditions affecting the Nisku Aquifer in the WCSB, identification of which factors dictate the presence of density effects or lack thereof are included in Section 5.2, for each individual area of the basin (Figure 4.2), in order to link it with local hydrodynamic regimes.

5.2 Synthesis of Groundwater Flow in the Nisku Aquifer

This section presents a synthesis of groundwater flow in the Nisku Aquifer at selected areas of the WCSB. Reference to the geographic location of those areas follows the designations shown in Figure 4.2. p(d) plots were constructed for most of those areas in
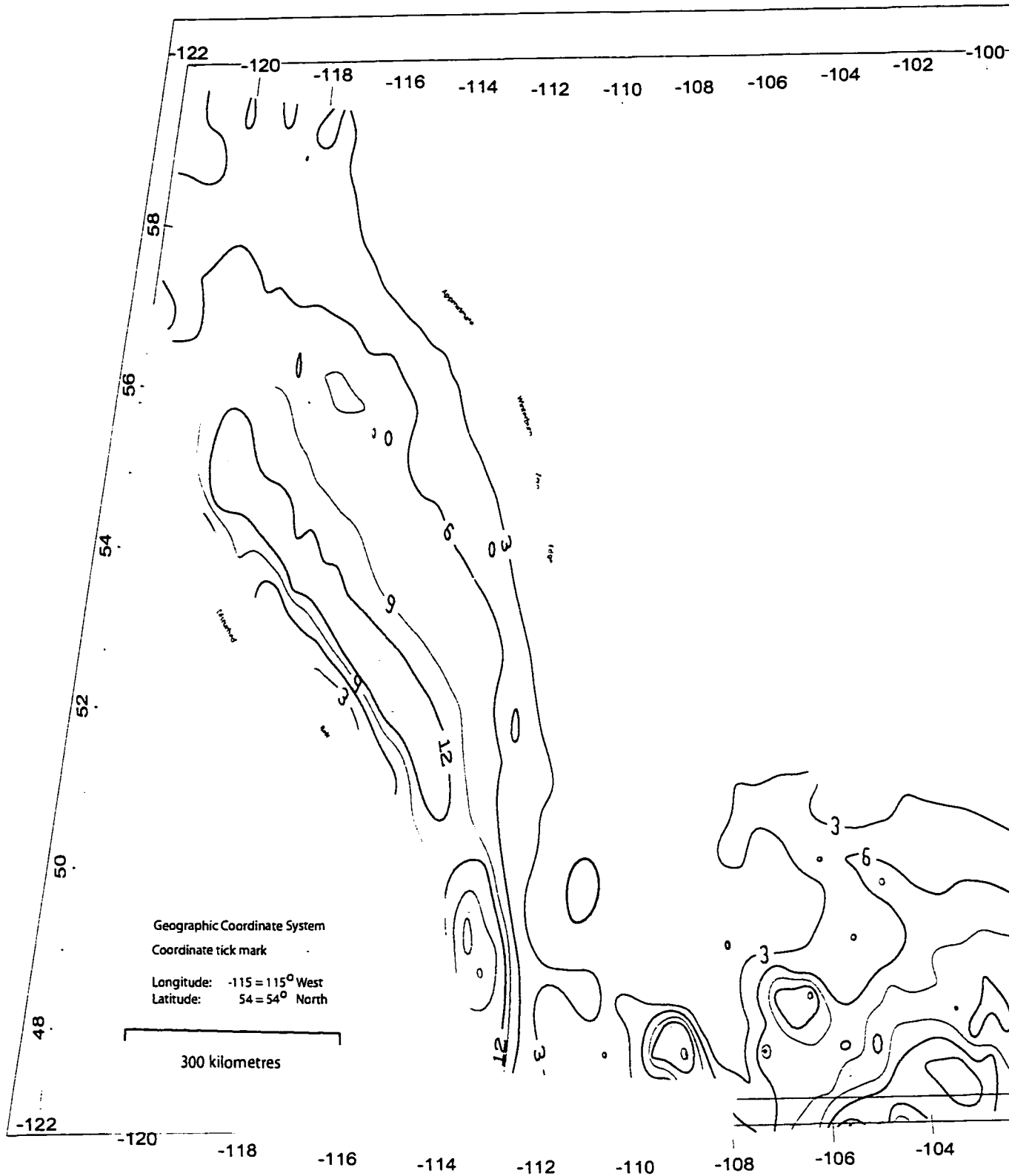
Figure 5.3 Magnitude of structural gradients for the Nisku Aquifer, WCSB (C. I. = 3 m/km).
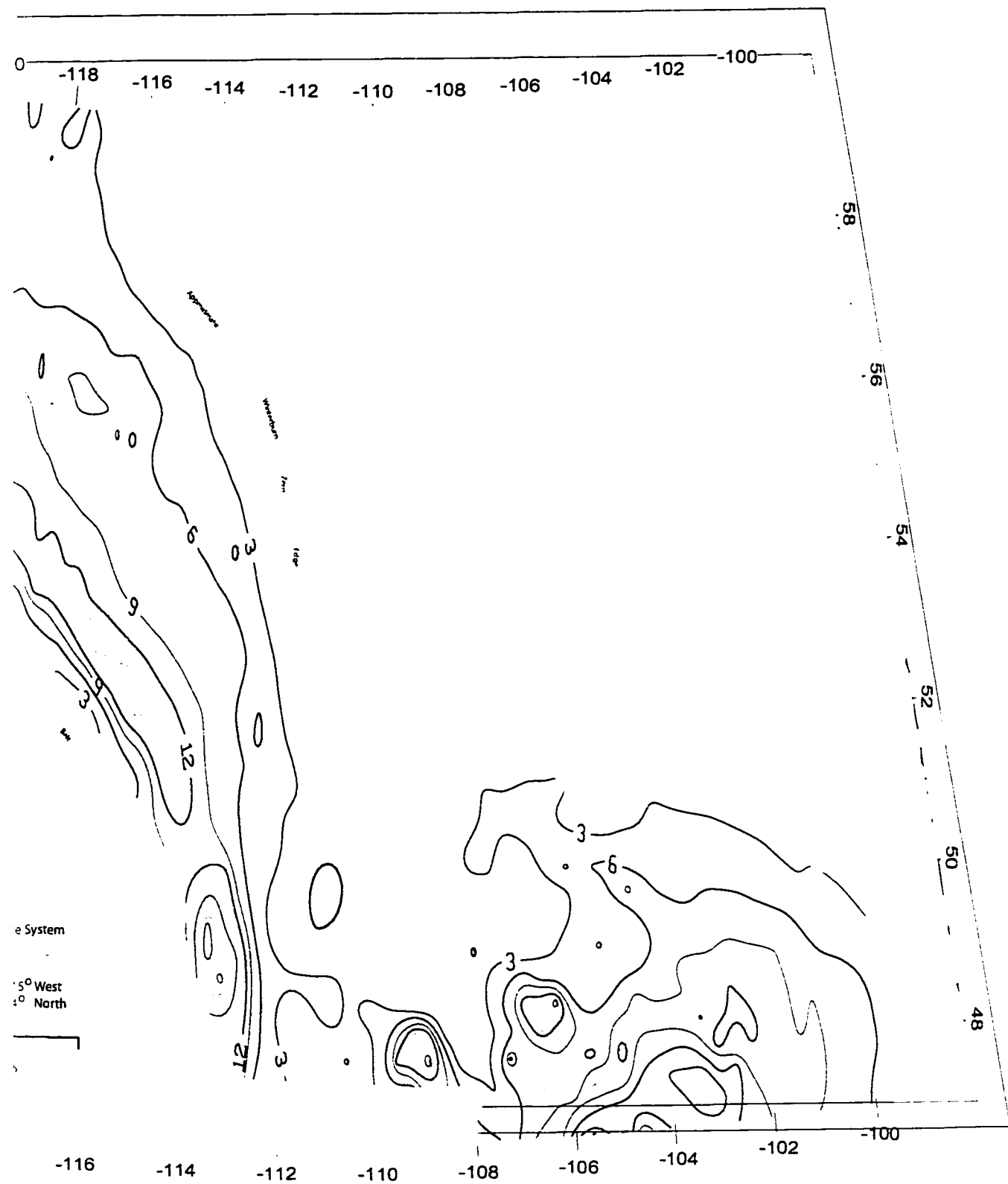
uctural gradients for the Nisku Aquifer, WCSB (C. I. = 3 m/km).
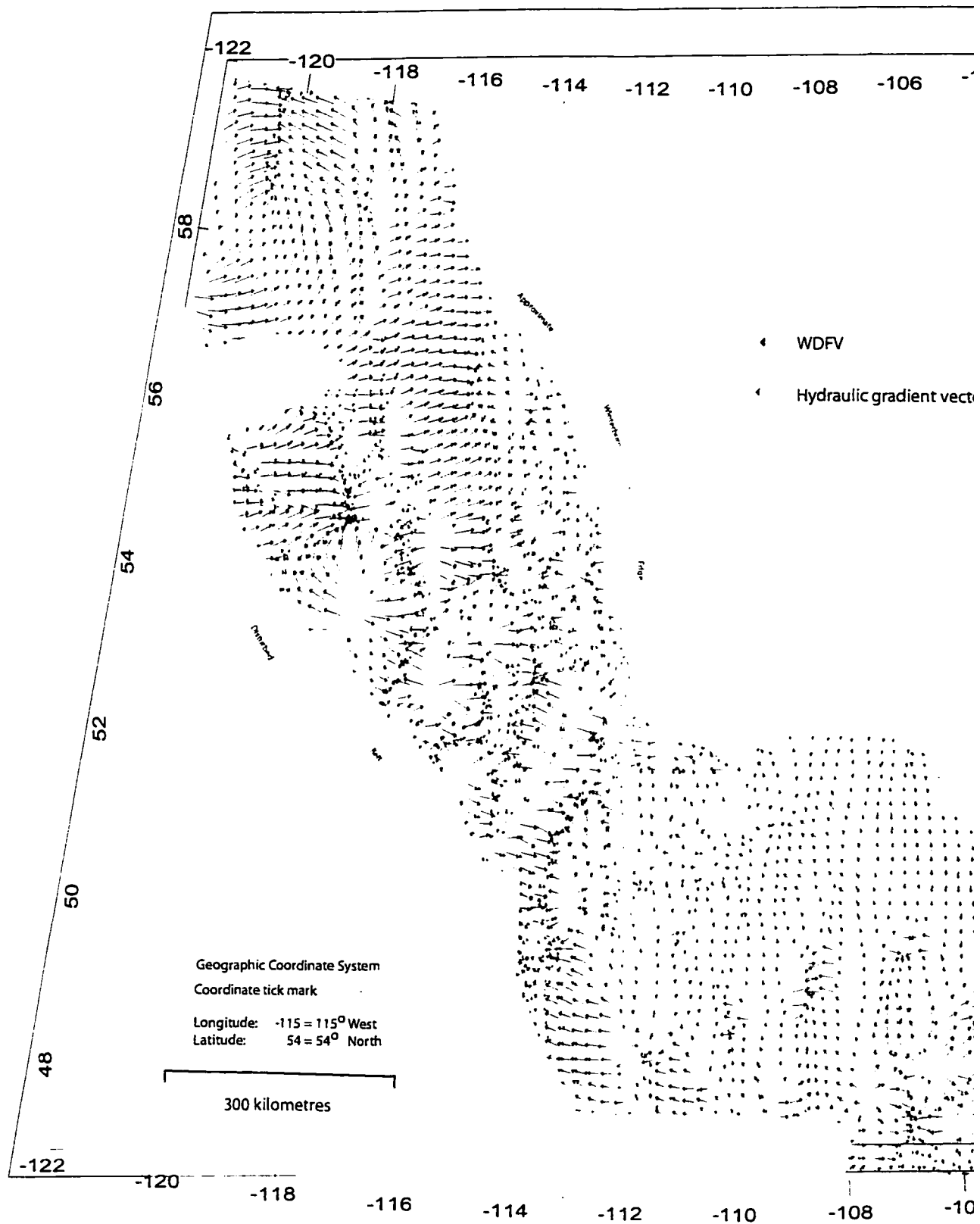
Figure 5.4 Comparison between hydraulic gradient vectors and WDFV's in the Nisku Aquifer, WCSI
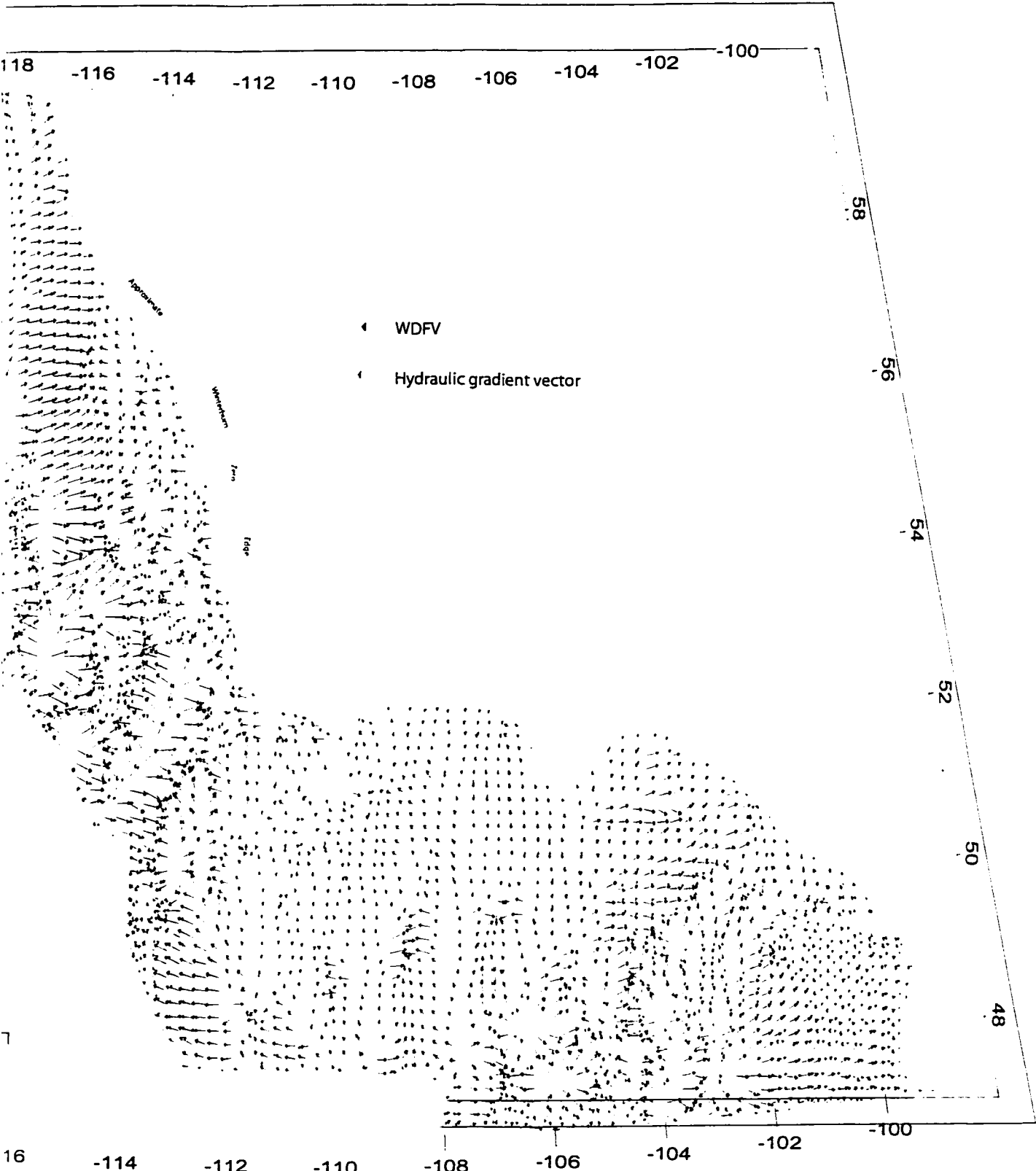
Hydraulic gradient vectors and WDFV's in the Nisku Aquifer, WCSB.
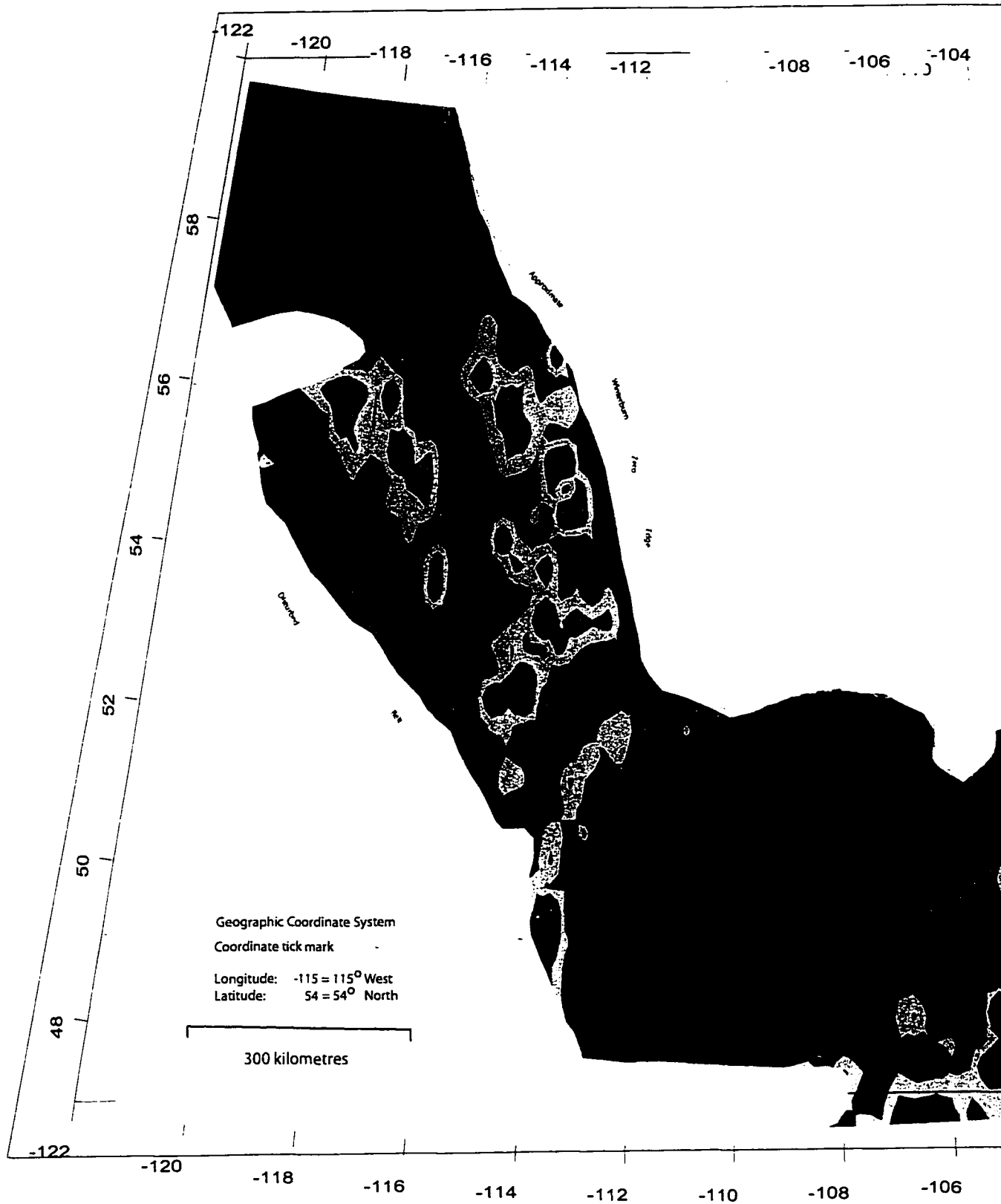
Figure 5.5 Map of angular differences between the orientation of hydraulic gradient vectors and WD
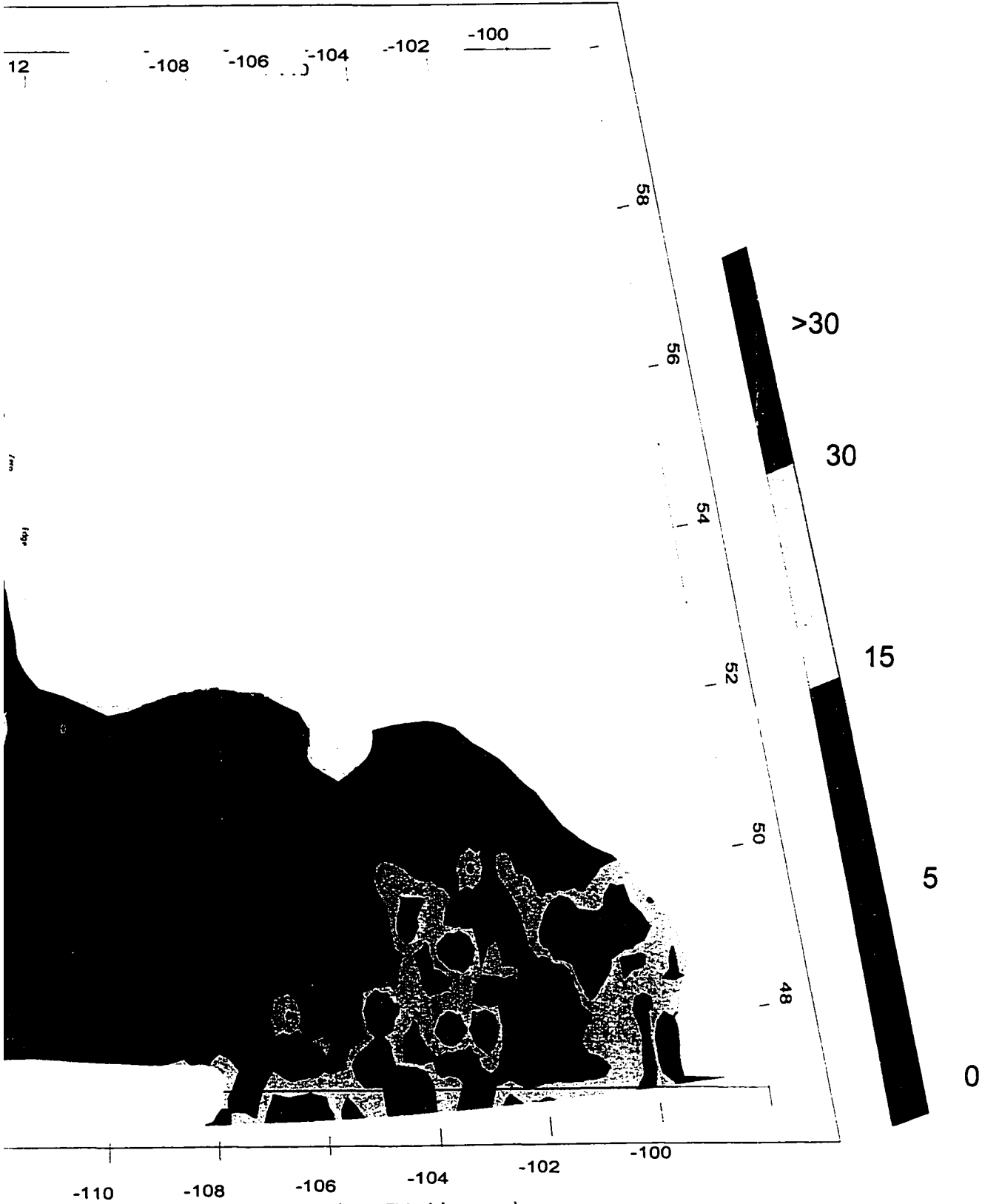
of hydraulic gradient vectors and WDFVs (degrees).

order to further understand the pressure regime in the geologic succession and assess possible vertical movement of groundwater, and how groundwater flow in the Nisku Aquifer relate to it. Observations made from the p(d) plots may vary for each area such that it will highlight the particular hydrogeological feature affecting the Nisku Aquifer. Geographic locations of the p(d) plots are also shown in Figure 4.2. Relevant TDS, density effects, and vertical temperature gradient anomalies falling within those areas are also interpreted.

5.2.1 South Central Alberta Area

Geological and hydrogeological evidences indicate that the northeast-southwest trending high hydraulic heads in the Nisku Aquifer of south central Alberta (area E, Figure 4.2) are caused by breaching in the Ireton Aquitard, associated with ascending groundwater flow from the underlying Leduc Aquifer. Geological and hydrogeological evidences in parts of the area were previously presented by several workers including Paul (1994), Rostron (1995), Rostron et al. (1997), Anfort (2001), and are supported here with a regional p(d) plot. Flow is directed to the northwest, southeast, and east. Effects of groundwater density on the flow are minimal close to the Bashaw reef trend, and increase away from it.

A regional p(d) plot was constructed in the area in order to characterize the flow system in a vertical sense (Figure 5.6). It is observed that two distinct pressure regimes are present in the sedimentary succession. An upper system which extends from surface to a depth of approximately 1.4 km. This system is underpressured, and adjusting to local present day topography. The Underpressuring is identified by pressure values being significantly less than those of the freshwater pressure gradient. The pattern of change in p(d) gradients in response to land surface topography suggest a system that is affected by local topography. The p(d) data show increase of p(d) gradients with the decrease of KB elevation ranges where pressures were observed. A p(d) trendline observed at KB elevation range of 800-850 m shows a p(d) gradient of 11.4 MPa/km, while that of KB elevation range of 950-1000 m shows a p(d) gradient of 6.2 MPa/km (Figure 5.6).

A second lower system, extending from a depth of 1.4 to 2.5 km and encompassing data from the Nisku Aquifer is observed. This system is characterized by a general p(d)
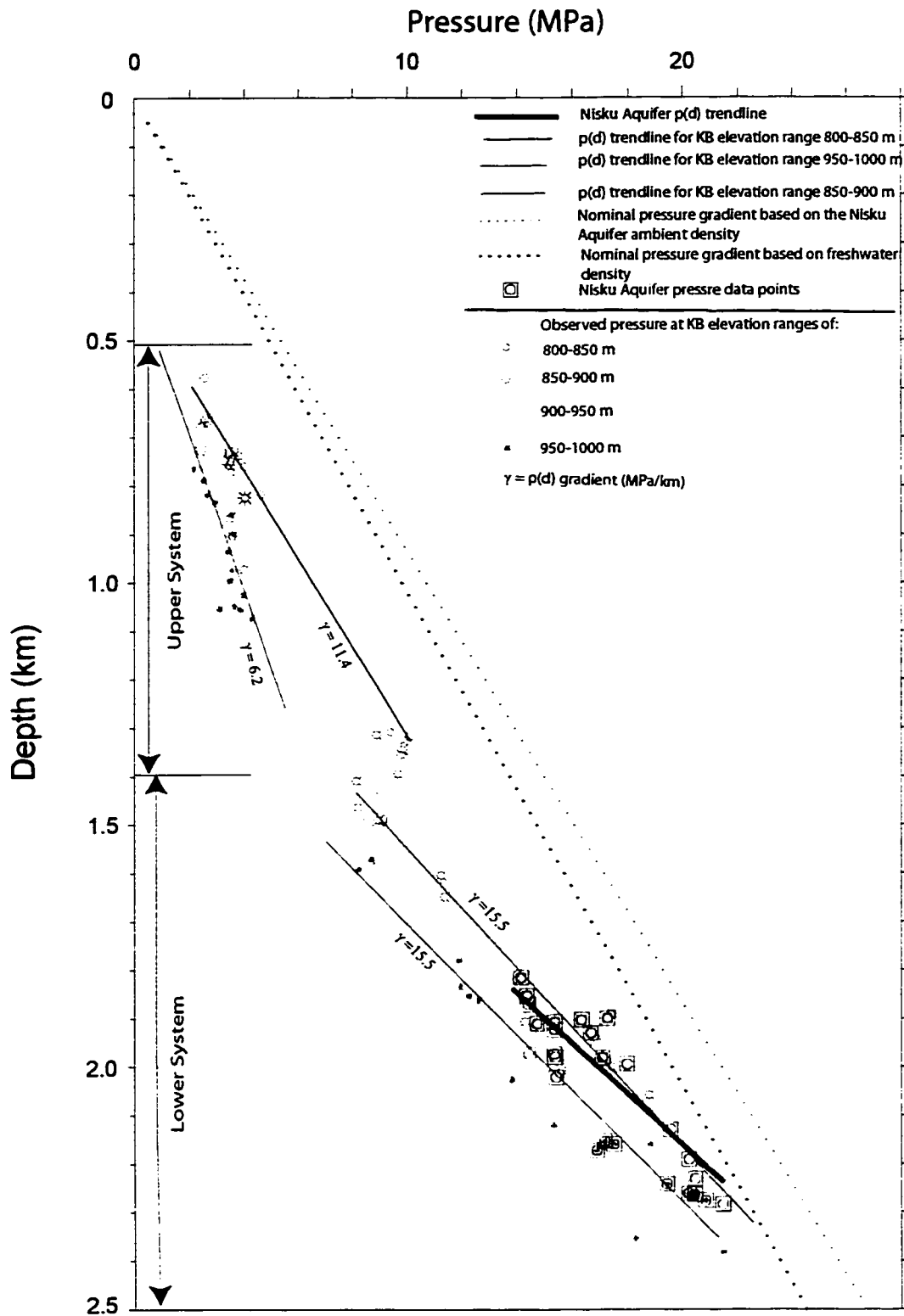
Figure 5.6 Regional p(d) plot for the south central Alberta
area (see Figure 4.2 for location)

gradient of approximately 15.5 MPa/km calculated for pressure observations at KB elevation ranges of 850-900 and 950-1000 m, which is greater than the nominal p(d) gradient in the area calculated according to the ambient groundwater density in the Nisku Aquifer. This indicates a significant component of vertically upward flow. The aquifers, including the Nisku Aquifer are underpressured, but the underpressuring becomes lesser in magnitude with increasing depth. Nisku Aquifer p(d) trendlines also demonstrate p(d) gradients greater than nominal p(d) gradients based on ambient Nisku Aquifer density.

Based on the above observations, and previous studies performed in parts of the area indicating breaches in the underlying Ireton Aquitard (Rostron, 1995; Hearn, 1996; Rostron et al., 1997) it can be concluded that the area of the Bashaw reef trend demonstrates relatively high hydraulic heads caused by vertically-upward cross-formational flow from the underlying Leduc Aquifer, and the Nisku Aquifer in the Area is underpressured.

The above conclusions raise the need for further examination to investigate the reason for 1) the underpressuring and 2) the mechanism that provided the energy to drive the flow upward. In general, it can be speculated that the underpressuring is caused by the removal of a thick sedimentary section in the Alberta basin (Nurkowski, 1984; Bustin, 1991), or due to discharge of aquifers at low topographic elevation a distance away from the p(d) plot area. On the other hand, the likely mechanisms that can provide energy to drive the cross-formational flow are 1) the response of the area to a regional topographic high at a distance, 2) energy that is preserved from compaction or compression during the formation of the foreland basin, or 3) hydrocarbon generation process. As noted by Rostron et al. (1997), the exact mechanism that provided the energy to this flow system is unknown.

Groundwater density effects on lateral flow in this area are reduced within proximity of the Bashaw reef trend (Figures 5.2, 5.4, 5.5), and increase in zones away from localities of cross-formational flow. Relatively high horizontal hydraulic gradients ranging between 3 and 6 m/km (Figure 4.3), developed as a result of the high hydraulic heads associated with cross-formational flow result in reduced DFR values (Figure 5.5), despite comparatively elevated structural gradients (Figure 5.3), and the relatively high groundwater density differences (Figure 4.5) which would otherwise increase the DFR.

Thus, it can be concluded that high fluid potentials, for which the energy is provided by cross-formational flow, causes the horizontal hydraulic gradient force vectors to dominate over the negative buoyancy driving force vector. Groundwater is directed outward and away from the northeast-southwest trending hydraulic head mound to the northwest, southeast, and northeast.

5.2.2 West Central Alberta Area

In the area of west central Alberta (area D, Figure 4.2), hydrogeological and geological evidences indicate that the anomalously high hydraulic heads are due to areas where overpressuring is preserved in rocks that are in poor hydraulic communication with the regional aquifer. Those rocks are in shale basins reported in west central Alberta (Putnam and Ward, 2001; Bachu et al., 2002). However, and within a close proximity to those anomalously overpressured rocks, cross-formational flow from underlying aquifers into the Nisku Aquifer causes the relatively elevated fluid potential in the area. The overpressuring in the Nisku Aquifer does not seem to influence the upward cross-formational system. Evidences to such syntheses come from previous geological and hydrogeological studies, and patterns observed from the hydraulic head map of the Nisku Aquifer (Figure 4.2), p(d) plot (Figure 5.7), and vertical temperature gradients (Figure 4.7).

This area has been reported by Putnam and Ward (2001) as having hydraulic heads reaching 4000 m. Putnam and Ward reported that such high hydraulic heads in the Nisku Aquifer are observed in locally developed shale basins. The observations made by Putnam and Ward (2001) were questioned by Bachu et al. (2002), who stated that Putnam and Ward (2001) did not show data to support the extent of the anomalously high fluid potential. Furthermore, Bachu et al. (2002) do not agree that the Nisku Aquifer is recharged from high elevations in the disturbed belt (Putnam and Ward, 2001) where the Nisku Formation outcrops (Putnam and Ward, 2001, Bachu et al., 2002). Bachu et al. supported their reasoning by previous hydrogeological work (Wilkinson, 1995; Hitchon and Friedman, 1969; Grasby and Hutcheon, 2001) and geochemical evidences (Connolly et al., 1990a, b; Machel et al., 1995, Manzano et al., 1997). On the basis of studies by

Wendte et al. (1998), Bachu et al (2002) attribute overpressuring as being localized to individual isolated reefs rather than an overpressuring affecting the general area.

A p(d) plot for west-central Alberta (Figure 5.7) shows three hydrogeological systems in the sedimentary succession: an upper system, a middle system, and a lower system. An upper system, extending to a depth of 2.4 km, where p(d) gradients increase as the KB elevation ranges where pressures were observed decrease, suggesting an influence by local topography. Trendlines through pressure measurements at elevation ranges of 700-800 and 1100-1200 m have p(d) gradients of 9.6 and 7.6 MPa/km, respectively. In the middle system, no clear trends in the p(d) data are observed, and thus this zone is probably a transition between the upper and the lower system. The lower system, in contrast, has p(d) trendlines of similar slopes of about 15 MPa/km, which is greater than the Nominal p(d) gradient at the Nisku Aquifer's ambient density, suggesting vertically upward movement of groundwater. This pattern extends from a depth around 2.6 to 4.2 km. p(d) trendline through data from the Nisku Aquifer suggest a p(d) gradient close 15 MPa/km.

Upward movement of groundwater is also suggested by vertical temperature gradients (Figure 4.7). In west central Alberta, relative increases in vertical tempereture gradients in the Nisku Aquifer are observed, reaching 40 °C/km where at similar depths along strike of the Nisku Formation (Figure 2.6), exhibit vertical temperature gradients of 28-32 °C/km. Ascending fluids can cause such elevated vertical gradients at any location in the basin, given that fluids are ascending from depths (Hitchon, 1984).

Upward cross-formational flow in west central Alberta is further substantiated by geological evidences. As reprted by Skilliter (2000), breaches in the Ireton Aquitard below the Nisku Aquifer are present in the area. Also, maps and cross sections show the Ireton Formation (Switzer et al., 1994) showing a lithofacies change in the area from shale to dolomite as well as continuities between reefs of the Leduc and Nisku formations. Putnam and Ward (2001) also alluded to such a presence of hydraulic continuity between the Leduc (the underlying aquifer) and the Nisku aquifers.

The presence of low permeability zone in this region is confirmed by the high hydraulic gradients observed in the Nisku Aquifer hydraulic head map (Figure 4.2) where there is a
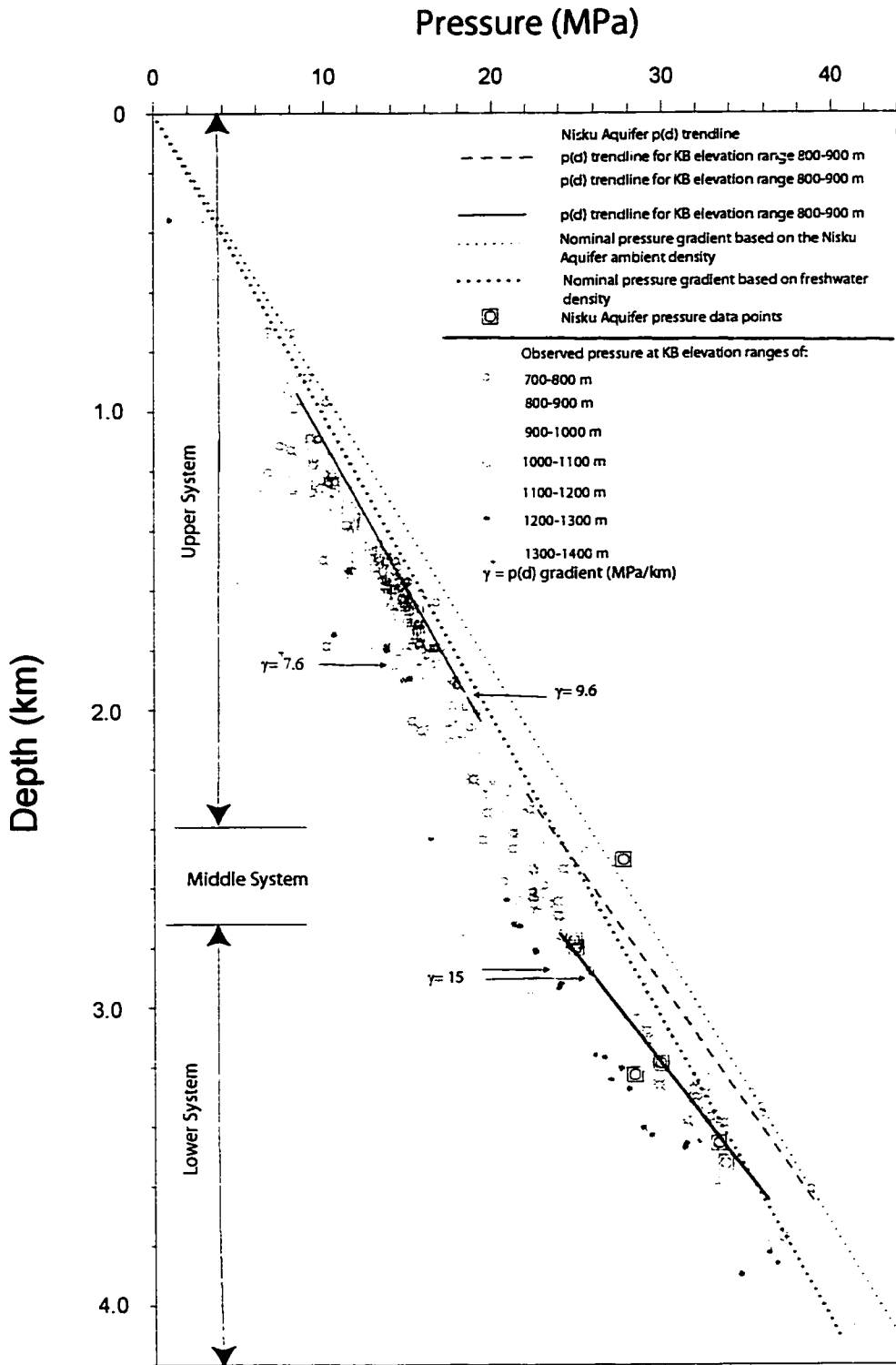
Figure 5.7   Regional p(d) plot west-central Alberta area (see Figure 4.2 for location)

significant drop in energy, expressed by the high horizontal hydraulic gradients (Figure 4.3) due groundwater flows in the relatively lower permeability rocks.

While the anomalously high hydraulic heads observed are likely to be restricted to localized zones of poor hydraulic communication with the regional hydrogeologic regime, relatively high hydraulic heads, of less magnitude than those caused by overpressuring, are present in the area and have been previously presented in hydraulic head maps of the Nisku Aquifer (Simpson 1999). This high hydraulic head forms a zone where flow is directed radially outward which is a further evidence that groundwater is being introduced into the Nisku Aquifer through cross-formational flow.

Groundwater density effects are minimized in west central Alberta due to high horizontal hydraulic gradients (Figure 4.3). High horizontal hydraulic gradients reduce the DFR values to below 0.5 despite the relatively high structural gradients (Figures 5.2 and 5.3) and high density differences between freshwater and groundwater in the Nisku Aquifer (Figure 4.5).

To summarize, the west central Alberta area demonstrates high hydraulic heads, partly due to some localized overpressuring, and mostly due to upward cross-formational flow. The proximity of overpressuring to areas of cross-formational flow may lead to misinterpretation that the high hydraulic heads are purely due to ascending fluids. The whole scenario is elucidated by the consideration of previous studies (Putnam and Ward, 2001; Bachu et al. 2002), and by the construction of a p(d) plot to assess the fluids vertical fluid movement. High hydraulic gradients reduce the effects of high-density groundwater from significantly affecting the flow regime.

5.2.3 West Pembina Area

In West Pembina area, the localized high hydraulic heads (Figure 4.2) are likely to be caused by hydrocarbon generation, although other mechanisms cannot be ruled out. Hydraulic heads, reaching more than 1200 m and dropping to 600 m over a relatively short distance, direct the flow radially away from the area. Evidences include previous geological and petroleum geochemical studies, hydraulic head distribution (Figure 4.2), and observations from the p(d) plot constructed for the area (Figure 5.8). Groundwater

95

density effects are reduced in areas of high horizontal hydraulic gradients, but become significant away from them.

In the p(d) plot, two primary pressure systems are observed. A system that is underpressured extends from 0.4 to 4.0 km in depth in the sedimentary succession. Another normally to overpressured system extends between the 1.4 and 3.5 km in depth. Pressure data from the Nisku Aquifer fall in under-, normally-, and overpressured systems. The overpressuring is mostly in the pressure measurements made in the hydrocarbon phase (oil and gas).

Overpressuring in the hydrocarbon phase is a well-understood phenomenon (Neuzil, 1995) and is usually attributed to differences in density between groundwater and the hydrocarbon phase. The magnitude ranges of such overpressuring can be related to the hydrocarbon column height in a structural trap or updip lateral extent of a stratigraphic trap and the density differences (Appendix B). Observed magnitudes of overpressuring the West Pembina area is in the range of 8 MPa. Such magnitude would require an excessively long column and a continuous gas phase and oil in the case of a structural trap, and an excessively large pool in the case of a structural trap (Appendix B). Thus, the overpressuring in West Pembina, based on the analysis in appendix B, is not caused by density differences. Detailed analyses of the continuity of the hydrocarbon phases in West Pembina are beyond the scope of this study, but such high hydrocarbon columns are unlikely based on the sizes of pools in the area (Chevron Exploration Staff, 1978; Switzer et al., 1994). Thus, it is concluded that overpressuring is caused by a regionally overpressured aquifer. This conclusion is also supported by pressure measurements in the water phase, which were used to generate the hydraulic head map.

Reported hydrocarbon generation in the area (Chevron Exploration Staff, 1978; Fowler et al., 2001) provides possible mechanism for overpressuring. Preservation of overpressuring can be attributed to the low permeability rocks. High permeability rocks of the Zeta Lake member of the Nisku Formation (Chevron Exploration Staff, 1978) are probably encased by lower permeability rocks on a basinal scale. Another indicator of the low permeability on a regional scale is the high horizontal hydraulic gradients observed around West Pembina (Figures 4.2 & 4.3), which suggest a high rate of energy loss of fluid potential.
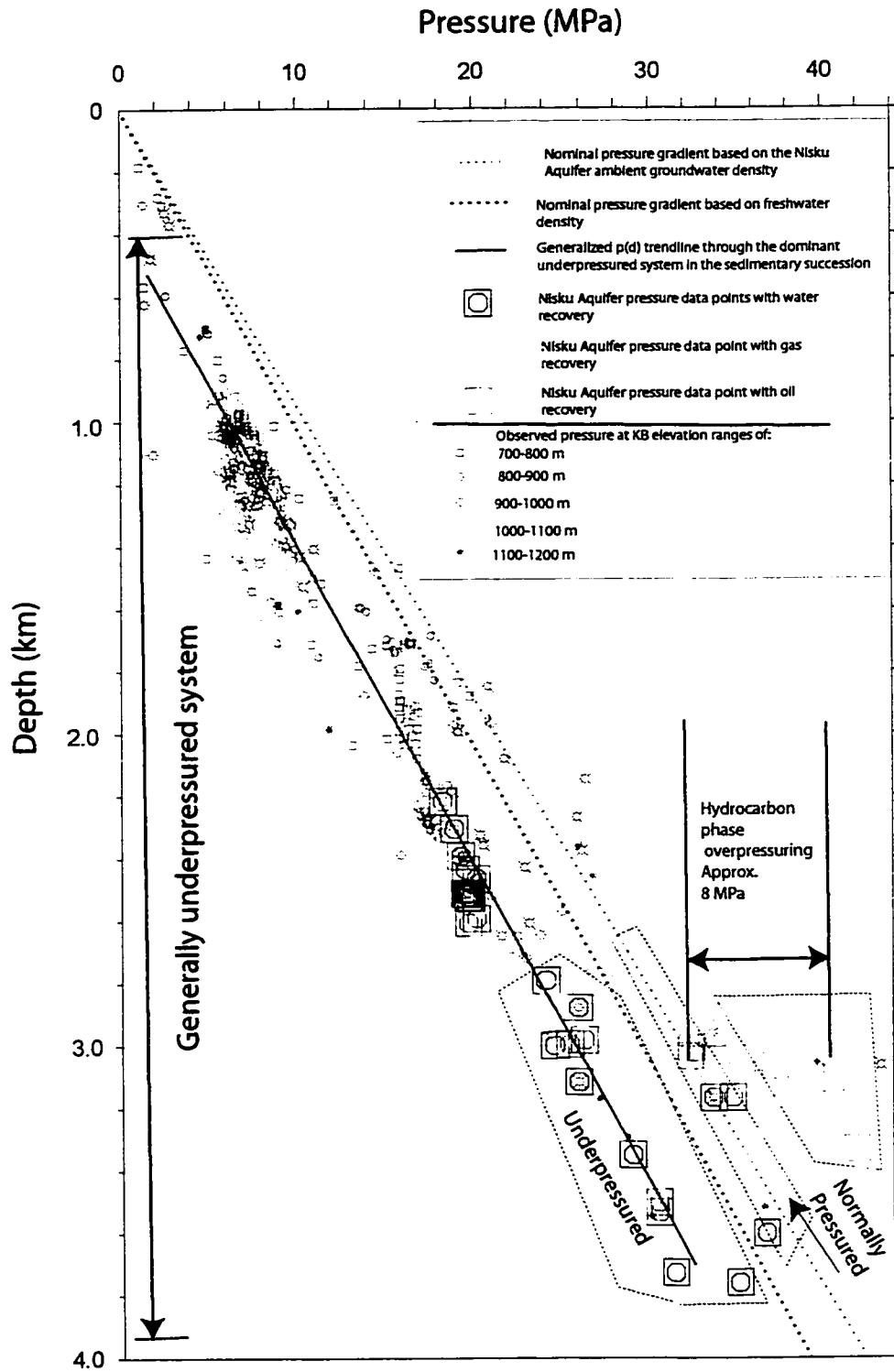
Figure 5.8 Regional p(d) plot for West Pembina area (see Figure 4.2 for location)

97

High horizontal hydraulic gradients in West Pembina, reaching to 15 m/km (Figure 4.3) at certain locations, lead to reduced values of the DFR (Figure 5.2) and thus leading to reduced effects of density effects on lateral groundwater flow in the whole area affected high hydraulic gradients (Figures 5.4 & 5.5). However, where the horizontal hydraulic gradients are reduced to the north and south of the area, the DFR value increases to values around 1.

5.2.4 East Central Alberta Area

The area of east central Alberta represents a regional low in hydraulic heads where the Nisku Aquifer demonstrates an upward directed flow, and probably makes a transition from a regional to local flow system. Such understanding is substantiated by a p(d) plot, basin-scale topography, vertical temperature gradients, and published models of flow in the WCSB. Density effects on lateral groundwater flow in east central Alberta are significant primarily due to reduced horizontal hydraulic head gradients associated with relatively elevated structural gradients.

The p(d) plot for east central Alberta exhibits three major flow systems (Figure 5.9). An upper zone extends from the land surface to a depth of about 0.9 km. This zone is characterized by increasing data scatter from the land surface and maximized at the depth of 0.9 km. The slopes of the lines defining the maximum and the minimum trends of this scatter are 10.4 and 7.0 MPa/km, respectively. Pressure data in the upper system can be divided into two subsystems: A and B as shown in Figure 5.9. Both system A and B are underpressured, but the underpresuring is more pronounced in system B. Both of the systems demonstrate change in the p(d) gradient corresponding to changes of the KB where pressures were observed, and show a pattern of a system adjusting to present day topography. Those two systems are interpreted to be representing local flow systems as per Tóth's model of gravity driven flow (1963). Few pressure data from the Nisku Aquifer fall in system B. A middle system, overlapping the upper system at the depth of 0.8 km and extending to a depth of about 1.4 km, has a pressure gradient of 11.4 MPa/km, which is greater than the nominal pressure gradient based on the Nisku Aquifer ambient density. Most of the Nisku Aquifer data fall in this system, whose pressure gradient suggests an upward directed flow. A third system with much less dense data
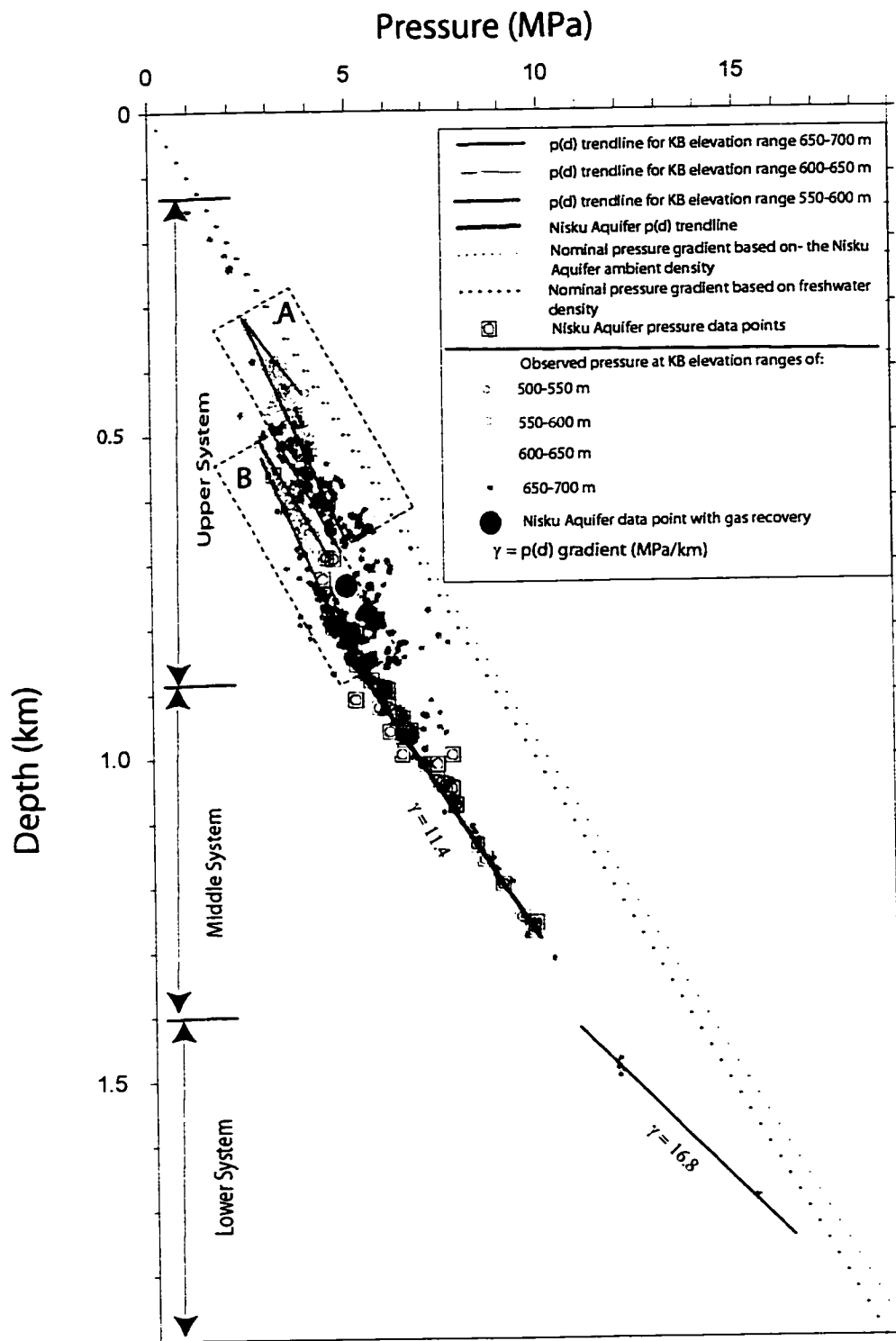
Figure 5.9 Regional p(d) plot for east central Alberta (see Figure 4.2 for location).

population spans a depth of 1.4 to about 2.0 km, and exhibits a pressure gradient of 16.8 MPa/km suggesting a strong component of an upward directed flow.

The area of east central Alberta also represents a basin-scale low land surface topography (Figure 4.9). Published models of flow in the Alberta basin (Hitcheon, 1969a, b; Bachu 1995a, 1999) define this region as being a discharge zone for the Alberta basin. Vertical temperature gradients in this area (Figure 4.7) are in the range of 36-48 °C/km which is relatively high compared to the basin average, and probably caused by upward moving fluids as suggested by Hitchon (1984).

Flow in the Nisku Aquifer in east central Alberta is highly affected by density variations in groundwater due to reduced horizontal hydraulic gradients (Figure 4.3) and comparatively higher structural gradients (Figure 5.3). Directions of the WDFVs are highly variable (Figure 5.4), but are mostly directed to the east. Horizontal hydraulic gradients are low in the region (Figure 4.3), and the differences in density range between 70 to 30 kg/m^3 (Figure 4.5). The structural gradients range between 3 to 5 m/km. The DFR values exceed 0.5 in major parts, and anglular differences between hydraulic gradients and WDFVs are in the range of 20 to 40 degrees (Figure 5.5).

5.2.5 Hamlet North Area

Anomalously low hydraulic heads in the Nisku Aquifer in the Hamlet North area (Figure 4.2, area A) are probably caused by a combination of two factors: 1) erosional rebound and

2) the aquifer is encased by thick low permeability rocks. This is supported by the large areal extent of the low hydraulic head area, previous geological studies, and a p(d) plot. Flow is directed inward towards the minimum hydraulic head, and density effects on lateral groundwater flow are minimized in this area due to high hydraulic head gradients. This area represents a regional sink, where flow is directed inward towards a minimum hydralic head of −50 m, the lowest for the Nisku Aquifer in the WCSB. Underpressuring in the gas phase for data points from the Nisku Aquifer, as observed from the p(d) plot (Figure 5.10), spans a depth of 0.9 to 2. km. Pressure data from other aquifers with water recoveries are normally- to underpressured, but their underpressuring is much less in
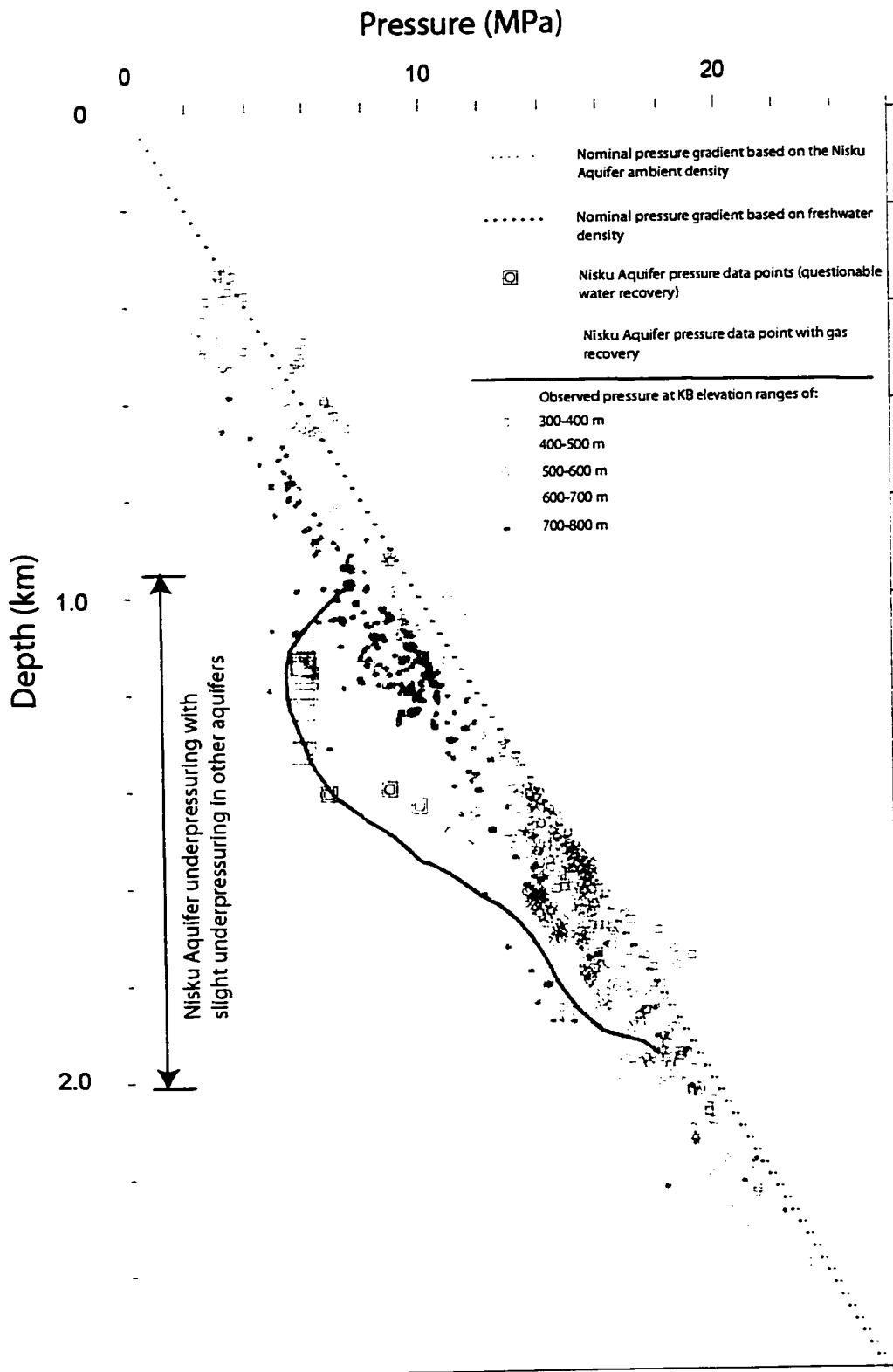
Figure 5.10 Regional p(d) plot for Hamlet North area (see Figure 4.2 for location)

magnitude. Underpressuring in the gas phase of the Nisku Aquifer reaches a maximum of 7 MPa at a depth of 1.3 km. Such a high magnitude of underpressuring and its depth extent probably suggest a mechanism operating on a basinal scale. Some values from other aquifers are also underpressured, probably influenced by this regional sink in the Nisku Aquifer.

Geological evidence that the Nisku Aquifer in the Hamlet North area is encased by low permeability rocks comes from Switzer et al. (1994) and Hudema (1991). Both of those studies have suggested that the Nisku Aquifer (the Jean Marie Formation) is overlain by shales of the Redknife silty shale, underlain by the Fort Simpson shale, and pinches out in the Fort Simpson shales. Thickness of the Nisku Aquifer is generally in the range of 12 m (Hudema, 1991), but increases to some 160 m in some localized regions.

Erosional rebound, the mechanism suggested here as causing such underpressuring in the Nisku Aquifer, has been ruled out by Bachu (1997), and the reasoning given by Bachu is questioned here. First, Bachu (1997) suggested that the "... phenomena is localized and areally constrained . . ." (p. 727). Data from this study show a progressive decrease in hydraulic heads towards the minimum value over a large area in northern Alberta and British Columbia. Second, Bachu suggests that the thickness of the overburden removed is three to four times less than that observed in southwerstern Alberta (Kalkreuth and McMechan, 1988). This view considers only one component of factors causing the underpressuring caused by rebound, which is the removal of overburden from the sedimentary succession. However, the equation describing the mathematical representation of flow in combination with the effects of rebound (Nuezil, 1995) show that hydraulic properties of the rock framework have an equally important factor in creating the underpressuring. Bachu's justification does not consider this other equally important factor.

Bachu (1997) attributes the underpressuring to either production from the gas fields, or to local diagenetic processes. The first reason has been ruled out by the CII criteria of pressure data used for mapping in this study, and the underpressuring is recognized in pressure measurements that were taken prior to any production influence at these points. The digenetic reasoning can still be a plausible suggestion, but the areal extent of underpressuring requires a mechanism operating on a regional scale. Detailed evaluation

of factors causing the underpressuring in the Nisku Aquifer would require a more detailed investigation to this particular region, which is beyond the scope of this study.

In the Hamlet North area, flow in the Nisku Aquifer is oriented towards the north, and the equipotential lines are more congested, indicating a major change in the flow regime and a relatively lower permeability zone in the northern part of the Alberta Basin. The flow is directed toward the center of the low potential area.

High horizontal hydraulic gradients in this area (Figure 4.3) lead to reduced values of the DFR for groundwater in the Nisku Aquifer (Figure 5.2), and thus, there is no significant influence of density on lateral flow in the Nisku Aquifer in this region (Figures 5.4 & 5.5).

5.2.7 Southeastern Saskatchewan

The pressure in the Nisku Aquifer in southeastern Saskatchewan seems to be adjusted to present day topography, and the p(d) plot appear to be falling in a midline area of the regional gravity driven flow system in the Williston basin. Previous hydrogeological studies, the p(d) plot constructed for this area, and basin topography are evidences to this characterization. Flow is directed mostly to the northeast, with varying effects of groundwater density on groundwater flow directions.

Descriptions of flow system in the Williston basin by previous studies have suggested that the aquifers are adjusted to present-day topography (Downey, 1982; Downey and Dinwiddie, 1988; Bachu and Hitchon, 1996), and that the system recharges at areas of high elevations in the southwest of the basin, and discharge at regional topographic lows. By examining the p(d) plot for this area (Figure 5.11), the following can be observed. There are two primary systems in the sedimentary succession: an upper system, and a lower system. Slight underpressuring is observed in the upper system, which extends between depths of 1.0 to 1.3 km and constitutes a minor portion of the data from the Nisku Aquifer. By visual examination, it can also be observed that the p(d) gradients for different KB elevation ranges are greater than nominal pressure gradients. Such observations can lead to the conclusion that the vertical component of flow in this system is upward. However, data in the lower system, including those from the Nisku Aquifer, fall on the nominal pressure gradient based on the Nisku Aquifer ambient density, which
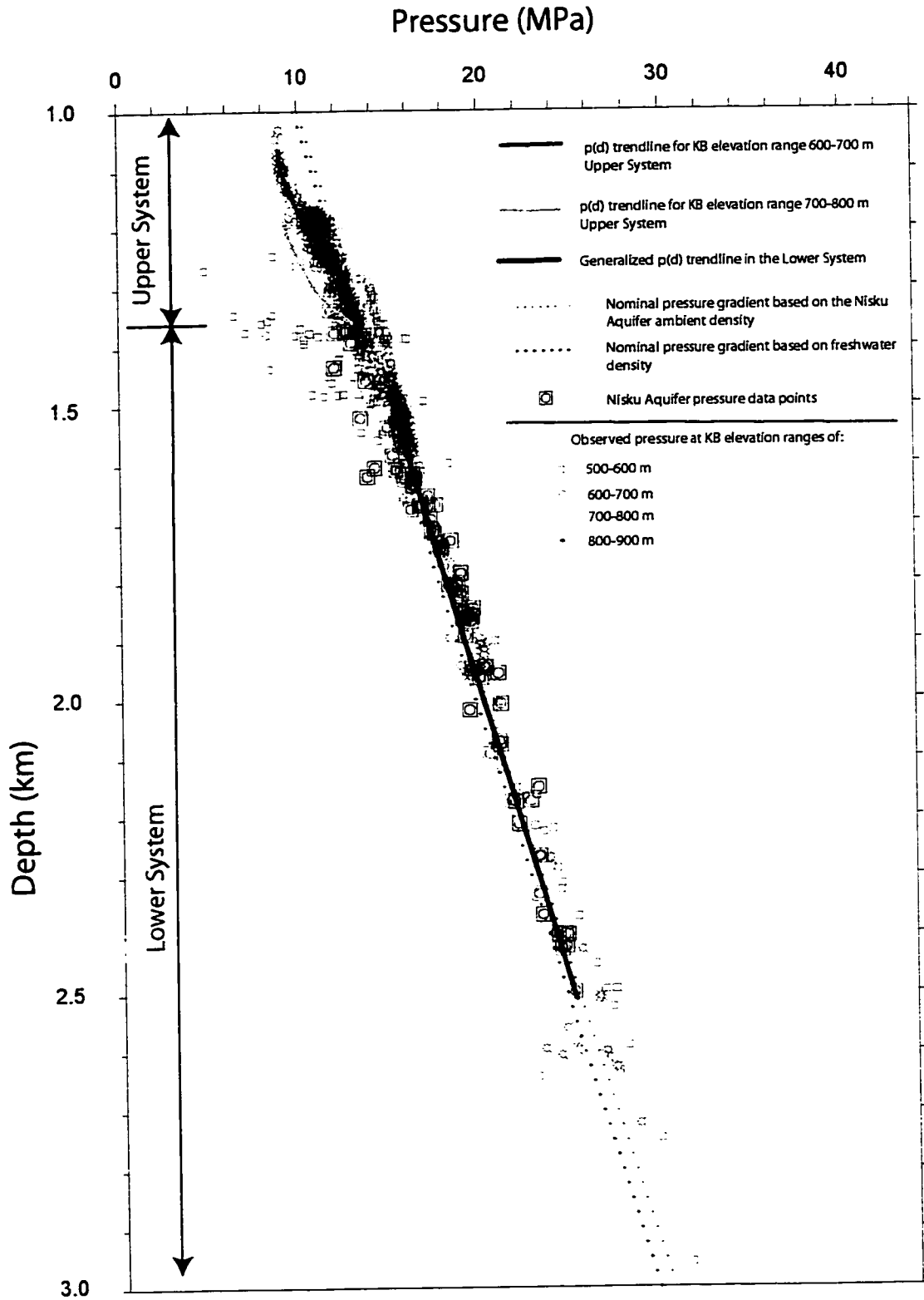
Figure 5.11 Regional p(d) plot for southeast Saskatchewan (see Figure 4.2 for location)

suggests the lack of a regionally significant vertical component of groundwater flow in the sedimentary section including the Nisku Aquifer, as shown from the p(d) plot. It has to be emphasized here that vertical components of flow are likely to be present, but are not as significant as those observed in the Bashaw area and in west central Alberta.

Large sections of this area are influenced by density component of flow in the Nisku Aquifer due to the reduced horizontal hydraulic gradients (Figure 4.3) and relatively elevated structural gradients and density differences between freshwater and ambient groundwater density in the Nisku Aquifer (Figures 5.3, 5.4, & 5.5).

5.2.8 Montana Area

The pressure in the Nisku Aquifer in Montana area (Figure 4.2, area G) appears to be adjusted to present day topography, and the p(d) plot indicates that the area is a regional recharge zone. However, observations from pressure data in the sedimentary succession shows an anomalous feature that may suggest that the Nisku Aquifer demonstrates a slightly different hydrogeological character. Topographic elevations, as well as vertical temperature gradients, suggest that this area is a regional recharge zone. Limited data availability prohibited the construction of the p(d) plot from the land surface (Figure 5.12). Pressure values from the Nisku Aquifer appear to be normally pressured to subnormally pressured. The general regional trend of the data show a pressure gradient that is less than nominal pressure gradient based on freshwater density. However, pressure data points from the Nisku Aquifer show a p(d) gradient greater than nominal pressure gradient based on the Nisku Aquifer ambient density. This may suggest a vertically upward-directed flow in the Nisku Aquifer, in this particular area.

Relatively higher topographic elevations in this area (Figure 4.9) and low values of vertical temperature gradients (Figure 4.7) suggest that this area is indeed showing a dominant downward vertical component of flow. Resolving the apparent contradiction between regional p(d) trend and that of the Nisku Aquifer is difficult due to limited data availability for the Nisku Aquifer in the area.

Flow in the Nisku Aquifer is highly affected by groundwater density in the Montana area, caused by relatively reduced hydraulic gradients (Figure 4.3) and relatively elevated structural gradients (Figure 5.3) and differences in density between groundwater

and freshwater (Figure 4.5). The total dissolved solids in this area are in the range of 300 g/l (Figure 4.4). The DFR value (Figure 5.2) exceeds 0.5 in most of the this area. The influence of the high DFR doesn't necessarily translate into the deflection flow based on hydraulic gradients, and may only reduce the water driving force as shown in some parts of the Williston basin. This is because in force vector addition, if the orientations of the added vectors are 180 degrees apart, the resultant vector will take the direction of the higher magnitude of the added vectors, and thus the original vector will not change in direction. Such scenario is seen in this area where the WDFVs are shorter than the hydraulic gradient vectors due to the angle between the structural dips and hydraulic gradients in the area being around 180 degrees (Figure 5.4).

To summarize the groundwater flow regime in this area, it can be said that the Nisku Aquifer is normally to subnormally pressured, and adjusted to present day local topography. Groundwater flow is directed radially to the northeast, to the north, and to the northwest, and is highly affected by groundwater density variations.

5.2.9 Southern Alberta and Northwestern Montana Area

The Nisku Aquifer in southern Alberta and northwestern Montana (area F, Figure 4.2) is affected by two flow systems relating to energy distribution in the sedimentary succession. One of those systems is driven by topographic elevations at the outcrop of the Nisku Formation in northwestern Montana, and the other system is affected by the general underpressuring in southern Alberta. These conclusions are supported by knowledge of the topographic elevations, location of the Nisku Formation outcrop (Figure 4.9), and by observations drawn from the p(d) plot in the area. Density effects on groundwater flow in the Nisku Aquifer are minimal, but increase towards areas of high structural gradients and TDS towards the west.

The p(d) plot constructed for the area (Figure 5.13) demonstrate three patterns of p(d) gradients and pressure systems. An upper system extending from the land surface to a depth of about 0.95 km where pressure values vary from slightly overpressured to slightly underpressured (features in this upper system need further examination which is beyond the scope of this study). In the depth range of 0.95 to 1.3 km, a different system that is slightly overpressured, and clearly distinguished from the upper system, is

106

Pressure (MPa)
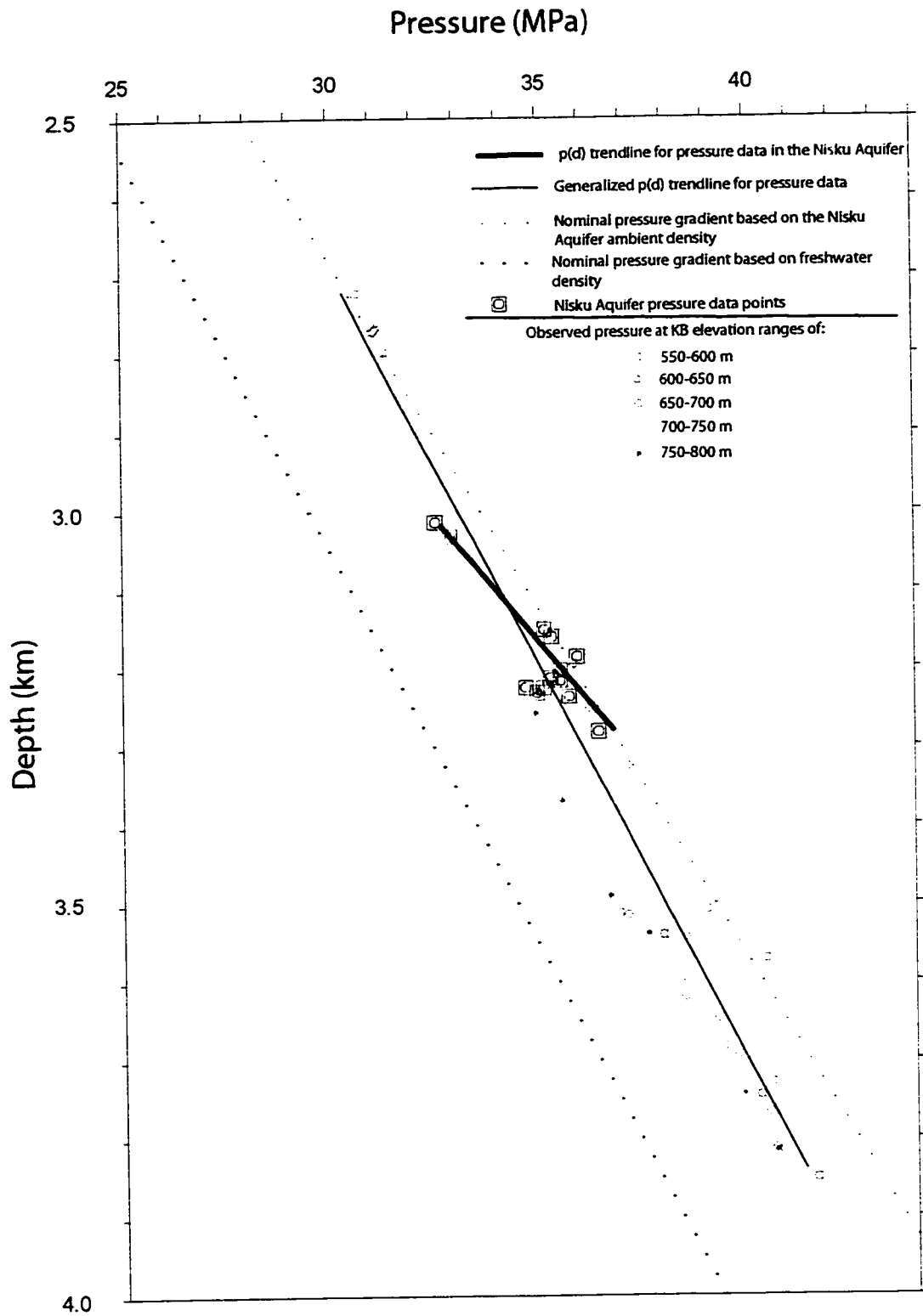
Figure 5.12 Regional p(d) plot for Montana area (see Figure 4.2 for location).

107
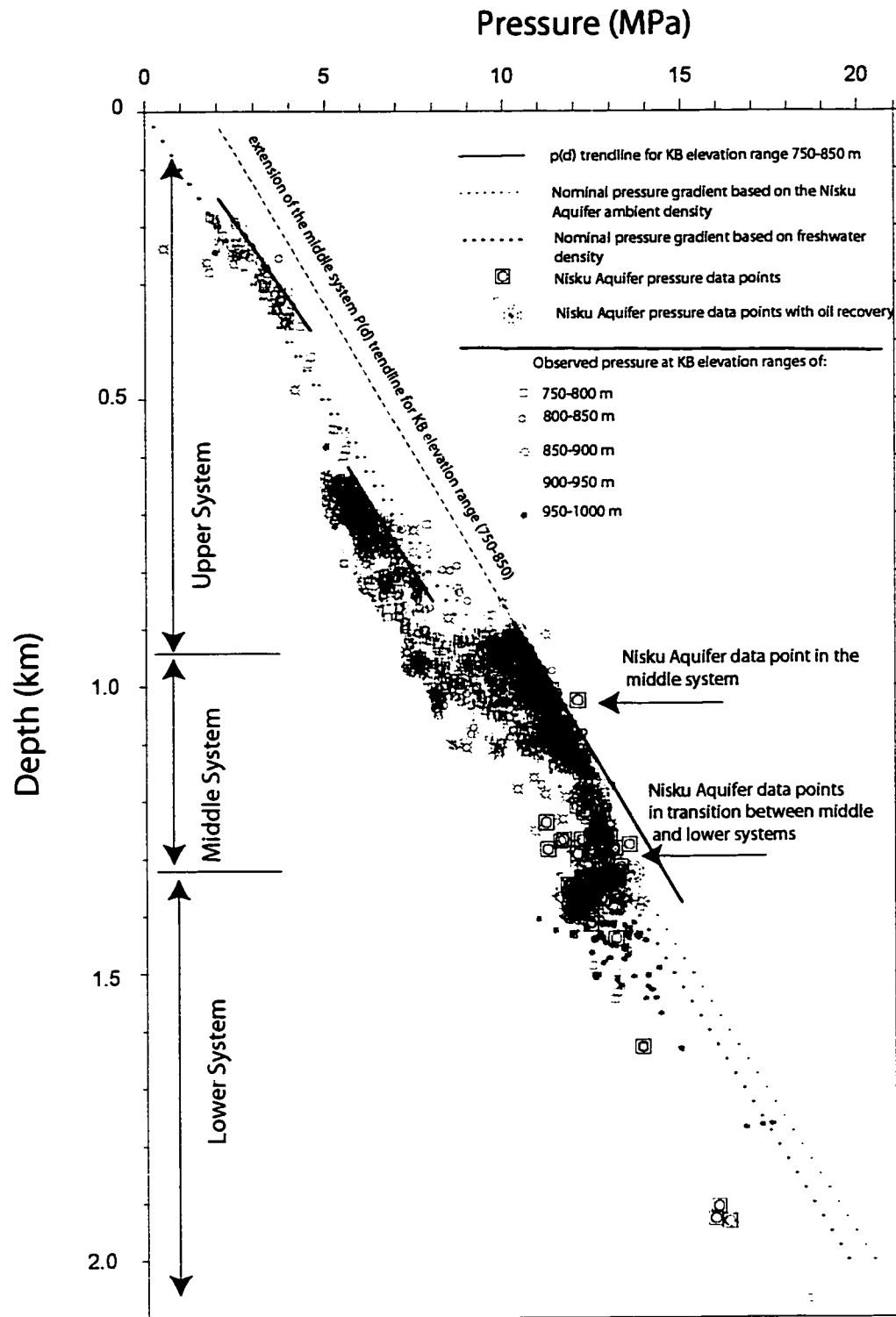
Figure 5.13 Regional p(d) plot for southern Alberta and northwestern Montana

108

observed. The middle system exhibits a p(d) gradient that is slightly less than the nominal freshwater p(d) gradient, indicating a vertically downward component of flow in the system. The projection of a trend line passing through the maximum pressure data points crosses the depth axis (0 MPa) above land surface elevation in this area, which indicates that the energy is provided by a source other than the local present-day topography. The pressure data below the depth of 1.3 km do not show a clear trend out of which a p(d) trend can be confidently drawn. However, it can be confidently said that the pressure system at this depth zone is significantly different from the slightly overpressured middle system. This lower system is slightly underpressured. Pressure data from the Nisku Aquifer, for both water and hydrocarbon recoveries, cluster at the depth of the divide between the middle zone and the lower zone. One pressure data point from the Nisku Aquifer falls along the middle, overpressured system (Figure 5.13).

The three systems shown in the p(d) plot represent the energy levels present in the sedimentary succession in the region. From the surface to a depth of about 0.95 km, the pressure gradient is responding to the local topography, due to the fact that no significant overpressuring is observed. From a depth of 0.95 to 1.3 km, an over-pressured system with a p(d) gradient less than hydrostatic, indicating a slight downward component of flow. The p(d) trendline projected above the local land surface in this area is interpreted as being due to the Nisku Aquifer (and other aquifers constituting this zone) being in more effective hydraulic communication with the outcrop of the Nisku Formation (and other formations) at higher elevations (Figure 4.9), a distance away from the p(d) plot area (Figure 4.9). Such a hydrogeological scenario as a cause for overpressuring has been explained by Dahlberg (1994). The lower system, where most of the Nisku Aquifer data are present, extends below the depth of 1.3 km. Data for this system indicate a different flow regime, which is subnormally pressured. This indicates that the Nisku Aquifer in the p(d) plot area is under the influence of two hydrogeological regimes: 1) a system influenced by the high topographic elevations of the outcrop in northwestern Montana and 2) a flow system with dissipated energy similar to that observed at the Bashaw area in south central Alberta area (Section 5.2.1).

Due to the relatively low density difference between freshwater in this area which ranges in value from less than 20 to 60 kg/m^3 (Figure 4.5), and the relatively low structural

109

gradient in most of the area, the flow is not significantly influenced by groundwater density variations except at the areas immediately adjacent to the disturbed belt where the structural gradient reaches values between 15 to 27 m/km and the flow is deflected from the orientation of the hydraulic gradient by 5 to 15 degrees (Figure 5.5).

5.2.10 Karr Basin Area

In the Karr basin area (area B, Figure 4.2), localized underpressuring in the Nisku Aquifer drives groundwater flow inward towards a hydraulic head minimum, probably affected by rebound. The speculation that this is caused by rebound is supported by the depositional environment of the Nisku Formation at the Karr basin, basin history, and the p(d) plot constructed for the area.

In the Karr basin area, the p(d) plot for the sedimentary section (Figure 5.14) shows three major trends reflecting an upper system, a middle system, and a lower system. An upper system that is normally pressured to underpressured extends to a depth of 2.25 km. The p(d) gradient for the upper system is less than nominal pressure gradient based on freshwater density. Underpressuring in the upper system is at its maximum at the transitions to the middle system. In the middle and the lower systems, the pressure data can be divided into two observable patterns, and so do the pressure data from the Nisku Aquifer. One of the trends becomes more normally pressured with depth and the other becomes more underpressured. This is interpreted as being caused by some permeability barriers, causing the more underpressured system to adjust at a slower rate to present day topography. The rates of adjustment create areas with relatively lower fluid potential to which flow is directed.

The variable permeability distribution is possible due depositional environment of the Nisku Aquifer around and at the Karr basin, which reflects restricted basin deposition (Switzer et al, 1994). The basin's rebound has been suggested by Bachu (1995, 1999) as a driving mechanism in the Alberta basin, based on the Alberta basin history of erosion (Nurkowski, 1984; Bustin, 1991) and observed pressure patterns by several workers (Tóth and Corbet, 1986; Corbet and Bethke, 1992; Parks and Tóth, 1993; Bachu and Undershultz, 1995).

110
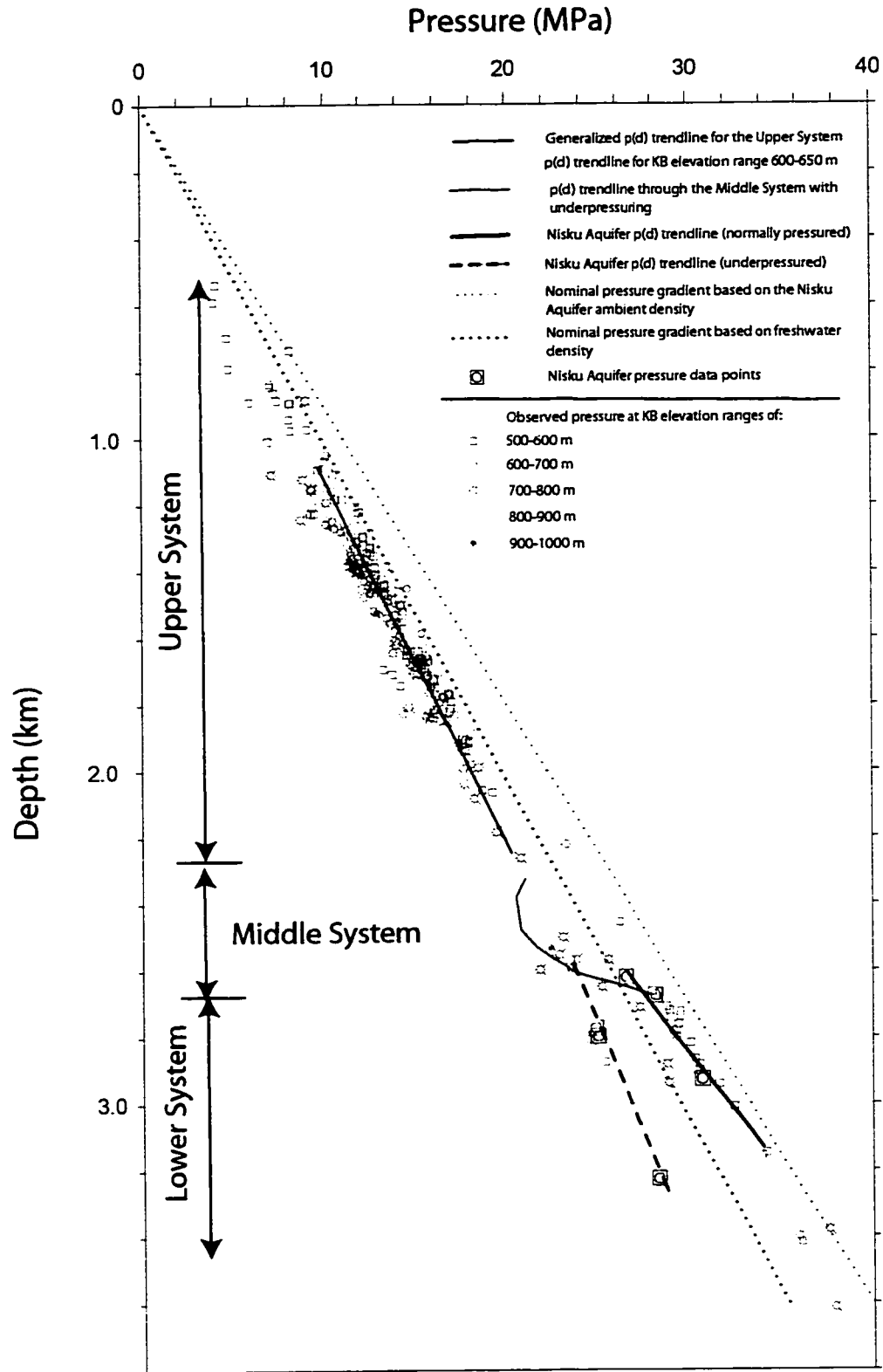
Figure 5.14 Regional p(d) plot for the Karr basin area (see Figure 4.2 for location)

Flow in the Nisku Aquifer around the Karr basin is highly influenced by density variations in groundwater. Elevated differences between freshwater and actual Nisku Aquifer water, reaching values of 120 kg/m³ (Figure 4.5) lead to elevated DFR values. Thus, the angular difference between the hydraulic gradient and WDFV in this area reaches values of up to 20 degrees (Figure 5.5), despite the relatively high horizontal hydraulic   gradients.

5.2.11 Flow at the Basin Divide:

The Area between the Alberta and the Williston basins (area I, Figure 4.2) represent a flow convergence zone in the Nisku Aquifer, probably due to two factors. From the Williston basin side, it represents a relatively lower topographic elevation, and from the Alberta basin side, it represents an area adjacent to the potentiometric high at the Bashaw reef complex in south central Alberta.

The WDFVs from both sub-basins converge at this general region (Figure 5.4). This zone of convergence forms a curving trend extending from 113° west longitude and 50° north latitude to approximately 112° west longitude and 52° north latitude north. Values of the DFR are slightly elevated in this region (Figure 5.2), owing mostly to the reduced hydraulic gradient and slightly increased density difference between freshwater and Nisku formation water. As a result, differences in angles between the hydraulic head gradients and the WDFV fall in the range between 5 to 30 degrees (Figure 5.5).

5.3 Petroleum Hydrogeology of the Nisku Aquifer in the WCSB

Moving groundwater has direct influence on hydrocarbon migration and entrapment as described by Hubbert (1953), Schowalter (1979), Tóth (1980), Davis (1987, 1991), and others. Thus, based on the characterization of groundwater movement in the Nisku Aquifer described so far, a direct consequence is that such movement affects the distribution of hydrocarbons in the aquifer. This section present a quantification of basinal scale effects of moving groundwater on hydrocarbons, based on the mapped WDFVs, ODFVs, and tilt on the oil water contact. First, a series of maps representing those quantities are presented. Second, preferred sites of hydrocarbon accumulations

based on hydrogeological factors are given, with an interpretation which links basinal scale hydrogeological factors to patterns of oil migration as a separate phase. Maps of quantities that have direct influence on the migrations patterns are presented in order to aid in the interpertations.

5.3.1 ODFVs For Gas-Saturated Oils in the Nisku Aquifer, WCSB

Patterns of oil migration in the Nisku Aquifer can be understood from maps representing force vectors driving hydrocarbons in the aquifer. Arrows representing those vectors, based on the fomulation of the ODFV given in Section 1.5 give an indication of possible migration pathway and accumulation sites. A series of such maps are presented here, for API gravity ranges observed in the Nisku Aquifer: 15, 35, and 55.

The oil driving force vectors for 15 API gravity oil in the Nisku Aquifer show several patterns of flow in the basin (Figure 5.15). Major areas of convergence of vectors include the area of the Hamlet North, at the Karr basin, on either flanks of the Bashaw reef complex in south central Alberta, at the flanks of the potentiometric high of west central Alberta, and the western northern, and eastern flanks of the potentiometric high of southern Alberta and northwestern Montana (Compare Figures 5.15 and 4.2). Few other converging ODFV zones occur in both the Williston basin and the Alberta basin. Converging vectors also occur in the approximate line separating the Alberta and the Williston basins, corresponding to the general structural high of the Nisku Aquifer (Figure 2.6). Other parts of the basin demonstrate ODFVs directed updip. One zone, falling in the area bounded by $50.8°$ to $51.5°$ north latitude and $110°$ to $112°$ west longitude, demonstrates an area of reduced magnitude of the ODFVs.

For 35 API gravity oil shown in Figure 5.16, features in the ODFVs mimic, to some degree, those observed in the 15 API gravity oil, however, minor observable differences exist. First is that the areas of converging ODFVs have become of less areal extent and some force vectors around convergence zones are oriented more towards the structural updip. The second difference is that the area of reduced magnitudes of ODFVs is showing an increase in magnitude expressed by the increased lengths of the arrows. For the 55 API oil, shown in Figure 5.17, the driving force vectors still converge in the areas
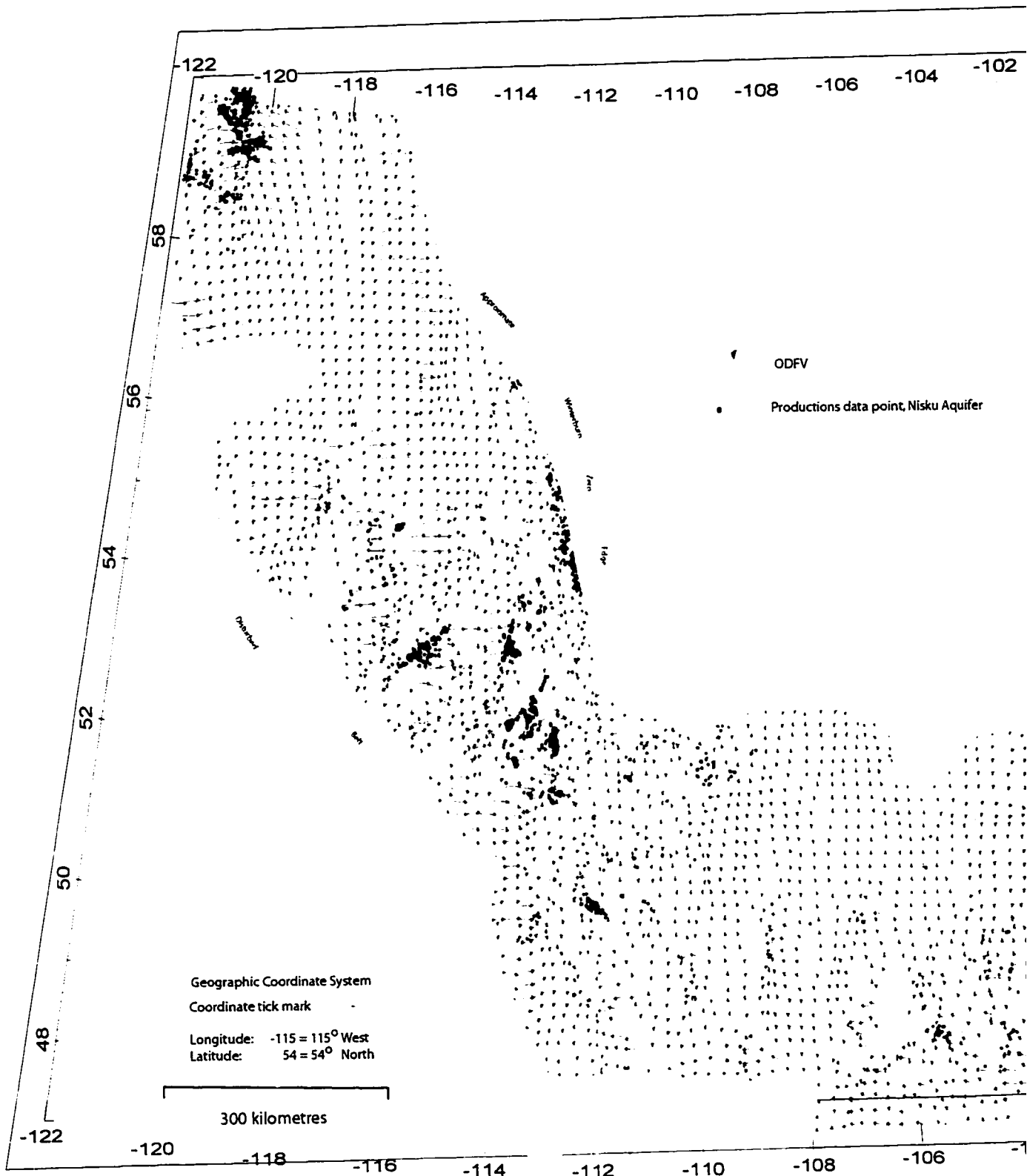
Figure 5.15 Distribution of the ODFV for a gas-saturated 15 API gravity oil in the Nisku Aquifer, WCSB.

-118 -116 -114 -112 -110 -108 -106 -104 -102 -100

58

56

54

52

50

48

ODFV

Productions data point, Nisku Aquifer

System

West
North

-116 -114 -112 -110 -108 -106 -104 -102 -100

ODFV for a gas-saturated 15 API gravity oil in the Nisku Aquifer, WCSB.

114
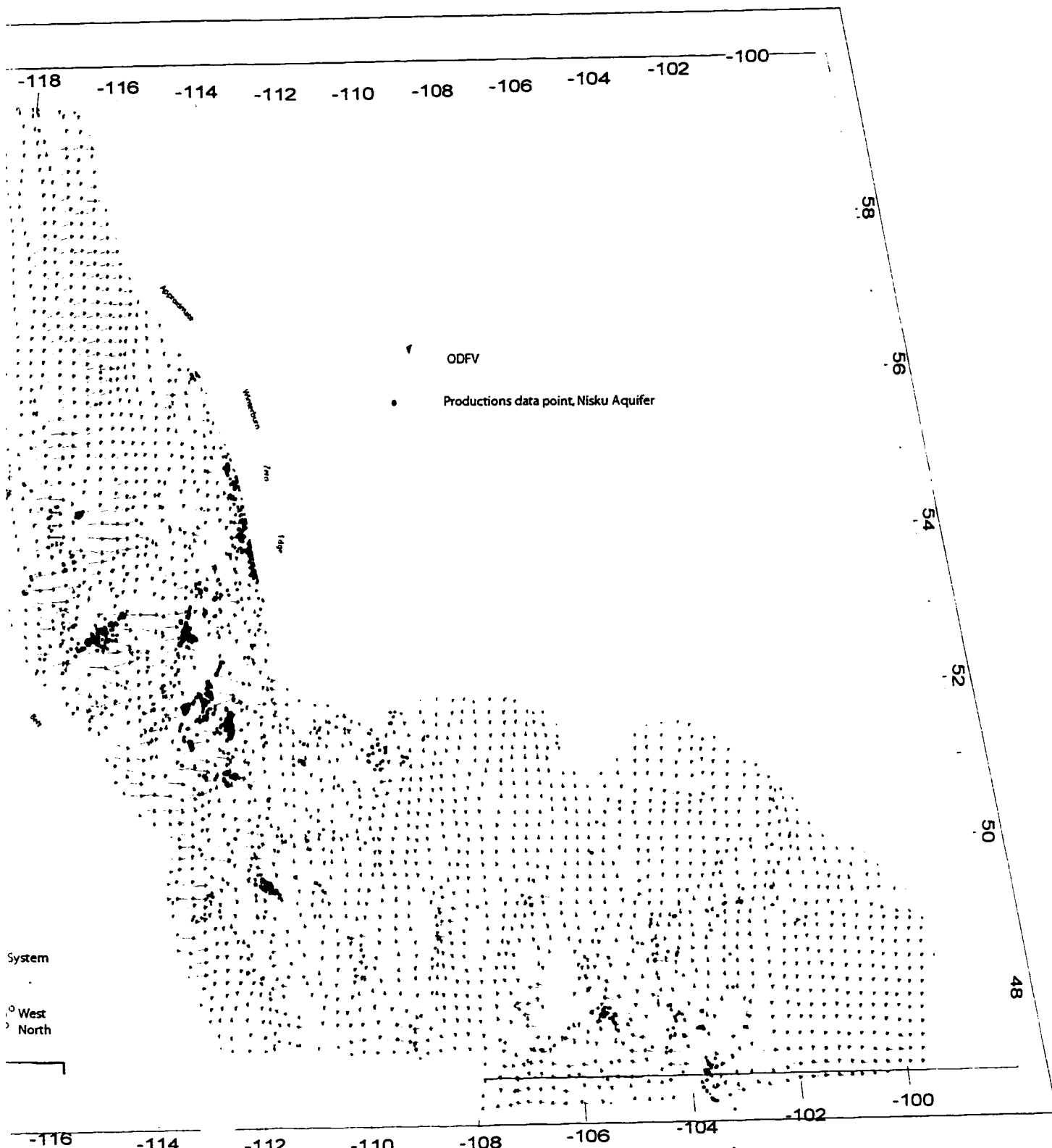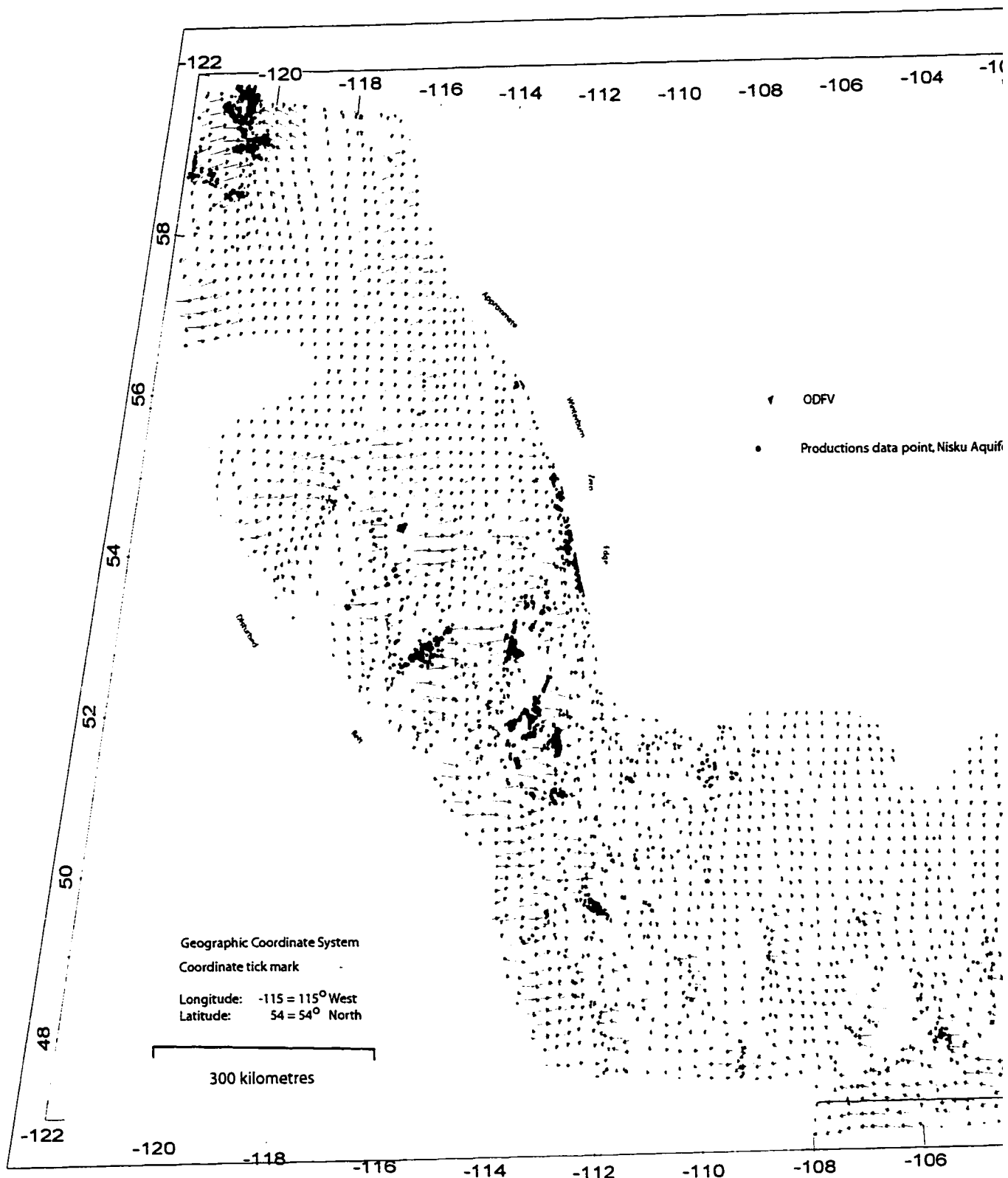
Figure 5.16 Distribution of ODFV for a gas-saturated 35 API gravity oil in the Nisku Aquifer, WCSB.

-116 -114 -112 -110 -108 -106 -104 -102 -100

58

56

54

52

50

48

-114 -112 -110 -108 -106 -104 -102 -100

ꞁ ODFV

• Productions data point, Nisku Aquifer

...s-saturated 35 API gravity oil in the Nisku Aquifer, WCSB .

115
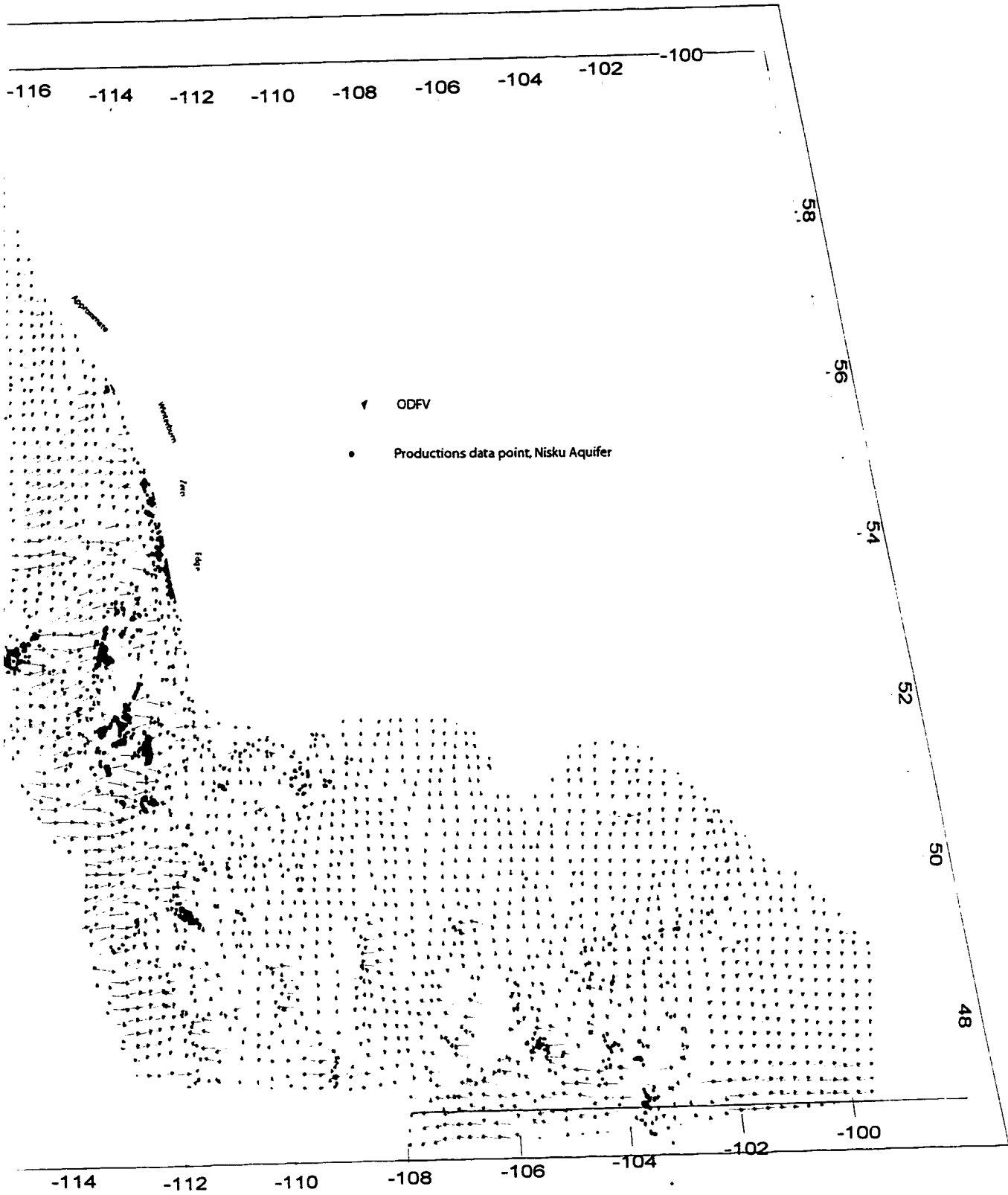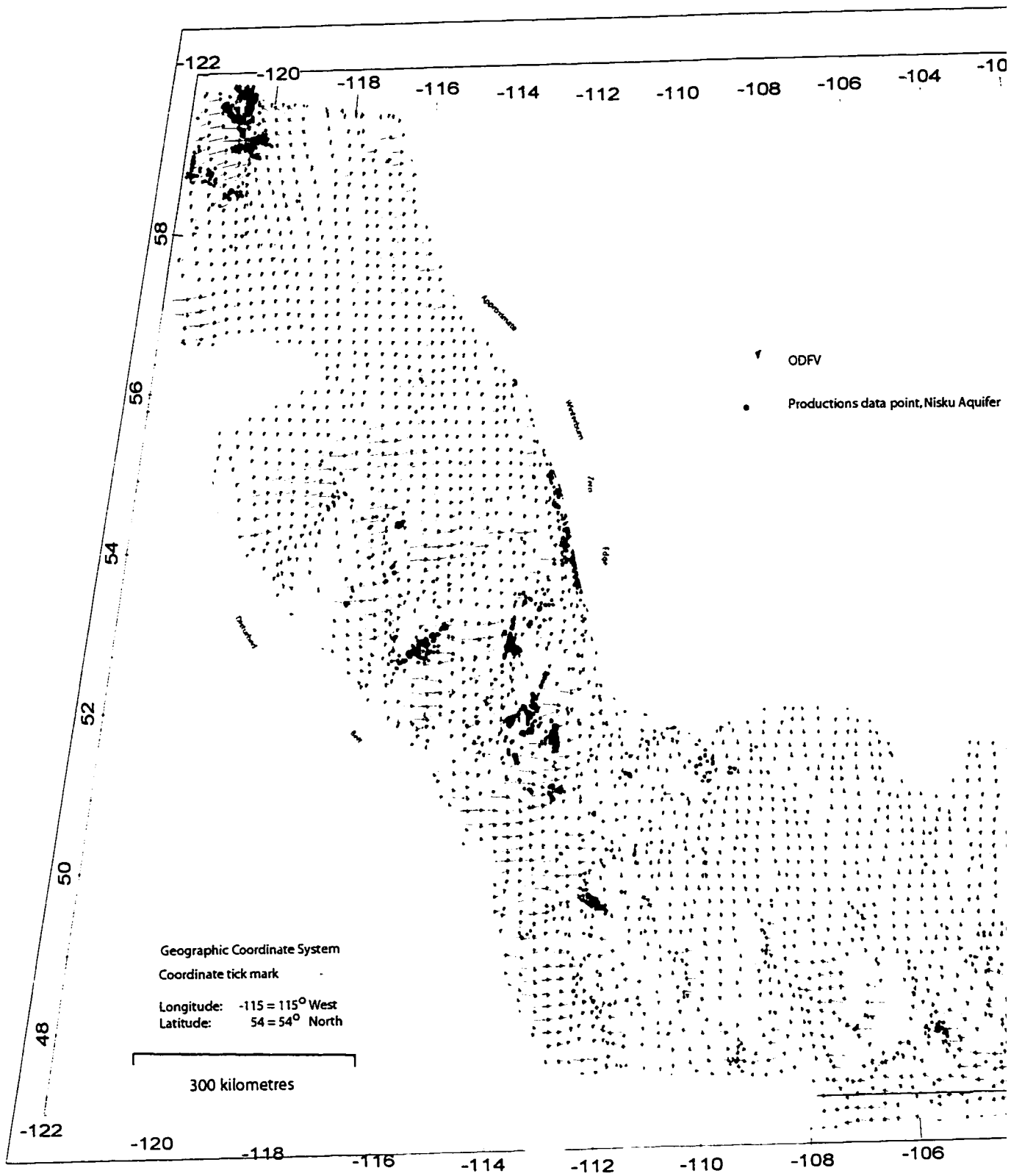
Figure 5.17 Distribution of ODFVs for a gas-saturated 55API gravity oil in the Nisku Aquifer, WCSB.

-116 -114 -112 -110 -108 -106 -104 -102 -100

⏚ ODFV

• Productions data point, Nisku Aquifer

-114 -112 -110 -108 -106 -104 -102 -100
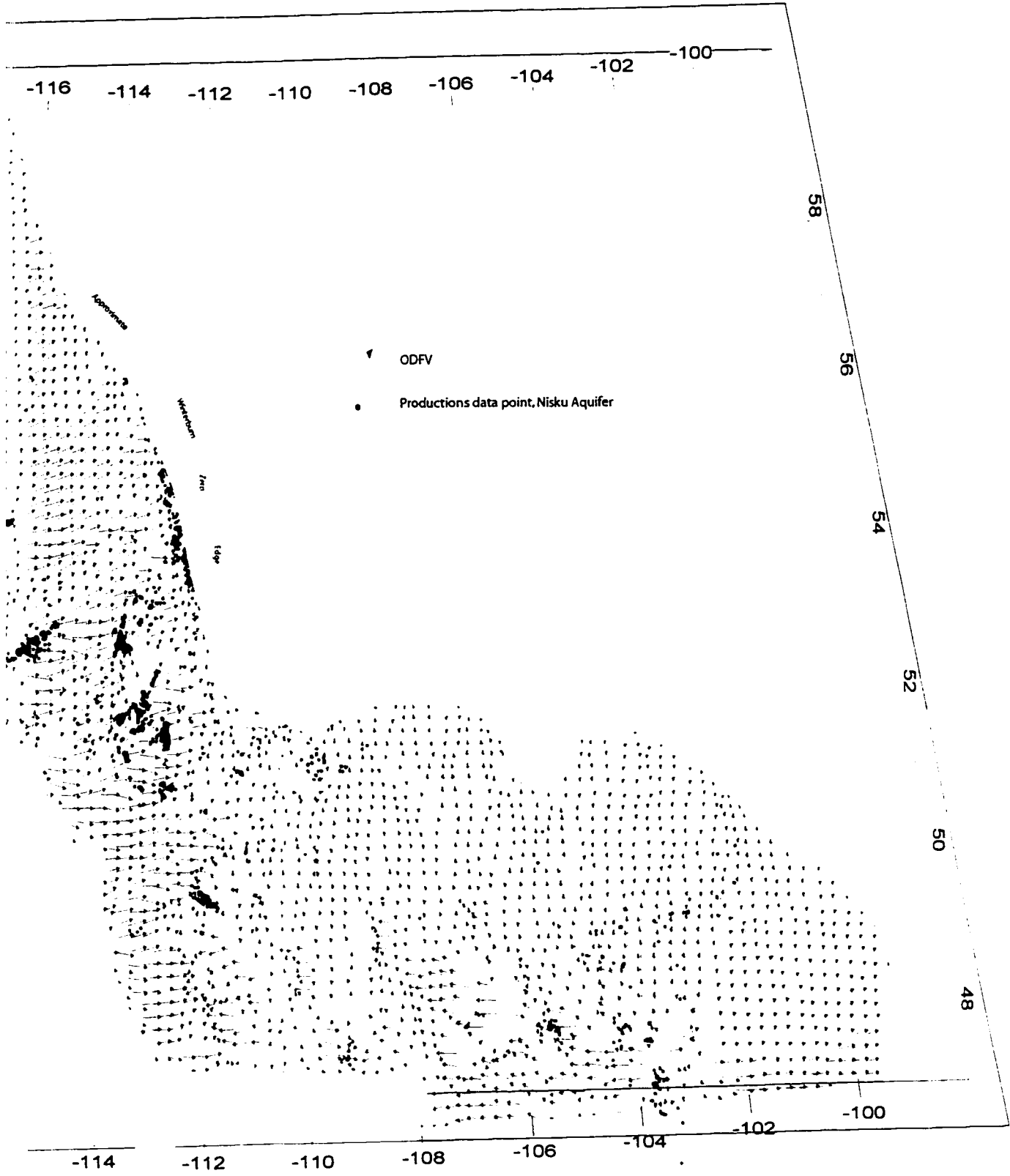
s-saturated 55API gravity oil in the Nisku Aquifer, WCSB.

recognized in the heavier hydrocarbons in west central Alberta, around the area of West Pembina, in Southern Alberta and North Western Montana, and at the flanks of the Bashaw reef complex. However, the areal extent is observably less and differs significantly from the 15 API gravity map. Most vectors are now oriented structurely updip.

5.3.2 Potential Tilt of Oil Water Contact in the Nisku Aquifer, WCSB

The potential tilt maps show the calculated tilt, based on the calculated WDFVs and the densities of both formation water and oil, as discussed in Section 1.6. Tilt maps of oils at API gravities of 15, 35, and 55 are presented (Figures 5.18 to 5.20). This may help in understanding the distribution of oil APIs in the Nisku Aquifer (Figure 4.8), as will be discussed later.

It is observed that for a 15 API oil, the potential tilt for the majority of the basin is 5 to 10 m/km (Figure 5.18). However, a few areas of the basin demonstrate elevated values of potential tilt in the Nisku Aquifer. On the flanks of the potentiometric high at the south central Alberta, the potential tilt reaches more than to 20 m/km. In West Central Alberta, the potential tilt in the Nisku Aquifer reaches values up to 60 m/km as well as in the area of Hamlet North. For the 55 and API gravity oils, the values of the potential tilt are reduced from those observed for the 15 API oil.

5.3.3 Hydrogeological Influances on Oil Movement in the Nisku Aquifer

In order to highlight areas affected by moving groundwater, i.e., hydrodynamic forces, a set of maps with relevant explanations are presented here. Those include oil driving force ratio (ODFR), angular differences between ODFVs and BDFVs, magnitude differences between ODFVs and BDFVs.

The ODFR, defined as the ratio of the magnitude of BDFV to WDFV, for gas-saturated 35 API gravity oil in the Nisku Aquifer is shown in Figure 5.21. From the definition, the smaller the DFR, the greater the influences of groundwater flow. The ODFR ranges in value from less than 0.25 to 5.5. The highest values, reaching 5.5, are southeastern part of the Williston basin and east-central Alberta while the lower values are seen in southern Alberta and north western Montana, west central Alberta, Hamlet North area,

117
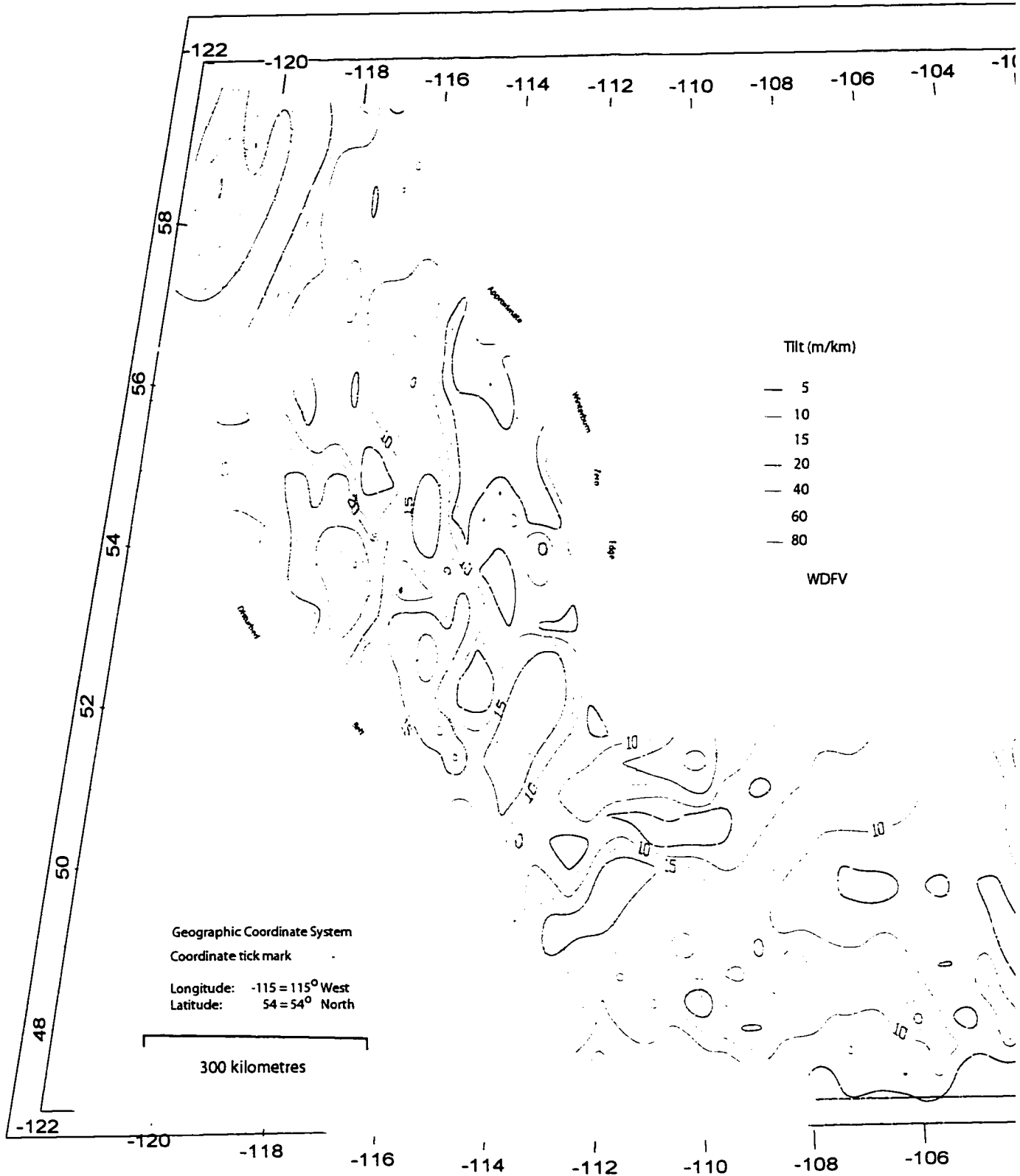
Figure 5.18 Potential tilt map for a gas-saturated 15 API oil in the Nisku Aquifer, WCSB.

Tilt (m/km)

— 5
— 10
15
— 20
— 40
60
— 80

WDFV

s-saturated 15 API oil in the Nisku Aquifer, WCSB.

118
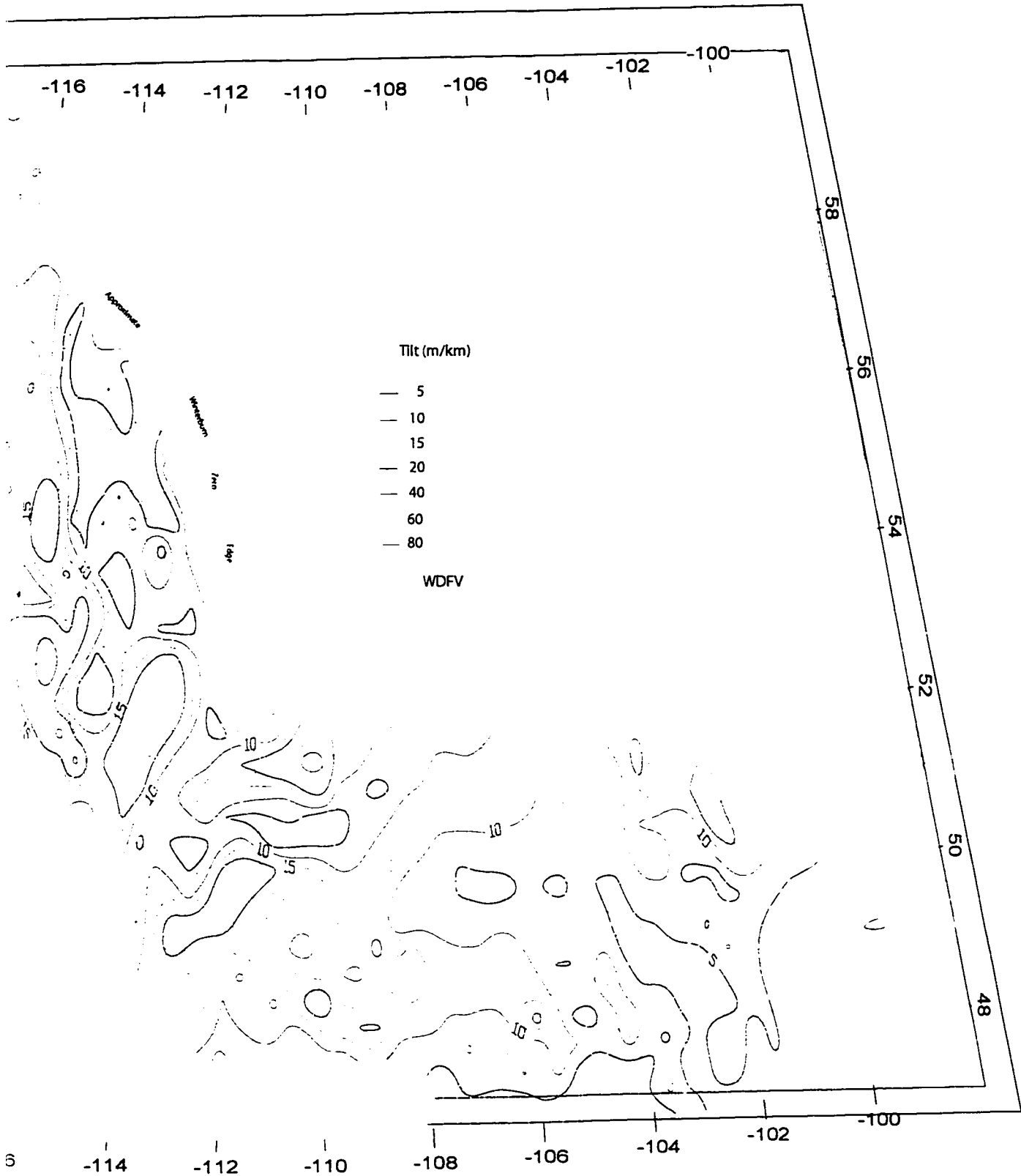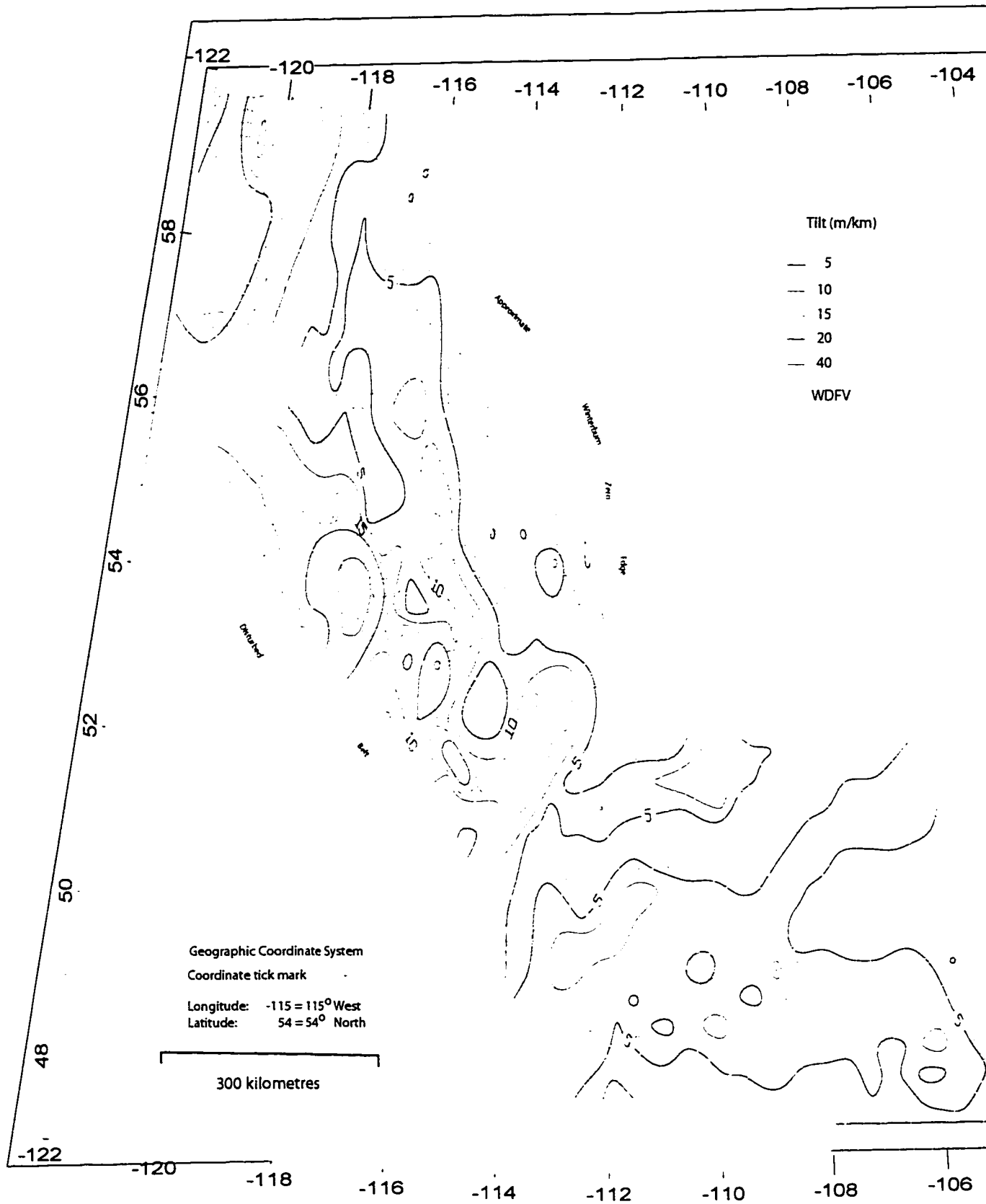
Figure 5.19 Potential tilt map for a gas-saturated 35 API gravity oil in the Nisku Aquifer, WCSB.

Tilt (m/km)

— 5
— 10
· · 15
— 20
— 40

WDFV

-116 -114 -112 -110 -108 -106 -104 -102 -100

58

56

54

52

50

48

-100

-114 -112 -110 -108 -106 -104 -102

rated 35 API gravity oil in the Nisku Aquifer, WCSB.

119
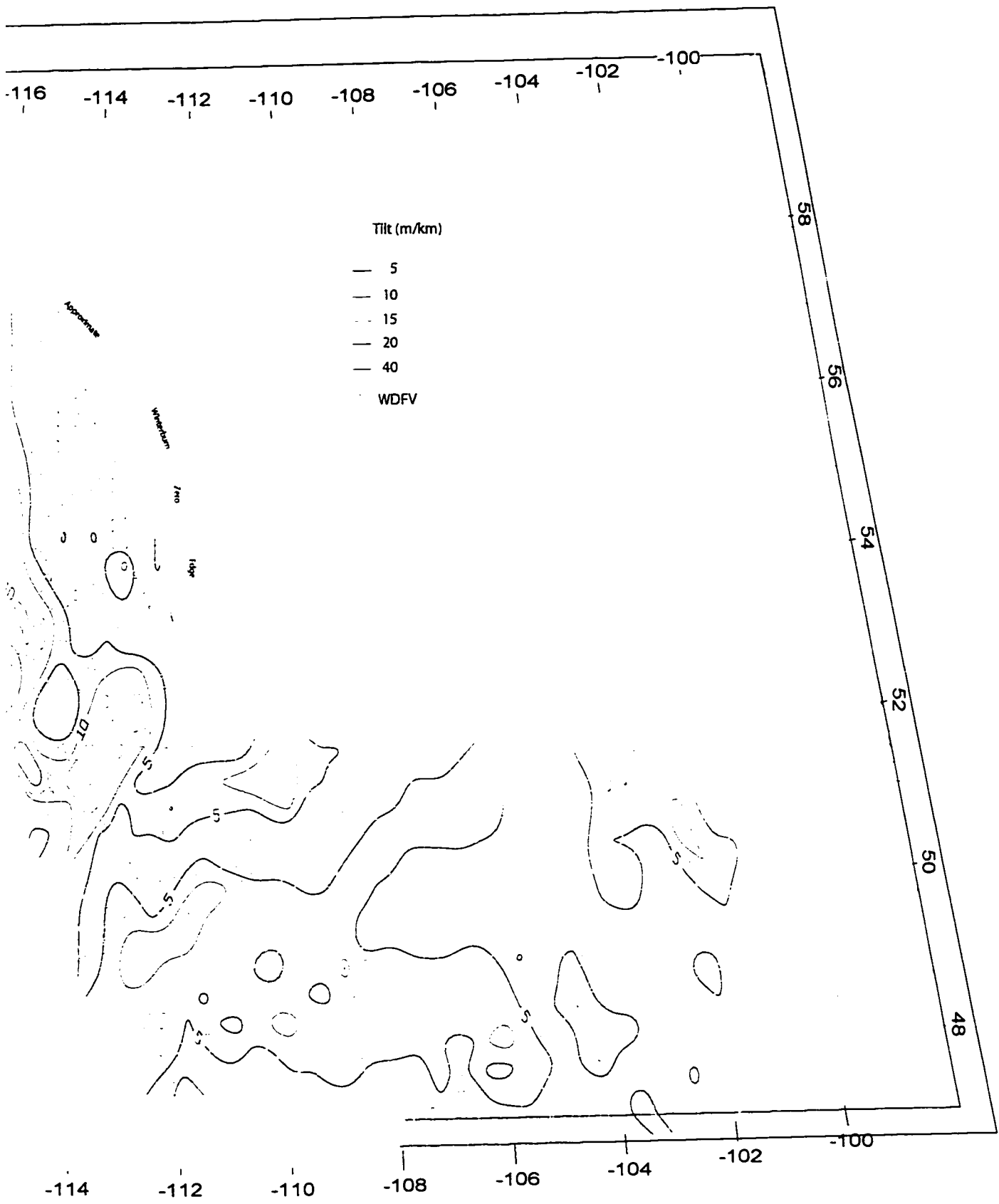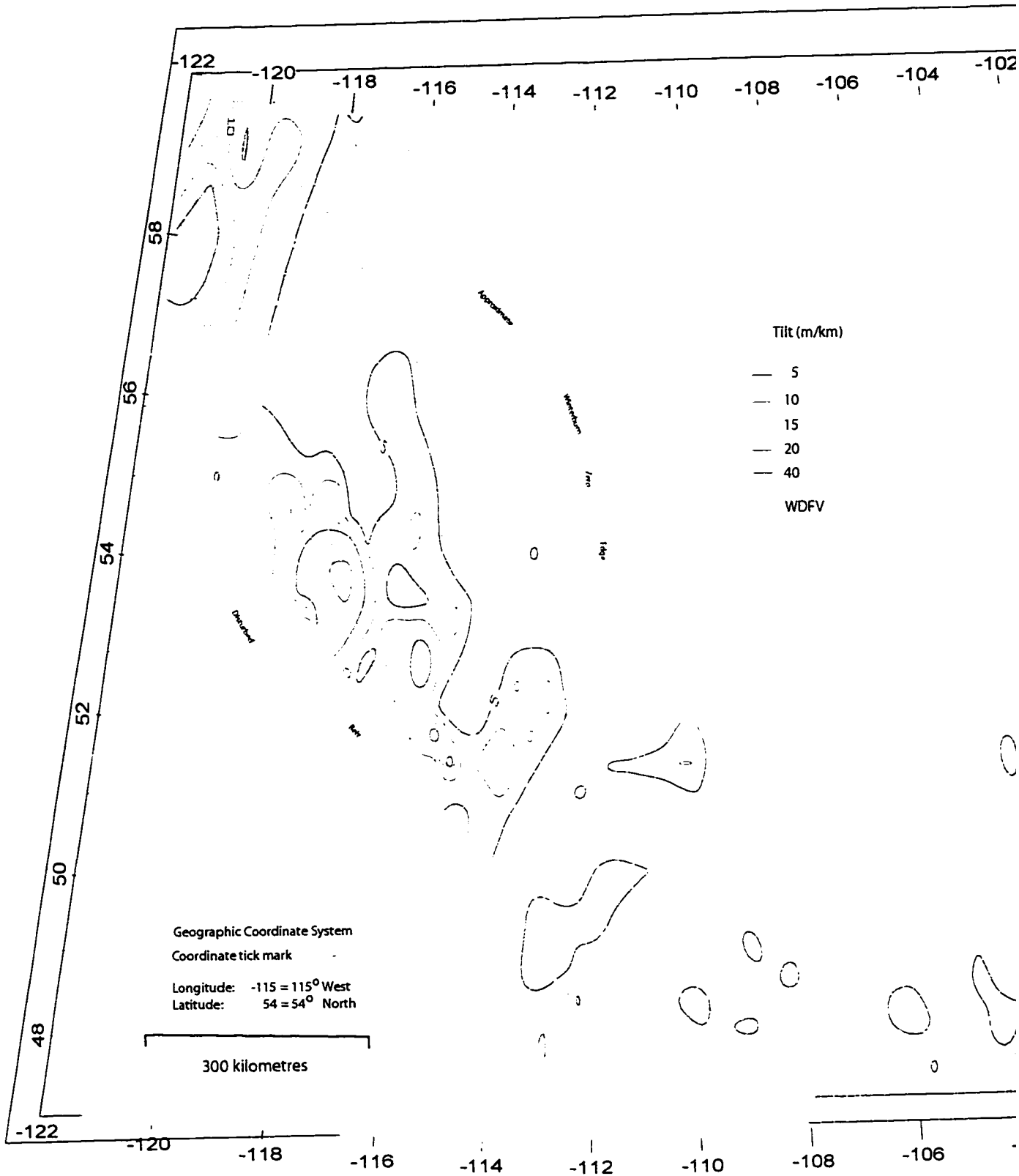
Figure 5.20 Potential tilt map for a gas-saturated 55 API gravity oin in the Nisku Aquifer, WCSB.

-116 -114 -112 -110 -108 -106 -104 -102 -100

58

56

54

52

50

48

Tilt (m/km)

— 5

— 10

15

— 20

— 40

WDFV

-114   -112   -110   -108   -106   -104   -102   -100

ⴑrated 55 API gravity oin in the Nisku Aquifer, WCSB.

120
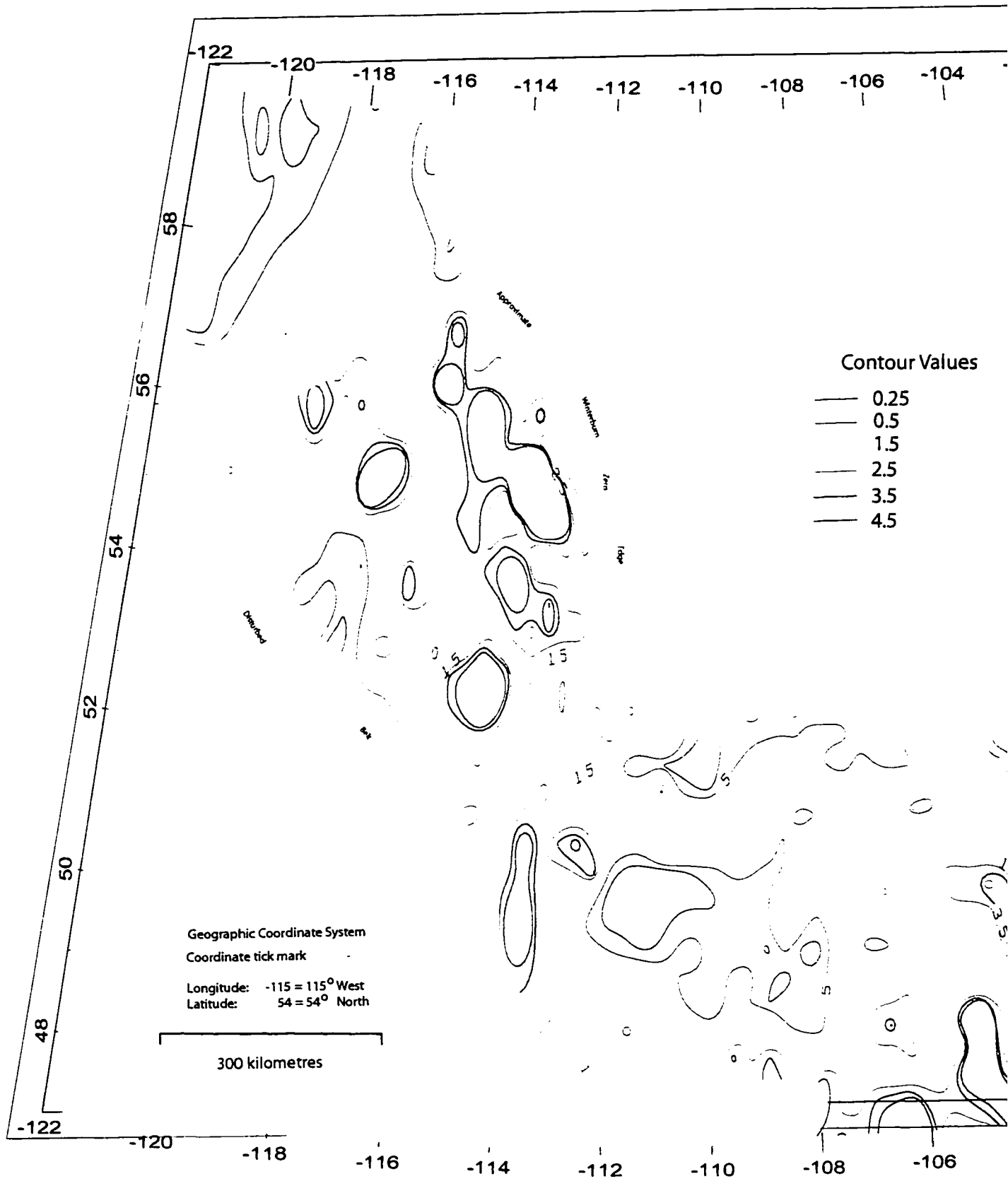
Figure 5.21 Distribution of the ODFR for a gas-saturated 35 API gravity oil in the Nisku Aquifer, WCSB.

-116 -114 -112 -110 -108 -106 -104 -102 -100

8

Contour Values

—— 0.25
—— 0.5
1.5
—— 2.5
—— 3.5
—— 4.5

58

56

54

52

50

48

-100

-102

-104

Approximate

Winterburn

Zem

Idge

0

15

15

5

5

5

1.5

3.5

2.5

2.5

6 -114 -112 -110 -108 -106 -104 -102 -100

a gas-saturated 35 API gravity oil in the Nisku Aquifer, WCSB.

121
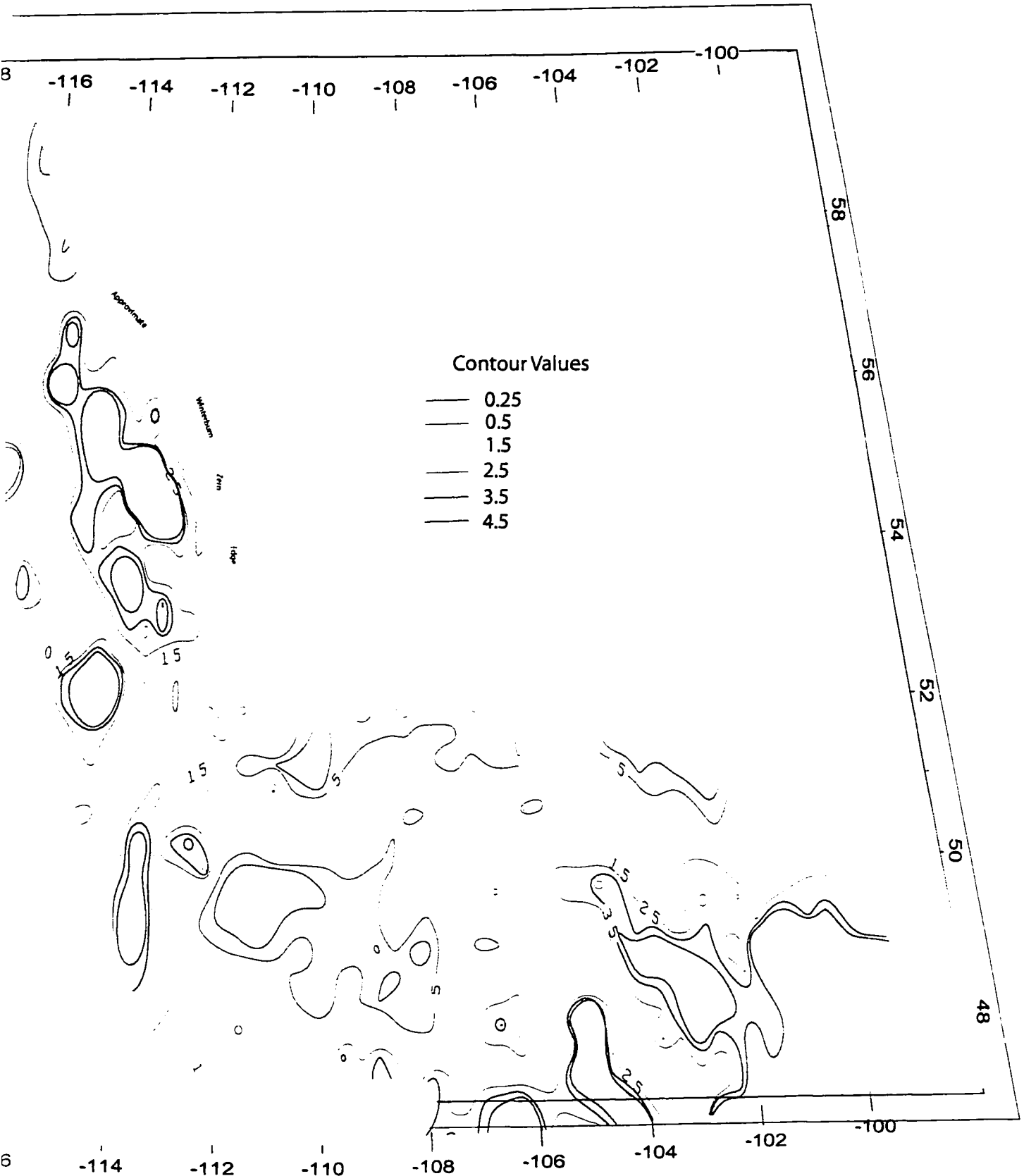
and at the Bashaw area in south central Alberta. Such areas, as have been discussed earlier, are characterized by being affected by energy sources of different types.

The angular difference map between the ODFV and the BDFV in the Nisku Aquifer is less than 5 degrees in the majority of the basin (Figure 5.22). However, as a consequence of the relatively higher influence of groundwater flow, several areas within the basin demonstrate elevated values. Those are observable in the areas of the Hamlet North, Karr basin, west central Alberta, West Pembina, south central Alberta, and in southern Alberta. In southern Alberta, Hamlet North, and Westcentral Alberta, the angular differences reach values of up to 80 degrees. In the areas of the south central Alberta and Karr Basin, the angular difference reaches 20-30 degrees.

The influence of groundwater flow on the magnitude of the ODFV can be revealed by comparing the magnitudes of the BDFVs to the ODFVs. In order to show such comparison, a map generated by subtracting the ODFVs from the BDFV is presented (Figure 5.23). It shows a range of values between −28 to 4 m/km (Figure 4.25). However, the absolute value of the difference increases significantly in several areas. In west central Alberta, the absolute value of the magnitude difference is reaching a value of 28 m/km. This area falls in the approximate area bound by 53° to 54.3° north latitude and 116° to 118° longitude west. This area corresponds to the potentiometric high of west central Alberta. Another major area with a high magnitude difference falls over the area of the Hamlet North, with absolute values of the difference reaching 10 m/km. This area is bounded by 57.5° to 60° latitude north and 120° to 122° longitude west. Other localized areas of high magnitude difference occur in the areas of the West Pembina, and along the Bashaw reef trend in south central Alberta.

The BDFV for oil is highly influenced by the differences in density between groundwater and oil. Density differences between groundwater in the Nisku Aquifer and a gas-saturated 35 API gravity oil (Figure 5.24) show values in the range of 200 to 550 kg/m^3. For both the Alberta basin and the Williston basin, the contour lines mimic the pattern observed in the structure map of the Nisku Formation (Figure 2.6). This pattern is expressed, as semi-parallel lines with the highest values of density difference in the deeper parts of the basin, and the orientation of the lines are subdued replica of the strike of the top of the Nisku Formation. This suggests that the pressure in the formation, which
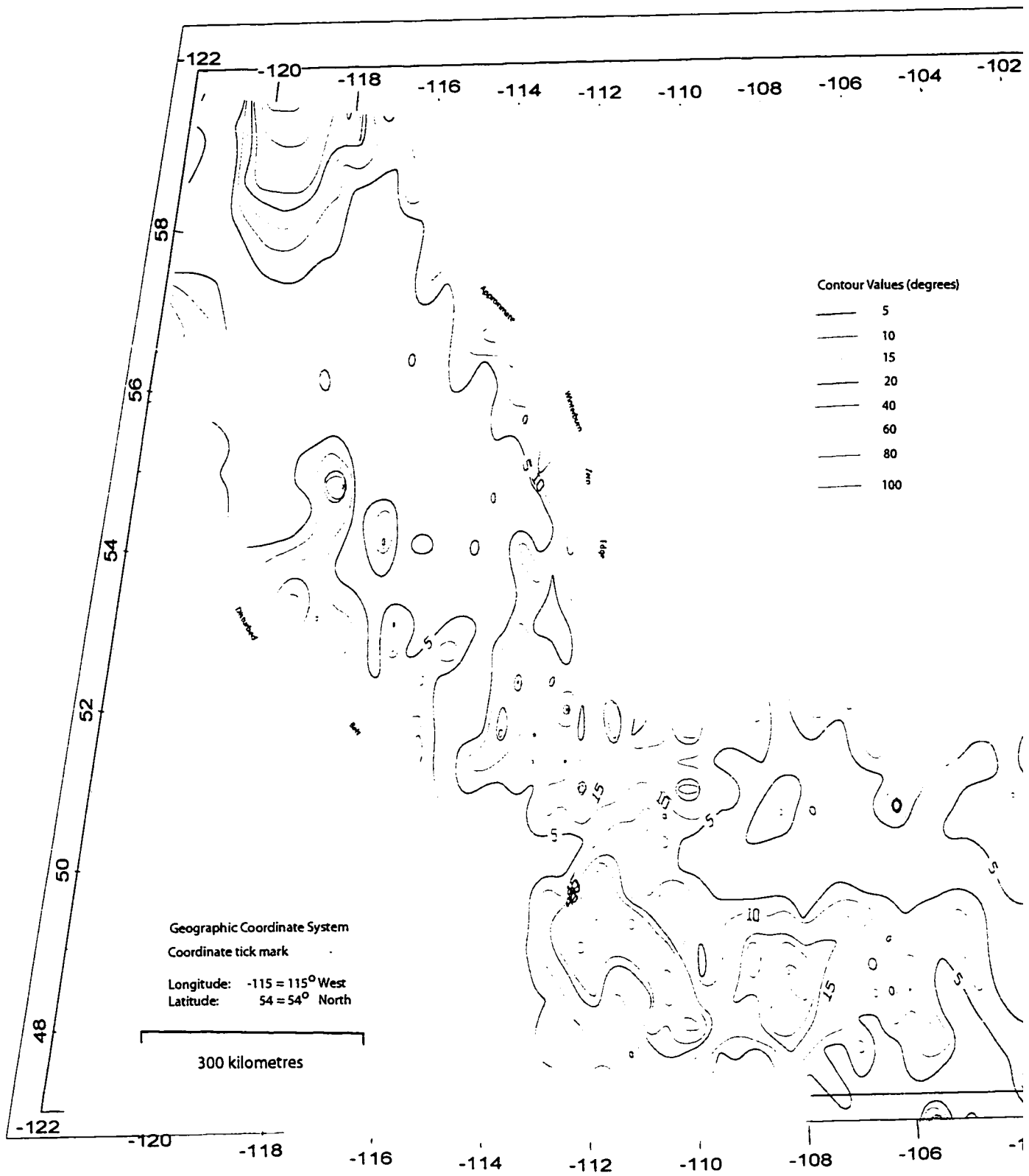
Figure 5.22 Angles of differences between the orientation of ODFVs and BDFVs.

Contour Values (degrees)

———	5
———	10
-	15
———	20
———	40
	60
———	80
———	100
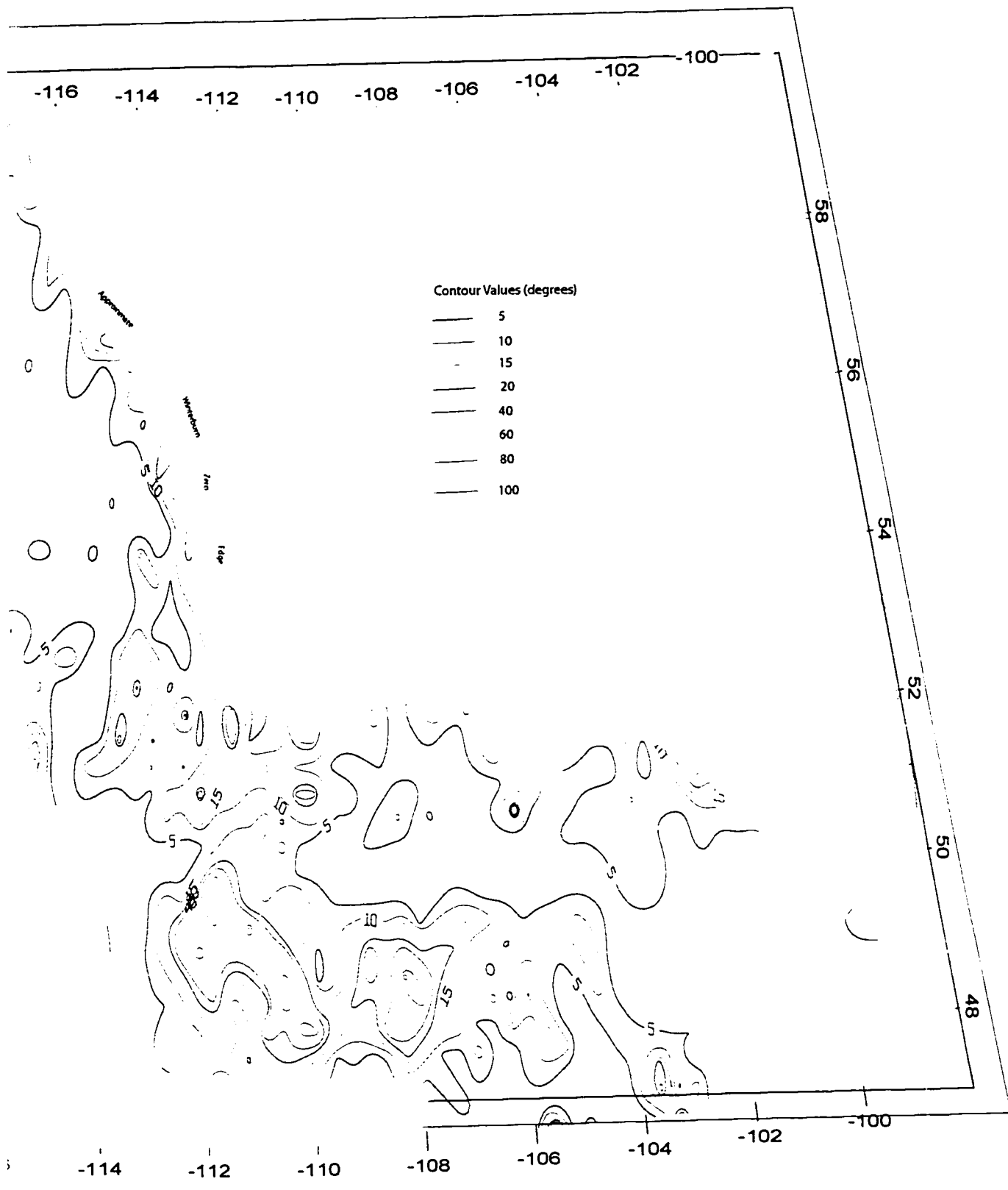
the orientation of ODFVs and BDFVs.
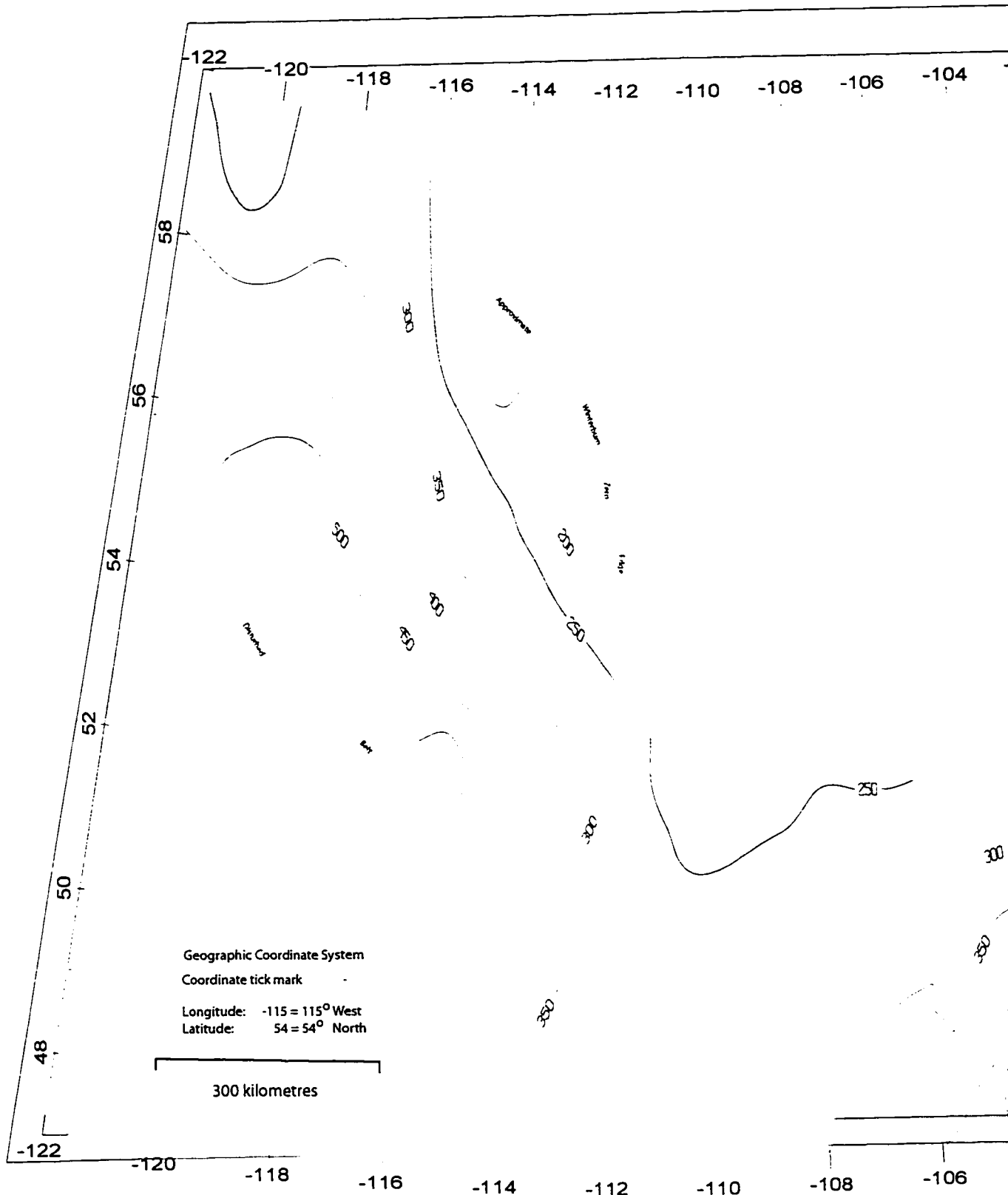
Figure 5.23 Differences in density between groundwater and a gas-saturated 35 API gravity oil (C. I. = 50

-116 -114 -112 -110 -108 -106 -104 -102 -100

58

56

54

52

50

48

-114 -112 -110 -108 -106 -104 -102 -100

124
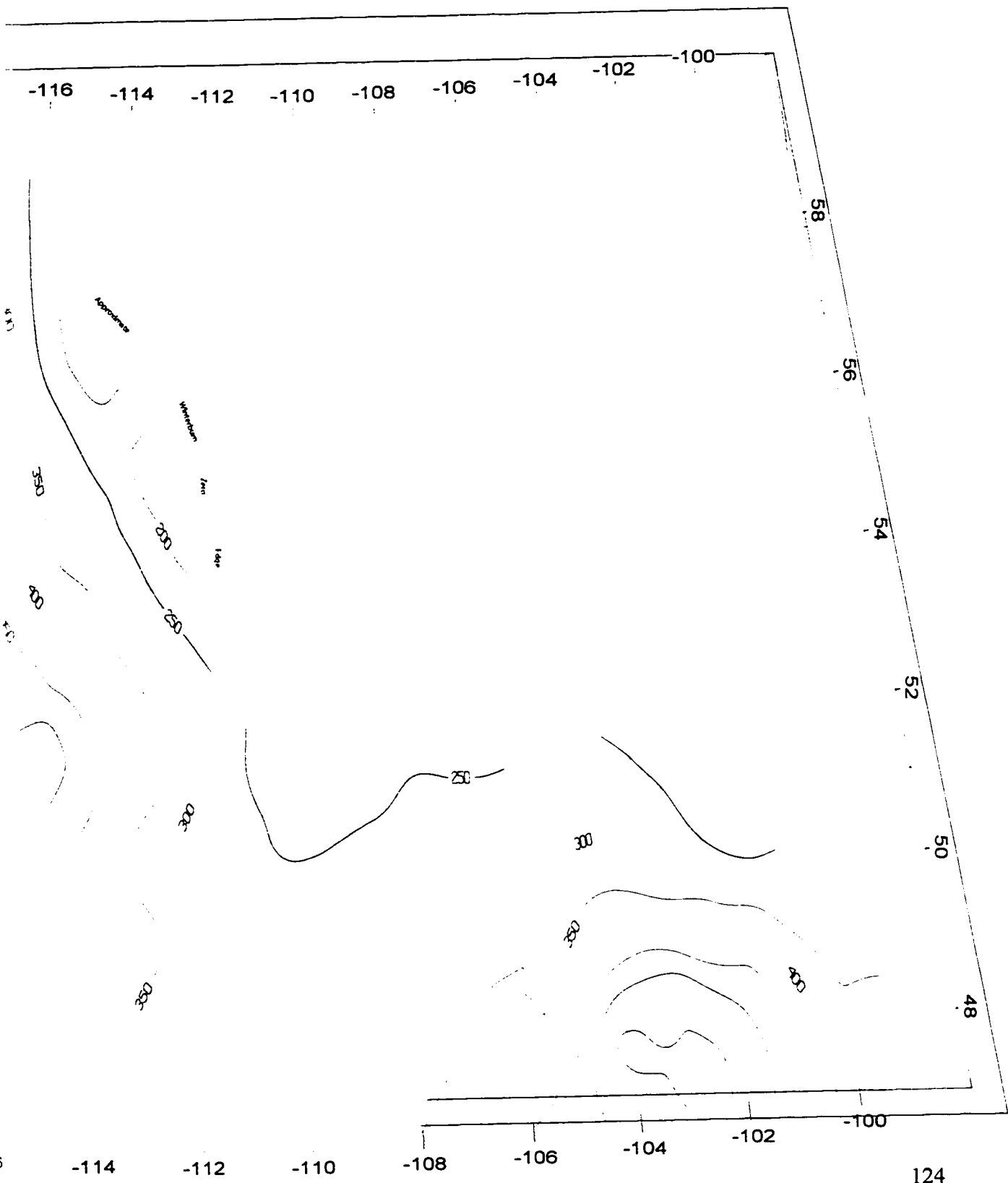
groundwater and a gas-saturated 35 API gravity oil (C.I. = 50 kg/m³).

is a function of depth, rather than the density of groundwater, controls the differences in density.

The dominance of hydrodynamic forces in certain areas of the basin is observed by comparing the patterns of the ODFR contour lines and those of density differences between oil and water. Contour lines of smaller values cut through the contour lines of density differences, highlighting the significance of hydrodynamic forces in the ODFVs in a particular area.

5.3.4 Hydrocarbon Accumulations and Hydrogeological Influences

The proposed modes of hydrocarbon migration suggested in Chapter 1, either as a separate phase or as a solution, necessitate the analysis for the movement of hydrocarbons from two perspectives. In the case of the transport in solution, which is more likely in lighter hydrocarbons due to their higher solubility, groundwater movement becomes the determining factor in the transport process, until thermodynamic conditions change in a way that those hydrocarbons are released from groundwater (Verweij, 1993). On the other hand, the transport of hydrocarbons as a separate phase is determined by the direction of the ODFV throughout the basin (Verweij, 1993). This section presents the ultimate result of the WDFVs and the ODFV analyses, which is the identification of sites preferred for hydrocarbon exploration, based on hydrogeological analyses.

5.3.4.1 Movement of Hydrocarbon as a Dissolved Phase

Hydrocarbon migration in the dissolved phase will persist until thermodynamic conditions are suitable for a compound to remain in solution. Thus, lighter hydrocarbons, which usually have more solubility in water, are going to migrate the farthest distance, which is opposite to the scenario for migration as a separate phase where heavier hydrocarbons will migrate the farthest distance. Examination of the WDFV in the Nisku Aquifer on a basinal scale reveals that water, and thus also the hydrocarbons in it, will take the following pattern. In the Williston basin, hydrocarbons will move to the northeast, to the north, and to the northwest. Areas of converging WDFVs are present at

125
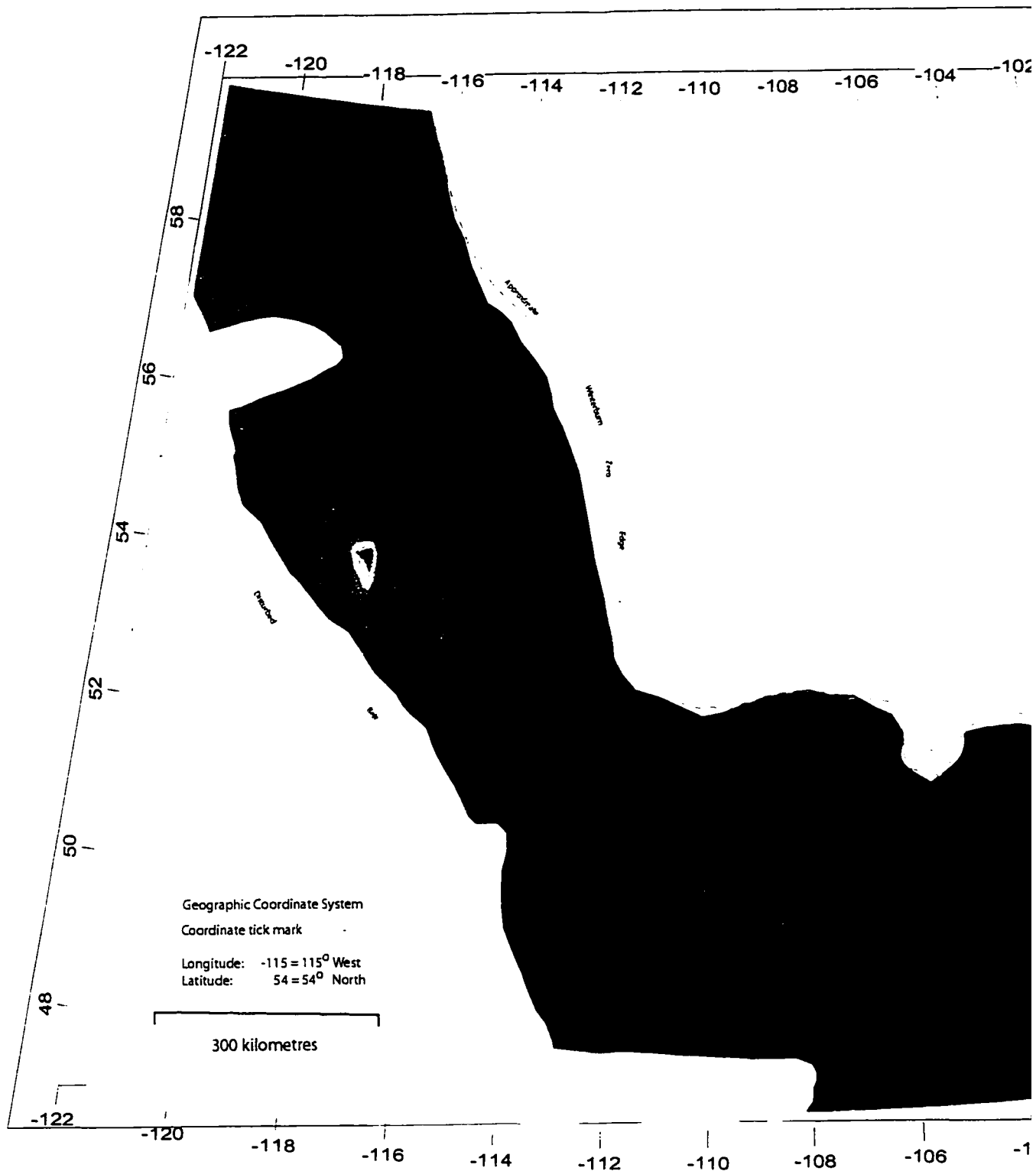
Figure 5.24 Differences in magnitude between BDFVs and ODFVs (BDFV-ODFV) for the Nisku Aquifer, W
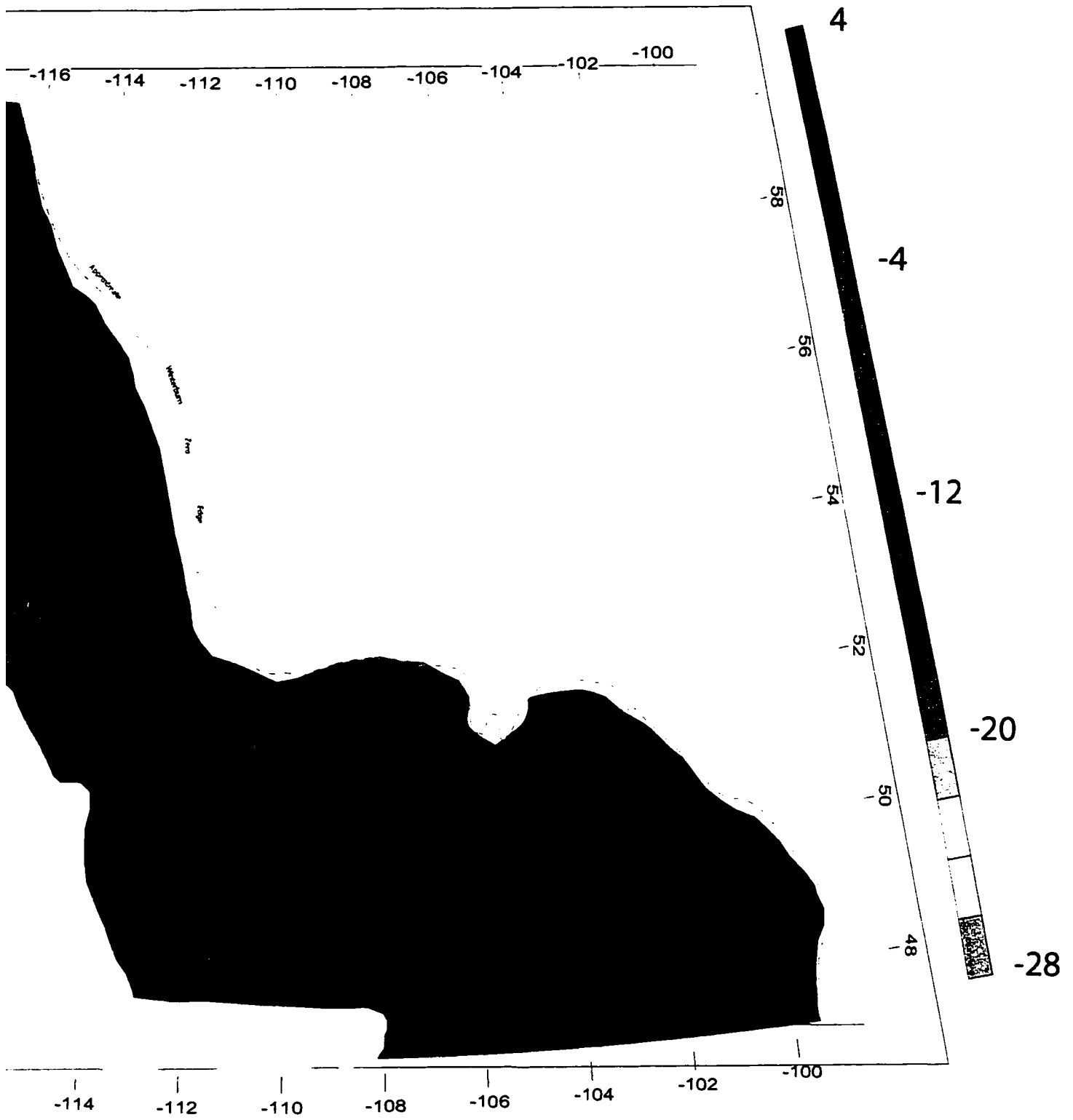
een BDFVs and ODFVs (BDFV-ODFV) for the Nisku Aquifer, WCSB (units: m/km).

several localities shown in Figure 5.25. Within the Alberta basin, migration of oil as a dissolved phase in the Nisku Aquifer will be directed from the southern border towards the north, with a major site of converging flow extending to the southern flank of the potentiometric high trend in south central Alberta.

Other major zones of convergence of flow are present in the Karr basin, the Hamlet North area, and in areas flanking the areas of cross-formational flow of the Bashaw reef trend in south central Alberta and that of west central Alberta.

Convergence zones of the WDFVs are created by both regional and relative minima in the hydraulic heads, which indicates areas of low potential. Those are created either as a result of regional energy sinks or resulting from two or more adjacent relative highs in fluid potential. Examples of regional sinks include Hamlet North area and the Karr basin area (Figure 5.25). An example of an area of a relative minimum resulting in area between two potential highs include that forming between west central Alberta and West Pembina (Figure 5.25). Factors that created this variation in the hydraulic head causing these basinal scale patterns have already been discussed.

5.3.4.2 The Movement of Hydrocarbon as a Separate Phase:

Effects of moving groundwater on the ODFVs for oils of different gravities and maps describing the dominance of a certain force in an area have been presented. An area by area description of such effects are given here, linking the hydrogeology of those areas to the pattern of ODFVs causing the dominance of a certain force or the convergence zones to develop.

In southeastern Saskatchewan, Montana, and North Dakota, where formation water density is elevated and the hydrocarbon density is reduced creating the maximum possible differences in density between oil and water (Figure 5.23), buoyancy forces dominate the driving mechanism of hydrocarbons within the Nisku Aquifer, as can be seen from the elevated ODFR values (Figure 5.21). The high pressure and temperature in the deeper parts of the basin play a role in reducing the density of the oil caused by both high OGR and by the fact that the oil density will decrease as the temperature increase. On the other hand, the hydraulic gradient is reduced in that area (Figure 4.3), reducing

127
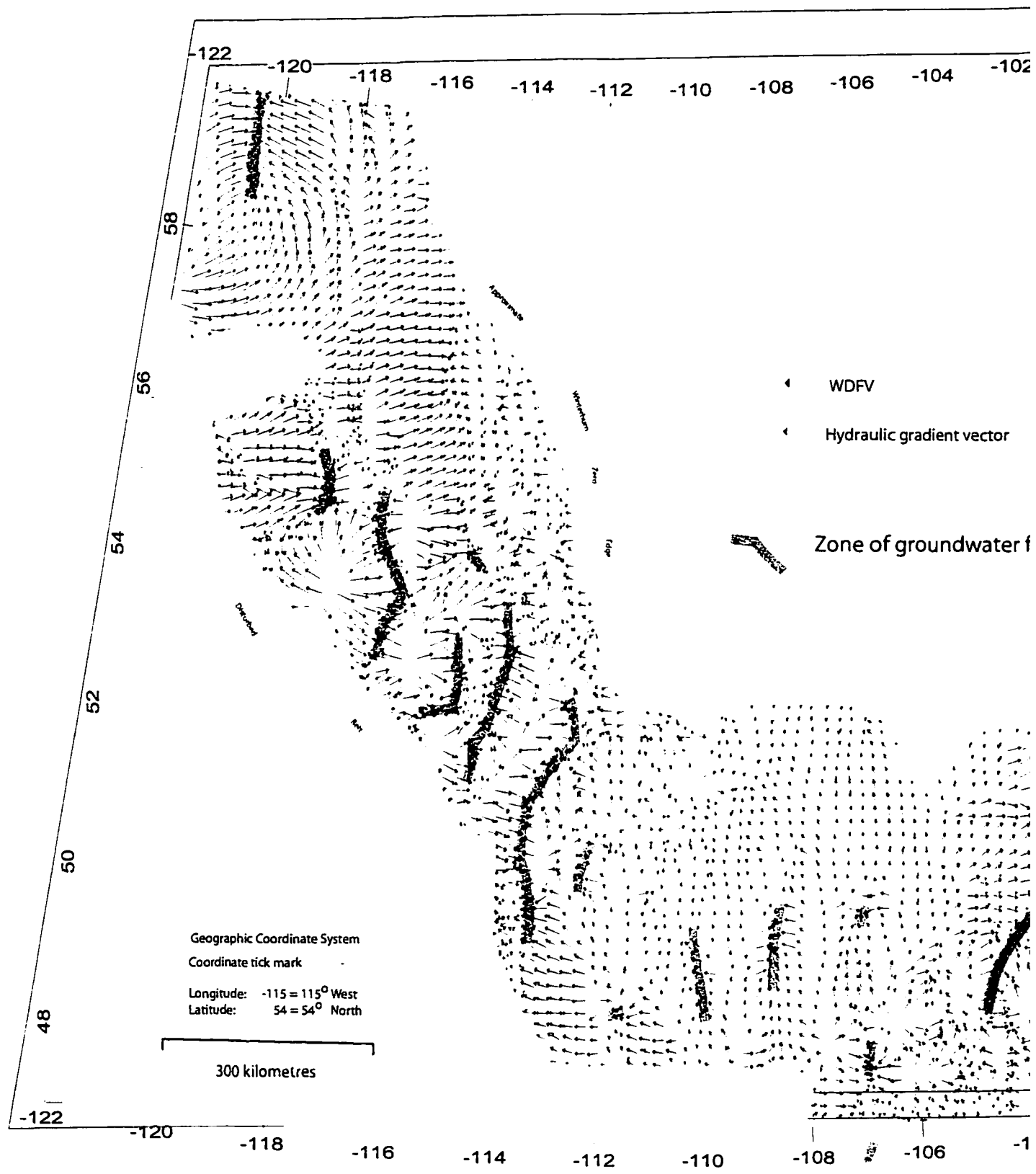
Figure 5.25 Map highlighting zones of converging groundwater flow, which are preferred sites for hydrocarb

Zone of groundwater flow convergence
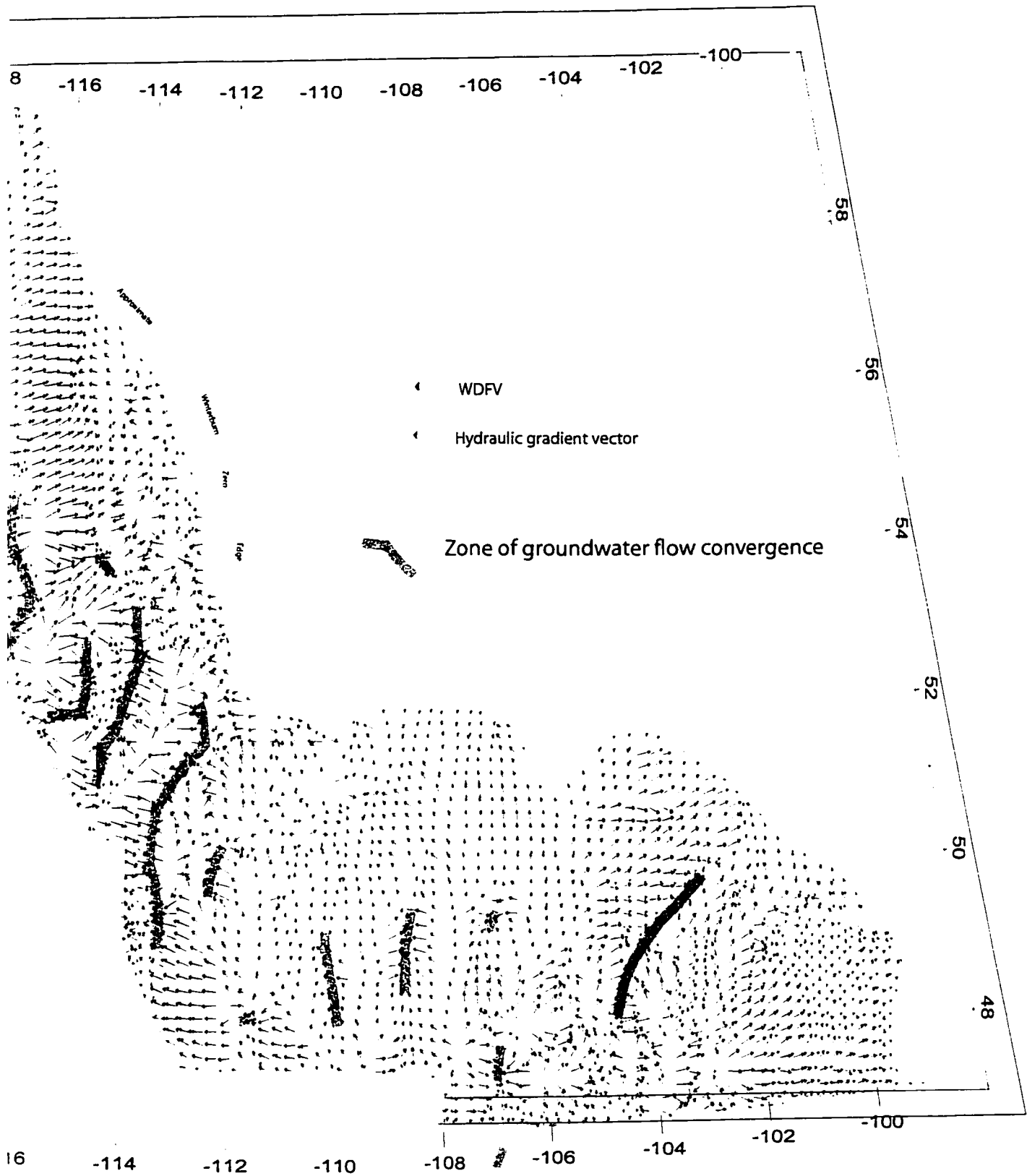
onverging groundwater flow, which are preferred sites for hydrocarbon accumulations.

128

the effects of hydrodynamic forces in the hydrocarbon flow regime. There are no indications of significant cross-formational flow in that area within the basin. However, since the flow is mainly updip, WDFVs are likely to enhance the hydrocarbon driving force vectors in the updip flow as can be observed from the reduced angles difference between ODFV and BDFV (Figure 5.22). Within this area, no indicators are present in the hydraulic head map that would indicate barriers to flow, which supports the occurrence of long distance hydrocarbon migration.

In southern Alberta and northwestern Montana, hydrodynamic forces dominate the oil driving forces for migration within the Nisku Aquifer, as can be concluded from the difference in angles between the BDFVs and the ODFVs, values reach up to 100 degrees, which represent the amount of diversion caused by the WDFVs. Also the ODFR values are reduced in this area (Figure 5.21), indicating that the BDFVs are becoming less dominant. Down dip groundwater flow dominates in this area, creating zones of convergence around the topographic high of southern Alberta and northwestern Montana. The energy provided by the higher elevations causes the hydraulic gradient to be relatively elevated, with heads corresponding to the highest topographic elevation in the area. The major zones of convergence of flow are primarily caused by the meeting of two types of ODFVs, one is dominated by buoyancy and thus acts updip, and another is dominated by the WDFVs and acting mostly downdip.

In the area of south central Alberta, where the Bashaw and Rimbey-Meadowbrook reef trends are located, the energy is provided by cross-formational flow of groundwater to the Nisku Aquifer from the underlying Leduc Aquifer as reported by Rostron et al. (1997), and observed in this study. It creates conditions for elevated magnitudes of WDFVs and thus that component of ODFV becomes more dominant. The dominance is indicated by the reduced ODFR values (Figure 5.21). The diversion of the ODFV creates two zones of convergence, on the southeast and the northwest of the Bashaw reef trend. The convergence to the northwestern flank is caused by oil driving forces being hydrodynamically diverted towards the Rimbey-Meadowbrook reef trend where there is a potentiometric low (Figure 4.2). Both of the convergence regions also have a general flow component in the updip direction to the northeast, probably directing the hydrocarbon transport towards the eastern subcrop of the Nisku Formation.

In Hamlet North area, the underpressuring provides the energy differences for the hydrodynamic forces to dominate, as can be concluded from the reduced values of the ODFR (Figure 5.21). The underpressuring creates a relatively large area of converging ODFV. Despite the Nisku Formation being dominated by fine clastics in much of the affected area, the presence of the reef trends may act as hydrocarbon conduits, collecting hydrocarbons and delivering them to the potentiometric minimum. The trapping of gas in the area of the North Hamlet is likely to be associated with the underpressuring.

In the area of west central Alberta, the regional p(d) plot suggests upward-directed cross-formational flow. The ODFVs radiate outward from the regional potentiometric high in west central Alberta, and is being dominated by hydrodynamic forces as can be observed from the reduced values ODFR (Figure 5.21). The high hydraulic gradient (Figure 4.2) around the flanks where the lithofacies of the Nisku Formation change from carbonates to fine clastics can be attributed to energy loss as flow crosses such a low permeability barrier. Such change in permeability may offer the capillary forces necessary for trapping the hydrocarbons at the lithofacies change, which form stratigraphic traps. As reported by Putnam and Ward (2001), the largest gas accumulations are found in the Nisku Formation in areas where hydraulic continuity exists between the Nisku and the Leduc aquifers.

In the area of the Karr Basin, it is observed that the ODFVs converge inward into a local potentiometric low caused by hydrodynamic forces. This is expressed by comparing the sink in hydraulic head (Figure 4.2) with the same location in the map of angle differences between the ODFVs and the BDFVs (Figure 5.22). The Nisku Formation lithofacies at the Karr basin is composed of evaporites, and away from evaporites, the Nisku Formation lithofacies change into fine clastics as shown in the regional cross-section by Switzer et al. (1994, Figure 12.36). The TDS in the area of the Karr basin is significantly elevated with the highest TDS corresponding to the geographic location of the Karr basin, which may indicate that dissolution which has been reported in the area (Switzer et al., 1994), and thus possible collapse features, to be present in the Nisku Formation in the Karr basin area. The Alberta basin, as described in chapter 3, has undergone compaction and then erosion of a thick sedimentary section. This erosion can

Favorable exploration sites where breaching in the under[...

Favorable exploration sites where the magnitudes of the [...

Favorable exploration sites where converging ODFVs are [...

•   Productions data point, Nisku Aquifer

Geographic Coordinate System

Coordinate tick mark   ·

Longitude: -115 = 115° West
Latitude: 54 = 54° North

300 kilometres
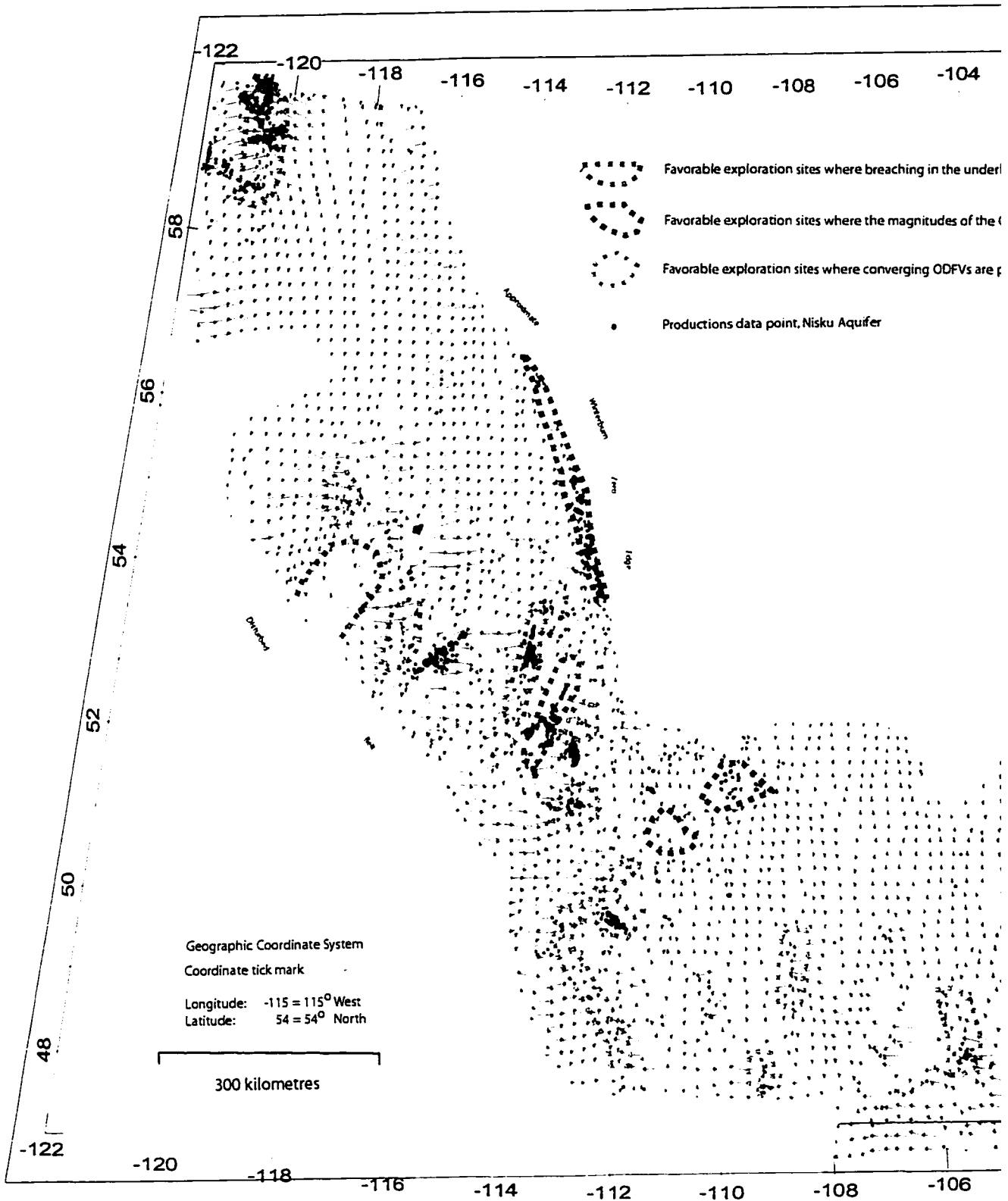
Figure 5.26 Favorable exploration sites in the Nisku Aquifer based on patterns in the ODFVs.

Favorable exploration sites where breaching in the underlying aquitard is likely

Favorable exploration sites where the magnitudes of the ODFVs are reduced

Favorable exploration sites where converging ODFVs are present

Productions data point, Nisku Aquifer
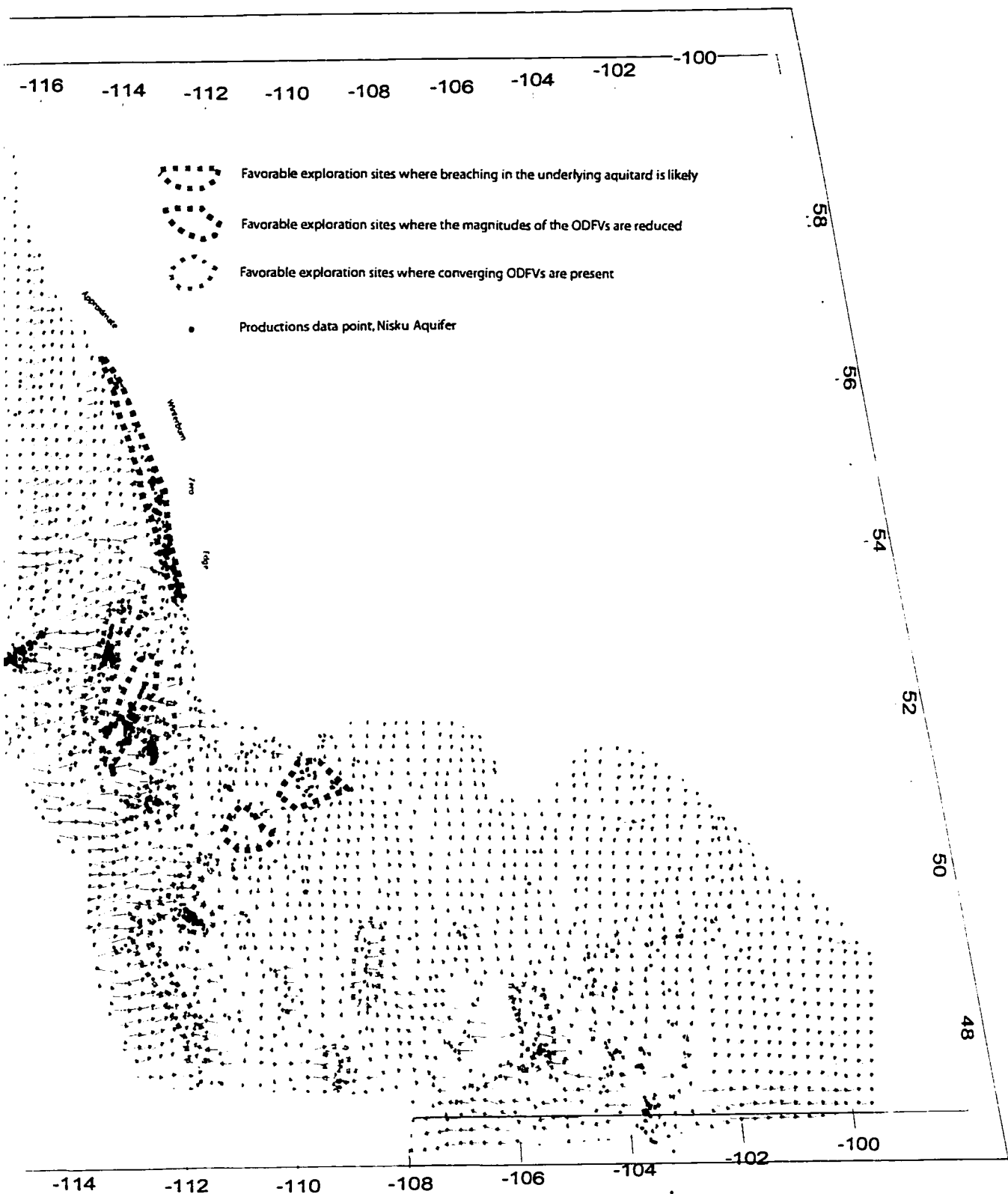
ı the Nisku Aquifer based on patterns in the ODFVs.

create a rebound, and if the Nisku Formation at the Karr basin indeed does have some collapse features, it is likely that those collapse features will form some relatively under-pressured zones, which can be significant reservoir to which hydrocarbons are likely to flow under hydrodynamically dominated migration system.

The east central Alberta area is a regional topographic low and a regional discharge zone as seen from the p(d) plot and temperature gradients. However, local variations in the surface topographic elevation in the area create local gravity-driven flow systems, which can influence the flow regime within the Nisku Aquifer as it becomes shallower. The p(d) plot of east central Alberta shows several relatively shallower localized topography driven flow systems, and the Nisku Aquifer falls in both shallower recharge zone and a deeper discharge zones of those systems. The presence of a recharge system in this area of significant hydrocarbon accumulations can possibly be acting to enhance the forces necessary for trapping mechanism in the region.

The area of the basin divide between the Alberta basin and the Williston basin may also be a favorable site for hydrocarbon accumulation for several reasons. First, the region is essentially a convergence zone. Furthermore, the area has several localities of reduced magnitudes of ODFVs. Low hydraulic gradient can result from either a zone of high permeability or a zone of dissipated flow-driving energy. In this area, there is a reduced hydraulic gradient coupled with a reduced structural gradient, which result in ODFVs of low magnitudes. In this zone, minor lithofacies changes can offer the capillary forces to create stratigraphic traps, since the forces mobilizing hydrocarbons are dissipated.

A map showing areas of areas with hydrogeologically favorable sites for exploration is presented in Figure 5.26.

5.3.4.3 Tilt in the Oil Water Contact

The systematic reduction in potential tilt with the increase in API gravity is due to the fact that the tilt amplification factor is directly proportional to the density of the hydrocarbon. The highest potential tilt values are again in areas of high hydraulic WDFVs. For the Nisku Aquifer, two areas are likely to have tilted OWC. Those are in west central Alberta and in the area flanking the elongated potentiometric high coinciding geographically with the Bashaw reef complex in south central Alberta. Two

reasons justify the possibility of tilt at those locations. First is that both areas fall where the Nisku Formation lithofacies can be considered to have higher values of permeability, from the knowledge of lithofacies associated with higher permeability. The second reason is that the high hydraulic gradient is caused by a significant source of energy, primarily the cross-formational flow in south central Alberta and in west central Alberta which creates areas of high-magnitude WDFVs.

In the area of the Hamlet North fields, and even though the potential tilt map shows a high values, it is very unlikely that tilt exists. As per the analysis by Hubbert (1953), water flowing in the aquifer is required in order to create the tilt. However, the Hamlet North area is likely to be saturated with gas (based on the p(d) plot) and no active groundwater flow under the gas.

5.3.4.4 Tilt in the Oil Water Contact and Possible Implication on Migration Patterns

Examination of Figure 4.8 shows a clear pattern of decreasing API gravity away from the potentiometric high of south central Alberta and a clearly distinguished relatively lower API gravity in the area coinciding with the Leduc Rimbey-Meadowbrook reef trend. This pattern can be explained by the fact that a main mechanism of delivering hydrocarbons into the Nisku Formation over the Bashaw reef complex is by cross-formational flow. Owing to strong hydrodynamic forces in the region, hydrocarbons can be impelled radially away from the potentiometric high. The lighter hydrocarbons are likely not to be flushed from drape structures above the Leduc reefs. But, however, relatively heavier hydrocarbons are going to be flushed from minor trapping structures, delivering them to trapping sites on either flanks of the potentiometric high in south central Alberta, which can explain the increase in density away from the clear trend of higher API around the Bashaw reef complex. Even if present-day hydrogeology cannot provide enough energy for flushing, a recent study by Haug et al. (2001) suggests a stronger paleoflow regime which would have more energy for more tilting and flushing of hydrocarbons.

133

6.0 Conclusions

1. Hydrogeological characterization of the Nisku Aquifer over the WCSB revealed varied evidences of active groundwater flow systems in the basin.

2. Basin-wide mapping of the potentiometric surface in the Nisku Aquifer revealed several features of mounds and depressions in the hydraulic head distribution. Those features are influenced by basinal-scale energy sources as well as lithological permeability controls. As a result of those variations, groundwater movement within the Nisku Aquifer is controlled by varying conditions, which in turn could potentially have influenced the movement of hydrocarbons.

3. In the areas of west-central and south-central Alberta, breaching in the aquitard coupled with elevated fluid potential in the underlying Leduc Aquifer set the stage for upward cross-formational flow leading to the formation of regional mounds in the potentiometric surface. The pressure system in this area is under-pressured. Despite the high TDS in the Nisku Aquifer in those areas, groundwater density does not affect the direction of flow due to the high hydraulic gradients present in those areas. Those high hydraulic gradients have created areas of high potential tilt in the oil water contact as well as regionally recognized convergence zones of ODFV. Adding to the hydrocarbon cross-formational flow, this study has shown that flow of hydrocarbons could have moved laterally away from the Bashaw reef complex and into the area above to the Leduc Rimbey-Meadowbrook trend in the Nisku and to the areas southeast of Bashaw. Correlation of API values in the area of south-central Alberta confirms the lateral migration patterns found in this study. High hydraulic gradients create areas of elevated potential tilt in the oil-water contact.

4. In the area of southern Alberta and northwestern Montana, the shallow depth of the Nisku aquifer coupled with relatively higher land surface topography created an area of elevated hydraulic heads forming a nose-like pattern of high

potentiometric surface. This high potentiometric surface created a zone of downdip groundwater flow to the north, east, and to the west. Also, this has influenced the ODFV in creating a vector field oriented to the north, and creating several vector convergence zones in southern Alberta and northwestern Montana.

5. In the northern Alberta basin and potentially in the Karr basin, basin rebound due to erosion has created a potentiometric minimum in the Nisku Aquifer, driving the flow inward towards the center of these minima. This has created ODFV fields dominated by groundwater flow, and correlation with present day distribution shows a large hydrocarbon accumulation in the Hamlet North area of northern British Columbia. The Karr basin is a site recommended for further investigation with potential significant hydrocarbon accumulations.

6. In east-central Alberta, a regional potentiometric minimum is present probably due to being at low regional land surface topography. The groundwater flow is highly affected by density variations probably due to the reduced hydraulic head gradient and relatively elevated structural gradient. Hydrocarbon accumulations in the Nisku Formation in east-central Alberta are potentially influenced by local flow systems where recharge is downward and enhancing the trapping mechanism.

7. In West Pembina, hydrocarbon generation provided the energy to raise the fluid potential in the Nisku Aquifer, expressed as a regional mound in the hydraulic head map. The system ranges from under-pressured, normally pressured, to over-pressured. Groundwater flow is outward from the area and high hydraulic gradients subdue the effects of groundwater density variations. The lithology in the area may prohibit significant hydrocarbon migration away from the source rocks in West Pembina, however, it can not be ruled out.

8. In the Williston basin, flow in the Nisku Aquifer within the study area is normally pressured. The flow patterns follow the regional pattern of topographically driven

flow. High density variations, coupled with increasing structural gradient to the depo-center of the basin and relatively reduced hydraulic head gradients introduce high degrees of deflection of groundwater flow. ODFVs are dominated by buoyancy forces in most of the area.

9. Petroleum hydrogeological analyses of the Nisku Aquifer in the WCSB revealed many favorable areas for exploration based on two modes of transport: 1) as a solution and 2) as a separate phase. Those are concluded from regionally recognizable converging forces driving oil and groundwater.

References

Adams, J. E., 1936, Oil pool of open reservoir type: AAPG Bulletin, v. 20, p. 780-796.

Ahern, J., and R. C. Ditmars, 1985, Rejuvenation of continental lithosphere beneath an intercratonic basin: Tectophysics, v. 120, p. 21-35.

Ahern, J. L., and S. R. Mrkvicka, 1984, A mechanical and thermal model for the evolution of the Williston basin: Tectonics, v. 3, p. 79-102.

Allan, J., and S. Creany, 1991, Oil families of the Western Canada sedimentary basin: Bulletin of Canadian Petroleum Geology, v. 39, p. 107-122.

Anfort, S. J., S. Bachu, and L. R. Bently, 2001, Regional-scale hydrogeology of the Upper Devonian-Lower Cretaceous sedimentary succession, south-central Alberta basin, Canada: AAPG Bulletin, v. 85, no. 4, p. 637-660.

Bachu, S., 1995a, Synthesis and model of formation water flow in the Alberta basin, Canada: AAPG, v. 79, p. 1159-1178.

Bachu, S., 1995b, Flow of variable-density formation water in deep sloping aquifers: review of methods of representation with case studies: Journal of Hydrology, v. 164, p. 19-39.

Bachu, S., 1997, Flow of formation waters, aquifer characteristics, and their relation to hydrocarbon accumulation in the northern part of the Alberta basin: AAPG Bulletin, v. 81, p. 712-733.

Bachu, S., 1999, Flow systems in the Alberta basin: patterns, types and driving mechanisms: Bulletin of Canadian Petroleum Geology, v. 47, p. 455-474.

Bachu, S., and B. Hitchon, 1996, Regional-scale flow of formation waters in the Williston Basin: AAPG Bulletin, v. 80, no. 2, p.248-264.

Bachu, S., and K. Michael, 2002, Flow of variable-density formation water in deep sloping aquifers: minimizing the error in representation and analysis when using hydraulic-head distributions: Journal of Hydrology, v. 259, p. 49-65.

Bachu, S., and J. R. Underschultz, 1993, Hydrogeology of formation waters, northeastern Alberta basin: AAPG Bulletin, v. 77, p. 1745-1768.

Bachu, S., and J. R. Underschultz, 1995, Large-scale erosional underpressuring in the Mississippian-Cretaceous succession, southwestern Alberta basin: AAPG Bulletin, v. 79, p. 989-1004.

Bachu, S., K. Michael, and B. E. Buschkuehl, 2002, The relation between stratigraphic elements, pressure regime, and hydrocarbons in the Alberta deep basin (with emphasis on select Mesozoic units): discussion: AAPG Bulletin, v. 86, no. 3, p. 525-528.

Barson, D. B., 1993, The hydrogeological characterization of oil fields in north-central Alberta for exploration purposes: Ph.D. thesis, University of Alberta, Edmonton, Alberta, Canada, 301 p.

Bear, J., 1972, Dynamics of fluids in porous media: New York, Elsevier, 764 p.

Belitz, K., and J. D. Bredehoeft, 1988, Hydrodynamics of the Denver basin: an explanation of subnormal fluid pressures: AAPG Bulletin, v. 72, p. 1334-1359.

Benn, A.A., and B. J. Rostron, 1998, Regional hydrochemistry of Cambrian to Devonian Aquifers in the Williston Basin, Canada-USA, in S. Bend, J. E. Christopher, C. F. Gilboy, and D. F. Paterson, eds., Proceedings of the eighth international Williston basin symposium: Saskatchewan Geological Society, Special Publication no. 13, p. 238-245.

Bethke, C. M., J. D. Reed, and D. F. Oltz, 1991, Long-range petroleum migration in the Illinois Basin: AAPG Bulletin, v. 75, no. 5, p. 925-945.

Block, D., 2001, Water resistivity atlas of western Canada CSPG (abs.): Rock the Foundation, abstracts of technical talks, posters, and core displays, Canadian Society of Petroleum Geologists Annual Convention, p. 359-369.

Bredehoeft, J. D., C. E. Neuzil, and P. C. D. Milly, 1983, Regional flow in the Dakota aquifer: a study of the role of confining layers: U. S. Geological Survey Water Supply Paper 2237, 45 p.

Bustin, R. M., 1991, Organic maturation of the Western Canadian sedimentary basin: International Journal of Coal Geology, v. 19, p. 319-358.

Chevron Exploration Staff, 1979, The geology, geophysics, and the significance of Nisku reef discoveries, West Pembina area, Alberta, Canada: Bulletin of Canadian Petroleum Geology, v. 27, p. 326-359.

Chiarelli, A., 1978, Hydrodynamic framework of eastern Algerian Sahara-influence on hydrocarbon occurrence: AAPG Bulletin, v. 62, p. 677-685.

Chierici, G. L., G. Long G, 1959, Compressibilité et masse spécifique des eaux de gisement dans les conditions du gisement, application à quelques problémes de reservoir engineering: Proceedings of the fifth World Petroleum Congress v. 2, p. 187-210.

Chierici, G. L., 1994, Principles of petroleum reservoir engineering, v. 1: Berlin, Springer-Verlag, 419p.

Cisyk, D. E., Stratigraphy, depositional settings, and diagenesis of carbonate rocks of the Upper Devonian Birdbear Formation, west-central Saskatchewan: Master's thesis, University of Regina, Regina, Saskatchewan, Canada, 148p.

Connolly, C. A., L. M. Walter, H. Baadsgaard, and F. Longstaffe, 1990a, Origin and evolution of formation waters, Alberta basin, Western Canada sedimentary basin: I. chemistry: Applied Geochemistry, v. 5, p. 375-395.

Connolly, C. A., L. M. Walter, H. Baadsgaard, and F. Longstaffe, 1990b, Origin and evolution of formation waters, Alberta basin, Western Canada sedimentary basin: II. isotope systematics and water mixing: Applied Geochemistry, v. 5, p. 397-413.

Corbet, T. F., and C. M. Bethke, 1992, Disequilibrium fluid pressures and groundwater flow in the Western Canada sedimentary basin: Journal of Geophysical Research, v. 97, no. B5, p. 7203-7217.

Crowley, K. D., J. L. Ahern, and C. W. Naeser, 1985, Origin and epeirogenic history of Williston basin: evidence from fission-track analysis of apatite: Geology, v. 13, p. 620-623.

Dahlberg, E. C., 1994, Applied hydrodynamics in petroleum exploration: New York, Springer-Verlag, 295 p.

Davies, P. B., 1987, Modeling areal, variable density, groundwater flow using equivalent freshwater head –analysis of potentially significant errors, in Solving groundwater problems with models: Proceedings of the National Water Well Association/International Groundwater Modeling Center Conference, p. 888-903.

Davis, R. W., 1987, Analysis of hydrodynamic factors in petroleum migration and entrapment: AAPG Bulletin, v. 71, no. 6, p. 643-649.

Davis, R. W., 1991, Integration of geological data into hydrodynamic analysis of hydrocarbon movement: Geological Society Special Publication, no. 59, p. 127-135.

DeWiest, R. J. M., 1965, Geohydrology: New York, Wiley, 366 p.

Downey, J. S., 1982, Hydrodynamics of the Williston basin in the northern Great Plains, in D. G. Jorgensen and D. C. Signor, eds., Geohydrology of the Dakota aquifer: Worthington, Ohio, National Water Well Association, p. 92-98.

Downey, J. S., 1984, Geohydrology of the Madison and associated aquifers in parts of Montana, North Dakota, South Dakota, and Wyoming: U.S. Geological Survey Professional Paper 1273-G, 47 p.

Downey, J. S., and G. A. Dinwiddie, 1988, The regional aquifer system underlying the northern Great Plains in parts of Montana, North Dakota, South Dakota, and Wyoming-Summary: U. S. Geological Survey Professional Paper 1402-A, 63 p.

Downey, J. S., J. F. Busby, and G. A. Dinwiddie, 1987, Regional aquifer and petroleum in the Williston basin region of the United States, in J. A. Peterson, D. M. Kent, S. B. Anderson, R. H. Pilatske, and M. W. Longman, eds., Williston basin: Anatomy of a cratonic oil province: Denver, Colorado, Rocky Mountain Association of Geologists, p. 299-312.

England, W. A., A. S. Mackenzie, D. M. Mann, and T. M. Quingley, 1987, The movement and entrapment of petroleum fluids in the subsurface: Journal of the Geological Society, London, v. 144, p. 327-347.

Fowler M. G., L. D. Stasiuk, M. Hearn, and M. Obermajer, 2001, Devonian hydrocarbon source rocks and their derived oils in the Western Canada sedimentary basin: Bulletin of Canadian Petroleum Geology, v. 49, no.1, p. 117-148.

Freeze, R. A., and J. A. Cherry, 1979, Groundwater: New Jersey, Prentice-Hall, 604 p.

Freeze, R. A., and P. Witherspoon, 1966, Theoretical analysis of regional groundwater flow, 1. analytical and numerical solutions to the mathematical model: Water Resources Research, vol. 2, no. 4, p. 641-656.

Freeze, R. A., and P. A. Witherspoon, 1967, Theoretical analysis of regional groundwater flow, 2. Effect of water-table configuration and subsurface permeability variation: Water Resources Research, v. 3, no. 2, p. 623-634.

Ge, S., and G. Garven, 1989, Tectonically induced transient groundwater flow in foreland basins, in A. E. Beck, L. Stegena, and G. Garven, eds.,The origin and evolution of sedimentary basins and their energy and mineral resources: American Geophysical Union Geodynamics Series Monograph 48, p. 145-157.

Ge, S., and G. Garven, 1994, A theoretical model for thrust-induced deep groundwater expulsion with application to Canadian Rocky Mountains: Journal of Geophysical Research, v. 99, p. 13851-13868.

Gerhard, L. C., S. B. Anderson, J. A. LeFever, and C. G. Carlson, 1982, Geological development, origin, and energy mineral resources of Williston basin, North Dakota: AAPG Bulletin, v.66, p. 989-1020.

Glassø, Ø., 1980, Generalized pressure-volume-temperature correlations: Journal of Petroleum Technology, v. 32, p.785-95.

Goebel, L. A., 1950, Cairo Field, Union County, Arkansas: AAPG Bulletin, v. 34, no. 10, p. 1954-1980.

Grasby, S. E., and I. Hutcheon, 2001, Controls on the distribution of thermal springs in the southern Canadian Cordillera: Canadian Journal of Earth Sciences, v. 38, p. 427-440.

Gretener, P. E., 1981, Geothermics: using temperature in hydrocarbon exploration: AAPG Education Course Note Series no. 17, 170 p.

Halabura, S. P., Depositional environments of the Upper Devonian Birdbear Formation, Saskatchewan: Master's thesis, University of Saskatchewan, Saskatoon, Saskatchewan, Canada, 182p.

Hannon, N., 1987, Subsurface water flow patterns in the Canadian Sector of the Williston basin, in J. A. Peterson, D. M. Kent, S. B. Anderson, R. H. Pilatske, and M. W. Longman, eds., Williston basin: Anatomy of a cratonic oil province: Denver, Colorado, Rocky Mountain Association of Geologists, p. 313-322.

Haug, K, B. Rostron, and C. Mendoza, 2001, Numerical modeling of a saline plume in the Mannville Group Aquifer, Alberta basin: Proceedings of the 2nd joint International Association of Hydrogeologists and The Canadian Geotechnical Society specialty conference, p. 1264-1271.

Hearn, M. R., 1996, Stratigraphic and diagenetic controls on aquitard integrity and hydrocarbon entrapment, Bashaw reef complex, Alberta, Canada: Master's thesis, University of Alberta, Edmonton, Alberta, Canada, 135 p.

Hearn, M. R., and B. J. Rostron, 1997, Hydrogeologic, stratigraphic, and Diagenetic controls on petroleum entrapment in Devonian reefs, Bashaw area, Alberta, in J. Wood and B. Martindale, compilers, Sedimentary Events - Hydrocarbon Systems: Canadian Society of Petroleum Geologists and Society of Economic Paleontologists and Mineralogists core conference abstracts, p. 89-103.

Hitchon, B., 1969a, Fluid flow in the Western Canada sedimentary basin 1: effect of topography: Water Resources Research, v. 5, p.186-195.

Hitchon, B., 1969b, Fluid flow in the Western Canada sedimentary basin 2: effect of geology: Water Resources Research, v. 5, p.460-469.

Hitchon, B., 1984, Geothermal gradients, hydrodunamics, and hydrocarbon occurrences, Alberta, Canada: AAPG Bulletin, v. 68, p. 713-743.

Hitchon, B., and M. Brulotte, 1994, Culling criteria for "standard" formation water analyses: Applied Geochemistry, v. 9, p. 637-645.

Hitchon, B., and I. Friedman, 1969, Geochemistry and origin of formation waters in the Western Canada sedimentary basin, I. stable isotopes of hydrogen and oxygen: Geochemica and Cosmochimica Acta, v. 33, p. 1321-1349.

Hubbert, M. K., 1940, The theory of groundwater motion: Journal of Geology, v. 48, no. 8, p. 785-944.

Hubbert, M.K., 1953, Entrapment of petroleum under hydrodynamic conditions: AAPG Bulletin, v.37, no. 8, p. 1954-2026.

Hudema, T. C., 1991, Stratigraphy and sedimentology of the uppermost Fransian Jean Marie Formation of northeastern British Columbia and adjoining Northwest Territories: Master's thesis, University Saskatchewan, Saskatoon, Saskatchewan, Canada, 134 p.

Hugo, K. J., 1985, Hydrodynamic flow associated with Leduc reefs: Master's thesis, University of Calgary, Calgary, Alberta, Canada, 149 p.

Iampen H. T., and B. J. Rostron, 2000, Hydrogeochemistry of pre-Mississippian brines, Williston basin, Canada-USA: Journal of Geochemical Exploration, v. 69-70, p. 29-35.

Jiao J. J. and C. Zheng, 1998, Abnormal fluid pressures caused by erosion and subsidence of sedimentary basins: Journal of Hydrology, v. 204, p. 124-137.

Kalkreuth, W., and M. McMechan, 1988, Burial history and thermal maturity, Rocky Mountain Front Ranges, foothills, and foreland, east-central British Columbia and adjacent Alberta, Canada: AAPG Bulletin, v.72, p. 1395-1410.

Kirste, D, 2000, Compositional variation in formation fluids and their relation to fluid flow and water-rock interaction in Devonian to Lower Cretaceous sedimentary rocks of southern Alberta: Ph.D. thesis, University of Calgary, Calgary, Alberta, Canada, 219 p.

Kissling, D. L., 1997, Upper Devonian Nisku resrviors in a barrier-lagoon complex, south Alberta and northwest Montana plains, J. Wood and B. Martindale, compilers, Sedimentary Events - Hydrocarbon Systems: Canadian Society of Petroleum Geologists and Society of Economic Paleontologists and Mineralogists core conference abstracts, p. 105-120.

Lasater, J. A., 1958, Bubble point pressure correlations: American Institute of Mining Engineers Transactions, v. 213, p. 379-381.

Lusczynski, N. J., 1961, Head and flow of ground water of variable density: Journal of Geophysical Research, v. 66, no. 12, p. 4247-4255.

Machel, H. G., 1986, Limestone diagenesis of Upper Devonian Nisku carbonates in the subsurface of central Alberta: Canadian Journal of Earth Science, v. 23, p. 1804-1822.

Machel, H. G., and J. H. Anderson, 1989, Pervasive subsurface dolomitization of the Nisku Formation in central Alberta: Journal of Sedimentary Petrology, v.59, p. 891-911.

Machel, H. G., H. R. Krouse, L. R. Riciputi, and D. R. Cole, 1995, Devonian Nisku sour gas play, Canada: a unique laboratory for study of thermochemical sulfate reduction, in M. A. Vairavamurthy and M. A. A. Schoonen, eds., Geochemical transformation of sedimentary sulfer: American Chemical Society Symposium Series 612, p. 439-454.

Machel, H. G., P. A. Cawell , and K. S. Patey, 1996, Isotopic evidence for carbonate cementation and recrystallization, and for tectonic expulsion of fluids into the Western Canada sedimentary basin: Geological Society of America Bulletin, v. 108, p. 1108-1119.

Manzano, B. K., M. G. Fowler, and H. G. Machel, 1997, The influence of thermochemical sulfate reduction on hydrocarbon composition in Nisku reservoirs, Brazeau River area, Alberta, Canada: Organic Geochemistry, v. 27, p. 507-521.

MBOGC, 2002, Online data, <http: //bogc.dnrc.state.mt.us/OnlineData.htm> Acessed 2001-2002.

Michael, K., 2002, Flow of formation water in the Alberta basin adjacent to the Rocky Mountains thrust and fold belt, west-central Alberta, Canada: Ph.D. thesis, University of Alberta, Edmonton, Alberta, Canada. 332 p.

Mossop, G. D., and I. Shetsen, comp., 1994, Geological Atlas of the Western Canada sedimentary basin: Calgary, Canadian Society of Petroleum Geologists and Alberta Research Council, 510 p.

Munn, M. J., 1909, The anticlinal and hydraulic theories of oil and gas accumulation: Economic Geology, v. 4, no. 6, p. 509-529.

National Geophysical Data Center, 2002, NGDC 5-Minute Gridded Elevation Data Selection, <http: //www.ngdc.noaa.gov/mgg/global/seltopo.html> Accessed 2001-2002.

NDIC, 2000, Oil in North Dakota, 2000 production statistics, 645 p.

Nesbitt, B. E., and K. Muehlenbachs, 1993, Synorogenic fluids of the Rockies and their impact on paleohydrogeology and resources of the Western Canada sedimentary basin, in G. M. Ross, ed., Alberta Basement Transect Workshop: LITHOPROBE Report 31. LITHOPROBE Secretariate, University of British Columbia, p. 60-62.

Neuzil, C. E., 1995, Abnormal pressure as hydrodynamic phenomena: American Journal of Science, v. 295, p. 742-786.

Neuzil, C.E., and D.W. Pollock, 1983, Erosional unloading and fluid pressures in hydraulically "tight" rocks: Journal of Geology, v. 91, p. 179-193.

Nurkowski, J. R., 1984, Coal quality, coal rank variation and its relation to reconstructed overburden, Upper Cretaceous and Tertiary plains coals, Alberta, Canada: AAPG Bulletin, v. 68, p. 285-295.

Obermajer, M., K. G. Ostadetz, M. G. Fowler, and L. R. Snowdon, 1999, Geochemistry and familial association of crude oils from the Birdbear Formation in southeastern Saskatchewan, Williston Basin: Bulletin of Canadian Petroleum Geology, v. 47, p. 255-269.

Orr, E. D., and C. W. Kreitler, 1985, Interpertation of pressure-depth data from confined underpressured aquifers exemplified by the Deep-Basin Brine aquifer, Palo Duro Basin, Texas: Water Resources Research, v. 21, no. 4, p. 533-544.

Ostadetz, K. G., P. W. Brooks, and L. R. Snowdon, 1992, Oil families and their sources in the Canadian Williston basin (southern Saskatchewan and southwestern Manitoba): Bulletin of Canadian petroleum geology, v. 40, p. 254-273.

Parks, K. P., and J. Tóth, 1995, Field evidence for erosion-induced underpressuring in Upper Cretaceous and Tertiary strata, west-central Alberta, Canada: Bulletin of Canadian Petroleum Geology, v. 43, p. 281-292.

Paul, D., Hydrogeology of the Devonian Rimbey-Meadowbrook reef trend of central Alberta, Canada: Master's thesis, University of Alberta, Edmonton, Alberta, Canada, 152 p.

Peterson, J. A., and L. M. MacCary, 1987, Regional stratigraphy and general petroleum geology of the U.S. portion of the Williston basin and adjacent areas,

in J. A. Peterson, D. M. Kent, S. B. Anderson, R. H. Pilatske, and M. W. Longman, eds., Wiilliston basin: Anatomy of cratonic oil province: Denver, Colorado, Rocky Mountain Association of Geologists, p. 9-44.

Price, L. C., 1976, Aqueous solubility of petroleum as applied to its origin and primary migration: AAPG Bulletin, v. 60, p. 213-244.

Putnam E., and G. S. Ward, 2001, The relation between stratigraphic elements, pressure regime, and hydrocarbons in the Alberta deep basin (with emphasis on select Mesozoic units): AAPG Bulletin, v. 85, no. 4, p. 691-714.

Rostron, B., 1993, Numerical simulations of how cap rock properties can control differential entrapment of oil: Proceedings Society of Petroleum Engineers Annual Technical Conference and Exhibition, Formation Evaluation and Reservoir Geology Volume, p. 263-275.

Rostron, B. J, 1994, A new method for culling pressure data used in hydrodynamic studies: AAPG Annual Meeting Abstracts - American Association of Petroleum Geologists and Society of Economic Paleontologists and Mineralogists, P. 247

Rostron, B., 1995, Cross-formational fluid flow in Upper Devonian to Lower Cretaceous strata, west-central Alberta, Canada: Ph.D. thesis, University of Alberta, Edmonton, Alberta, Canada, 201 p.

Rostron, B. J., and J. Tóth, 1997, Cross-formational fluid flow and the generation of a saline plume of formation waters in the Mannville Group, west-central Alberta, in S. G. Pemberton and D. P. James, eds., Petroleum geology of the Cretaceous Mannville Group, Western Canada: Canadian Society of Petroleum Geologists Memoir 18, p. 169-190.

Rostron, B. J., J. Tóth, and H. G. Machel, 1997, Fluid flow, hydrochemistry and petroleum entrapment in Devonian reef complexes, south-central Alberta, Canada, in I. P. Montanez, J. M. Gregg, and K. L. Shelton, eds., Basin-wide diagenetic patterns: integrated petrologic, geochemical, and hydrologic consideration: SEPM Special Publication 57, p. 139-155.

Schowalter, T. T., 1979. Mechanics of secondary hydrocarbon migration and entrapment: AAPG Bulletin, vol. 63, no. 5, p. 723-760.

Simpson, G., 1999, Sulfate reduction and fluid chemistry of the Devonian Leduc and Nisku formations in south-central Alberta: Ph.D. thesis, University of Calgary, Calgary, Alberta, Canada, 288 p.

Skilliter, C. C., 2000, A stratigraphic and geochemical investigation of Upper Devonian shale and marl aquitards, west-central Alberta, Canada: Master's thesis, University of Alberta, Edmonton, Alberta, Canada, 227 p.

Spencer, C. W., 1987, Hydrocarbon generation as a mechanism for overpressuring in Rocky Mountains region: AAPG Bulletin, v. 71, p. 368-388.

Stokes, F. A., and S. Creany, 1985, Sedimentology of a carbonate source rock: the Duvernay Formation of Alberta, Canada, in M. W. Longman, K. W. Shanley, R. F. Lindsay, and D.E. Eby, eds., Rocky Montain carbonate reservoirs-a Core Workshop: SEPM Core Workshop No. 7, p.343-375.

Stone, D. S., and R. L. Hoeger, 1973, Importance of hydrodynamic factor in formation of lower cretaceous combination traps, Big Muddy-South Glenrock area, Wyoming: AAPG Bulletin, v. 57, no. 9, p. 1714-1733.

Switzer, S. B., Holland, W.G., Christie, D.S., Graf, G.C., Hedinger, A. G., McAuley, R.J., Wierzbicki, R.A. and J.J. Packard, 1994, Devonian Woodbend-Winterburn strata of the Western Canada sedimentary basin, in G.D. Mossop and I. shetsen comps., Geological atlas of the Western Canada sedimentary basin, Canadian Society of Petroleum Geologists and Alberta Research Council, p. 165-202.

Toop, D. C., 1992, Petroleum hydrogeology and hydrochemistry of south-central Saskatchewan: Master's thesis, University of Alberta, Edmonton, Alberta, Canada, 172 p.

Tóth, J., 1962, A theory of groundwater motion in small drainage basins in central Alberta, Canada: Journal of Geophysical Research v. 67, p. 4375-4387.

Tóth, J., 1963, A theoretical analysis of groundwater flow in small drainage basins: Journal of Geophysical Research, v. 68, p. 4795-4812.

Tóth, J., 1978, Gravity-induced cross-formational flow of formation fluids, Red Earth region, Alberta, Canada: Analysis patterns, and evolution: Water Resources Research, v. 14, p. 805-843.

Tóth, J., 1980, Cross-formational gravity-flow of groundwater: a mechanism of the transport and accumulation of petroleum (the generalized hydraulic theory of petroleum migration), in W. H. Roberts III, and R. J. Cordell, eds., Problems of petroleum migration: AAPG Studies in Geology 10, p. 121-167.

Tóth, J., 1995, Hydraulic continuity in large sedimentary basins: Hydrogeology Journal, v. 3, no. 4, p. 4-15.

Tóth, J., and T. F. Corbet, 1986, Post-Paleocene evolution of regional groundwater flow systems and their relation to petroleum accumulations, Taber area, southern Alberta, Canada: Bulletin of Canadian Petroleum Geology, v. 34, p. 339-363.

Tóth, J. and R. Millar, 1983, Possible effects of erosional changes of the topographic relief on pore pressures at depth: Water Resources Research, v. 19, no 6, p. 1585-1597.

Tóth, J., and K. Rakhit, 1988, Exploration for reservoir quality rock bodies by mapping and simulation of potentiometric surface anomalies: Bulletin of Canadian Petroleum Geology, v. 36, no. 4, p. 362-378.

Verweij, J. M., 1993, Hydrocarbon migration system analysis: New York, Elsevier, 276 p.

Wendte, J., J. J. Dravis, L. D. Stasiuk, H. Qing, S. L. O. Moore, and G. Ward, 1998, High temperature saline (thermoflux) dolomitization of Devonian Swan Hills platform and bank carbonates, Wild River area, west-central Alberta: Bulletin of Canadian Petroleum Geology, v. 46, p. 210-265.

Whittaker, S. G., and E. W. Mountjoy, 1996, Diagenesis of an Upper Devonian carbonate-evaporite sequence: Birdbear Formation, Southern Interior Plains, Canada: Journal of Sedimentary Research, v. 66, no. 5, p. 965-975.

Wilkinson, P. K., 1995, Is fluid flow in Paleozoic formations of west central Alberta affected by the Rocky Mountain thrust belt: Master's thesis, University of Alberta, Edmonton, Alberta, Canada, 102 p.

Appendix A: Accuracies and Resolutions of Selected DST Pressure Gauges.

Make and Model	Accuracy	Resolution	Pressure Range psi
Geophysical Research Corporation Amerada) RPG 3, 4, and 5	0.25	0.05%	500-25000
Kuster KPG K-2, 3, and 4	0.25	0.05%	800-22000
Johnson J-200	0.25	0.005%	1600-20000
Sperry Sun MRPG	0.05	0.005%	1000-10000
Johnson J-300	0.10	0.02	0-10000
Hewlett Packard HP-2811B	0.025	0.01 pis	0-10000
Flopetrol SSDR	0.05	0.02 psi	0-10000
Flopetrol SSDR	0.035	0.01 psi	0-10000
Flopetrol CRG	0.035	0.01 psi	0-10000
Panex Corporation 1420	0.07	0.0001%	500-15000
Squire_Whistenghouse 6800	0.025	0.01 psi	0-15000

[a] Manufacturer's specification, percent of full scale.
[b] Manufacturer's specification, percent of full scale or psi.

Table A1 Accuracies of selected pressure gauges used in DSTs (Courtesy of Hugh W. Reid & Associates Ltd, Calgary, Alberta, Canada)

148

Appendix B: Overpressuring Due to Hydrocarbon Phase

Overpressuring in the subsurface due to measurements of pressure in the hydrocarbon (HC) phase is attributed to difference in density between groundwater and the HC phase. The illustrations in Figure B1 shows schematics of how such over pressuring is created. For the case of a stratigraphic trap, the overpressuring at the point of pressure measurement p is p_{α}, that can be related to the of updip length of continuous-phase hydrocarbon, ΔX and the dip of the reservoir (formation) H/L.

$$p_{\alpha} = \Delta Z (g\rho_{GW} - g\rho_{HC}) = \Delta X \frac{H}{L}(g\rho_{GW} - g\rho_{HC})$$

Where ρ_{GW} is the density of groundwater, ρ_{HC} is the density of hydrocarbon, and g is the gravity constant, but

$$\frac{H}{L} = \text{structural gradient}$$

Thus, the required length of continuous phase HC, ΔX, to create the overpressuring p_{α} is

$$\Delta X = \frac{p_{\alpha}}{\frac{H}{L}(g\rho_{GW} - g\rho_{HC})}$$

Figure B2 shows the calculated length of continuous phase hydrocarbon, which represents the updip length of a pool in a stratigraphic trap to cause certain amount of overpressuring. The calculations were also carried out for hydrocarbon p(d) gradients. The overpressuring is read from the X-axis, while the required length of continuous HC phase to create such overpressuring in a stratigraphic trap is read from the Y-axis. It was assumed for Figure B2 that the structural gradient is 12 m/km and the and the p(d) gradient of groundwater is 10 MPa/m.

A similar analysis applies to a structural trap condition, as shown in Figure B1. In this case, the required hydrocarbon column, ΔZ, to create an overpressuring p_{α} is

$$\Delta Z = \frac{p_{\alpha}}{(g\rho_{GW} - g\rho_{HC})}$$

Figure B3 shows the calculated column of hydrocarbon phase in a structural trap that can cause a certain overpressuring. The amount of overpressuring is read from the X-axis, while the required HC column is read from the Y-axis, for different HC p(d) gradients.
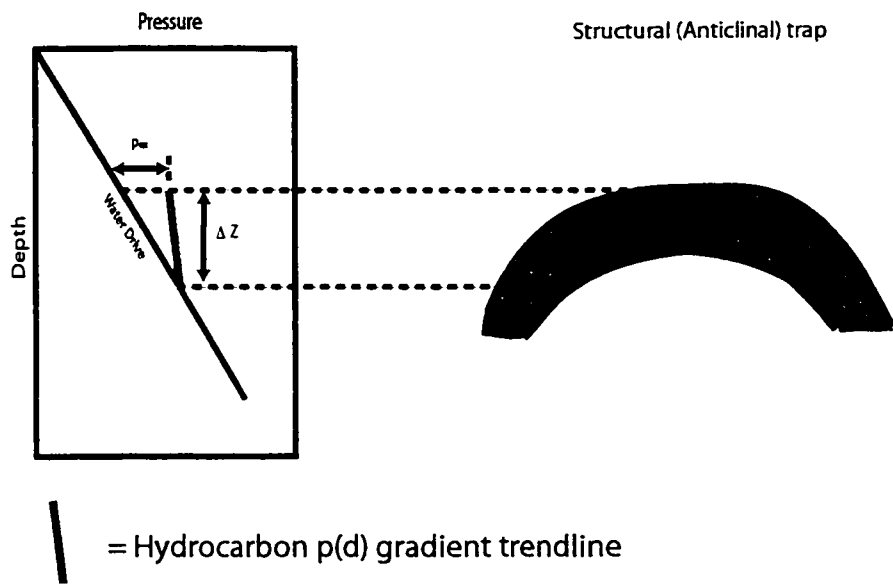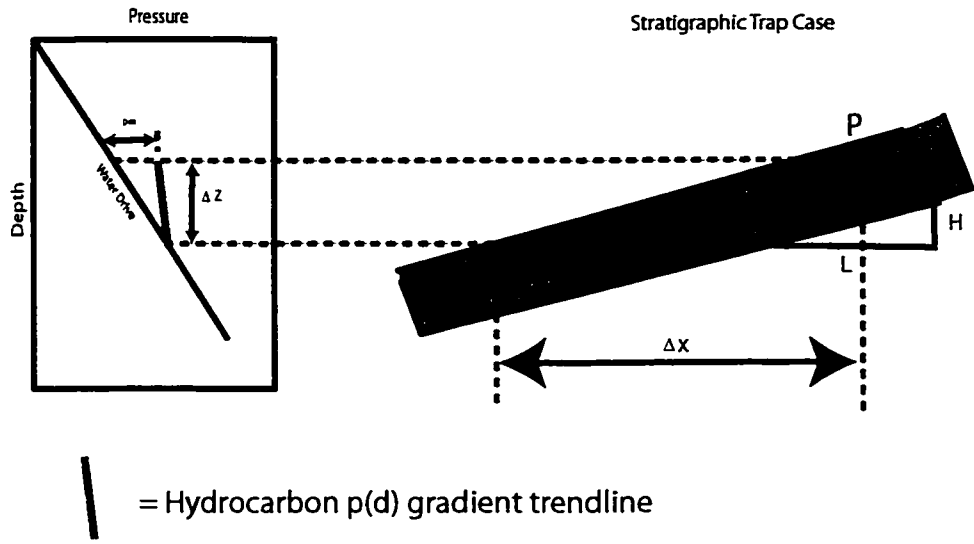
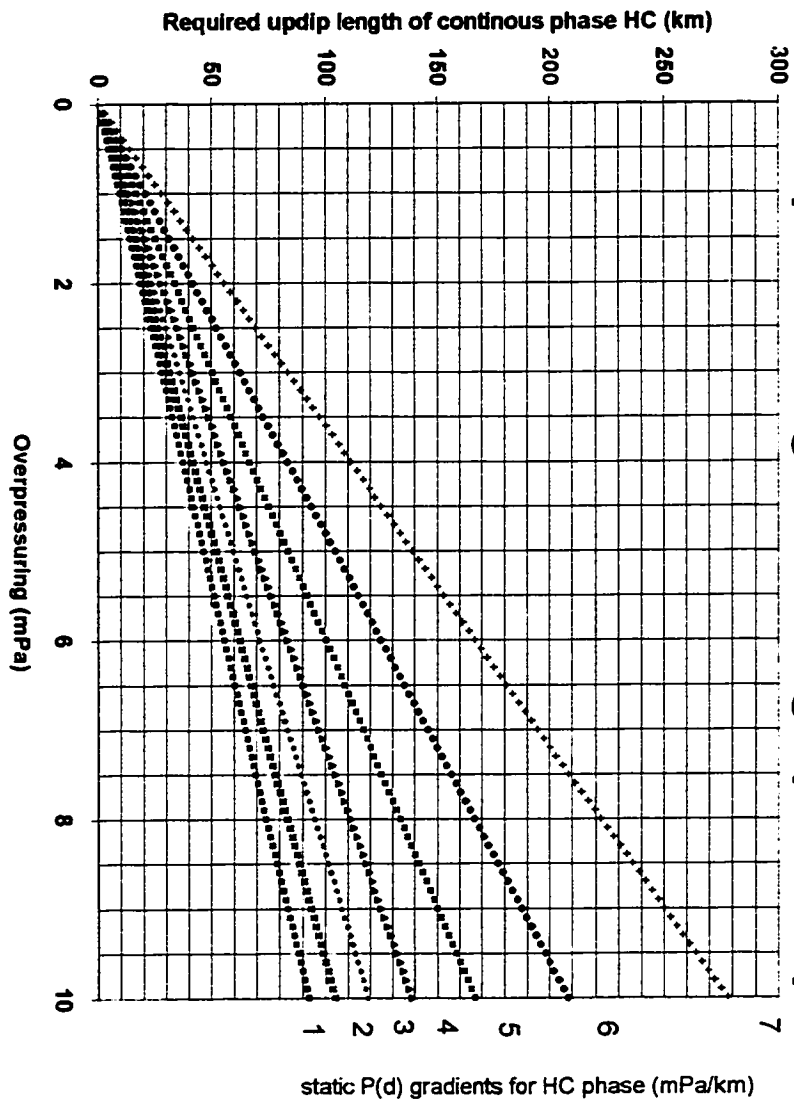Figure B1 Schematic of a stratigraphic and a structural trap with the relevant p(d) plot.

Figure B2 Required updip pool length to create overpressuring

151

Overpressuring for Structural Trap

Required HC Column (km) — axis: 0, 0.5, 1, 1.5, 2, 2.5, 3, 3.5

Overpressuring (mPa) — axis: 0, 2, 4, 6, 8, 10

static P(d) gradients
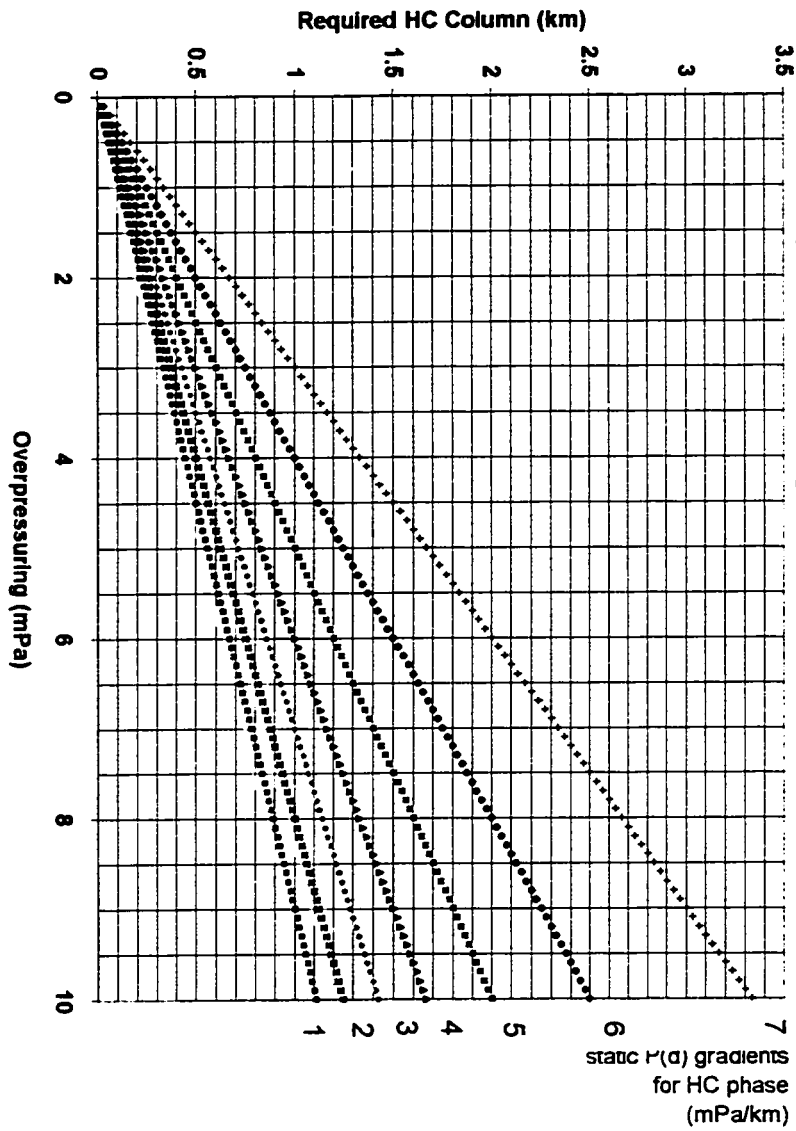for HC phase
(mPa/km): 1, 2, 3, 4, 5, 6, 7

Figure B3 Required column height to create overpressuring